

PhD Thesis

School of Chemistry

Cardiff University



The direct synthesis of hydrogen peroxide
in water at ambient temperature: A study
of reaction conditions, catalyst design and
implementation.

Thesis submitted in accordance with the requirements of the
University of Cardiff for the degree of doctor in philosophy by:

David Alexander Crole

2017

Summary

The research presented in this thesis focuses on the process of direct synthesis of hydrogen peroxide from molecular hydrogen and oxygen. This reaction potentially offers an approach which is greener and more sustainable when compared to the current industrial indirect auto-oxidation process. The work presented herein examines some of the key factors in determining the viability of the process in a water solvent at ambient temperature, conditions which would represent a very economically and environmentally attractive option, if feasible.

The first part of this thesis investigates the ways in which changing reaction conditions affects the fundamental reaction processes of the direct synthesis reaction – synthesis of hydrogen peroxide and its subsequent degradation by decomposition and hydrogenation. It was found that moving to a water solvent and ambient temperature results in significantly lower yields and greater degradation comparative to previously used water/methanol solvents and 2°C reactions.

The second part of this thesis explores the design of catalysts which are active for the direct synthesis of hydrogen peroxide while limiting degradation activity, to increase the yield in water at ambient temperature. A series of supported metal catalysts of the nominal formulation 0.5 wt. % Pd - 4.5 wt. % 'base metal' were prepared and treated with a cyclic oxidative-reductive-oxidative heat treatment. This produced highly stable catalysts with activity for the synthesis of hydrogen peroxide, but low to no activity for both decomposition and hydrogenation pathways. These catalysts also fulfilled a secondary aim of producing economically attractive catalysts due to the low loadings of precious metals used.

The third and final part of this thesis studies the implementation of these highly selective catalysts in both gas and gas/liquid phase flow reactors. The production of hydrogen peroxide in a gas phase flow system is shown to be attainable although most likely not a commercially viable option. The direct synthesis of hydrogen peroxide in a gas/liquid flow system is shown to proceed with selectivities greater than those previously reported for different catalysts under similar conditions. Tests also show that hydrogen peroxide can be produced under 'real world' conditions of high flow rates, a hard water solvent and a dilute hydrogen in air gas mix. These studies could be used to inform future work on high throughput water cleaning technologies.

Acknowledgements

I would like to express my gratitude to my research supervisor Professor Graham Hutchings for providing me with the opportunity to conduct this research as a member of the Cardiff Catalysis Institute. The guidance and insights received throughout this work from Professor Hutchings were invaluable. I also wish to acknowledge Selden Research Ltd, in particular Peter Woodhead for his ideas and enthusiasm throughout this project.

I would like to thank Dr. Peter Miedziak, Dr. Simon Freakley, Dr. Gregory Shaw and Dr. Nicholas Dummer for their advice during the three years of laboratory work as well as during the writing of this thesis, which has been greatly appreciated. My gratitude is extended to Prof. Pelham Hawker, Dr. Brian Harrison, Dr. Mark Howard, Prof. Hans Niemantsverdriet and Prof. Jacob Moulijn for their advice and constructive recommendations on their numerous visits to Cardiff. I gratefully acknowledge the staff in the chemistry department at Cardiff University, in particular the men without whom the lab would cease to operate: Chris Morgan, Steve Morris, Alun Davies and Lee Wescombe.

I would like to thank all of the PhD students and post docs who I have had the pleasure to work alongside. In particular I would like to thank Dr. Richard Lewis for his never-ending help and support, beginning with the training he provided on my very first day and continuing throughout my PhD. I would also like to thank the past and present members of the '*Hydrogen peroxide team*': Dr. Adeeba Akram, Dr. Ouardia Adkim, Dr. Richard Lewis, Ricci Underhill and Jonathan Harray in addition to Dr. Benjamin Yeo, Dr. Samuel Pattison, Dr. James Carter and Dr. James Hayward all of whom have been incredibly generous in lending a helping hand when needed.

Finally, I would like to thank Caroline Shearer whose positive energy managed to brighten up even the worst days, my close friends who do a fantastic job of taking my mind off my studies when necessary and my family who have been a constant support in everything I undertake.

TABLE OF CONTENTS

1. Introduction.....	1
1.1. Fundamentals of catalysis.....	1
1.2. Hydrogen peroxide.....	3
1.2.1. History and importance.....	3
1.2.2. Anthraquinone (auto-oxidation) process.....	4
1.3. Direct synthesis of H ₂ O ₂	6
1.3.1. Fundamentals of the reaction.....	6
1.3.2. The mechanism of direct synthesis of H ₂ O ₂	7
1.3.3. Palladium catalysts.....	9
1.3.4. Gold-palladium catalysts.....	14
1.3.5. Other metals.....	16
1.3.6. Support effects.....	17
1.4. Reaction parameters in the direct synthesis of H ₂ O ₂	18
1.4.1. Solvent.....	18
1.4.2. Acid and halide additives.....	20
1.4.3. Gas feed diluent.....	22
1.4.4. Temperature.....	22
1.5. Reactor types for the direct synthesis of H ₂ O ₂	24
1.5.1. Batch.....	24
1.5.2. Membrane.....	24
1.5.3. Flow.....	25
1.6. Thesis aims.....	26
1.7. References.....	28
2. Experimental.....	33
2.1. Materials and Reagents.....	33
2.2. Catalyst Preparation.....	34
2.2.1. Gold-Palladium catalyst preparation by wet impregnation.....	34

2.2.2. Various supported metal catalysts preparation by wet impregnation.....	34
2.3. Catalyst Testing	35
2.3.1. Batch H ₂ O ₂ Synthesis.....	35
2.3.2. Batch H ₂ O ₂ Degradation.....	37
2.3.3. Batch Blank Reactions	38
2.3.4. Batch Catalyst Re-use.....	39
2.3.5. Liquid/gas flow H ₂ O ₂ synthesis	39
2.3.6. Gas phase flow H ₂ O ₂ synthesis	41
2.4. Gas Chromatography.....	43
2.4.1. Gas Chromatography theory	43
2.4.2. Gas Chromatography analysis for H ₂ O ₂ synthesis reactions.....	44
2.5. X-Ray Photoelectron Spectroscopy	45
2.6. Electron Microscopy and Element Analysis.....	46
2.6.1. Transmission Electron Microscopy	46
2.6.2. Scanning Transmission Electron Microscopy	47
2.6.3 Energy-dispersive X-Ray Spectroscopy and Electron Energy Loss Spectroscopy	48
2.8. X-Ray Diffraction.....	49
2.9. Temperature Programmed Reduction	51
2.10. Microwave Plasma Atomic Emission Spectroscopy	52
2.11. Surface Area Analysis.....	53
2.11.1. Surface Area Analysis by Physisorption	53
2.11.2. Surface Area Analysis by Chemisorption.....	54
2.12. Infrared spectroscopy	55
2.13. References	58
3. The effect of reaction conditions on the direct synthesis of hydrogen peroxide using supported gold-palladium catalysts	59
3.1. Introduction	59
3.2. Results and Discussion.....	61

3.2.1. Time-on-line studies for hydrogen peroxide synthesis and degradation using 2.5 wt. % Au-2.5 wt. % Pd/TiO ₂ at 20°C - 25°C in varied solvent compositions	61
3.2.2. The effect of temperature on hydrogen peroxide synthesis and degradation using 2.5 wt. % Au - 2.5 wt. % Pd/TiO ₂ in H ₂ O	65
3.2.3. The effect of varied H ₂ O/MeOH solvent ratios on hydrogen peroxide synthesis and degradation using 2.5 wt. % Au - 2.5 wt. % Pd/TiO ₂ at 20°C.....	67
3.2.4. The effect of pressure and H ₂ /O ₂ gas ratio on hydrogen peroxide synthesis using 2.5 wt. % Au - 2.5 wt. % Pd/TiO ₂ at 20°C.....	69
3.2.5. The effect of catalyst mass on hydrogen peroxide synthesis and degradation using 2.5 wt. % Au - 2.5 wt. % Pd/TiO ₂ at 20°C	73
3.2.6. Henry's constants for the solubility of H ₂ and O ₂ in H ₂ O and MeOH.....	76
3.2.7. The effect of solution pH on hydrogen peroxide synthesis and degradation using 2.5 wt. % Au - 2.5 wt. % Pd/TiO ₂ at 20°C.....	78
3.2.8. The effect of dissolved ions on hydrogen peroxide synthesis using 2.5 wt. % Au - 2.5 wt. % Pd/TiO ₂ at 20°C	81
3.2.9. The effect of using N ₂ diluent gas on hydrogen peroxide synthesis using 2.5 wt. % Au - 2.5 wt. % Pd/TiO ₂ at 20°C	92
3.3. Conclusions	95
3.4. References	97
4. The design of stable and selective catalysts for the direct synthesis of hydrogen peroxide.....	100
4.1. Introduction	100
4.2. Results and discussion	102
4.2.1. Metal Screening	102
4.2.2. Pd-Pt Catalysts.....	104
4.2.3. Pd-M bi-metallic screening	107
4.2.4. Pd-Ni catalysts	109
4.2.5. Oxidation-Reduction-Oxidation treatment of Pd-Ni catalysts.....	111
4.2.6. The use of varied supports for Pd-Ni catalysts	117
4.2.7. The effect of precursor salt and preparation pH for Pd-Ni catalysts	120

4.2.8. Pd-Ga catalysts	123
4.2.9. Further Pd-‘M’ ORO catalysts	126
4.2.10. Pd-Ni ORO performance under varied reaction conditions	131
4.3. Characterisation.....	136
4.3.1. – STEM	136
4.3.2. – XPS	140
4.3.3. – CO DRIFTS	142
4.3.4. – CO Chemisorption	144
4.3.5. – XRD	145
4.3.6 – TPR.....	147
4.4. Conclusions	149
4.5. References	152
5. The implementation of gas and liquid flow systems for the direct synthesis of hydrogen peroxide	155
5.1. Introduction	155
5.2. Results.....	157
5.2.1. Gas phase flow reactions using Au-Pd/TiO ₂ catalysts	157
5.2.2. Gas phase flow reactions using Pd-Ni/TiO ₂ and Pd-Ga/TiO ₂ catalysts ...	163
5.2.3. Liquid/gas phase flow reactions using 0.5 wt. % Pd – 4.5 wt. % Ni/TiO ₂ ORO.....	167
5.2.4. The effect of pressure on liquid/gas phase flow reactions using 0.5 wt. % Pd – 4.5 wt. % Ni/TiO ₂ ORO.....	170
5.2.5. The effect of catalyst mass on liquid/gas phase flow reactions using 0.5 wt. % Pd – 4.5 wt. % Ni/TiO ₂ ORO	172
5.2.6. The effect of solvent flow rate on liquid/gas phase flow reactions using 0.5 wt. % Pd – 4.5 wt. % Ni/TiO ₂ ORO	173
5.2.7. The effect of gas flow rate on liquid/gas phase flow reactions using 0.5 wt. % Pd – 4.5 wt. % Ni/TiO ₂ ORO	176
5.2.8. Liquid/gas phase flow reactions using 0.5 wt. % Pd – 4.5 wt. % Ga/TiO ₂ ORO.....	177

5.2.9. The effect of using an N ₂ diluent on liquid/gas phase flow reactions using 0.5 wt. % Pd – 4.5 wt. % Ni/TiO ₂ ORO	179
5.2.10. The effect of using a ‘hard water’ solvent on liquid/gas phase flow reactions using 0.5 wt. % Pd – 4.5 wt. % Ni/TiO ₂ ORO	181
5.3. Conclusions	183
5.4. References	187
6. Future work and conclusions	188
6.1. Conclusions	188
6.2. Future work.....	192
6.2.1. Further catalyst optimisation and design.....	192
6.2.2. Use of Pd-M ORO catalysts in further reactions	193
6.2.3. Further flow system testing.....	195
6.2.4. Characterisation	196
6.3. References	198

1. INTRODUCTION

In this Chapter the fundamentals of catalysis are outlined and the state-of-the-art of the literature relating to the direct synthesis of hydrogen peroxide is discussed.

1.1. Fundamentals of catalysis

The existence of a so-called 'catalytic force' was first reported by J. J. Berzelius, who noted that there were substances which had the effect of accelerating the rate of a reaction whilst remaining unchanged in the process.¹ These substances later became known as catalysts and the resulting acceleration of a rate of reaction from their use became known as catalysis. A catalyst can be more accurately described as a substance which alters the kinetics but not the thermodynamics of a chemical reaction by lowering the activation energy (E_a) of a reaction through providing an alternative, lower energy pathway (as shown in Figure 1.1). This happens *via* the reactant molecule(s) forming bonds to the catalyst, allowing them to react through a lower energy process than would occur in the absence of a catalyst, to form a product which unbinds from the catalyst, leaving it unchanged.²

The rate constant of a given reaction can be expressed by the Arrhenius equation:

—

Where k = rate constant, A = pre-exponential factor, E_a = activation energy, R = molar gas constant, T = temperature.

Thus it can be seen that when a reaction proceeds *via* an alternative, lower activation energy pathway, in the case from using a catalyst, a greater rate constant is the result (all other factors being equal).

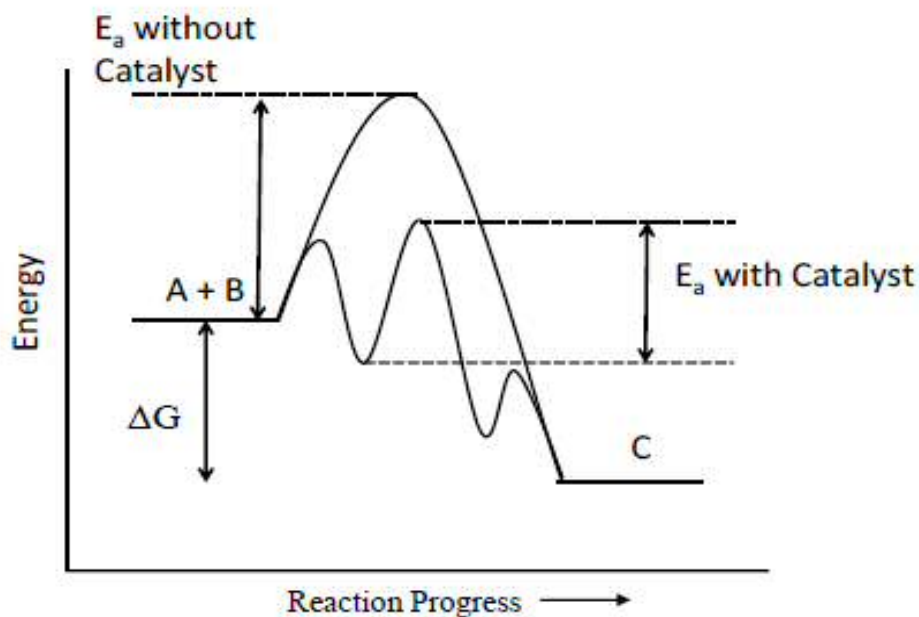


Figure 1.1 – An energy level diagram illustrating an uncatalysed reaction and an alternative, lower activation energy pathway for a catalysed reaction.

Catalysis is incredibly important in the modern world with the chemical industry employing catalytic processes in the production of the majority of consumer and platform chemicals. One such example and perhaps the single most important application of catalysis is the Haber-Bosch process, which employs a heterogeneous iron catalyst to synthesise ammonia. The majority of this ammonia is used to create artificial fertilisers, which are vital to meet the current population's food demands.³

Catalysts are generally split into three categories: homogeneous, heterogeneous and biological. Homogeneous catalysts exist in the same phase as the reactants, most commonly as liquids, and generally are effective catalysts, but present problems for separation and re-use. Heterogeneous catalysts exist in a different phase to the reactants, generally solid catalysts in liquid or gaseous reactant mixtures, and while they tend to exhibit less efficacy than homogeneous catalysts, they are physically robust and easy to separate and re-use. For this reason, heterogeneous catalysts represent the majority of industrially employed catalysts. Finally, biological catalysts or enzymes display unparalleled efficacy, but are generally active only for a specific reaction under very specific conditions and therefore are not usually industrially viable.

1.2. Hydrogen peroxide

1.2.1. History and importance

Hydrogen peroxide (H_2O_2) is the simplest molecule containing a peroxide group, that is, a single oxygen-oxygen bond. It was first discovered by Louis Jacques Thénard in 1818⁴ and has since become an important commodity chemical, with annual usage now exceeding 3 million tonnes per annum and increasing.⁵ H_2O_2 has many important industrial applications, including a number of selective oxidation processes, paper, pulp and textile bleaching and use in the manufacture of percarbonates and perborates, which find use as mild bleaches in laundry detergents.⁶ Due to its anti-microbial and oxidising properties, hydrogen peroxide can be used for the treatment of waste waters and industrial wastes. Hydrogen peroxide is a powerful oxidant in aqueous solution, effectively destroying chlorine, hypochlorite, thiocyanate, nitrate and many other chemicals which are potentially toxic if present in water streams. It also exhibits a high atom economy and only produces water as a waste product when employed as an oxidant, which makes it a 'green' alternative to commonly used chlorine containing oxidants such as sodium hypochlorite.⁷

For the treatment of waste water, hydrogen peroxide can be used alone, but is more effective in the presence of Fe^{2+} or Mn^{4+} species which decompose the peroxide to hydroxyl and hydroperoxyl radicals. When hydrogen peroxide is used in conjunction with a Fe catalyst, it is known as Fenton's reagent. The radical species produced are powerful non-selective oxidants which participate in secondary reactions; this is useful for the total oxidation of many organic contaminant species to harmless carbon dioxide and water.^{8,9} Other catalysts can be employed and conditions changed for the effective destruction of certain contaminants, for example the use of hydrogen peroxide with a copper catalyst at pH 8.5 – 11.5 efficiently destroys cyanide.¹⁰

Hydrogen peroxide is increasingly used as an oxidant in organic and inorganic chemical syntheses. Much of this has been made possible by the development of a ZSM-5 type titanium-silicate molecular sieve catalyst, TS-1, which has the ability to catalyse many different oxidation reactions using hydrogen peroxide. These include direct ammoxidation of cyclohexanone to cyclohexanone oxime,¹¹ oxidation of sulfoxides and thioethers,¹² selective oxidation of alcohols and hydroxylation of aromatics.⁸ A fairly recent major use of hydrogen peroxide industrially is Degussa/Uhde's HPPO process, shown in Figure 1.2, a single step epoxidation of propene which produces water as the only by product.¹³ Propene oxide is an

important commodity chemical which is used to for the plastic polyurethane as well as solvents, flame retardants and surfactants.¹⁴

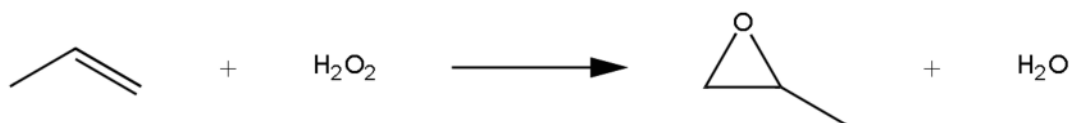


Figure 1.2 – Reaction schematic of the Degussa/Uhde HPPO process

1.2.2. Anthraquinone (auto-oxidation) process

Currently, over 95% of the world's supply of H_2O_2 is produced by the anthraquinone (AQ) process, also known as the auto-oxidation (AO) process. This process is an indirect synthesis of H_2O_2 which proceeds by the hydrogenation of a 2-alkyl anthraquinone (AQ) over a palladium, platinum or nickel catalyst.¹⁵ This forms the corresponding 2-alkyl anthrahydroquinone (AHQ), followed by reaction with oxygen, regenerating the 2-alkyl anthraquinone and forming H_2O_2 . The AHQ molecule can also undergo further hydrogenation to the corresponding 2-alkyl tetrahydroanthrahydroquinone (THAHQ), which reacts with oxygen to yield H_2O_2 and 2-alkyl tetrahydroanthroquinone (THAQ), as illustrated in Figure 1.3. This process is generally carried out at mild temperatures and pressures, with operating conditions of approximately 50°C and 4 bar H_2 commonly used. The process was developed by Ridel and Pfeleiderer, building upon work by Manchot, who originally showed that under alkaline conditions, peroxides are produced by the auto-oxidation of hydrobenzenes and hydroquinones.¹⁶ The above description represents the most basic form of the AO process; there have since been many iterative advances and updates, with the current version representing an efficient production method, optimised to give high H_2 selectivity towards H_2O_2 .

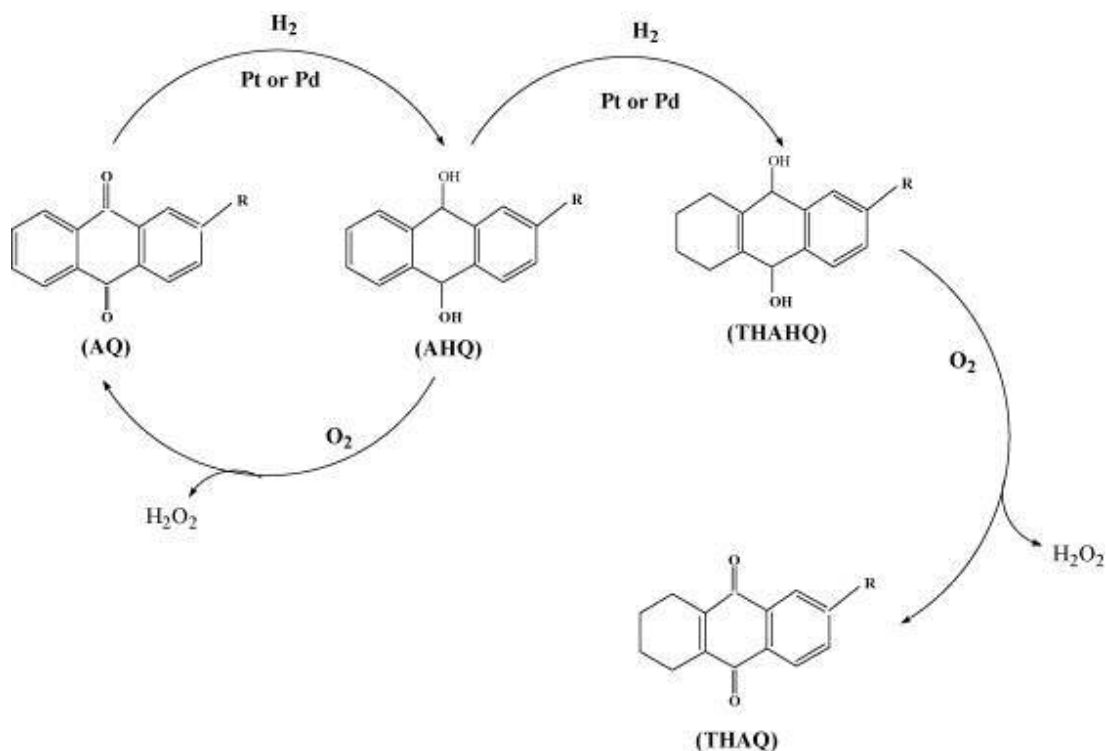


Figure 1.3 – Schematic representation of the anthraquinone process.⁷

There are however inherent problems with the AO process. It proves to only be economically viable when operated at a large scale, typically in the order of 10⁵ tons/annum, and hence production currently has to be centralised at large processing plants. As such there is a need to store and/or transport the H₂O₂, usually as a concentrated solution (c.a. 70 wt %), which presents safety challenges due to its oxidising nature. Generally the addition of a stabiliser in the form of an acid or halide is also required. Therefore in the final application, dilution and potentially removal of stabilisers may be necessary for many uses, particularly bleaching applications when H₂O₂ is used in a dilute solution (3-8 vol%).⁷ These extra steps can require time and energy input at the point of use.

The AO process also suffers from loss of the AQ, this occurs both through the formation of derivatives which do not take part in the H₂O₂ formation cycle (such as THAQ) and through decomposition over the hydrogenation catalyst. Due to these losses, the efficiency of the process will decrease over time, necessitating the addition of AQ to the system to keep yield sufficiently high, reducing the 'green' credentials of the process.^{8, 16-19}

1.3. Direct synthesis of H₂O₂

1.3.1. Fundamentals of the reaction

H₂O₂ can be synthesised by the direct combination of molecular hydrogen (H₂) and oxygen (O₂) with use of a suitable catalyst. This synthesis of H₂O₂ presents a 100% atom efficient reaction and thus a far 'greener' method of H₂O₂ production when compared to the AO process. However, the direct synthesis of H₂O₂ is not without its challenges, predominantly in the form of the parallel combustion reaction of H₂ and O₂ and the subsequent degradation of synthesised H₂O₂ via hydrogenation and decomposition reactions, all of which form water. These reaction pathways and their corresponding free energy and enthalpy values are illustrated in Figure 1.4.

To further compound these issues, the catalysts which are active for the desired direct combination of H₂ and O₂ to form H₂O₂ are generally also active catalysts for the undesired combustion reaction and the hydrogenation of H₂O₂. The decomposition reaction, which is also undesired, occurs even without the presence of a catalyst due to the instability of H₂O₂, however the rate of this too can be enhanced by many of the H₂O₂ synthesis catalysts. All the reactions detailed are highly exothermic and therefore favourable, however the combustion reaction and the hydrogenation reaction are significantly more favourable than the desired direct combination of H₂ and O₂. Therefore, these side reactions must be limited to increase the efficiency with which available H₂ is used and to reduce the destruction of synthesised H₂O₂ to a minimum.

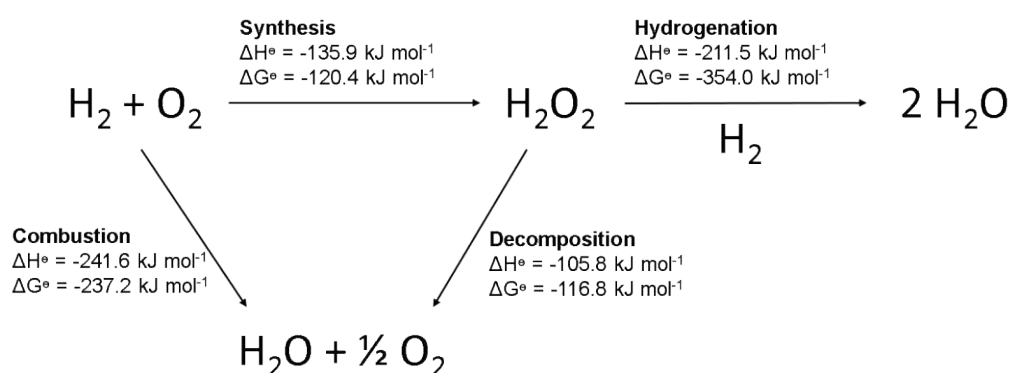


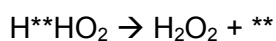
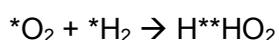
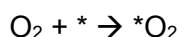
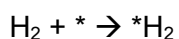
Figure 1.4 – Schematic representation of the reaction pathways involved in the direct synthesis of H₂O₂ and the corresponding enthalpy and free energy values.

The potential rate at which H₂O₂ can be practically synthesised in this way is also limited by the need to use dilute O₂ and H₂ gas streams for safety reasons. High pressure O₂ and H₂ mixes present a danger due to their explosive nature in the range of 4% to 94% volume of H₂ in O₂ at room temperature. Thus to remove the risk of explosion, the reagent gases are diluted to a level outside this explosive regime, which in practical terms means a limit of the maximum possible yield of H₂O₂.^{7,8}

1.3.2. The mechanism of direct synthesis of H₂O₂

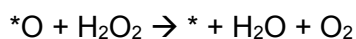
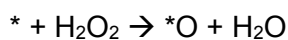
Suggested reaction mechanisms for the direct synthesis of H₂O₂ and the degradation pathways, decomposition and hydrogenation, will be discussed in a chronological order of publication. Strukul and co-workers²⁰ put forward a mechanism in which protons are directly involved in the direct synthesis of hydrogen peroxide on “large, non-defective” Pd surfaces (in this study present as supported nanoparticles on alumina membranes). They propose that O₂ first non-dissociatively chemisorbs on the surface, followed by reaction with a proton to form an OOH⁺ surface intermediate, which then reacts with H₂ in solution to form H₂O₂ and regenerate a proton. On surfaces which are of higher energy, for example defects and edge sites, dissociative chemisorption of O₂ and H₂O₂ occurs and the surface species formed react with chemisorbed H atoms to form water through combustion and H₂O₂ hydrogenation respectively.

A different mechanism is proposed by Zhou and Lee²¹ in their patent. It is claimed that H₂ and O₂ both non-dissociatively bind to adjacent Pd atoms. There is then a sequential transfer of hydrogen atoms to first form adjacent surface bound OOH and H species and then H₂O₂. Voloshin *et al.*²² derived rate equations from the mechanism proposed by Zhou and Lee in addition to 3 further feasible mechanisms proposed by the authors. They then obtained kinetic data for the direct synthesis of H₂O₂ and compared this to the rate laws derived from the 4 proposed mechanisms. They found that the kinetic data most close fit the mechanism originally proposed by Zhou and Lee which they expressed as follows:

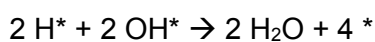
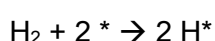


(* = catalytic site)

Further studies from Voloshin *et al.*^{23, 24} sought to propose and test mechanisms for the catalytic decomposition and hydrogenation of H₂O₂. For the catalytic decomposition of H₂O₂, they reject a mechanism involving homolytic dissociation of H₂O₂ on the catalyst and instead they propose the following scheme *via* correlation with kinetic data:



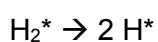
For the catalytic hydrogenation of H₂O₂, they propose the mechanism that fits with their experimental kinetic data is as follows:



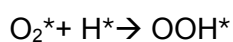
Hutchings and co-workers²⁵ outlined a Langmuir-Hinshelwood style mechanism in which H₂ dissociatively chemisorbs on the surface. One adsorbed H reacts with non-dissociated adsorbed O₂ to first form an OOH intermediate, then the second adsorbed H also reacts to form H₂O₂. They propose that if O₂ dissociatively chemisorbs, reaction with adsorbed H occurs, resulting in the combustion reaction yielding H₂O. A mechanism for catalytic decomposition of H₂O₂ identical to that proposed by Voloshin is also suggested.

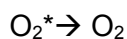
Iwamoto and co-workers²⁶ have suggested a mechanism closer to an Eley-Rideal style mechanism in which H₂ dissociatively chemisorbs, then free O₂ reacts with an adsorbed H species to form an OOH species, which then reacts with the second adsorbed H to form H₂O₂. However in later papers^{27, 28} their kinetic data appear to support the mechanism proposed by Hutchings. Computational studies by Nørskov and co-workers²⁹ and by Ding and co-workers³⁰ simulating H₂O₂ synthesis on Au clusters also concur with the mechanism proposed by Hutchings. A stepwise expression of this mechanism was clearly detailed by Yoshizawa and co-workers³¹ in a review and can be expressed as follows:

For all hydrogenations to take place, H₂ must adsorb and dissociate:

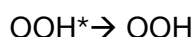
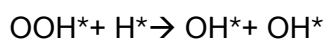
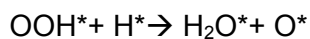
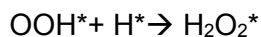


For the reactant O₂:

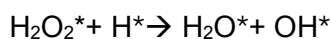
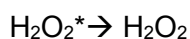




For the intermediate OOH:



For the product H_2O_2 :



Hence the majority of literature agrees that a Langmuir-Hinshelwood style, two step hydrogenation of oxygen is the pathway by which H_2O_2 is synthesised.

However, in a recent theoretical study Flaherty and co-workers³² have proposed a reaction mechanism for the direct synthesis of hydrogen peroxide over Pd clusters which proceeds via heterolytic reaction pathways involving successive proton then electron transfer, first to surface bound O_2 to form OOH intermediates, then again to these intermediates to form H_2O_2 . Therefore there is not unanimous agreement on the mechanism of direct H_2O_2 synthesis and as such it is necessary for continued studies in this area to elucidate full mechanistic details.

1.3.3. Palladium catalysts

A catalysed direct synthesis of H_2O_2 was first patented in 1914 by Henkel and Weber³³ but the technology was not used in a commercial setting. The process used a palladium catalyst and since their findings much of the further work in this area has studied palladium based catalysts. Pd catalysts have been studied in multiple forms, such as bulk metal surfaces, supported nano-particles, colloidal Pd and modified membranes.^{5, 7, 15, 34, 35}

Choudhary and co-workers have performed extensive studies using Pd catalysts. This has included a Pd film deposited on a γ -alumina membrane,³⁶ but the majority of studies employ supported Pd nanoparticle catalysts using carbon or oxide supports such as CeO_2 , Ga_2O_3 , Al_2O_3 and SiO_2 .³⁷⁻⁴³ Choudhary utilises both heat treatments under a hydrogen rich atmosphere to yield Pd^0 surfaces and heat treatments under an oxygen rich atmosphere to yield PdO surfaces, however catalysts have also been treated with oxidising agents such as perchloric acid,⁴⁴ bromide salts⁴⁵ and combinations of bromide and fluoride salts⁴⁶ to further tune surface properties.

Choudhary showed that for palladium catalysts to be effective for the direct synthesis of H_2O_2 , they must be calcined under an oxidative environment to produce bulk or sub-surface PdO in the nano-particles. If the calcination takes place under a reductive atmosphere, forming Pd^0 nano-particles, the catalysts displayed a very high rate of H_2O_2 decomposition and therefore low selectivity, which is undesirable.^{44, 47}

Strukul and co-workers have performed studies on tubular catalytic membranes, similar to those studied by Choudhary. These catalytic membranes are composed of mesoporous α -alumina. These membranes are either coated with carbon, onto which Pd is supported as small (5-10 nm) nanoparticles by deposition-precipitation (DP); or a 1-10 μm thick layer of Pd is coated onto the membrane by electroless plating deposition (EPD). The catalysts prepared by EPD were heat treated both at 500°C in air, producing an ordered surface of large crystallites and 800°C under an inert gas, producing an unordered microcrystalline surface. Catalysts prepared by DP and catalysts prepared by EPD with both morphologies of Pd layers were active for the direct synthesis of H_2O_2 . Strukul found that for DP catalysts, those with an average Pd crystallite size of 8 nm were more active and selective than those with a smaller average particle size. Similarly, it was found that the EPD catalysts with larger, ordered crystallites were more active and selective than those with disordered microcrystallites. Strukul concluded that a "smooth metallic surface", free of defects and with limited edge and corner sites, is necessary to limit decomposition and therefore improve synthesis yields.^{20, 48, 49}

Lunsford and co-workers have extensively studied Pd catalysts in various forms, this has included a homogeneous system of PdCl_2 dissolved in HCl (which exists in equilibrium with colloidal Pd in solution)^{50, 51} and heterogeneous catalysts such as Pd supported on SiO_2 ⁵⁰⁻⁵⁶, Al_2O_3 , ZrO_2 ¹⁹ and carbon black⁵⁷. These colloidal and supported Pd catalysts are shown to be effective catalysts for the production of H_2O_2 ,

with concentrations approaching 2 wt% reached in an acid and bromide salt promoted aqueous medium.

However, Lunsford argues that colloidal Pd is the predominantly active form of Pd and that this can arise from both the reduction of PdCl_4^{2-} ions or through leaching of surface Pd from supported Pd^0 catalysts in the presence of ≥ 0.1 N HCl. It was observed that when the solid Pd/SiO₂ catalyst was removed from the reaction mixture after 2 h, the rate of reaction remained unchanged.⁵² Furthermore, Lunsford shows that the rate of reaction is “approximately proportional” to the concentration of Pd colloid in solution. This shows that the direct synthesis of H₂O₂ with supported Pd⁰ catalysts under the aforementioned conditions is in fact catalysed by colloidal Pd and therefore not a true heterogeneous process.⁵⁰⁻⁵²

Colloidal Pd is an effective catalyst and an interesting system for academic study, however it is very unlikely to be useful in a practical industrial scenario. The difficulty of separating a colloid and the deposition of the majority of colloidal Pd on reactor walls and frits after a 24 h reaction time shown by Lunsford⁵¹ would most likely both prove prohibitive to use. Schematics of the various forms which Lunsford proposed that Pd can assume through a reaction is shown in Figure 1.5.

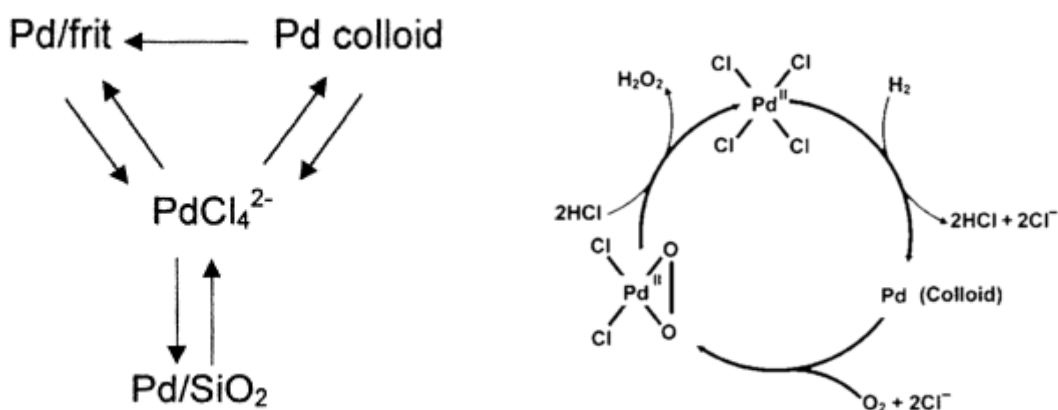


Figure 1.5 – Proposed mechanisms of the formation of colloidal Pd from chloride salts and supported catalysts.^{19, 52}

Salmi and co-workers use a range of supported Pd catalysts in their various studies on reactor engineering for the direct synthesis of H₂O₂. These catalysts were generally prepared by incipient wetness impregnation of Pd onto supports such as carbon, SiO₂, ZrO₂, sulphonated CeO₂ and sulphonated ZrO₂ and were heat treated in air.⁵⁸⁻⁶¹ In their paper comparing Pd catalysts on these various supports, it was found that sulphonated ceria and zirconia give the greatest productivity and

selectivity. It was reasoned that this is primarily due to the strong increase in acidity brought about by sulphonation, however retardation of surface crystallisation and increases in surface area and pore size could also be contributing factors. Salmi suggests that the use of strongly acidic supports will lead to the most productive supported Pd catalysts.^{59, 61}

The work of Song and co-workers studies similar catalysts consisting of Pd on sulphonated supports. This has various consisted of sulphonated SiO₂, TiO₂, ZrO₂ and SBA-15 and MCF (both forms of mesoporous silica).⁶²⁻⁶⁵ In all of these studies a consistent finding was that as the acidity of the support increased, so too did the selectivity towards H₂O₂ synthesis and catalyst productivity as the support acted as an *in-situ* acidic promoter. Song also studied Pd/HZSM-5 catalysts and found a 'volcano curve' relationship between yield and Si/Al ratio, as shown in Figure 1.6. However, productivity was found to positively correlate with the number of Brønsted acid sites.⁶⁶

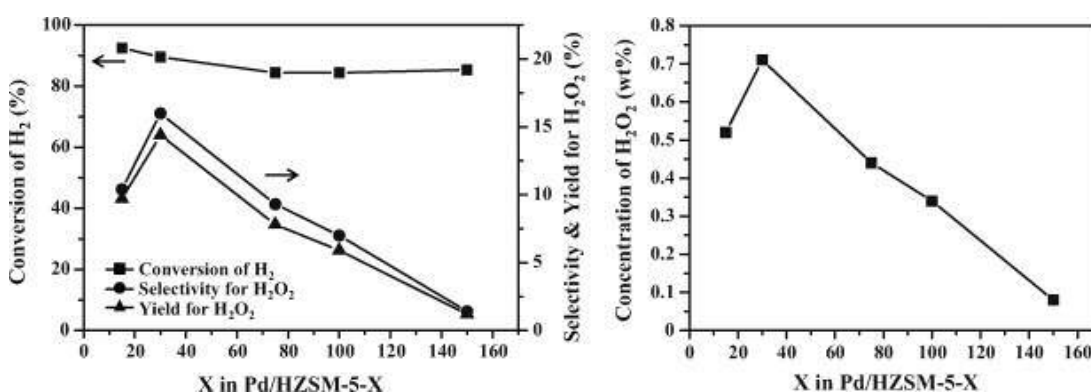


Figure 1.6 – Relationship of Si/Al atomic ratio (X) in Pd/HZSM-5 and conversion of H₂, selectivity for H₂O₂ and yield of H₂O₂.⁶⁶

Tangential studies by Song and co-workers focus on the use of heteropolyacid (HPA) catalysts with Pd catalysts. HPAs were exchanged with Pd ions, in addition to being used as co-catalysts to Pd/SiO₂, used as supports, co-supported with Pd species and incorporated into a support.⁶⁷⁻⁷² Again, the trend of the findings of these studies was that as the acidity of the HPA/supports increased, so too did the selectivity and productivity of the catalyst(s) for H₂O₂ synthesis.

From the same research department, Lee and co-workers have studied encapsulated Pd colloids, using porous SiO₂, ZrO₂ and SiO₂-Al₂O₃ frameworks to immobilise and stabilise Pd nanoparticles.⁷³⁻⁷⁶ Preparing Pd colloids with c.a. 4 nm diameter and

encapsulating them inside metal oxide frameworks yielded catalysts with very high dispersions of Pd and as such greater activity per gram of Pd than SiO₂ supported catalysts.⁷³ Further studies showed that colloids of approximately 4 nm diameter were more selective than those with a smaller diameter, due to a greater proportion of high energy edge and defect sites in smaller colloids, which cleave O-O bonds and lead to combustion and degradation reactions.⁷⁴ Lee also showed that if a yolk-shell structure is created with a void in between the Pd colloid and the metal oxide framework, mass transport of reactant gas can be improved, leading to greater productivities.⁷⁵ It was also shown that increasing the number of Brønsted acid sites in the framework through tuning a ratio of SiO₂-Al₂O₃ mixed oxide framework increased productivity and therefore yield.⁷⁶

Hutchings and co-workers have performed extensive studies on supported Pd catalysts, generally prepared by wet impregnation and heat treated in air. Various supports have been used in these studies including carbon, TiO₂, SiO₂, Fe₂O₃, CeO₂, Al₂O₃ and zeolite USY.^{25, 77-88} Testing data for a selection of stable Pd catalysts tested by Hutchings and co-workers is displayed in Table 1.1. These data show that an acid-washed SiO₂ support displays superior productivity, corroborating the findings of Salmi and Song, as detailed previously.

Table 1.1 – Testing data for various supported metal catalysts from Hutchings and co-workers.^{25, 78, 79, 88}

Conditions: 30 min reaction time, 5.6 g MeOH/2.9 g H₂O solvent, 100 mL autoclave, 2°C, 1200 rpm stirring, 10 mg catalyst, 420 psi H₂/CO₂ + 160 psi O₂/CO₂.

Catalyst	H₂O₂ productivity / mol H₂O₂ kg_{cat}⁻¹h⁻¹	H₂O₂ degradation /%	H₂O₂ decomposition /%
5 wt. % Pd/Al₂O₃	9	11	1
5 wt. % Pd/TiO₂	31	16	12
5 wt. % Pd/MgO	29	29	18
5 wt. % Pd/C	55	6	5
5 wt.% Pd/α- Fe₂O₃	4	n.d.	n.d.
5 wt. %Pd/acid- washed SiO₂	85	18	n.d.

n.d. = not determined

1.3.4. Gold-palladium catalysts

In 2002 Hutchings and co-workers reported the high selectivity of supported Au catalysts for the direct synthesis of H_2O_2 .⁸⁹ Further work discovered that supported bimetallic Au-Pd nano-particle catalysts benefit from enhanced activity and selectivity when compared to Pd analogues.⁷⁷ This synergistic increase in productivity and selectivity is shown in Figure 1.7. As such a great number of studies into the properties, optimum reaction conditions and synthesis methods for these catalysts followed.^{5, 25, 77-88, 90-99} It was found that heating of the catalysts to sufficiently high temperatures (generally 400°C , 3 h, static air) is a necessary step to ensure the stability of the catalyst to metal loss. Catalysts which have not been heat treated initially display a higher activity than heat treated catalysts, due to colloidal metal particles acting as effective catalysts (as proposed by Lunsford⁵⁰), but subsequently decrease in activity due to loss of the active metal.⁷⁸

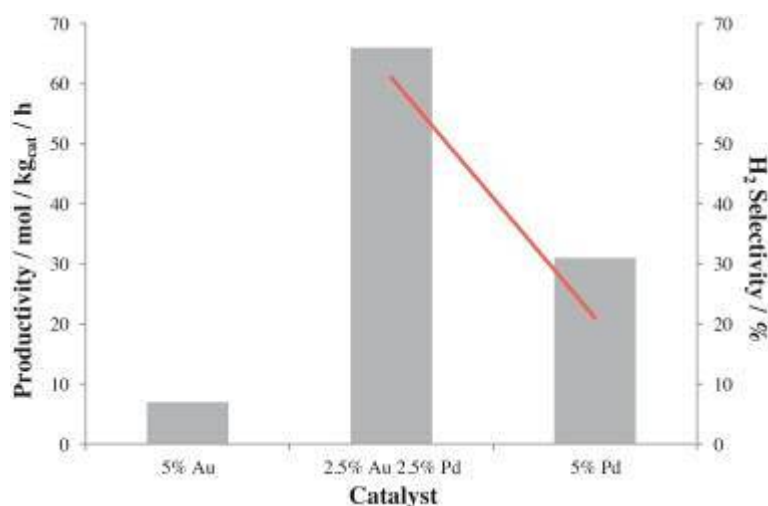


Figure 1.7 – Data from Hutchings and co-workers illustrating the synergistic increases in both productivity (bars) and selectivity (line) for Au-Pd catalysts versus monometallic analogues.³⁵

Metal oxide supported Au-Pd catalysts heat treated in an oxidative environment were found to have an $\text{Au}_{\text{core}}\text{-PdO}_{\text{shell}}$ nanoparticle morphology *via* XPS and STEM analyses. Untreated catalysts were found to be formed of random alloys, thus it was concluded that the core-shell morphology forms upon heat treatment.⁸⁰ Carbon supported Au-Pd catalysts differ from metal oxide supported catalysts as the nanoparticles display a random alloy structure both before and after heat treatment. Imaging of these catalysts is displayed in Figure 1.8. These carbon supported catalysts give greater productivity for H_2O_2 synthesis than metal oxide supported

analogues, primarily due to an increase in selectivity.⁸¹ This suggests that a random alloy Au-Pd nano-particle structure is preferable to Au_{core}-Pd_{shell} nanoparticles for minimising the degradation of H₂O₂.

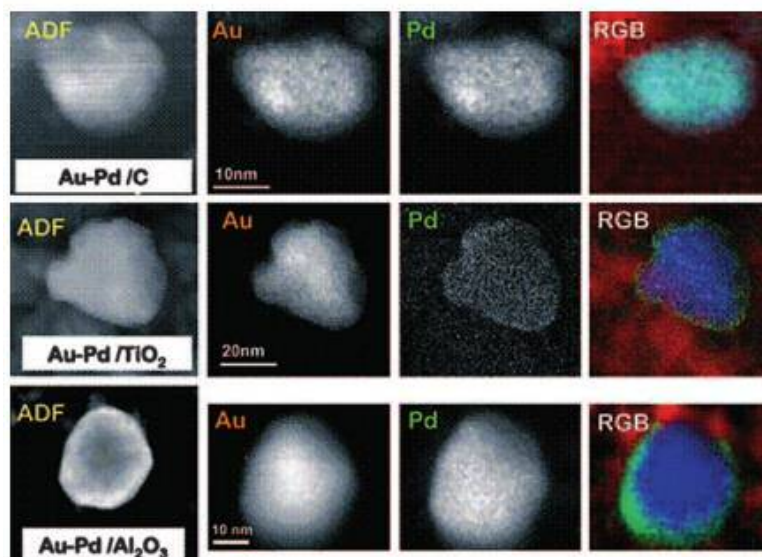


Figure 1.8 – Columns l-r: Montage of high-angle annular dark-field image, Au map, Pd map and RGB reconstructed overlay map (Au-blue, Pd-green). Rows t-b: calcined AuPd/C, calcined AuPd/TiO₂ and calcined AuPd/Al₂O₃.⁸³

Au-Pd catalysts prepared by impregnation show high activity for H₂O₂ synthesis, however catalysts with identical composition prepared by deposition precipitation (DP) show very low activity for H₂O₂ synthesis.⁷⁸ This is believed to be due to the size distribution of the metal nano-particles. Au-Pd/TiO₂ catalysts prepared by impregnation exhibit a bi-modal size distribution, with a mixture of small (2-10 nm) particles and much larger (>25 nm) particles. DP prepared catalysts however display a consistent small (<5 nm) particle size, which are believed to have very low activity for H₂O₂ synthesis.^{78, 83}

The reason for the synergistic nature of Au-Pd catalysts for H₂O₂ synthesis has been attributed to two effects. The first is the geometric/ensemble effect, where Au atoms break up continuous arrays of Pd atoms, which are believed to be active for the hydrogenation reaction.¹⁰⁰ The second is the ligand/electronic effect, where Au causes an increase in the filling of d-band in Pd via charge transfer. This increase in d-band filling raises the Pd d-band centre further above the Fermi level. As a result this causes a decrease in the strength of binding between Pd and the reactants and products, decreasing the extent of O-O cleavage, which increases selectivity.¹⁰¹

1.3.5. Other metals

Other supported metals have also exhibited activity for H_2O_2 in studies; Ru-Pd and Ru-Au alloys were shown to be active by Hutchings and co-workers, however they require high temperature ($>600^\circ\text{C}$) treatment to form stable catalysts, which decreases activity comparative to treatment at 400°C .¹⁰² Choudhary and co-workers found the addition of Ru to a 2.5 wt. % Pd/ ZrO_2 catalyst to decrease productivity. Similar results were found for the addition of Rh, both of which were attributed to increased decomposition and/or combustion activity. The addition of Pt was found to enhance activity, albeit not as effectively as the addition of Au.⁴⁷ Earlier studies by Choudhary which investigated Pd-Ag alloys in membrane type catalysts found that Ag containing alloys have very high decomposition activity, leading to very low productivities and selectivity towards H_2O_2 .³⁶

The use of Pt-Pd alloys has also been investigated by others, with Lunsford and co-workers reporting the addition of very small amounts of Pt (5 atom%) to a 0.5 wt. % Pd/ SiO_2 catalyst producing a 2.5 fold increase in activity of the catalyst.¹⁰³ Strukul and co-workers found that addition of Pt to a 2.5 wt. % Pd/C catalyst resulted in an increase in both activity and selectivity, with an optimum Pd/Pt ratio of 18.⁴⁹ In another study by Strukul, Pd-Pt coatings on membrane type catalyst were found to give significantly greater productivity than those with only Pd coatings.¹⁰⁴ A study by Biasi *et al.* reports a small decrease in productivity but a significant increase in selectivity from the addition of a modest amount of Pt (0.1 wt. %) to a 1 wt. % Pd catalyst. It was found that higher Pt loadings decreased activity, believed to be due to the poisoning of Pt sites by strong chemisorption of the formed H_2O_2 .¹⁰⁵ Hutchings and co-workers have also investigated Au-Pd-Pt tri-metallic catalysts, finding that addition of Pt to 1:1 Au:Pt catalyst formulations supported on ceria resulted in greater productivities and selectivities. A catalyst composition of 0.2 wt. % Pt 2.4 wt. % Au 2.4 wt. % Pd/ CeO_2 was found to be optimal, giving a productivity greater than double that of an AuPd analogue with equal metal loading. XPS analyses showed that samples containing Pt display a surface Pd/Au ratio far greater than those without, with Pd/Au increasing from 7.1 for 2.5 wt. % Pd 2.5 wt. % Au/ CeO_2 to 58 for 0.2 wt. % Pt 2.4 wt. % Au 2.4 wt. % Pd/ CeO_2 . This suggests that Pt addition encourages the formation of $\text{Au}_{\text{core}}\text{-PdO}_{\text{shell}}$ structures to a greater degree of metal segregation than what was observed previously for supported AuPd catalysts.^{5, 106}

In a recent paper in *Science*, Hutchings and co-workers detail a series of Pd-'base metal' bi-metallic catalysts with selectivities towards H_2O_2 greater than 95%. Sn, Ni, Ga, In, Co and Zn were all successfully utilised as a secondary metal (along with Pd) to result in highly selective and stable catalysts when a cycled oxidative-reductive-oxidative (ORO) heat treatment was applied. At the time of publication, Pd-Sn catalysts had been studied in the greatest detail. Through a combination of XPS, STEM and EELS analyses, it was hypothesised that the high degree of selectivity arose from a tin oxide layer covering small, unselective Pd particles, while larger selective Sn-Pd alloyed particles remained uncovered. A schematic diagram of this effect and STEM-EELS images are shown in Figure 1.9.¹⁰⁷ Further studies on these selective 'Pd-base metal' catalysts are detailed in Chapter 4 of this work.

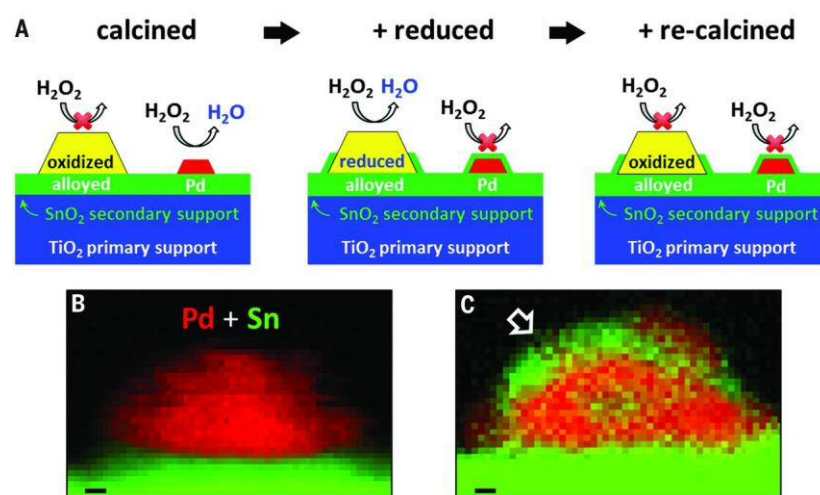


Figure 1.9 – (A) Hypothesised mechanism for limiting H_2O_2 hydrogenation by small Pd particles through encapsulation by SnO_x after an ORO cycle. This step prevents these NPs from decomposing and hydrogenating the H_2O_2 product. (B and C) STEM-EELS mapping of a 5 wt % Pd/ SnO_2 model catalyst at the oxidized (B) and ORO (C) stages, showing partial encapsulation of the Pd particle (red) by SnO_x (green) after the ORO heat treatment cycle. Scale bars: 1 nm.

1.3.6. Support effects

Hutchings and co-workers have studied the variation in the H_2O_2 synthesis activity of Au-Pd catalysts using different supports, it was found that the activity of the catalysts follows the trend carbon > SiO_2 > TiO_2 > Al_2O_3 > Fe_2O_3 .⁸¹ It was proposed that this trend was linked to the isoelectric point of the supports, with acidic supports (e.g. carbon and SiO_2) generally displaying greater activity than basic supports (e.g. MgO and Al_2O_3); this is shown in Figure 1.10.²⁵ It is reasoned that basic supports catalyse decomposition and hydrogenation reactions, leading to lower H_2O_2 selectivity and

productivity. A later investigation showed that H_2O_2 degradation pathways can be effectively 'switched off' by pre-treatment of carbon supports with dilute HNO_3 .⁸⁶ Similar results were observed by acid washing TiO_2 and SiO_2 , albeit to a lesser extent.^{85, 88} XPS and STEM analyses revealed that acid pre-treated catalysts showed a greater number of smaller Au-Pd alloy nanoparticles which 'decorate and inhibit' active sites for degradation on the carbon support.

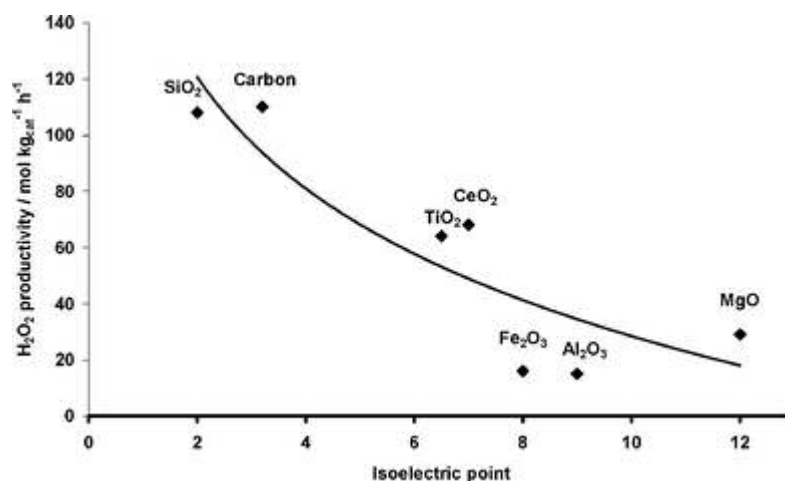


Figure 1.10 – The relationship between isoelectric point of the support and H_2O_2 productivity for supported 2.5 wt. % Au - 2.5 wt. % Pd nanoparticle catalysts.

As detailed in Section 1.3.3, a consistent finding over many studies by Song and co-workers in addition to those by Lee and co-workers and Salmi and co-workers was an increase in catalyst productivity and selectivity in line with increasing acidic nature of the support material. Many of these studies also reported an increase in supported metal dispersion, in line with that observed by Hutchings and co-workers. Song also proposed the positive effects of an acidic support were due to the support acting as an *in-situ* promoter, suppressing dissociation of H_2O_2 .^{59, 62-65, 76}

1.4. Reaction parameters in the direct synthesis of H_2O_2

1.4.1. Solvent

Some early studies⁷⁷ used supercritical CO_2 as a solvent due to the high solubility of the reactant gasses (H_2 and O_2), however high rates of decomposition necessitated the use of a different solvent system. The reactant gasses display good solubility in alcohols; data by Lunsford shows that the maximum dissolved hydrogen

concentration at 25°C is 3.96 mM in methanol, compared to 0.81 mM in H₂O.¹⁹ As such methanol and ethanol, sometimes as a mixture with H₂O, are very commonly used as solvents for H₂O₂ synthesis.^{15, 34}

Hutchings and co-workers found that 80-93 wt. % methanol in water was an optimum solvent for maximising rate of H₂O₂ synthesis and minimising hydrogenation under the group's commonly used reaction conditions. At lower methanol proportions synthesis activity is decreased due to a reduced concentration of dissolved hydrogen. Conversely at higher methanol proportions, a greater concentration of dissolved hydrogen leads to an increase in hydrogenation, therefore a decrease in yield.⁹⁸ However the majority of studies from this group have used a methanol and water mixture in an approximate 2:1 ratio, generally in the absence of acid or halides.^{5, 78, 94}

Lunsford and co-workers utilised a water or ethanol solvent with the addition of chloride, bromide, hydrochloric acid and sulphuric acid promoters.⁵³⁻⁵⁶ Choudhary and co-workers utilise H₂O acidified with sulphuric or phosphoric acid, in most cases with one or more halide promoter.³⁷⁻⁴⁶ Song and co-workers use a solution of methanol with dissolved NaBr.⁶²⁻⁷² Salmi and co-workers generally use methanol in the absence of promoters,^{58, 59, 61, 105, 108-110} but have also used acidified, bromide-promoted aqueous solutions.⁶⁰

There are limited studies on the aqueous direct synthesis of H₂O₂ in the absence of promoters. A study by Hutchings and co-workers contained testing data for a 2.5 wt. % Au 2.5 wt. % Pd/C catalyst at 2°C in a 2:1 methanol and water solvent mixture, 20°C in the same solvent mixture and 20°C in water. These data are displayed in Table 1.2.¹¹¹ From this data we can see there is a negative effect of both increasing temperature and using a water only solvent, however the magnitude of productivity decrease from changing the reaction solvent is significantly greater. These data suggest that the synthesis of significant concentrations of H₂O₂ in a water only solvent is a significant challenge.

Table 1.2 – Testing data for a 2.5 wt. % Au 2.5 wt. % Pd/C catalyst. Conditions: 5% H₂/CO₂ (2.9 MPa) and 25% O₂/CO₂ (1.1 MPa), 8.5 g solvent, 0.01 g catalyst, 1200 rpm stirring, 30 min reaction.¹¹¹

Temperature / °C	Solvent	Productivity /mol kg _{cat} ⁻¹ h ⁻¹	Degradation / mol kg _{cat} ⁻¹ h ⁻¹
2	2:1 MeOH/H ₂ O	110	117
20	2:1 MeOH/H ₂ O	98	352
20	H ₂ O	4	799

If the generation of H₂O₂ in aqueous solution without additives becomes viable, it would negate the necessity for the extraction of synthesised H₂O₂ from the anthraquinone process solvents. Furthermore, the removal of stabilisers (as with anthraquinone process produced H₂O₂) or promoters (as may be necessary for H₂O₂ produced by acid or halide promoted direct synthesis) would not be required. The ability to efficiently generate H₂O₂ in a water stream also presents opportunities for water cleaning technologies to be developed.

1.4.2. Acid and halide additives

Multiple studies have highlighted the promotional effect of H⁺ ions on H₂O₂ synthesis, primarily by inhibiting decomposition and hydrogenation.^{39, 40, 46, 53, 85} The addition of some form of H⁺ is commonly employed to achieve high productivity of H₂O₂ synthesis, especially with Pd catalysts. However high concentrations of acid must be avoided as this can lead to dissolution of the active metals from the catalyst, causing a decrease in activity and lack of re-usability.⁵⁶

The use of halides as promoters for the synthesis of H₂O₂ is widely reported and utilised by many groups. It is believed that halides act to stabilise the O-O bond, which affects the reaction in 3 ways. Molecular O₂ dissociates to a lesser extent, reducing the rate of combustion, therefore increasing selectivity. Surface OOH intermediate species are stabilised, which serves to increase the rate of synthesis. Finally synthesised H₂O₂ is dissociated to a lesser extent, which reduces the rate of degradation and therefore increases selectivity. The combined effect of these processes is an increase in H₂O₂ yield.^{42, 43, 56, 62, 92}

It was noted by Pospelova in 1961 that the addition of halo-acids significantly increased H₂O₂ synthesis activity of Pd based catalysts.¹¹² More recent work by

Choudhary and co-workers which investigated the effect of many different acids on H_2O_2 synthesis reactions found that addition of halo-acids of Cl^- , Br^- and I^- decrease decomposition and hydrogenation reactions, whilst slightly decreasing conversion. Conversely oxo-acids had a lesser effect on the selectivity of the reaction. Thus it was shown that halides also play a role in suppressing the combustion and hydrogenation reactions³⁸. Whilst halides can be added in the form of metal salts, this study shows that a combination of halides and acids (as provided by using halo-acids) leads to the greatest increase in H_2O_2 synthesis productivity.

Choudhary suggested the increase in selectivity from halides is due to site blocking, which at low concentrations breaks up large Pd arrays which are active for hydrogenation/decomposition. There is however an optimum concentration of halide in the reaction solution, above which productivity will decrease due to indiscriminate site blocking causing a decrease in the activity of the catalyst for the desired synthesis reaction as well as degradation.⁴¹ Halides can also be incorporated into the catalysts themselves during preparation as a means of selective poisoning. This again sees an increase in selectivity of the catalysts when Cl^- , Br^- and I^- are used, with Br^- proving the most effective promoter,⁴⁵ however F^- was shown to act as a promoter of undesired side reactions.⁴³

The mechanism(s) through which acid addition decreases degradation and increases yield are not agreed upon. Early studies by Pospelova and co-workers^{112, 113} showed that acid promoters were necessary to achieve high yields with supported Pd catalysts, with the rationale that the decomposition pathway is base-catalysed, thus acid addition mitigates degradation via decomposition. Choudhary and co-workers showed that non-halide acids give a moderate decrease in degradation in reactions using a Pd/C catalyst and thus an increase in yield, however leaching of Pd was observed at concentrations above 0.05 M H_2SO_4 or 0.3 M H_3PO_4 .³⁷

Lunsford and co-workers showed that in an ethanol solvent, no H_2O_2 is produced with use of a Pd/ SiO_2 catalyst in the absence of acid promoters, but significant yields are produced above 1 M H_2SO_4 . It is argued that base catalysed degradation and the abatement of such is only a minor factor in the promotion effect seen from acid addition. Lunsford states that in the aforementioned reaction in the absence of acidic promoters, H_2 is consumed through combustion, but no H_2O_2 is produced. Acid addition vastly reduces the extent of combustion and allows for the synthesis of H_2O_2 . Lunsford states that the exact role of protons is unclear, but that they play “a very

positive but largely indirect role” in the direct synthesis reaction, possibly due to influencing the electronic state of surface palladium atoms on the catalyst.⁵⁶

As detailed in Section 1.3.2 both Strukul and co-workers²⁰ and Flaherty and co-workers³² have proposed mechanisms in which protons are directly involved in the fundamental reaction processes. As protons are directly involved in the synthesis of H₂O₂ in Strukul and Flaherty’s proposed mechanisms, it follows that a decrease in pH, *i.e.* an increase in the concentration of protons in solution, will increase the rate of synthesis and thus achieve a greater yield of H₂O₂.

1.4.3. Gas feed diluent

A diluent in the gas feed is commonly used to remain outside the explosive regime which exists between 4 vol. % and 94 vol. % H₂ in O₂. The two most commonly used diluent gasses are N₂ and CO₂. N₂ is used because it is completely inert under the conditions of the direct synthesis of H₂O₂ and is cheap and abundant. Furthermore, if an implementation of the direct synthesis of H₂O₂ is to use a gas feed of H₂ generated from the electrolytic or photo-catalytic splitting of water combined with air, as is envisioned by some, N₂ becomes the gas feed diluent by default.⁷

A CO₂ gas feed diluent was used by Hutchings and co-workers, initially because this slightly narrows the explosive regime, allowing for an increased concentration of H₂ to be used safely. However, it was soon realised that if water is present in the solvent, CO₂ will form carbonic acid, which acts as an *in-situ* promoter. This promotional effect is significant, and as such many groups use CO₂ as a diluent to enhance the productivity of the reaction.^{5, 35}

1.4.4. Temperature

The Gibbs free energy and enthalpy of the processes involved in the direct synthesis of H₂O₂ were presented in Figure 1.4 in Section 1.3.1. From the Figures presented there, it can be observed that the entropy change for the synthesis reaction is negative, whereas the entropy change for both the hydrogenation and decomposition reactions are positive. Therefore, a decrease in temperature serves to decrease the Gibbs free energy for the synthesis reaction and increase the Gibbs free energy for the undesired hydrogenation and decomposition reactions.

It has been observed experimentally that decreasing the temperature at which the direct synthesis process is performed has a greater suppression effect on the hydrogenation and decomposition reactions than the synthesis reaction.^{5, 7} In addition, decreased temperature raises the solubility of CO₂ in methanol, which increases H₂ solubility in the mixture. Therefore in cases where a CO₂ diluent gas and methanol containing solvent are used, decreasing temperature increases the concentration of reactant H₂.

Due to these factors, the direct synthesis of hydrogen peroxide is generally performed at room/ambient or sub-ambient temperatures. Choudhary and co-workers,^{37-40, 42, 44, 45, 47} Strukul and co-workers^{20, 48, 49, 104, 114, 115} and Song and co-workers⁶²⁻⁷² have all used exclusively ambient temperature reactions in their studies. Lunsford and co-workers have generally used a temperature of 10°C,^{52-55, 57, 103} Hutchings and co-workers regularly use a temperature of 2°C^{25, 77-90, 92, 93, 95-97, 102, 106} and Salmi and co-workers have used a range of temperatures from ambient to -10°C.^{58, 59, 61, 105, 108-110, 116}

Salmi and co-workers produced a study in which temperatures in the range of 5-35°C were tested for the direct synthesis of H₂O₂ in a continuous trickle bed reactor. Using a Pd/C catalyst, various masses and catalyst bed concentrations were tested at a liquid (NaBr and H₃PO₄ promoted H₂O) flow rate of 1 ml/min and a gas flow rate of 4 ml/min at 5, 15, 25 and 35°C. The consistent finding across all catalyst masses/concentrations was a decrease in the rate of H₂O₂ production as temperature increased, with a decrease in production rate of 15 - 30% for reactions performed at 35°C relative to those performed at 5°C.⁶⁰

Hutchings and co-workers have also studied the effect of temperature for the direct synthesis of H₂O₂ in a batch reactor using a 2.5 wt. % Au 2.5 wt. % Pd catalyst and a 2:1 methanol-water solvent. This study found a more pronounced negative effect of increased temperature, with the rate of H₂O₂ synthesis at 22°C falling approximately 50% relative to the rate at 2°C.⁹⁴

While there is agreement in the literature about the beneficial effect of decreased temperature in the direct synthesis of H₂O₂, cooling to sub-ambient temperatures requires an energy input. Furthermore, in processes which use a solvent composition with a high proportion of water, problems due to freezing of the solvent may be encountered with excessive cooling. Therefore the operation of this process

at ambient temperature represents the most economic, green and practical condition.

1.5. Reactor types for the direct synthesis of H₂O₂

1.5.1. Batch

The reactor type which has been predominately used in studies of the direct synthesis of H₂O₂ is a batch autoclave reactor. Reactors in this style range from glass reactors operated at atmospheric pressure like those used by Lunsford and co-workers and Choudhary and co-workers to stainless steel autoclaves operated at pressures of up to 40 bar, as used by Hutchings and co-workers and Song and co-workers. The method of introducing reactant gasses can also differ slightly, with Lunsford, Choudhary and Song generally favouring the method of passing a gas stream through the catalyst/solvent mixture, whereas Hutchings uses a method of charging the reactor with reactant gasses once at the beginning of the reaction.^{37, 51, 62, 78}

In a batch reactor, the catalyst is placed in the reactor with the solvent and sealed. Performing experiments with short residence time is not usually feasible, therefore there is necessarily a long contact time between the catalyst and both reactants and products. As batch reactor tests only allow for measurement of H₂O₂ concentration at a certain reaction time, it is difficult to measure the absolute rate of H₂O₂ synthesis as the contribution of all reaction pathways detailed in Section 1.3.1 cannot easily be separated. Therefore any measured rate is an observed rate, k_{obs} , to which the synthesis, hydrogenation and decomposition pathways all contribute; furthermore, any measure of H₂ conversion must also account for the combustion of H₂.

1.5.2. Membrane

Mixtures of H₂ and O₂ are explosive between the limits of 4% and 94% H₂ in O₂ by volume at room temperature.⁵ As such, most studies use a diluted gas mixture in the non-flammable regime to reduce the potential hazards of the direct synthesis process. However, the addition of a diluent increase mass transport limitations and thereby reduces reaction rates.³⁴

Some studies have used a membrane style reactor, which allows the majority of reactant H₂ and O₂ to be separated, with only a very small fraction coming into contact at the catalyst active site. This allows for high concentration or pure feeds of reactant

gasses to be used. Many differing reactor designs have been used, however the basic premise remains the same. H_2 and O_2 are fed to opposite sides of a porous membrane catalyst with a pore size through which reactant flux is very low. All of the H_2 which is able to pass into the pores is dissociated at the active site, where it reacts with adsorbed O_2 to form H_2O_2 without any significant mixing of H_2 and O_2 . An example of a catalytic membrane contact style reactor is illustrated in Figure 1.11. Membrane catalysts broadly fall into two categories, those coated in a single layer of Pd or an alloy such as Pd-Ag (which serves to improve mechanical stability), or those decorated with Pd or Pd-M bi-metallic nanoparticles. Despite the ability to use high concentration reactant gasses, the diffusion of the reactants to the active site can be slow, as such the productivity of these systems have not significantly outperformed supported metal catalysts in batch reactors. A challenge for membrane catalyst systems is the design of a robust membrane that does not suffer from loss of surface active metal which also exhibits high diffusion rates.^{20, 34, 36, 48, 49, 104, 117-120}

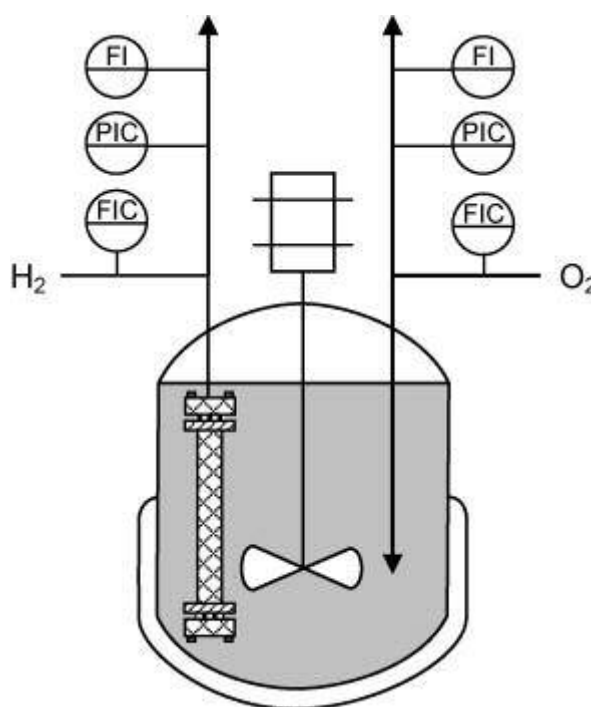


Figure 1.11 – Schematic representation of catalytic membrane contactor style reactor.¹¹⁷

1.5.3. Flow

Flow reactors operate via the pumping of solvent and reactant gasses through a catalyst bed. As flow rates and volumes can be altered, this allows for control of the contact time between reactants and the catalyst. Through reducing contact time,

subsequent decomposition and hydrogenation reactions can theoretically be suppressed, as the synthesised H_2O_2 is in contact with the catalyst for less time therefore is statistically less likely to undergo cleavage and degradation. Flow reactor systems which have been implemented in past studies have included <1 mm diameter micro-reactors which are efficiently packed to eliminate void space, allowing for high concentration reactant gasses as bulk mixing is avoided. This style of reactor has displayed high productivities with supported Pd catalysts, however they have low throughputs and are expensive and difficult to construct and pack with catalyst.^{22, 109, 121}

Larger fixed bed reactors in which flows of gas and liquid are passed through a secured mass of powdered or pelletized catalyst are used ubiquitously in the chemical industry, especially in petrochemicals. They can be constructed and operated fairly easily and allow for good mass transfer of the reactants to the active site. A flow system, especially fixed bed, therefore represents the most practically desirable implementation of the direct synthesis of H_2O_2 , allowing for continuous operation, recycling of unreacted gasses to increase conversion and the potential for high throughputs.^{35, 99, 122} The efficient direct synthesis of H_2O_2 in water in a flow system would also be a very attractive process for potential water cleaning technologies.

1.6. Thesis aims

This project aims to design and fully test catalysts which are active for the synthesis of hydrogen peroxide in water at ambient temperature. Proposed applications which have been identified for this technology include on-site generation of H_2O_2 in tap water streams, with potential for *in-situ* cleaning of waste water streams. As such the catalysts will be required to be robust to poisoning by a range of common tap water ions, including sodium, calcium and carbonate, and also should display tolerance to differing pH levels which may occur in waste streams. The catalysts must be active in a pure water solvent system as there can be no addition of alternative solvents (such as methanol or ethanol) or additives such as halides or acids, which are known to be beneficial to the reaction. The catalysts must be active using dilute H_2 in air gas streams, both so the explosive $\text{H}_2\text{-O}_2$ regime is avoided and so the system could potentially be practically implemented in-line with an electrolyser for the generation of hydrogen.

Therefore, initially this project will fully study the effects of reaction conditions with the aim of moving to the conditions outlined above from the conditions that have been extensively used by the Hutchings group in the past.⁷⁸ This will include the effect of solvent, temperature, reaction time, diluent gas, total reactant gas pressure, solution pH and the presence of a range of ions.

Secondly this project aims to develop catalysts which are highly active and selective for the direct synthesis of H_2O_2 under these conditions. The findings from the first part of the study will be considered so the challenges presented by the given conditions can be addressed. Ideally, design will result in a catalyst or a series of catalysts which are active, selective and composed of metals which are abundant and not subject to supply constraints or large price swings due to such.

Finally, the catalysts which have been designed will be implemented in a fixed bed flow reactor with conditions close to those which would be necessary for practical implementation. This will include use of a dilute H_2 in air gas supply in a water solvent and the addition of common tap water ions.

1.7. References

1. J. J. Berzelius, *Edinburgh New Philosophical Journal*, 1836, XXI, 223.
2. M. Boudart, B. H. Davis and H. Heinemann, in *Handbook of Heterogeneous Catalysis*, Wiley-VCH Verlag GmbH, 2008, DOI: 10.1002/9783527619474.ch1, pp. 1-48.
3. V. Smil, *Nature*, 1999, 400, 415-415.
4. H. M. Smith, in *Torchbearers of Chemistry*, Academic Press, 1949, DOI: <http://dx.doi.org/10.1016/B978-1-4831-9805-7.50233-4>, p. 237.
5. J. K. Edwards and G. J. Hutchings, *Angewandte Chemie*, 2008, 47, 9192-9198.
6. R. Hage and A. Lienke, *Angewandte Chemie International Edition*, 2006, 45, 175-175.
7. C. Samanta, *Applied Catalysis A: General*, 2008, 350, 133-149.
8. J. M. Campos-Martin, G. Blanco-Brieva and J. L. Fierro, *Angewandte Chemie*, 2006, 45, 6962-6984.
9. E. Neyens and J. Baeyens, *Journal of hazardous materials*, 2003, 98, 33-50.
10. A. R. Yeddou, S. Chergui, A. Chergui, F. Halet, A. Hamza, B. Nadjemi, A. Ould-Dris and J. Belkouch, *Minerals Engineering*, 2011, 24, 788-793.
11. J. Sudhakar Reddy, S. Sivasanker and P. Ratnasamy, *Journal of Molecular Catalysis*, 1991, 69, 383-392.
12. D. J. Robinson, L. Davies, N. McGuire, D. F. Lee, P. McMorn, D. J. Willock, G. W. Watson, P. C. Bulman Page, D. Bethell and G. J. Hutchings, *Physical Chemistry Chemical Physics*, 2000, 2, 1523-1529.
13. G. Blanco-Brieva, M. C. Capel-Sanchez, M. P. de Frutos, A. Padilla-Polo, J. M. Campos-Martin and J. L. G. Fierro, *Industrial & Engineering Chemistry Research*, 2008, 47, 8011-8015.
14. T. A. Nijhuis, M. Makkee, J. A. Moulijn and B. M. Weckhuysen, *Industrial & Engineering Chemistry Research*, 2006, 45, 3447-3459.
15. Y. H. Yi, L. Wang, G. Li and H. C. Guo, *Catalysis Science & Technology*, 2016, 6, 1593-1610.
16. J. H. Clark and C. W. Jones, in *Applications of Peroxide and Derivatives*, RSC, 1999, DOI: 10.1039/9781847550132-00001, pp. 1-36.
17. A. S. Hashmi and G. J. Hutchings, *Angewandte Chemie*, 2006, 45, 7896-7936.
18. R. Burch and P. R. Ellis, *Applied Catalysis B: Environmental*, 2003, 42, 203-211.
19. J. Lunsford, *Journal of Catalysis*, 2003, 216, 455-460.
20. S. Abate, G. Centi, S. Melada, S. Perathoner, F. Pinna and G. Strukul, *Catalysis Today*, 2005, 104, 323-328.
21. B. Zhou and L. K. Lee, U.S. Patent 6,919,065 B2, 2005.
22. Y. Voloshin, R. Halder and A. Lawal, *Catalysis Today*, 2007, 125, 40-47.
23. Y. Voloshin, J. Manganaro and A. Lawal, *Industrial & Engineering Chemistry Research*, 2008, 47, 8119-8125.
24. Y. Voloshin and A. Lawal, *Appl. Catal. A-Gen.*, 2009, 353, 9-16.
25. E. Ntainjua N, J. K. Edwards, A. F. Carley, J. A. Lopez-Sanchez, J. A. Moulijn, A. A. Herzing, C. J. Kiely and G. J. Hutchings, *Green Chemistry*, 2008, 10, 1162.
26. T. Deguchi and M. Iwamoto, *Journal of Catalysis*, 2011, 280, 239-246.
27. T. Deguchi, H. Yamano and M. Iwamoto, *Catalysis Today*, 2015, 248, 80-90.
28. T. Deguchi and M. Iwamoto, *The Journal of Physical Chemistry C*, 2013, DOI: 10.1021/jp4056297, 130828083551006.

29. L. Grabow, B. Hvolbæk, H. Falsig and J. Nørskov, *Topics in Catalysis*, 2012, 55, 336-344.
30. F. Wang, D. Zhang, H. Sun and Y. Ding, *Journal of Physical Chemistry C*, 2007, 111, 11590-11597.
31. J. Li and K. Yoshizawa, *Catalysis Today*, 2015, 248, 142-148.
32. N. M. Wilson and D. W. Flaherty, *Journal of the American Chemical Society*, 2016, 138, 574-586.
33. H. Henkel and W. Weber, *US Patent 1,108,752*, 1914.
34. R. Dittmeyer, J. D. Grunwaldt and A. Pashkova, *Catalysis Today*, 2015, 248, 149-159.
35. J. K. Edwards, S. J. Freakley, R. J. Lewis, J. C. Pritchard and G. J. Hutchings, *Catalysis Today*, 2015, 248, 3-9.
36. V. R. Choudhary, A. G. Gaikwad and S. D. Sansare, *Angewandte Chemie - International Edition*, 2001, 40, 1776-1779.
37. V. Choudhary and C. Samanta, *Journal of Catalysis*, 2006, 238, 28-38.
38. V. R. Choudhary, C. Samanta and T. V. Choudhary, *Journal of Molecular Catalysis A: Chemical*, 2006, 260, 115-120.
39. V. Choudhary and P. Jana, *Journal of Catalysis*, 2007, 246, 434-439.
40. V. R. Choudhary, C. Samanta and P. Jana, *Applied Catalysis A: General*, 2007, 317, 234-243.
41. V. R. Choudhary, C. Samanta and P. Jana, *Industrial and Engineering Chemistry Research*, 2007, 46, 3237-3242.
42. C. Samanta and V. R. Choudhary, *Catalysis Communications*, 2007, 8, 2222-2228.
43. C. Samanta and V. R. Choudhary, *Chemical Engineering Journal*, 2008, 136, 126-132.
44. V. R. Choudhary, A. G. Gaikwad and S. D. Sansare, *Catalysis Letters*, 2002, 83, 235-239.
45. V. R. Choudhary, C. Samanta and A. G. Gaikwad, *Chemical Communications*, 2004, 10, 2054-2055.
46. V. R. Choudhary and P. Jana, *Applied Catalysis A: General*, 2009, 352, 35-42.
47. V. R. Choudhary, C. Samanta and T. V. Choudhary, *Applied Catalysis A: General*, 2006, 308, 128-133.
48. S. Melada, F. Pinna, G. Strukul, S. Perathoner and G. Centi, *Journal of Catalysis*, 2005, 235, 241-248.
49. S. Melada, F. Pinna, G. Strukul, S. Perathoner and G. Centi, *Journal of Catalysis*, 2006, 237, 213-219.
50. D. P. Dissanayake and J. H. Lunsford, *Journal of Catalysis*, 2002, 206, 173-176.
51. D. P. Dissanayake and J. H. Lunsford, *Journal of Catalysis*, 2003, 214, 113-120.
52. S. Chinta and J. H. Lunsford, *Journal of Catalysis*, 2004, 225, 249-255.
53. Y. Han and J. Lunsford, *Journal of Catalysis*, 2005, 230, 313-316.
54. Y. F. Han and J. H. Lunsford, *Catalysis Letters*, 2005, 99, 13-19.
55. Q. Liu and J. Lunsford, *Journal of Catalysis*, 2006, 239, 237-243.
56. Q. Liu and J. H. Lunsford, *Applied Catalysis A: General*, 2006, 314, 94-100.
57. Q. Liu, J. C. Bauer, R. E. Schaak and J. H. Lunsford, *Angewandte Chemie*, 2008, 47, 6221-6224.
58. P. Biasi, F. Menegazzo, F. Pinna, K. Eränen, P. Canu and T. O. Salmi, *Industrial and Engineering Chemistry Research*, 2010, 49, 10627-10632.
59. P. Biasi, P. Canu, F. Menegazzo, F. Pinna and T. O. Salmi, *Industrial & Engineering Chemistry Research*, 2012, 51, 8883-8890.

60. P. Biasi, J. García-Serna, A. Bittante and T. Salmi, *Green Chemistry*, 2013, 15, 2502.
61. P. Biasi, F. Menegazzo, P. Canu, F. Pinna and T. O. Salmi, *Industrial & Engineering Chemistry Research*, 2013, DOI: 10.1021/ie4011782, 130916123939006.
62. S. Park, J. C. Jung, J. G. Seo, T. J. Kim, Y.-M. Chung, S.-H. Oh and I. K. Song, *Catalysis Letters*, 2009, 130, 604-607.
63. S. Park, T. J. Kim, Y.-M. Chung, S.-H. Oh and I. K. Song, *Catalysis Letters*, 2009, 130, 296-300.
64. S. Park, J. G. Seo, J. C. Jung, S.-H. Baeck, T. J. Kim, Y.-M. Chung, S.-H. Oh and I. K. Song, *Catalysis Communications*, 2009, 10, 1762-1765.
65. S. Park, S.-H. Baeck, T. J. Kim, Y.-M. Chung, S.-H. Oh and I. K. Song, *Journal of Molecular Catalysis A: Chemical*, 2010, 319, 98-107.
66. S. Park, J. Lee, J. H. Song, T. J. Kim, Y.-M. Chung, S.-H. Oh and I. K. Song, *Journal of Molecular Catalysis A: Chemical*, 2012, 363-364, 230-236.
67. S. Park, S. Lee, S. Song, D. Park, S. Baeck, T. Kim, Y. Chung, S. Oh and I. Song, *Catalysis Communications*, 2009, 10, 391-394.
68. S. Park, T. J. Kim, Y.-M. Chung, S.-H. Oh and I. K. Song, *Research on Chemical Intermediates*, 2010, 36, 639-646.
69. S. Park, D. R. Park, J. H. Choi, T. J. Kim, Y.-M. Chung, S.-H. Oh and I. K. Song, *Journal of Molecular Catalysis A: Chemical*, 2010, 332, 76-83.
70. S. Park, D. R. Park, J. H. Choi, T. J. Kim, Y.-M. Chung, S.-H. Oh and I. K. Song, *Journal of Molecular Catalysis A: Chemical*, 2011, 336, 78-86.
71. S. Park, J. H. Choi, T. J. Kim, Y.-M. Chung, S.-H. Oh and I. K. Song, *Catalysis Today*, 2012, 185, 162-167.
72. S. Park, J. H. Choi, T. J. Kim, Y.-M. Chung, S.-H. Oh and I. K. Song, *Journal of Molecular Catalysis A: Chemical*, 2012, 353-354, 37-43.
73. H. Lee, S. Kim, D.-W. Lee and K.-Y. Lee, *Catalysis Communications*, 2011, 12, 968-971.
74. S. Kim, D.-W. Lee, K.-Y. Lee and E. A. Cho, *Catalysis Letters*, 2014, 144, 905-911.
75. M. G. Seo, S. Kim, H. E. Jeong, D. W. Lee and K. Y. Lee, *J. Mol. Catal. A-Chem.*, 2016, 413, 1-6.
76. M. G. Seo, S. Kim, D. W. Lee, H. E. Jeong and K. Y. Lee, *Appl. Catal. A-Gen.*, 2016, 511, 87-94.
77. P. Landon, P. J. Collier, A. F. Carley, D. Chadwick, A. J. Papworth, A. Burrows, C. J. Kiely and G. J. Hutchings, *Physical Chemistry Chemical Physics*, 2003, 5, 1917-1923.
78. J. Edwards, B. Solsona, P. Landon, A. Carley, A. Herzing, C. Kiely and G. Hutchings, *Journal of Catalysis*, 2005, 236, 69-79.
79. J. K. Edwards, B. Solsona, P. Landon, A. F. Carley, A. Herzing, M. Watanabe, C. J. Kiely and G. J. Hutchings, *Journal of Materials Chemistry*, 2005, 15, 4595.
80. B. E. Solsona, J. K. Edwards, P. Landon, A. F. Carley, A. Herzing, C. J. Kiely and G. J. Hutchings, *Chemistry of Materials*, 2006, 18, 2689-2695.
81. J. K. Edwards, A. Thomas, B. E. Solsona, P. Landon, A. F. Carley and G. J. Hutchings, *Catalysis Today*, 2007, 122, 397-402.
82. G. Li, J. Edwards, A. F. Carley and G. J. Hutchings, *Catalysis Today*, 2007, 122, 361-364.
83. J. K. Edwards, A. F. Carley, A. A. Herzing, C. J. Kiely and G. J. Hutchings, *Faraday Discussions*, 2008, 138, 225.
84. J. K. Edwards, A. Thomas, A. F. Carley, A. A. Herzing, C. J. Kiely and G. J. Hutchings, *Green Chemistry*, 2008, 10, 388.

85. J. K. Edwards, E. Ntainjua, A. F. Carley, A. A. Herzing, C. J. Kiely and G. J. Hutchings, *Angewandte Chemie*, 2009, 48, 8512-8515.
86. J. K. Edwards, B. Solsona, E. N. N, A. F. Carley, A. A. Herzing, C. J. Kiely and G. J. Hutchings, *Science*, 2009, 323, 1037-1041.
87. E. N. Ntainjua, M. Piccinini, J. C. Pritchard, J. K. Edwards, A. F. Carley, C. J. Kiely and G. J. Hutchings, *Catalysis Today*, 2011, 178, 47-50.
88. J. K. Edwards, S. F. Parker, J. Pritchard, M. Piccinini, S. J. Freakley, Q. He, A. F. Carley, C. J. Kiely and G. J. Hutchings, *Catalysis Science & Technology*, 2013, 3, 812.
89. P. Landon, P. J. Collier, A. J. Papworth, C. J. Kiely and G. J. Hutchings, *Chemical Communications*, 2002, DOI: 10.1039/b205248m, 2058-2059.
90. G. Li, J. Edwards, A. F. Carley and G. J. Hutchings, *Catalysis Communications*, 2007, 8, 247-250.
91. J. A. Lopez-Sanchez, N. Dimitratos, P. Miedziak, E. Ntainjua, J. K. Edwards, D. Morgan, A. F. Carley, R. Tiruvalam, C. J. Kiely and G. J. Hutchings, *Physical Chemistry Chemical Physics*, 2008, 10, 1921-1930.
92. N. E. Ntainjua, M. Piccinini, J. C. Pritchard, J. K. Edwards, A. F. Carley, J. A. Moulijn and G. J. Hutchings, *ChemSusChem*, 2009, 2, 575-580.
93. E. Ntainjua, M. Piccinini, J. C. Pritchard, Q. He, J. K. Edwards, A. F. Carley, J. A. Moulijn, C. J. Kiely and G. J. Hutchings, *ChemCatChem*, 2009, 1, 479-484.
94. M. Piccinini, E. Ntainjua, J. K. Edwards, A. F. Carley, J. A. Moulijn and G. J. Hutchings, *Physical chemistry chemical physics : PCCP*, 2010, 12, 2488-2492.
95. J. C. Pritchard, Q. He, E. N. Ntainjua, M. Piccinini, J. K. Edwards, A. A. Herzing, A. F. Carley, J. A. Moulijn, C. J. Kiely and G. J. Hutchings, *Green Chemistry*, 2010, 12, 915.
96. J. K. Edwards, J. Pritchard, M. Piccinini, G. Shaw, Q. He, A. F. Carley, C. J. Kiely and G. J. Hutchings, *Journal of Catalysis*, 2012, 292, 227-238.
97. E. N. Ntainjua, M. Piccinini, S. J. Freakley, J. C. Pritchard, J. K. Edwards, A. F. Carley and G. J. Hutchings, *Green Chemistry*, 2012, 14, 170.
98. M. Piccinini, J. K. Edwards, J. A. Moulijn and G. J. Hutchings, *Catalysis Science & Technology*, 2012, 2, 1908.
99. S. J. Freakley, M. Piccinini, J. K. Edwards, E. N. Ntainjua, J. A. Moulijn and G. J. Hutchings, *ACS Catalysis*, 2013, 3, 487-501.
100. L. Ouyang, G.-j. Da, P.-f. Tian, T.-y. Chen, G.-d. Liang, J. Xu and Y.-F. Han, *Journal of Catalysis*, 2014, 311, 129-136.
101. F. Gao and D. W. Goodman, *Chemical Society reviews*, 2012, 41, 8009-8020.
102. E. N. Ntainjua, S. J. Freakley and G. J. Hutchings, *Topics in Catalysis*, 2012, 55, 718-722.
103. Q. Liu, J. C. Bauer, R. E. Schaak and J. H. Lunsford, *Applied Catalysis A: General*, 2008, 339, 130-136.
104. S. Abate, S. Melada, G. Centi, S. Perathoner, F. Pinna and G. Strukul, *Catalysis Today*, 2006, 117, 193-198.
105. S. Sterchele, P. Biasi, P. Centomo, P. Canton, S. Campestrini, T. Salmi and M. Zecca, *Applied Catalysis A: General*, 2013, 468, 160-174.
106. J. K. Edwards, J. Pritchard, L. Lu, M. Piccinini, G. Shaw, A. F. Carley, D. J. Morgan, C. J. Kiely and G. J. Hutchings, *Angewandte Chemie*, 2014, 53, 2381-2384.
107. S. J. Freakley, Q. He, J. H. Harrhy, L. Lu, D. A. Crole, D. J. Morgan, E. N. Ntainjua, J. K. Edwards, A. F. Carley, A. Y. Borisevich, C. J. Kiely and G. J. Hutchings, *Science*, 2016, 351, 965-968.

108. D. Gudarzi, O. A. Simakova, J. R. Hernández Carucci, P. D. Biasi, K. Eränen, E. Kolehmainen, I. Turunen, D. Y. Murzin and T. Salmi, *Chemical Engineering Transactions*, 2010, 21, 925-930.
109. P. Biasi, S. Zancanella, F. Pinna, P. Canu and T. O. Salmi, *Chemical Engineering Transactions*, 2011, 24, 49-54.
110. N. Gemo, P. Biasi, P. Canu and T. O. Salmi, *Chemical Engineering Journal*, 2012, 207-208, 539-551.
111. S. J. Freakley, R. J. Lewis, D. J. Morgan, J. K. Edwards and G. J. Hutchings, *Catalysis Today*, 2015, 248, 10-17.
112. T. A. Pospelova, N. I. Kobozev and E. N. Eremin, *Zhurnal Fiz. Khimii*, 1961, 35, 298-305.
113. T. A. Pospelova and N. I. Kobozev, *Zhurnal Fiz. Khimii*, 1961, 35, 535-542.
114. S. Melada, R. Rioda, F. Menegazzo, F. Pinna and G. Strukul, *Journal of Catalysis*, 2006, 239, 422-430.
115. F. Menegazzo, M. Signoretto, M. Manzoli, F. Boccuzzi, G. Cruciani, F. Pinna and G. Strukul, *Journal of Catalysis*, 2009, 268, 122-130.
116. P. Biasi, F. Menegazzo, F. Pinna, K. Eranen, T. O. Salmi and P. Canu, *Chemical Engineering Journal*, 2011, 176, 172-177.
117. A. Pashkova, K. Svajda and R. Dittmeyer, *Chemical Engineering Journal*, 2008, 139, 165-171.
118. T. Inoue, Y. Tanaka, D. A. P. Tanaka, T. M. Suzuki, K. Sato, M. Nishioka, S. Hamakawa and F. Mizukami, *Chemical Engineering Science*, 2010, 65, 436-440.
119. A. Pashkova, R. Dittmeyer, N. Kaltenborn and H. Richter, *Chemical Engineering Journal*, 2010, 165, 924-933.
120. M. Selinsek, M. Bohrer, B. K. Vankayala, K. Haas-Santo, M. Kraut and R. Dittmeyer, *Catalysis Today*, 2016, 268, 85-94.
121. T. Inoue, J. Adachi, K. Ohtaki, M. Lu, S. Murakami, X. Sun and D. F. Wang, *Chemical Engineering Journal*, 2015, 278, 517-526.
122. J. García-Serna, T. Moreno, P. Biasi, M. J. Cocero, J.-P. Mikkola and T. O. Salmi, *Green Chemistry*, 2014, DOI: 10.1039/c3gc41600c.

2. EXPERIMENTAL

This chapter outlines the experimental procedures which were followed for the catalyst preparation, testing and characterisation which is discussed herein.

2.1. Materials and Reagents

PdCl_2 – Johnson Matthey (99.99% trace metal basis)

$\text{Pd}(\text{NO}_3)_2$ – Johnson Matthey (99.99% trace metal basis)

HAuCl_4 – Johnson Matthey (99.99% trace metal basis)

H_2PtCl_6 – Johnson Matthey (99.99% trace metal basis)

RhCl_3 – Sigma Aldrich (99.98% trace metal basis)

NiCl_2 – Sigma Aldrich (99.99% trace metal basis)

$\text{Ni}(\text{NO}_3)_2$ – Sigma Aldrich (99.999% trace metal basis)

GaCl_3 – Sigma Aldrich (99.999% trace metal basis)

$\text{Ga}(\text{NO}_3)_3$ – Sigma Aldrich (99.9% trace metal basis)

$\text{In}(\text{NO}_3)_3$ – Sigma Aldrich (99.99% trace metal basis)

$\text{Co}(\text{NO}_3)_2$ – Sigma Aldrich (ACS Reagent, >98%)

$\text{Zn}(\text{NO}_3)_2$ – Sigma Aldrich (ACS Reagent, >98%)

AgNO_3 – Sigma Aldrich (ACS Reagent, >99%)

$\text{Fe}(\text{NO}_3)_3$ – Sigma Aldrich (ACS Reagent, >98%)

$\text{Cu}(\text{NO}_3)_2$ – Sigma Aldrich (ACS Reagent, >98%)

$\text{Al}(\text{NO}_3)_3$ – Sigma Aldrich (ACS Reagent, >98%)

$\text{Ru}(\text{NO})(\text{NO}_3)_3$ – Sigma Aldrich (1.5% Ru in solution)

TiO_2 – Degussa p25 (99.5% trace metal basis, 20-30 nm particle size)

SiO_2 – Fisher Scientific (Silica 60A, 35-70 μm)

CeO_2 – Sigma Aldrich (powder, <5 μm , 99.9% trace metals basis)

SiC – Sigma Aldrich (nanopowder, <100 nm particle size)

BN – Sigma Aldrich (powder, ~1 μm , 98%)

Carbon – Sigma Aldrich (Darco G60, -100 mesh particle size)

H_2O – Sigma Aldrich (HPLC Grade)

MeOH – Sigma Aldrich (HPLC Grade)

50% H_2O_2 – Sigma Aldrich (Stabilised)

$\text{Ce}(\text{SO}_4)_2$ – Sigma Aldrich (>98%)

Ferroun indicator solution – Sigma Aldrich (0.1 wt% in H_2O)

$(\text{NH}_4)_2\text{Fe}(\text{SO}_4)_2 \cdot 6\text{H}_2\text{O}$ – Sigma Aldrich (>98%)

5% H_2/CO_2 – BOC (Specialty Gas)

25% O_2/CO_2 – BOC (Specialty Gas)

5% H_2/N_2 – BOC (Specialty Gas)

25% O_2/N_2 – BOC (Specialty Gas)

2% H_2/Air – BOC (Specialty Gas)

5% H_2/Ar – BOC (Specialty Gas)

CO – BOC (99.999%)

2.2. Catalyst Preparation

2.2.1. Gold-Palladium catalyst preparation by wet impregnation

Bi-metallic gold-palladium catalysts were prepared by wet co-impregnation of a TiO_2 support with a mixed metal salt solution of PdCl_2 dissolved in HAuCl_4 solution. Preparation of 1 g of a 2.5 wt. % Au - 2.5 wt. % Pd / TiO_2 catalyst was carried out according to a well-established procedure which has been previously reported in the literature¹.

PdCl_2 (0.042 g) was dissolved in HAuCl_4 (2.04 ml, 12.25 g Au / L) and water (1 ml) by heating to 80 °C with stirring. To this solution, TiO_2 (0.95 g) was added and the mixture heated and stirred at 80°C, allowing water to evaporate until a thick paste consistency was achieved. The catalyst paste was dried in an oven at a temperature of 110°C for 16 h and ground to a fine powder using a mortar and pestle. The dried catalyst powder was then calcined in a tube furnace under static air at a temperature 400°C for 3 h with a ramp rate of 20°C min⁻¹.

2.2.2. Various supported metal catalysts preparation by wet impregnation

Many different formulations of supported metal catalysts were prepared for this work. The metal salts and supports for these preparations are listed in Section 2.1 'Materials and reagents'. All catalysts were prepared by wet impregnation. The general procedure for preparation of 1 g of 5 wt. % catalyst is as follows.

Stock solutions of the required metal salts were prepared in water with stirring and heating, if necessary. The concentration of the stock solution was then accurately determined by MP-AES analysis (see Section 2.10). To the required volume of stock

solution, diluted as necessary, TiO_2 (0.95 g) was added and the mixture heated and stirred at 80°C , allowing water to evaporate until a thick paste consistency was achieved. The catalyst paste was dried in an oven at a temperature of 110°C for 16 h and ground to a fine powder using a mortar and pestle. Tube furnace heat treatments for the prepared catalysts varied in temperature in duration, for all catalysts the medium under which heat treatment was performed was either static air (oxidative heat treatment) or flowing 5% H_2/Ar (reductive heat treatment).

2.3. Catalyst Testing

2.3.1. Batch H_2O_2 Synthesis

The direct synthesis of H_2O_2 from H_2 and O_2 was evaluated using a Parr Instruments stainless steel autoclave with a volume of either 100 ml or 50 ml and a maximum working pressure of 14 MPa, a schematic of an autoclave reactor is shown in Figure 2.1. The following reaction conditions were used.

The autoclave was charged with catalyst (0.010 g) and solvent (8.5 g HPLC grade H_2O and/or HPLC grade methanol) and sealed. The autoclave was then purged three times with 5% H_2/CO_2 before filling with 5% H_2/CO_2 to a pressure of 2.9 MPa (420 psi) followed by the addition of a further 1.1 MPa (160 psi) 25% O_2/CO_2 . After reaching the desired temperature for the experiment (generally 20°C), the reaction mixture was stirred at 1200 rpm for 30 min, however reaction temperature and duration were systematically varied for some studies.

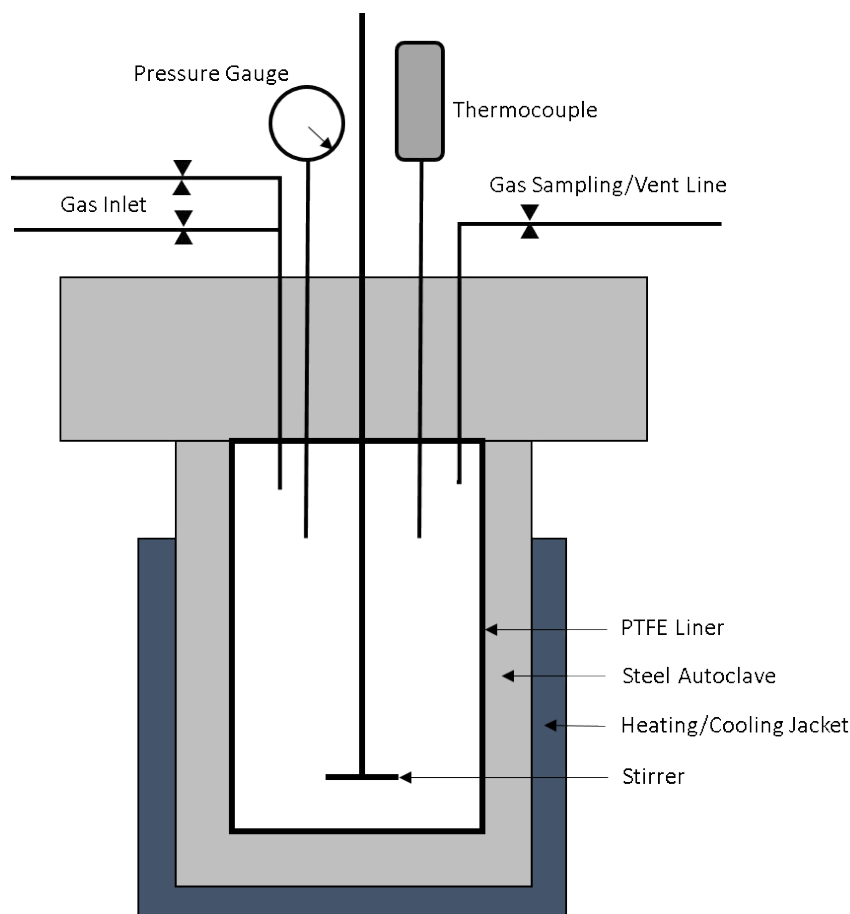


Figure 2.1 – Schematic of a high pressure autoclave reactor

H_2O_2 yield was determined by titrating accurately weighed aliquots (generally *c.a.* 1-2 g) of the filtered post-reaction solution with acidified $\text{Ce}(\text{SO}_4)_2$ solution (*c.a.* 0.01 M) in the presence of Ferroin indicator (*c.a.* 0.1 ml). The concentration of this $\text{Ce}(\text{SO}_4)_2$ solution was separately determined by titration against an accurately weighed amount (*c.a.* 0.030 g) of $(\text{NH}_4)_2\text{Fe}(\text{SO}_4)_2 \cdot 6\text{H}_2\text{O}$, in the presence of a Ferroin indicator.

The relative catalytic performance of various catalysts was compared by determining productivity for each catalyst, this was the average hourly rate of H_2O_2 production when normalised for the mass of catalyst used in each reaction. Productivity is reported with units of $\text{mol}_{\text{H}_2\text{O}_2} \text{h}^{-1} \text{kg}_{\text{cat}}^{-1}$. Absolute H_2O_2 yield for a given reaction is also quoted as ppm (weight). The equations used to obtain values for both catalyst productivity and H_2O_2 yield in ppm are shown below:

2.3.2. Batch H₂O₂ Degradation

H₂O₂ degradation represents the combined processes of H₂O₂ hydrogenation and H₂O₂ decomposition. Experiments can be performed to determine either the total degradation activity of a catalyst or the decomposition activity of a catalyst, thus net hydrogenation can be determined by subtracting the measured value for decomposition activity from the measured value for total degradation activity, assuming that the reactions happen independently of each other. The combined degradation processes are the dominant unselective pathways (relative to combustion) in the direct synthesis of H₂O₂ process and also correlate positively with combustion activity. Therefore, the total H₂O₂ degradation activity of a catalyst

can be used as an efficient proxy measure of the selectivity of a catalyst to H_2O_2 , with a low degradation activity representing a selective catalyst and *vice versa*.²

H_2O_2 degradation and decomposition experiments were carried out with identical reactors, total solvent mass and catalyst mass to that of H_2O_2 synthesis experiments. In these experiments, the reactor was only charged with a single gas, 420 psi (2.9 MPa) 5% H_2/CO_2 or 420 psi (2.9 MPa) 25% O_2/CO_2 for degradation tests or decomposition tests, respectively. Furthermore, a reaction solution containing 4 wt. % H_2O_2 was used for degradation/decomposition experiments. The total mass of solution used was always 8.5 g, the solution was prepared by the addition of concentrated H_2O_2 solution (50 wt. %, 0.68 g) to H_2O and/or methanol (7.82 g total mass). The concentration of H_2O_2 in the reaction solution was accurately determined before and after the reaction by titrating aliquots (c.a. 0.05 g) of the reaction solution with acidified $\text{Ce}(\text{SO}_4)_2$ in the presence of Ferriin indicator. Aside from the noted differences, reaction parameters were identical to those used for synthesis reactions. Degradation, decomposition and net hydrogenation activities of tested catalysts were generally expressed as a percentage of H_2O_2 which was degraded in the course of a test (generally 30 min), activity can also be expressed as a normalised degradation activity, similar to the previously defined catalyst productivity, and reported with units of $\text{mol}_{\text{H}_2\text{O}_2} \text{h}^{-1} \text{kg}_{\text{cat}}^{-1}$.

2.3.3. Batch Blank Reactions

Blank synthesis and degradation reactions are performed as outlined in Sections 2.3.1 and 2.3.2 respectively, however no catalyst is added to the reaction mixture. Blank reactions serve dual purposes. Primarily, they provide important data on how a system behaves under a given set on conditions in absence of a catalyst. This allows for comparison with data collected for catalytic reactions and the attribution of any differences therein to catalytic activity. Secondly, blank reactions (both synthesis and degradation) are performed periodically to ensure that there are no catalytically active deposits on the reactor surfaces, which will add error to the results of any reactions performed. If the results from these blank reactions differ from previous results obtained with a clean reactor, the autoclave is washed with acid and water until an acceptable blank reaction result is obtained.

2.3.4. Batch Catalyst Re-use

Catalysts were tested for re-usability by first performing a synthesis experiment (as detailed in Section 2.3.1), charging the reactor with an increased catalyst mass to (0.02 g) to ensure that 0.01 g of catalyst could be recovered and subsequently tested. Once the synthesis reaction was complete, the catalyst was recovered by filtration and placed in a desiccator until completely dry (at least 24 h). Once the catalyst was dry, 0.01g was used to test for synthesis, degradation or decomposition activity.

2.3.5. Liquid/gas flow H₂O₂ synthesis

Catalysts were tested for H₂O₂ synthesis and degradation in a continuous liquid/gas flow system, a schematic of the reactor used for this testing is shown in Figure 2.2. The reactor was constructed from Swagelok tubing of 1/4 inch internal diameter with a removable section in which the catalyst bed was installed. Gas flows were controlled using three Brooks mass flow controllers and pressure controlled and maintained via a Swagelok back pressure regulator at the end of the system. The solvent flow was supplied and controlled through an Agilent infinity 1260 series isocratic HPLC pump.

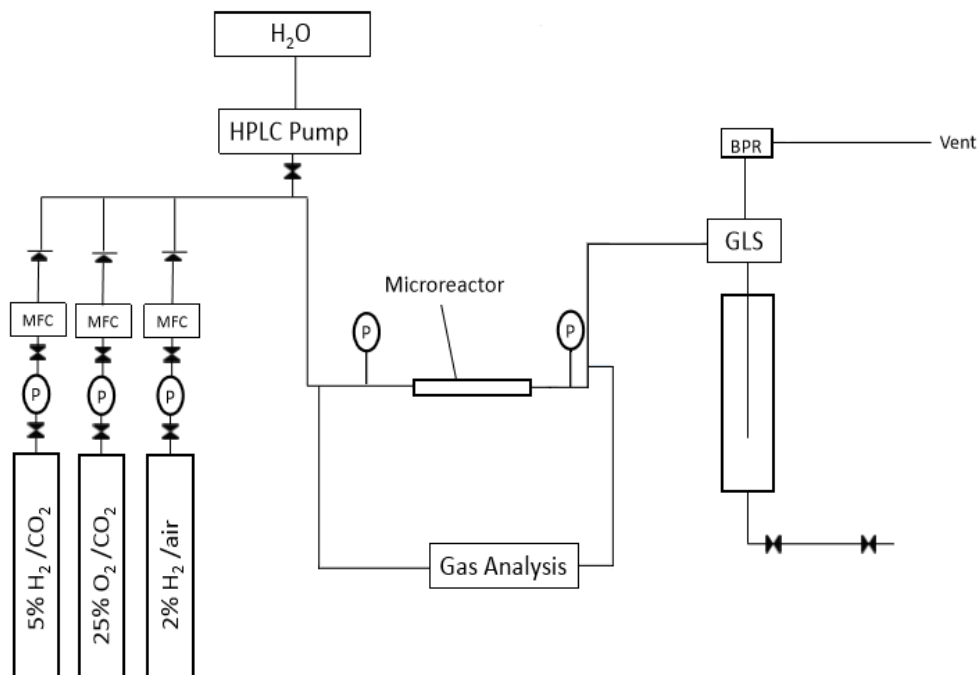


Figure 2.2 - Schematic of the reactor used to test H₂O₂ synthesis in a liquid/gas flow regime

P = pressure gauge, MFC = Mass flow controller, GLS = gas liquid separator, BPR = back pressure regulator.

One-way valves were fitted between the point at which gas enters into the reactor and the point at which liquid enters the reactor to prevent any back flow of liquid into the mass flow controllers. Pressure gauges were fitted on both sides of the catalyst bed to monitor for any pressure drops through the bed and to indicate if any blockages had occurred in the reactor. Solvent/ H₂O₂ was collected in a gas-liquid separator with a volume of 150 ml which acted as a sample bomb. Aliquots for analysis could be removed from this sample bomb with minimal pressure loss or disturbance to the gas dynamics of the system via a double locking tap system fitted to the bottom of the sample bomb. Upon opening the first tap, the solvent/ H₂O₂ was allowed to pass into a *c.a.* 5cm length of tubing, the first tap could then be closed and the second tap opened to release the *c.a.* 1.5 ml aliquot with minimal effect on the reactor.

50 – 250 mg of 425 – 600 micron pelleted catalyst was packed into the microreactor and secured using glass wool to prevent loss of catalyst downstream and any

blockages or malfunctions which may result from such. The microreactor/catalyst bed was fitted securely into the reactor and the reactor was pressurised to the necessary pressure using either a mixture of 5% H₂/CO₂ and 25% O₂/CO₂ or 2% H₂/air. Total gas flows used ranged from 42 to 363 ml min⁻¹. Once the reactor had reached the necessary pressure, solvent was pumped through the reactor at flow rates ranging from 0.25 to 5 ml min⁻¹. Aliquots for analysis were removed from the sample bomb after 10 min and repeated as necessary. The concentration of H₂O₂ produced was quantified by titration of accurately measured aliquots (c.a. 4.5 g) against an acidified Ce(SO₄)₂ solution (c.a. 0.01 M) in the presence of Ferroin indicator (c.a. 0.1 ml).

H₂O₂ degradation experiments were performed in the flow reactor by using only 5% H₂/CO₂ as a gas feed and replacing the water liquid phase with a 1 wt. % H₂O₂ solution. As described in Section 2.3.2, the concentration of H₂O₂ was accurately determined pre and post reaction by titration of accurately measured aliquots against an acidified Ce(SO₄)₂ solution (c.a. 0.01 M) in the presence of Ferroin indicator (c.a. 0.1 ml). Thus any loss of H₂O₂ that occurs when passing through the reactor/catalyst can be quantified.

2.3.6. Gas phase flow H₂O₂ synthesis

Catalysts were additionally tested for H₂O₂ synthesis in a continuous gas flow system, a schematic of the reactor used for this testing is shown in Figure 2.3. The reactor was constructed from Swagelok tubing of 1/8 inch internal diameter with a removable 3/8 inch internal diameter section of approximately 5 cm length in which the catalyst bed was installed. The gas flow was controlled via a needle valve and internal pressure controlled and maintained via a Swagelok back pressure regulator at the end of the system.

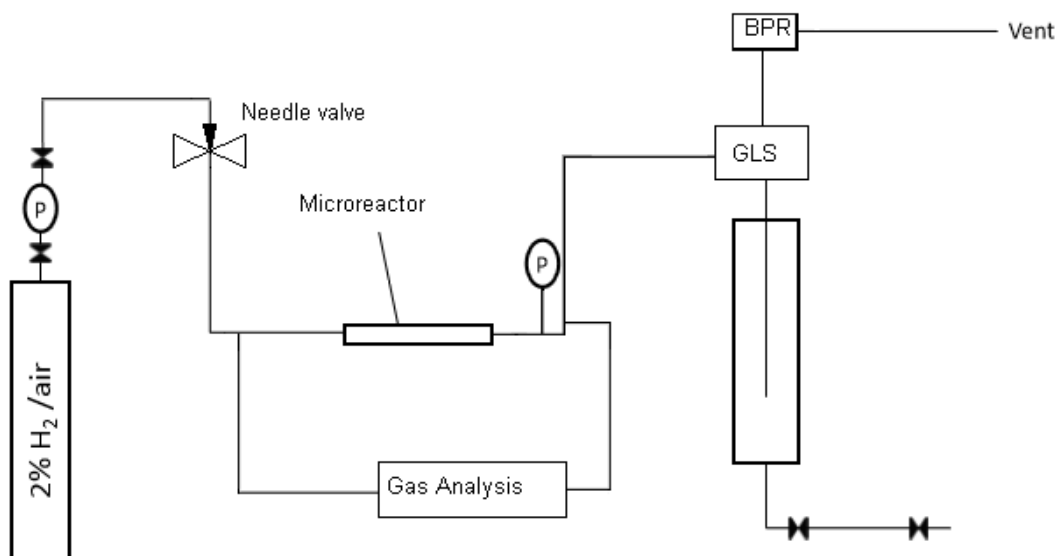


Figure 2.3 - Schematic of the reactor used to test H_2O_2 synthesis in a gas flow regime

P = pressure gauge, GLS = gas liquid separator, BPR = back pressure regulator.

A pressure gauge was fitted after the catalyst bed to monitor pressure of the reactor. H_2O_2 was collected in a gas-liquid separator with a volume of 150 ml which acted as a sample bomb. In this sample bomb *c.a.* 20 cm^3 of 2% H_2SO_4 solution was placed before the experiments to act as a stabiliser for collected peroxide. At completion of the reaction, the entire sample bomb was drained via the tap fitted at the bottom; the catalyst bed and bomb were then rinsed through three times with *c.a.* 20 cm^3 of H_2O to collect all residual H_2O_2 .

10 – 250 mg catalyst was packed into the microreactor and secured using quartz wool to prevent loss of catalyst downstream and any blockages or malfunctions which may result from such. The microreactor/catalyst bed was fitted securely into the reactor and the reactor was pressurised to the necessary pressure using 2% H_2/air . A gas flow of 50 ml min^{-1} was used, this was measured by digital flow meter both before and after the catalyst bed to ensure there were no blockages or pressure build-ups. Once the reactor had reached the necessary pressure, it was left for the duration of the reaction (generally 16 h). Upon completion the produced H_2O_2 was collected as previously described. The total moles of H_2O_2 produced was quantified by titration of the total product against an acidified $\text{Ce}(\text{SO}_4)_2$ solution (*c.a.* 0.01 M) in the presence of Ferroin indicator (*c.a.* 0.1 ml).

2.4. Gas Chromatography

2.4.1. Gas Chromatography theory

Gas Chromatography (GC) is an analytical technique used for separation and subsequent identification and quantitation of compounds in a mixture, a schematic of a GC machine is shown in Figure 2.4. It involves injection of a vaporised liquid or gaseous compound into a chromatographic column through which differing analytes elute at differing rates. A chromatographic column can be either packed or capillary style. A packed column consists of a 2-4 mm internal diameter glass, quartz or stainless steel tube filled with an inert stationary support material such as diatomaceous earth or silica gel, onto which a 'stationary phase' liquid of high boiling point, usually a waxy polymer, is adsorbed. A capillary column has an internal diameter of less than 1 mm and consists of either an inert support and adsorbed stationary phase or just stationary phase liquid coated directly onto the walls of column. The column is housed in a temperature regulated oven, which can either be held at a constant temperature or programmed for a ramped increase through analysis to affect the rate of elution of analytes.

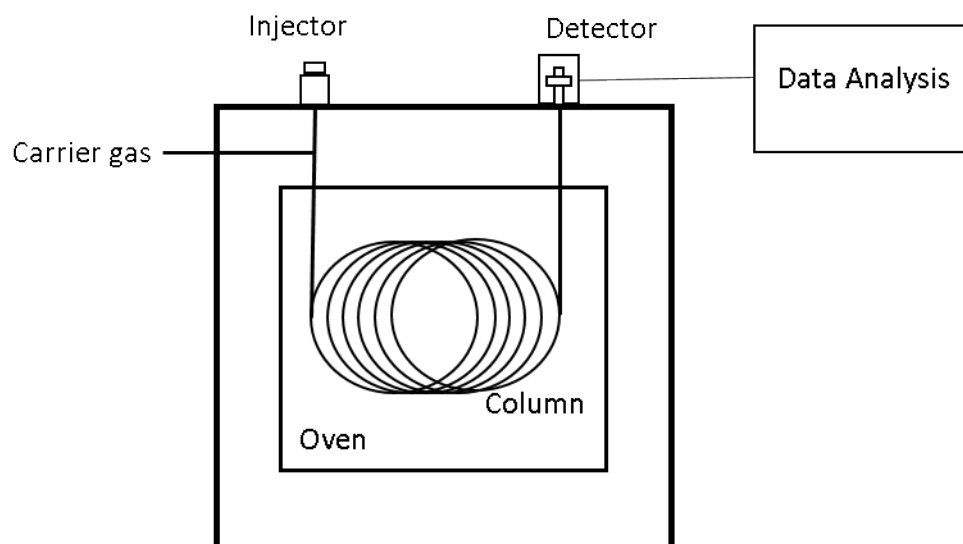


Figure 2.4 – Schematic of a gas chromatograph

Once a sample is injected it is carried through the column by a flow of an inert gas, such as Helium, Nitrogen or Argon, which is known as the mobile phase. Injected samples may remain in the gas phase, adsorb on the stationary phase, dissolve into the stationary phase, or a combination of any of these. How a sample behaves with respect to the stationary phase affects how long it takes to elute from the column; this time between injection and the peak elution of a compound is referred to as the retention time. With selection of an appropriate column and oven temperature, GC allows for differing retention times and therefore full separation of components in mixed samples.

Many types of detector can be used to evaluate changes in the gas eluted from the column, two of the most commonly use are a thermal conductivity detector (TCD) and a flame ionisation detector (FID). A TCD contains heated filaments held at a constant temperature over which pass a stream of carrier gas alone and a stream of the gas eluted from the column. The power required to keep the filaments at a constant temperature is measured and recorded, which allows for differences in the thermal conductivity (and therefore gas identity) of the eluted gas stream and the stream of carrier gas to be detected. TCDs which use one filament over which passes a rapidly switching gas stream of carrier gas and eluted gas are also used. An FID requires the eluted gas to be mixed with air and hydrogen, before a small jet of the mixture is ignited. Pyrolysis of organic compounds produce ions and electrons which are attracted to a cathode situated above the flame burner tip, over which a large electrical potential is applied. The movement of the electrons and ions to the cathode produce a current which is measured and recorded. FIDs are very sensitive for the detection of organic compounds and allow for quantitative analysis due to a generally linear response rate and high signal to noise ratio.³

2.4.2. Gas Chromatography analysis for H₂O₂ synthesis reactions

Reaction gas mixtures from the direct synthesis of H₂O₂ was analysed with the use of a Varian 3800 gas chromatogram (GC) fitted with a thermal conductivity detector (TCD) and a CP-wax 52 CB column, which was held at 30°C in an oven to allow for separation of H₂, O₂ and CO₂. To allow for accurate calculation of reactant (H₂) conversion and product (H₂O₂) selectivity of catalysed reactions, there must be comparison between a given catalysed reaction and a 'blank' synthesis reaction. A blank reaction is performed under identical conditions to the given catalysed reaction, however no catalyst is added to the reactor. Comparison of a catalysed reaction

sample with a 'blank' reaction sample (as opposed to a directly sampled mixture of reactant gasses) serves to eliminate any discrepancies of reactant gas composition that are simply due to dissolution of gasses in the reaction solvent and not any catalytic activity. Each sample was analysed for 22 min, which is sufficient to allow for all gasses under analysis to pass through the column, the retention times for the gasses analysed are shown in Table 2.1.

Table 2.1. Retention times of gasses analysed from H₂O₂ direct synthesis experiments.

Gas	Retention time / min
H₂	1.64
O₂	2.25
CO₂	9.22

By integrating the peaks for the gasses and comparing the H₂: CO₂ ratio of the 'blank' sample to the H₂: CO₂ ratio of the reaction sample, hydrogen conversion can be calculated. From the calculated hydrogen conversion value, hydrogen selectivity can further be calculated by factoring in the moles of H₂O₂ synthesised in the direct synthesis reaction and therefore producing a value for the hydrogen selectivity towards synthesised H₂O₂.

2.5. X-Ray Photoelectron Spectroscopy

X-ray photoelectron spectroscopy (XPS) allows for analysis of the elemental composition and electronic (oxidation) state of elements present in the surface atomic layers (generally a depth <10 nm) of a sample. XPS spectra are produced by placing a sample under ultra-high vacuum and subjecting it to irradiation from a beam of low energy X-rays. A detector is then used to count and measure the kinetic energy of core-level electrons which are subsequently emitted from the sample. The energy of emitted electrons is a function of the electrons' binding energy and is characteristic of a given element in a given oxidation state; the intensity of a signal can also be used to give quantitative information. Therefore XPS enables identification of all surface elements (with the exception of hydrogen), information on the electronic state(s) of these elements and elemental ratios present

at a catalyst surface.⁴ A schematic representation of XPS apparatus is shown in Figure 2.5.

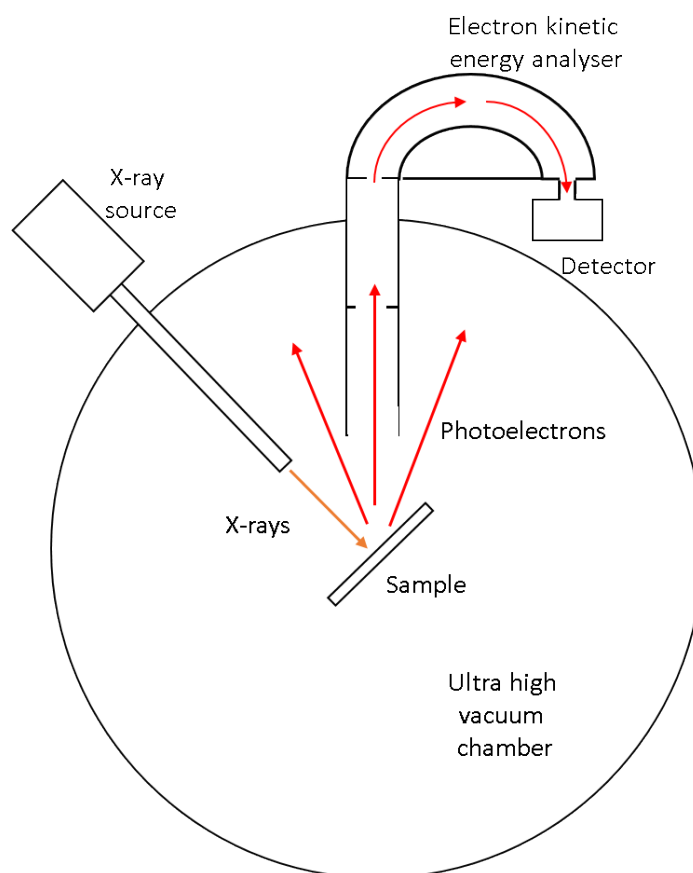


Figure 2.5 – Schematic of a XPS system

XPS analysis was performed using a VG EscaLab 220i spectrometer, fitted with a 300 W Al-K α X-ray source and an analyzer pass energy of 20 eV.

2.6. Electron Microscopy and Element Analysis

2.6.1. Transmission Electron Microscopy

Transmission electron microscopy (TEM) uses a high energy electron beam which passes through a thin sample to produce images at resolutions far higher than is possible with visible light microscopy, with resolutions of 0.5 nm common. A high intensity electron beam passes through condensers and apertures which causes the beam to become parallel and coherent while excluding high angle electrons. This beam is focussed on a sample, which it partially passes through, dependant on electron transparency and thickness of the sample. The transmitted electron beam

forms an image on an electronic detector such as a charge coupled device camera or an imaging detector such as a phosphor screen. The image produced has darker areas where less electrons are transmitted (thicker regions or elements with higher atomic numbers) and light areas where more electrons are transmitted; this image is called a 'bright field'. A 'dark field' image is also obtained from electrons which have undergone Bragg diffraction, these are detected slightly off angle from the transmitted portion of the electron beam. For successful TEM imaging of supported metal catalysts, there generally needs to be adequate contrast in electron transparency between the metal particles and the support, the support must also be thin, generally below 100 nm.⁵

2.6.2. Scanning Transmission Electron Microscopy

Scanning Transmission Electron Microscopy (STEM) is a combination of TEM and Scanning electron Microscopy (SEM); STEM is distinguished from TEM by the use of a narrower beam of electrons which is rastered over the surface being imaged. STEM allows for many simultaneous detection methods to be employed (SEM, TEM, EDX, EELS, HAADF) and therefore can give more information than conventional TEM imaging through the use of additional detectors. High angle annular dark-field (HAADF) imaging uses detectors set at a greater angle to the transmitted beam than those used for 'dark field' images in conventional TEM. These detectors collect electrons which have been elastically scattered at a high angle. Electrons from elements with greater atomic numbers undergo enhanced high angle scattering, with HAADF signal approximately proportional to $Z^{3/2}$, where Z is the atomic number of a given element which has caused the scattering. This technique allows for images with very good contrast by atomic number, with the resulting images also referred to as 'Z-contrast' images.⁵ A schematic representation of the various detectable signals generated by STEM is shown in Figure 2.6.

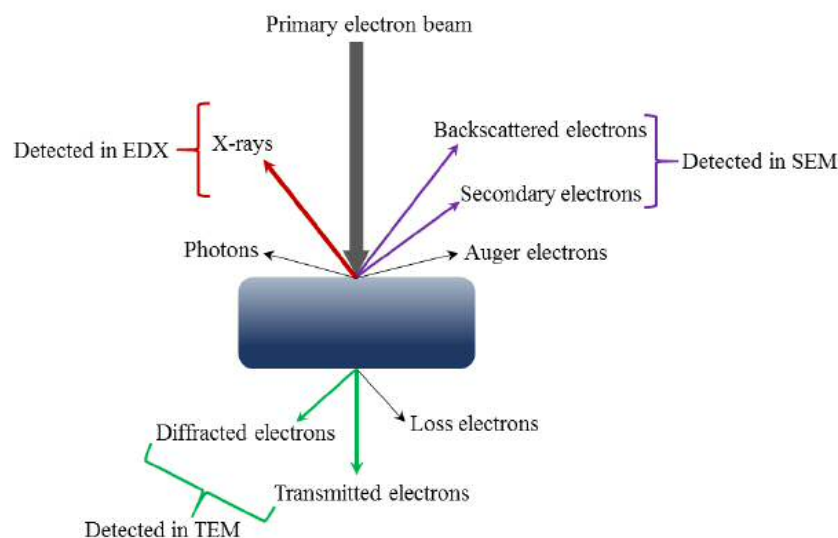


Figure 2.6 – Schematic representation of detectable signals generated by STEM

2.6.3 Energy-dispersive X-Ray Spectroscopy and Electron Energy Loss Spectroscopy

Energy-dispersive X-Ray Spectroscopy (EDX) is a complimentary technique to electron microscopy that is used for elemental analysis. When the incident electron beam interacts with the atoms in a sample undergoing microscopy, it can cause the emission of a core level electron, this leaves a vacancy which must be filled by an outer shell electron relaxing or ‘dropping down’ and in the process releasing excess energy in the form of an X-ray. The energy of this emitted X-ray is characteristic of the element from which it originated, therefore detection and measurement of these X-rays allows for facile qualitative elemental analysis and a degree of quantitative analysis of elemental composition. In scanning electron microscopy techniques (SEM, STEM), use of EDX allows for elemental ‘maps’ of a sample to be produced.⁶ A schematic representation of the electronic processes involved in EDX is shown in Figure 2.7.

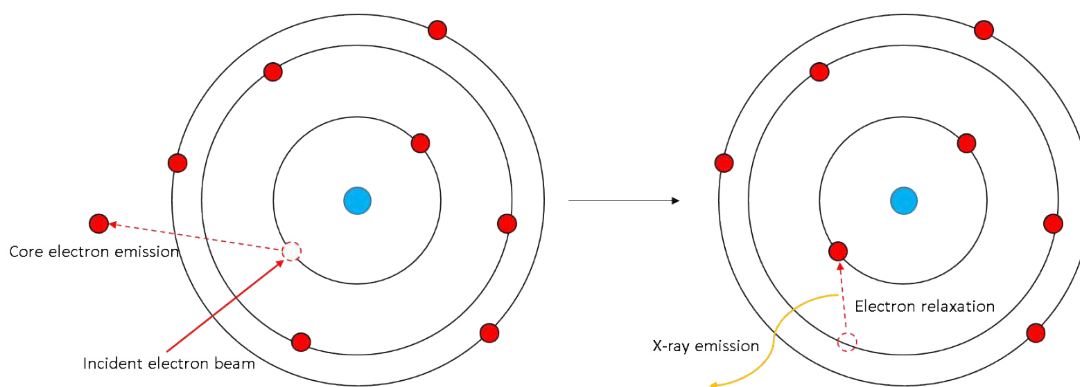


Figure 2.7 – Schematic representation of the electronic processes involved in EDX

Electron Energy Loss Spectroscopy (EELS) involves detection of the kinetic energy of scattered electrons from the sample and therefore allows for calculation of energy loss as the kinetic energy of the incident beam is known. The energy loss of the electrons is due to phonon interactions or vibrational excitations as well as aforementioned electronic transitions involved in EDX. EELS is complimentary to EDX as EDX allows for relatively facile identification of element identity, use of EELS can allow information to be gathered on atomic composition, chemical bonding and electronic properties of surfaces.⁷

2.8. X-Ray Diffraction

X-ray diffraction (XRD) is a bulk characteristic technique used to probe the crystal structure of samples. X-rays have wavelengths in the range of 10^{-10} m which is comparable to the separation of atoms in the ordered lattice of a crystalline material, this allows for elastic scattering of X-rays by atoms in an ordered lattice which creates characteristic interference patterns.

XRD requires the use of monochromatic X-rays; X-rays of a range of energies are first produced by a metal target (generally Cu or Mo) which is bombarded with high energy electrons. Collisions cause emission of metal electrons from the K-shell (1s), the resulting electronic vacancies are filled by the relaxation of electrons from the L (2p) or M (3p), which release X-rays of characteristic energy known as K_{α} and K_{β} , in addition to broad Bremsstrahlung radiation which is produced by deceleration of the incident electron beam. The X-rays are passed through a monochromator such as a

single germanium crystal to produce an X-ray beam of a very narrow range of wavelengths. This X-ray beam can then interact with the sample and undergo scattering to form interference patterns wherein the incidents of constructive interference are detected (commonly called a 'reflection'). In reference to Figure 2.8, the conditions for constructive interference can be expressed mathematically as $AB+BC = 2d \sin\theta = n\lambda$. Here $AB + BC$ is the additional distance travelled by the lower incident X-ray, if this additional distance is equal to a whole number of wavelengths the diffracted beams will be coherent and therefore display constructive interference.

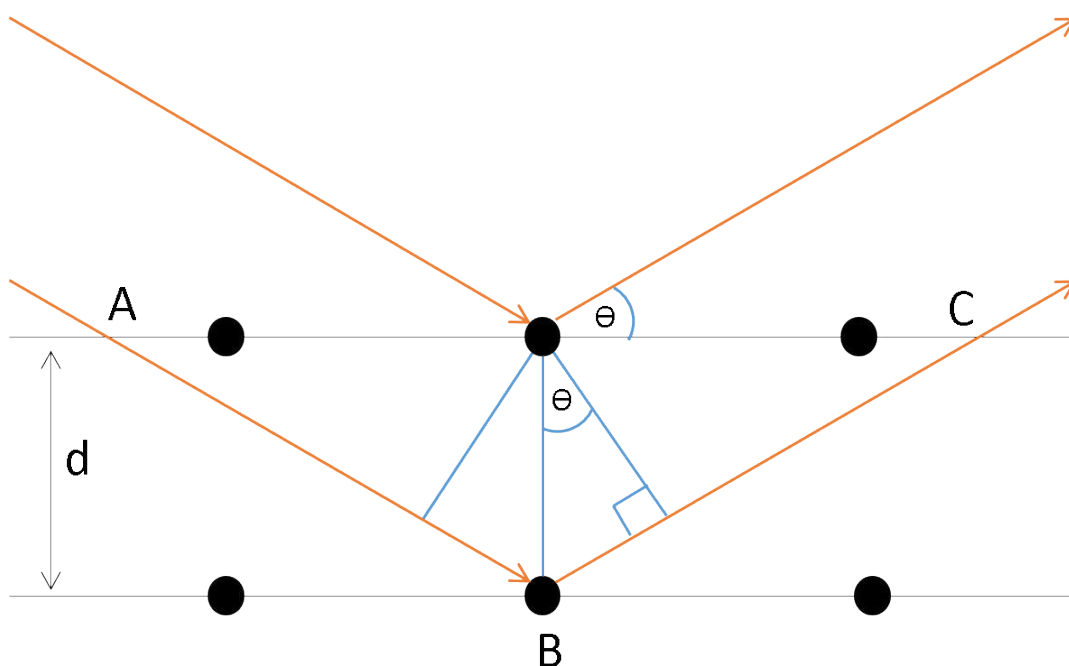


Figure 2.8 - Schematic of X-ray diffraction from lattice planes in a crystalline material. d = lattice spacing, θ = incident angle, normal to the plane

In the study of supported metal catalysts, powder XRD is predominately used. Finely ground powder samples have an extremely large number of randomly oriented crystallites, therefore there is always a small portion of the crystallites present in the powder that are oriented such that a certain crystal plane is at the correct angle to the incident beam to result in constructive interference. In powder XRD, the X-ray source is generally stationary and the detector moves around the sample to detect the angle (2θ) at which reflections (incidents of constructive interference) occur. Using Bragg's law, one can calculate lattice spacing from the previously defined relationship:

Where n = an integer, λ = X-ray wavelength, d = lattice spacing, θ = angle of incident X-ray beam, normal to the plane.

Calculated lattice spacings are characteristic of certain crystallites and can be compared to established standard databases to allow for crystal phase identification. Generally crystallites need to be of a size greater than 5 nm to allow for detection in powder XRD, as below this limit the scattering angles of the incident X-rays are too small to be measured.

For small crystallites, such as those regularly found in supported metal catalysts, line broadening in the diffraction pattern can occur as a result of partial destructive interference. The shape of the detected reflections can therefore give information in regards to the size of crystallites. The size of a crystalline particle can be estimated from the Scherrer equation⁶:

Where: τ = mean crystallite size, k = form factor, λ = X-ray wavelength, β = full width half maximum of the reflection peak, θ = diffraction angle.

XRD analyses were performed using a PANalytical X'pert Pro powder diffractometer fitted with an X'Celerator detector using a Cu K_{α} X-ray source operated at 40 KeV and 40mA. Analysis was generally performed on a back filled sample mounted on a zero-background sample holder, with each sample scanned for 40 minutes at 2θ values of $10 - 80^{\circ}$. Phase identification was implemented with the use of International Centre for Diffraction Data (ICDD) databases.

2.9. Temperature Programmed Reduction

Temperature Programmed Reduction (TPR) allows for monitoring of hydrogen uptake by a reducible material whilst temperature increases linearly with time at a user-defined rate. Hydrogen uptake by the material under test is monitored via a

change in conductivity of the gas mixture passing over the material, as detected by a TCD. This gives information about the temperature at which hydrogen adsorbs on and/or reduces the material under test and therefore can be used to inform reaction conditions and temperatures for reductive heat treatments.⁸

TPR data was collected with use of a Thermo 1100 series TPDRO. The sample tube was packed with an accurately weighed sample of c.a. 0.1 g secured with quartz wool. Pre-treatment was performed to remove residual water; the sample was heated under flowing Ar with a ramp rate of 10°C min⁻¹ to a maximum temperature of 110 °C, at which it was held for 60 min. Analysis was performed under 10% H₂/Ar with a ramp rate of 10°C min⁻¹, up to 600 °C.

2.10. Microwave Plasma Atomic Emission Spectroscopy

Microwave Plasma Atomic Emission Spectroscopy (MP-AES) is a quantitative analytical technique used to determine the concentration of a given element in a sample. Liquid samples are sprayed through a microwave and magnetically excited nitrogen plasma formed within a quartz torch which has a temperature of approximately 5000 K. The sample is atomised and the resultant atoms form a high population of excited states, these excited states then relax and emit photons of a characteristic wavelength for the element. These photons pass through a monochromator and mirror grating, which allows for the analysis of individual specific wavelengths as defined by the user, giving very low interference from other emissions.

The high temperatures of MP-AES allows for more electrons to enter into excited states, as such a greater emission is produced leading to an improved sensitivity over lower temperature AES techniques such as flame AES. The intensity of the signal from the emitted photons is proportional to the number of atoms of an element, therefore comparison of a recorded signal to a calibration from a known standard allows for accurate determination of the concentration of an element in a sample.⁹ In heterogeneous catalysis research, MP-AES is regularly used to accurately determine stock solution concentrations, examine reaction solutions for leached metal content and to assay digested catalysts to accurately determine metal weight loading.

Analyses were performed using an Agilent MP-AES 4100; samples were assayed using multiple wavelength calibrations to elemental standards supplied by Sigma Aldrich for each individual element. Reaction solutions were filtered to remove heterogeneous catalyst from the sample, first with fine filter paper followed by PTFE syringe filters (0.456 μm). Catalyst digestion was performed with 50 mg of catalyst sonicated for 16 h in 10 ml aqua regia, the sample was then diluted to 100 ml and filtered as above.

2.11. Surface Area Analysis

2.11.1. Surface Area Analysis by Physisorption

To determine the total surface area of a solid material, a measured volume of inert gas (such as N_2) can be physisorbed onto the surface and via interpretation of this measurement through Brunauer–Emmett–Teller (BET) theory, an estimated surface area can be calculated. This form of surface area analysis is often called BET analysis.

BET theory aims to explain multi-layer physical adsorption of gas on a solid surface and is an extension of Langmuir's adsorption model, which explains monolayer adsorption. The Langmuir model assumes that adsorption is limited to static monolayer coverage, that the solid surface is uniform with all sites equivalent and that the presence of adsorbed molecules on neighbouring sites does not affect the likelihood of a molecule adsorbing on a vacant site. BET extends this model to multi-layer adsorption by assuming molecules can physically adsorb on solid surfaces in layers infinitely, that each adsorption layer has no interaction with others, that Langmuir theory applies to all layers and that the uppermost layer is in an equilibrium state with the gas phase.¹⁰

The volume of gas adsorbed to form a monolayer on the surface can be related to pressure by use of BET theory through the following equation.

$$\frac{V}{V_m} \frac{P}{P_0 - P} = \frac{C}{1 + C} \frac{P_0}{P_0 - P} + \frac{C}{1 + C} \frac{P}{P_0 - P}$$

Where P = pressure of adsorbate gas, P_0 = saturation pressure, V = volume of gas adsorbed, V_m = volume of required to form a monolayer, C = BET constant.

Plotting this data in the form of $\frac{V_m}{P/P_0}$ versus $\frac{1}{P/P_0}$ yields a linear plot with an intercept of $\frac{V_m}{P/P_0}$ and a gradient of $\frac{V_m}{P/P_0}$, therefore V_m can be calculated. From V_m the surface area of the material can be calculated through the following equation:

$$S = \frac{V_m N_A}{M}$$

Where V_m = Volume of gas required for monolayer coverage, N_A = Avagadro's Number, S = Adsorption cross sectional area of gas, M = Molar volume of gas.

Surface area analysis was performed using a Micromeritics Gemini 2360. An accurately weighed sample of c.a. 100 mg was placed in a sample tube and degassed for 1 h at 120°C under a flow of N_2 to remove adsorbents such as water from the sample surface. Analysis was performed using N_2 as the inert adsorbate and a single point analysis programme, typically taking 5 points in the range $P/P_0 = 0.05 - 0.1$.

2.11.2. Surface Area Analysis by Chemisorption

To determine the total number of exposed active metal sites and therefore active metal surface area of a solid material, surface area techniques making use of small reactive gas molecules (e.g. CO , O_2) which chemically bond to exposed reactive metal sites (e.g. Pd , Pt) are used. The energy of monolayer chemisorption far exceeds the energy of adsorption in multilayers or on the support, therefore chemisorption occurs at lower pressures and can be distinguished and analysed separately. By measuring the number of reactant gas molecules necessary to saturate the active surface and considering the binding mode of the gas on the surface, the total number of surface metal sites and the exposed metal surface area can be determined. The choice of reactant gas molecule must be a species that reacts with only the surface of active metal under analysis, not the bulk or a support material, and binds irreversibly (under the given conditions) to the surface once reacted.

CO chemisorption can be performed in 'static' or 'pulsed' operational modes. Static operation proceeds in a manner analogous to BET analysis, with a constant rate of titration of an adsorbate gas onto the sample until all chemisorption sites are saturated, which generally occurs at a very low pressure. Pulsed operation involves the use of very small discreet pulses of adsorbate gas in carrier gas which are passed over the sample. Exit gas composition is determined by use of a TCD, therefore the

point at which no more adsorbate gas is taken up can be measured and thus the total volume of gas adsorbed can be calculated.

CO Chemisorption analysis was performed on a Quantachrome ChemBet equipped with a cold trap. An accurately weighed sample of *c.a.* 100 mg was pre-treated at 140 °C with a ramp-rate of 20 °C min⁻¹ under 10% H₂/Ar for 1 hr in order to reduce the surface and remove any adsorbates. CO chemisorption was performed in a pulsed mode, first by-passing the sample 3 times for calibration. Analysis was performed by titrating 113 µl CO in an Ar carrier gas over the sample until a stable TCD signal (δ (CO peak area) < 2%) was achieved.

2.12. Infrared spectroscopy

Infrared spectroscopy is generally performed as an absorption spectroscopy, where a sample is irradiated with UV light and the absorbance of the sample at given frequencies (generally reported as cm⁻¹) is measured. The commonly used 'mid-infrared' range, generally considered from 400-4000 cm⁻¹ gives information about the fundamental vibrational modes in a sample and therefore can be used for identification of compounds and binding modes of molecules.

A variant of infrared spectroscopy that is of particular use in heterogeneous catalysis research is CO Diffuse Reflectance Infrared Fourier Transform Spectroscopy (DRIFTS). The strong dipole in C–O bonds makes them ideal for study by infrared spectroscopy (as a vibration must display a change in dipole moment to be 'infrared active'); furthermore, the frequency of C–O stretch is informative about the environment and bonding of the molecule. Direct measurement of metal–C bond vibrations is not a facile process as the vibrations occur at low frequencies which require specialized equipment and suffer from background absorbance by the support, therefore changes in the C–O vibrations are used to give information about the metal–C bond.

CO can bind to a metal site in a linear, bridging (bonded to 2 metal atoms), three-fold or four-fold configuration. Generally, higher energy metal sites such as defects or edge sites will be more likely to bond in a linear configuration, whereas lower energy sites are more likely to bond in a 2-, 3- or 4-fold configuration. When the C is bound to more atoms the CO π^* anti-bonding orbital becomes more full, leading to a weakening of the C–O bond; this weakening causes the bond to vibrate at lower

frequencies. The exact frequencies of C–O vibrations depend on the binding metal, the structure of the surface and CO coverage, however from changes in the C–O vibration frequencies of adsorbed CO molecules, information about the relative energies of active sites on supported metal catalysts and the proportion thereof can be determined.¹¹

CO DRIFTS analysis was performed on a Bruker Tensor 27 spectrometer fitted with a mercury cadmium telluride (MCT) detector and ZnSe windows. A background measurement was first obtained using KBr as a standard. The sample holder in a Praying Mantis high temperature (HVC-DRP-4) *in-situ* cell was filled with finely ground sample and a 25 cm min⁻¹ flow of N₂ was passed over the sample. Spectra were recorded every minute at room temperature, first with an N₂ gas feed, followed by a 1% CO/N₂ gas feed and finally once the CO adsorption bands in the measured spectra ceased to change, the gas feed was changed back to N₂ and measurements continued until no change in subsequent spectra was observed.

2.13. Discussion of experimental uncertainty

For all data contained in this work, steps were taken to keep uncertainty in measurements to a minimum by using high precision instruments which were regularly calibrated. Experimental error was also minimised by performing each experiment three times, allowing for average values to be reported and anomalous results to be identified and repeated, if necessary.

Uncertainties arising from the measurement equipment and methods in this work were generally minor, allowing for a high degree of confidence in data trends. When considering a standard synthesis of H₂O₂, the uncertainty in measurement from weighing of both solvent and the final reaction solution, charging the reactor with reactant gasses and maintaining exact reaction duration is very small. The total percentage uncertainty attributed to apparatus used for these measurements is calculated to be no more than $\pm 0.25\%$. The majority of uncertainty for measurement of H₂O₂ synthesis arises from the titration of the reaction solution with acidified Ce(SO₄)₂ solution. The uncertainty in measurement for the burette which was used for all titrations is ± 0.05 ml. Reaction solution aliquot volumes were controlled such that titrations of <5 ml were not performed; as such the maximum percentage error from this titration process was $\pm 1\%$. Therefore, in this work the maximum limits of

uncertainty for H_2O_2 synthesis experiments is considered to be $\pm 1.25\%$. As degradation/hydrogenation experiments require 2 separate titration steps, the maximum limits of uncertainty on these experiments is considered to be $\pm 2.25\%$.

As outlined in Section 2.4.2., gas chromatography was used to measure reactant (H_2) conversion and product (H_2O_2) selectivity for synthesis reactions. For each of these measurements, a blank measurement was performed before each measurement of a reaction mixture to provide a baseline against which conversion can be compared. The constant partial pressure of CO_2 present in both blank and standard synthesis samples effectively acts as an internal standard, allowing for accurate quantification of reactant gasses. The relative uncertainty of the TCD is no more than $\pm 1\%$, therefore as quantification of conversion requires a comparison of 2 measurements, the relative uncertainty in conversion figures is $\pm 2\%$. The calculation of selectivity requires both a value for the amount of H_2O_2 synthesised and a value for conversion; via propagation of uncertainty, the relative uncertainty in measurements of selectivity is considered to be $\pm 2.5\%$.

2.14. References

1. J. Edwards, B. Solsona, P. Landon, A. Carley, A. Herzing, C. Kiely and G. Hutchings, *Journal of Catalysis*, 2005, 236, 69-79.
2. C. Samanta, *Applied Catalysis A: General*, 2008, 350, 133-149.
3. G. Schwedt, *The Essential Guide To Analytical Chemistry*, Wiley, 1997.
4. J. W. Niemantsverdriet, in *Spectroscopy in Catalysis*, Wiley-VCH Verlag GmbH & Co. KGaA, 2007, DOI: 10.1002/9783527611348.ch3, pp. 39-83.
5. J. W. Niemantsverdriet, in *Spectroscopy in Catalysis*, Wiley-VCH Verlag GmbH & Co. KGaA, 2007, DOI: 10.1002/9783527611348.ch7, pp. 179-216.
6. J. M. Thomas and W. J. Thomas, *Principles and practice of heterogeneous catalysis*, John Wiley & Sons, Second edn., 2014.
7. F. Hofer, F. P. Schmidt, W. Grogger and G. Kothleitner, *IOP Conference Series: Materials Science and Engineering*, 2016, 109, 012007.
8. I. Chorkendorff and J. W. Niemantsverdriet, *Concepts of modern catalysis and kinetics*, John Wiley & Sons, 2006.
9. E. Metcalfe, *Atomic absorption and emission spectroscopy*, Chichester : Wiley on behalf of ACOL, Chichester, 1987.
10. S. Brunauer, P. H. Emmett and E. Teller, *Journal of the American Chemical Society*, 1938, 60, 309-319.
11. J. W. Niemantsverdriet, in *Spectroscopy in Catalysis*, Wiley-VCH Verlag GmbH & Co. KGaA, 2007, DOI: 10.1002/9783527611348.ch8, pp. 217-249.

3. THE EFFECT OF REACTION CONDITIONS ON THE DIRECT SYNTHESIS OF HYDROGEN PEROXIDE USING SUPPORTED GOLD-PALLADIUM CATALYSTS

3.1. Introduction

Hydrogen peroxide (H_2O_2) is an important commodity chemical which is used in a number of selective oxidation processes, such as the synthesis of propene oxide from propene and H_2O_2 ,¹ and also non-synthetic applications which make use of its oxidative properties such as cleaning and bleaching. The existing indirect anthraquinone process for producing H_2O_2 is only economically viable at a large scale, hence production currently has to be centralised. H_2O_2 is then transported to the point of use in a high concentration (generally 70 vol. %) aqueous solution with added stabilisers, necessitating dilution and potentially removal of stabilisers for it to be effective for many uses, particularly bleaching applications when it is used in very dilute form (3-8 vol. %).²

The ability to produce H_2O_2 at a desired concentration at the point of use could prove to be a green and economical process. This could potentially be achieved *via* the direct synthesis of H_2O_2 from oxygen and hydrogen to localise the supply of H_2O_2 .

If generation of H_2O_2 in aqueous solution without additives becomes viable, it would negate the necessity for the extraction of synthesised H_2O_2 from the anthraquinone process solvents. Furthermore, the removal of stabilisers (as with anthraquinone process produced H_2O_2) or promoters (as may be necessary for H_2O_2 produced by acid or halide promoted direct synthesis) would not be required. The ability to efficiently generate H_2O_2 in a water stream also presents opportunities for water cleaning technologies to be developed. It is this latter application for which there is considerable current interest as H_2O_2 could then have the potential to replace chlorine as a disinfectant for water which would only be possible if stabiliser-free H_2O_2 can be produced in water.

Various solvents, generally consisting of water and/or alcohols, in combination with acid and/or halide promoters, have been used for the heterogeneously catalysed

direct synthesis of H_2O_2 . In the Hutchings group's previous studies on the direct synthesis of H_2O_2 ,³⁻⁵ reaction conditions have been standardised to allow differences in H_2O_2 yield to solely reflect differences in catalyst performance. The reaction parameters in these experiments were a 2.9 g H_2O /5.6 g methanol solvent mixture, temperature of 2°C , a reaction duration of 30 min and a 420 psi 5% H_2/CO_2 and 160 psi 5% O_2/CO_2 gas mix. The majority of work in the Hutchings group has focussed on achieving high yields of H_2O_2 in the absence of acid or halide promoters.

Lunsford and co-workers have utilised a water or ethanol solvent with the addition of chloride, bromide, hydrochloric acid and sulphuric acid promoters.⁶⁻⁹ Choudhary and co-workers utilised an aqueous medium acidified with sulphuric or phosphoric acid, in most cases with one or more halide promoter.¹⁰⁻¹⁹ Park and co-workers use a solution of methanol with dissolved NaBr .²⁰⁻³⁰ Biasi and co-workers generally use methanol in the absence of promoters,³¹⁻³⁷ but have also used acidified, bromide-promoted aqueous solutions.³⁸

In this work, the effect on the productivity and hydrogenation/decomposition rates of a 2.5 wt. % Au - 2.5 wt. % Pd / TiO_2 catalyst when reaction conditions are moved towards the use of water as a solvent and room temperature ($20 - 25^\circ\text{C}$) reactions are studied. This work also probes the effects of changing reactant gas ratios, total gas pressure and catalyst mass on the direct synthesis reaction, all of which are factors to consider when 'scaling up' the reaction from a small batch process. Furthermore, the effects of water quality (pH and dissolved ion concentration), in addition to moving to N_2/air as a diluent are studied, as these factors will also need to be considered for a potential practical implementation of H_2O_2 direct synthesis in a tap water stream using H_2 and O_2 produced by electrolytic or photocatalytic splitting of water, diluted with air.³⁹

These conditions studied in this work present a more environmentally friendly and economical reaction compared to the majority of aforementioned previously studied conditions as there are no energy demands for heating or cooling and the H_2O_2 requires no further extraction/purification. Using this work to help understand the effect of changing reaction parameters on all processes associated with the direct synthesis of H_2O_2 and identify challenges therein will allow for rational design of catalysts for optimal function in an aqueous / ambient temperature reaction condition.

3.2. Results and Discussion

3.2.1. Time-on-line studies for hydrogen peroxide synthesis and degradation using 2.5 wt. % Au-2.5 wt. % Pd/TiO₂ at 20°C - 25°C in varied solvent compositions

H₂O₂ synthesis activity and yield was determined at systematically varied reaction times at ambient temperatures (20°C - 25°C) in three different solvent compositions: water, water/methanol (2:1 ratio) and methanol. The results of these experiments are shown in terms of catalyst productivity in Figure 3.1 and in terms of H₂O₂ yield in Figure 3.2.

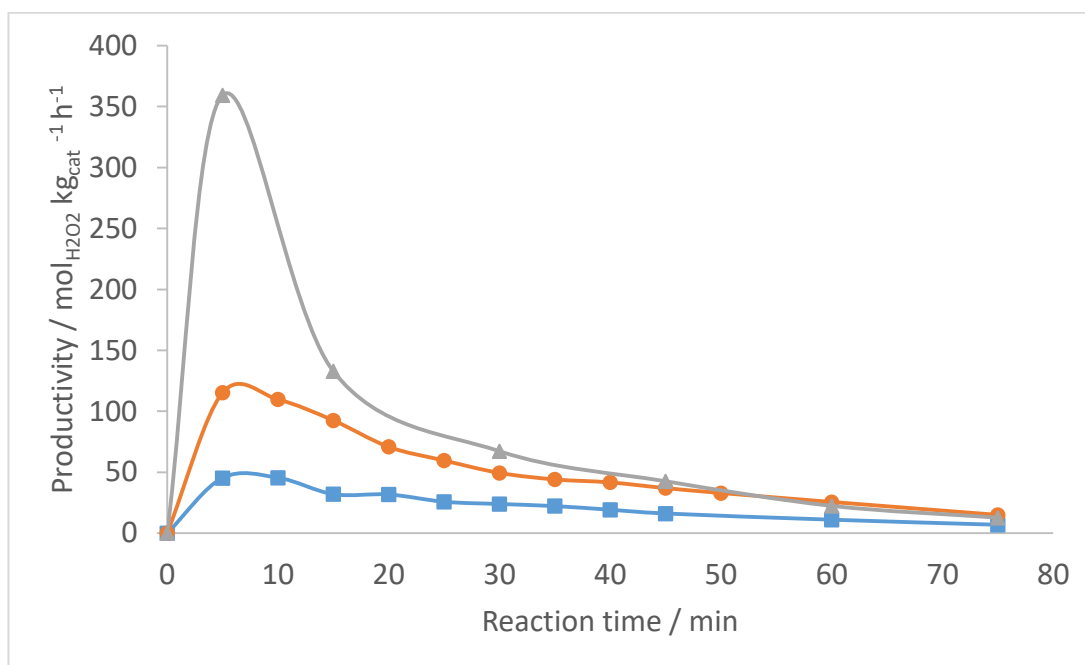


Figure 3.1 - Time on line H₂O₂ productivity in H₂O, 34% H₂O / 66% MeOH and MeOH solvent systems.

■ – H₂O, ● – 34% H₂O / 66% MeOH, ▲ - MeOH.

Conditions: Reaction time as indicated, 8.5 g solvent (as indicated), 100 mL autoclave, ambient temperature (20°C - 25°C), 1200 rpm, 10 mg 2.5 wt. % Au - 2.5 wt.% Pd/TiO₂ catalyst, 420 psi H₂/CO₂ + 160 psi O₂/CO₂.

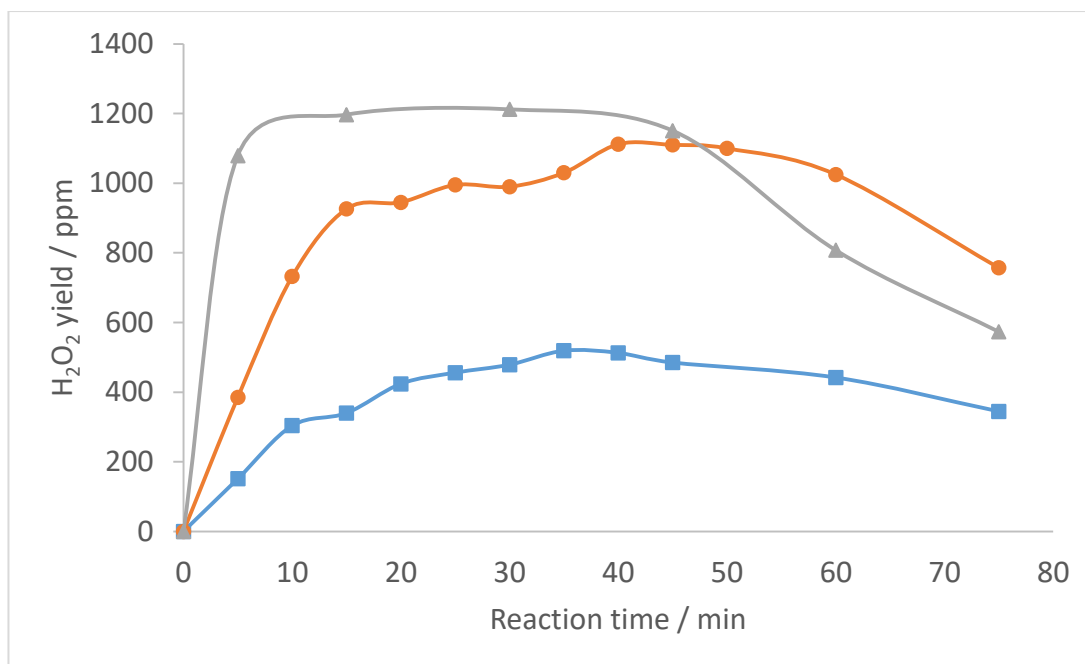


Figure 3.2 - Time on line H₂O₂ yield in H₂O, 34% H₂O / 66% MeOH and MeOH solvent systems.

■ – H₂O, ● – 34% H₂O / 66% MeOH, ▲ - MeOH.

Conditions: Reaction time as indicated, 8.5 g solvent (as indicated), 100 mL autoclave, ambient temperature (20°C - 25°C), 1200 rpm, 10 mg 2.5 wt. % Au - 2.5 wt.% Pd/TiO₂ catalyst, 420 psi H₂/CO₂ + 160 psi O₂/CO₂.

Figure 3.1 shows that the productivity is highest in each system at short reaction times as expected when the H₂ concentration will be highest and also the rates of H₂O₂ degradation will be minimal due to the low concentrations of H₂O₂ in the reaction mixtures. It is also clear that productivity is highest in a MeOH solvent and lowest in a H₂O solvent across the timescales investigated.

Figure 3.2 shows that reactions in H₂O have significantly lower peak yield than reactions in H₂O/MeOH or MeOH. It also appears that reactions in H₂O are proportionately less productive over shorter (0 – 15 min) timescales. In a MeOH solvent the majority (>85%) of maximum possible yield can be produced in the first 5 minutes of reaction, whereas in a H₂O solvent, approximately 30% of maximum yield is produced in the first 5 minutes of reaction. This is probably due to the greater solubility of H₂ in MeOH comparative to H₂O, which according to Henry's laws shows that hydrogen solubility is around an order of magnitude higher in MeOH compared to H₂O, with Henry's constant (H_{cp}) values at 20°C of $9.34 \times 10^{-3} \text{ mol atm}^{-1} \text{ L}^{-1}$ and

$8.04 \times 10^{-4} \text{ mol atm}^{-1} \text{ L}^{-1}$ respectively. Therefore in MeOH containing solvent compositions there is a high concentration of available H_2 at the start of the reaction, whereas in a H_2O only solvent there is a lower concentration of H_2 , thus the rate of H_2O_2 production is decreased due to mass transport limitations.

These observations indicate that the performance of the catalyst in the different solvent compositions is probably to be governed by gas solubility and mass transport effects.

The effect of gas solubility can also control the balance of the synthesis, hydrogenation and decomposition pathways. Hydrogenation and decomposition activity were similarly studied using systematically varied reaction times at ambient temperatures (20°C - 25°C) in water, water/methanol (2:1 ratio) and methanol solvent compositions. The results of these experiments are shown for decomposition in Figure 3.3 and net hydrogenation (total degradation less decomposition) in Figure 3.4.

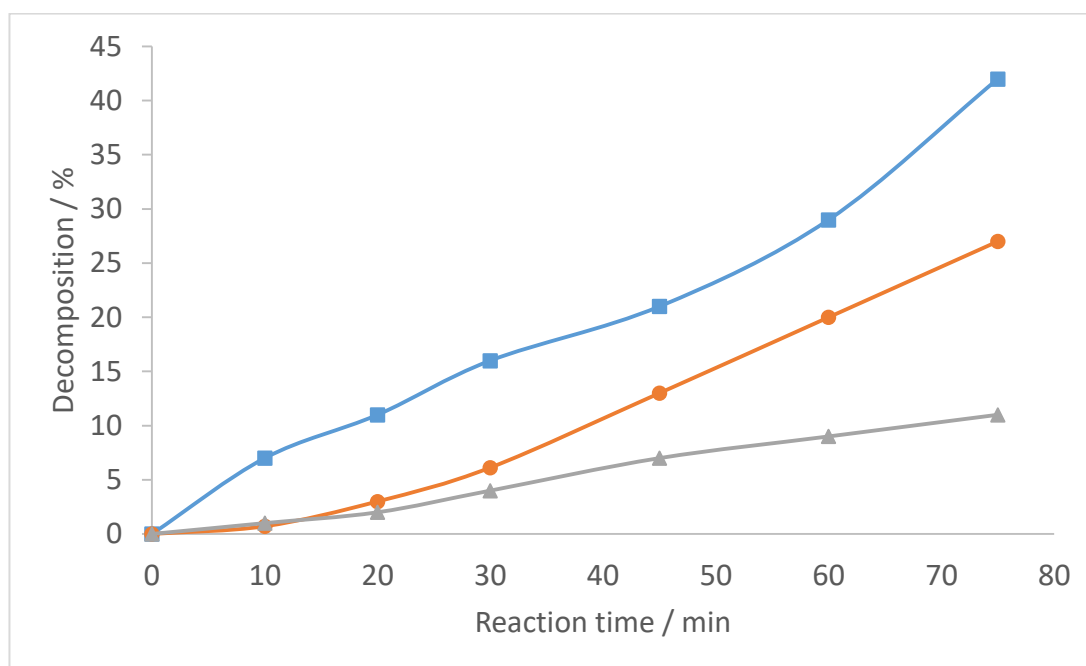


Figure 3.3 - Time on line decomposition in H_2O , 34% H_2O / 66% MeOH and MeOH solvent systems.

■ – H_2O , ● – 34% H_2O / 66% MeOH, ▲ - MeOH.

Conditions: Reaction time as indicated, 7.82 g solvent (as indicated) + 0.68 g 50% H_2O_2 solution, 100 mL autoclave, ambient temperature (20°C - 25°C), 1200 rpm, 10 mg 2.5 wt. % Au - 2.5 wt. % Pd/ TiO_2 catalyst, 420 psi O_2/CO_2 .

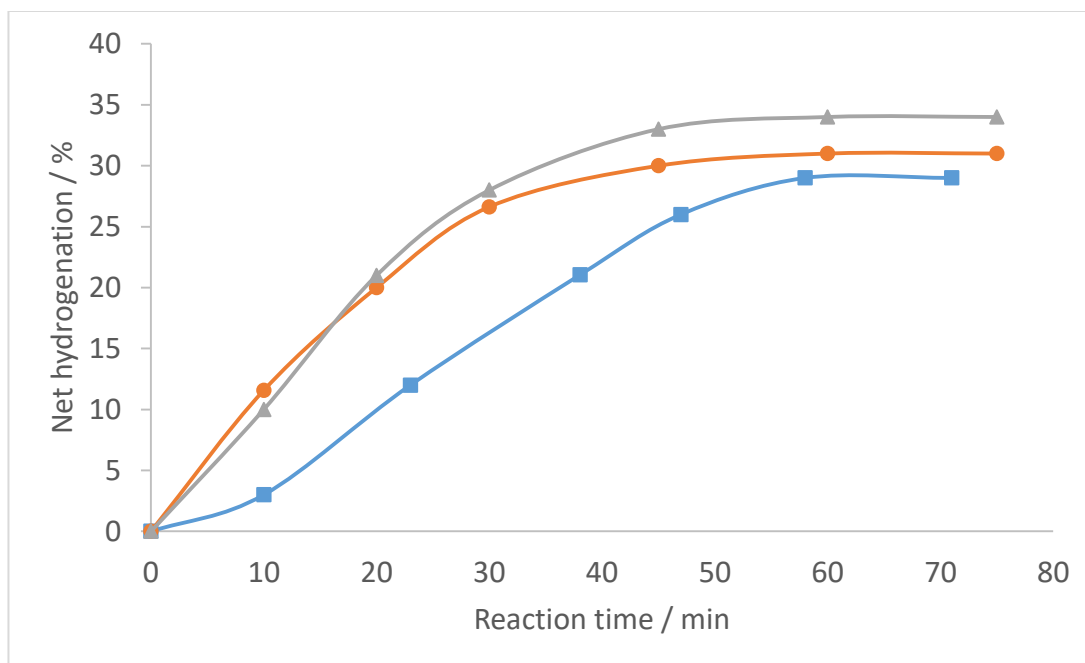


Figure 3.4 - Time on line net hydrogenation in H₂O, 34% H₂O / 66% MeOH and MeOH solvent systems.

■ – H₂O, ● – 34% H₂O / 66% MeOH, ▲ - MeOH.

Conditions: Reaction time as indicated, 7.82 g solvent (as indicated) + 0.68 g 50% H₂O₂ solution, 100 mL autoclave, ambient temperature (20°C - 25°C), 1200 rpm, 10 mg 2.5 wt. % Au - 2.5 wt.% Pd/TiO₂ catalyst, 420 psi H₂/CO₂.

For the decomposition reaction (Figure 3.3), it was observed that the relationship between the extent of decomposition and time is close to linear, with the least degree of decomposition in the MeOH solvent, followed by the H₂O/MeOH solvent and the greatest decomposition occurring in the H₂O solvent.

For hydrogenation (Figure 3.4), we see an inverse of the trend seen for decomposition, with the least extent of hydrogenation with respect to time in a H₂O solvent. MeOH and H₂O/MeOH solvent compositions appear to have very similar initial rates of hydrogenation, indicating that the addition of 66% methanol to H₂O reduces the mass transport limitations and the catalyst is most likely operating in the kinetic regime. These trends in hydrogenation activity are very likely due to the solubility of H₂ in the solvents; MeOH has greater hydrogen solubility, thus there is more available hydrogen for the hydrogenation reaction, leading to a faster initial rate and greater final extent of hydrogenation. The plots for hydrogenation plateau,

indicating that after an extended reaction the extent of hydrogenation becomes limited by the availability of hydrogen in solution, as the experimental procedure dictates that the reactor is charged with hydrogen only once at the start of the reaction. Therefore the rate of hydrogenation will decrease and eventually stop as the concentration of available hydrogen in solution decreases with time.

These observations indicate that when changing the reaction conditions for the direct synthesis, additional considerations need to be made in terms of catalyst design. If direct synthesis of H_2O_2 is to be successfully achieved in water as solvent, suppressing the decomposition reaction becomes an important factor in catalyst design, not only the suppression of the sequential hydrogenation, as has been the main focus in much of the previous research.^{3, 40-42}

3.2.2. The effect of temperature on hydrogen peroxide synthesis and degradation using 2.5 wt. % Au - 2.5 wt. % Pd/TiO₂ in H₂O

H_2O_2 yield and the activity of the two degradation processes, decomposition and hydrogenation, were determined for 30 minute reactions over a range of temperatures in a H_2O solvent system. These data are shown in Figure 3.5.

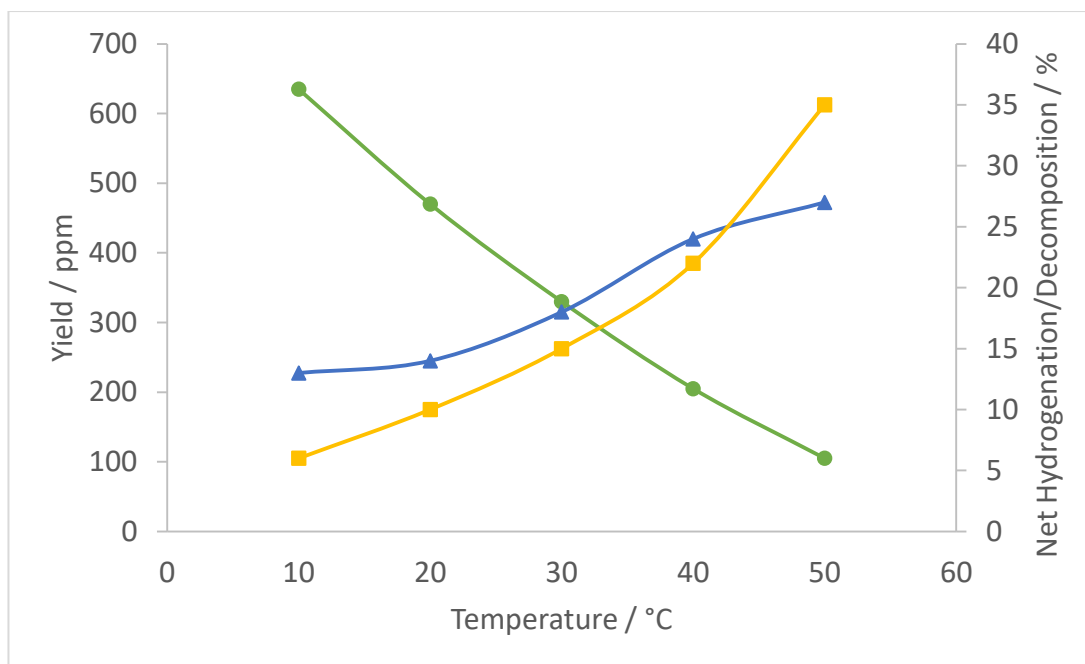


Figure 3.5 – The effect of temperature on yield, decomposition and net hydrogenation

● – Yield^[a], ■ – Decomposition^[b], ▲ - Net Hydrogenation^[c].

Conditions: 30 min reaction time, 50 mL autoclave, temperature as indicated, 1200 rpm, 10 mg 2.5 wt. % Au - 2.5 wt. % Pd/TiO₂ catalyst

[a]: 8.5 g H₂O solvent, 420 psi H₂/CO₂ + 160 psi O₂/CO₂

[b]: 7.82 g H₂O solvent + 0.68 g 50 wt. % H₂O₂, 420 psi O₂/CO₂

[c]: 7.82 g H₂O solvent + 0.68 g 50 wt. % H₂O₂, 420 psi H₂/CO₂

Yield was found to decrease significantly with increasing temperature in a relationship that is close to linear, this is tied to the fact that we observe an increase in both degradation processes with temperature. As temperature is increased, the extent of decomposition increases. The decomposition reaction only requires H₂O₂ as a reactant, therefore the increase in decomposition activity is most likely from an increase in the reaction rate which is caused by an increase in total energy of the system. Therefore the proportion of molecules with sufficiently high energy to react is greater when temperature is increased.

The extent of hydrogenation also increases with temperature, but does so to a lesser extent than degradation and appears to begin to plateau at higher temperatures. This is probably due to the fact that hydrogenation requires a reaction between H₂O₂ and dissolved H₂, of which there is a limited concentration, whereas decomposition requires no second reactant. The 'plateauing' of the extent of hydrogenation at higher

temperatures is most likely due to the decreasing solubility of H_2 with increasing temperature (see Section 3.2.6), which means there is a lesser concentration of H_2 in solution at high temperatures and thus less available reactant for the hydrogenation reaction. This decrease in available hydrogen at higher temperatures also contributes to decreased synthesis yield as there is less availability of reactant for the synthesis reaction, in addition to a greater rate of degradation for synthesised H_2O_2 .

3.2.3. The effect of varied $H_2O/MeOH$ solvent ratios on hydrogen peroxide synthesis and degradation using 2.5 wt. % Au - 2.5 wt. % Pd/ TiO_2 at 20°C

H_2O_2 synthesis yield and the extent of the two degradation processes, decomposition and hydrogenation, were determined for 30 minute reactions at 20°C over a range of H_2O and MeOH solvent compositions. These data are shown in Figure 3.6.

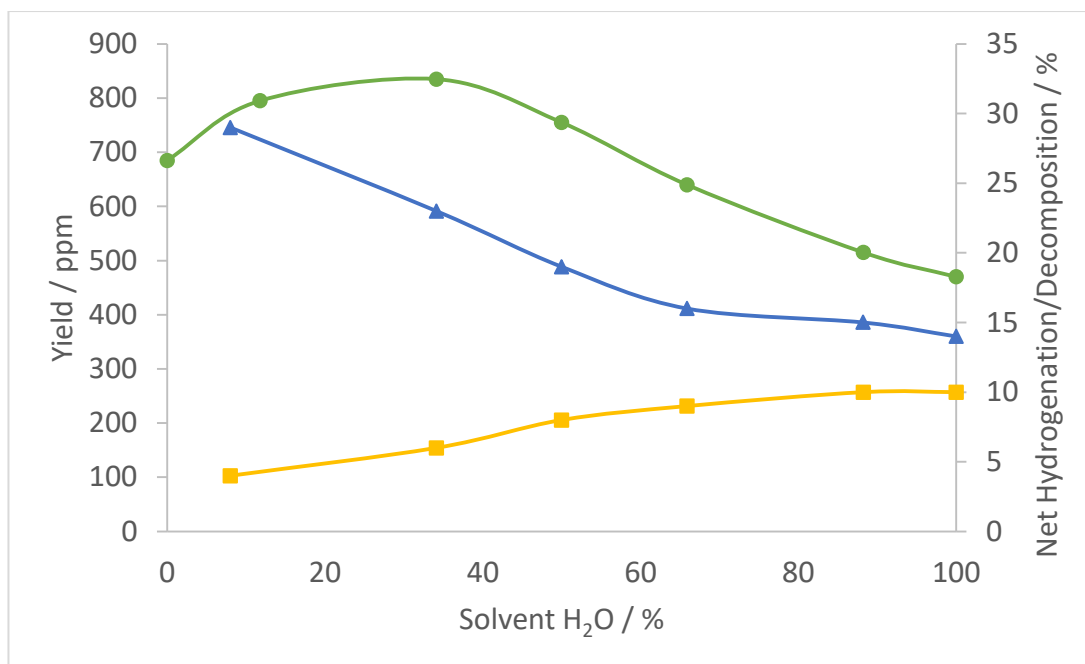


Figure 3.6 - The effect of solvent composition (H₂O/MeOH) on yield, decomposition and net hydrogenation.

● – Yield^[a], ■ – Decomposition^[b], ▲ - Net Hydrogenation^[c].

Conditions: 30 min reaction time, 50 mL autoclave, 20°C, 1200 rpm, 10 mg 2.5 wt. % Au - 2.5 wt. % Pd/TiO₂ catalyst, H₂O percentage of solvent as indicated (remainder MeOH)

[a]: 8.5 g solvent, 420 psi H₂/CO₂ + 160 psi O₂/CO₂

[b]: 7.82 g solvent + 0.68 g 50 wt. % H₂O₂, 420 psi O₂/CO₂

[c]: 7.82 g solvent + 0.68 g 50 wt. % H₂O₂, 420 psi H₂/CO₂

The extent of decomposition increases with an increasing H₂O content in the solvent and/or decreases with increasing MeOH content. Decomposition only involves H₂O₂ as a reactant, therefore the relative solubilities of H₂ and/or O₂ in the given solvent composition is assumed to have no effect. Therefore the reason for a decreased rate of decomposition of H₂O₂ in MeOH relative to H₂O is believed to be due to a stabilising effect of MeOH on H₂O₂ and/or a destabilising effect of H₂O.

The hydrogenation of H₂O₂ follows an opposite pattern to that of decomposition, increasing as the MeOH of the solvent increases. This is believed to be due to the increased solubility of H₂ in MeOH comparative to H₂O; this means there is a greater concentration of dissolved H₂ present in compositions with increased MeOH content and thus an increased rate of hydrogenation.

We observe a maximum measured yield of H₂O₂ in the 34% H₂O/66% MeOH composition, this is the solvent ratio used under 'standard conditions' of the Hutchings group which have previously been found to be optimal.⁴³ Moving to a greater proportion of MeOH decreases yield due to increased H₂ solubility allowing the hydrogenation of H₂O₂ to become a dominant process. Moving to a greater proportion of H₂O decreases yield due to less available dissolved H₂ limiting the rate of synthesis and an increased extent of H₂O₂ decomposition.

These results again highlight the need to design catalysts with reaction conditions in mind. In H₂O solvent, where H₂ availability is low compared to methanol rich solvent compositions, the hydrogenation and decomposition reactions occur with similar rate (600 mol kg_{cat}⁻¹ h⁻¹ net hydrogenation vs 450 mol kg_{cat}⁻¹ h⁻¹ decomposition) so catalyst design should focus on minimising both reactions equally. In MeOH rich solvent compositions the synthesis activity is increased due to the higher H₂ availability but as a consequence so is the H₂O₂ hydrogenation reaction. In a MeOH solvent the rates of hydrogenation are much higher than the rates of decomposition (790 mol kg_{cat}⁻¹ h⁻¹ net hydrogenation vs 110 mol kg_{cat}⁻¹ h⁻¹ decomposition) suggesting that when working at conditions with high hydrogen availability, de-convoluting the selective and unselective hydrogen activation is most important.

3.2.4. The effect of pressure and H₂/O₂ gas ratio on hydrogen peroxide synthesis using 2.5 wt. % Au - 2.5 wt. % Pd/TiO₂ at 20°C

H₂O₂ synthesis yield was determined for 30 minute reactions at 20°C in H₂O over a range of reactant gas compositions. There are two component gas feeds to the reactor, 5% H₂/CO₂ and 25% O₂/CO₂, therefore as the ratio of H₂ and O₂ (the 'reactant gasses') changes, so too does their total partial pressure and as such the partial pressure of CO₂ (the 'diluent gas'). It has been shown in previous studies from the Hutchings group⁴⁴ that CO₂ dissolves in a water (or water containing) solvent to form carbonic acid and act as an *in-situ* acid promotor. In the data presented in Figure 3.7, the partial pressure of CO₂ was not considered as the H₂O solvent will be saturated at all tested compositions, therefore the data solely reflects changes of H₂ and O₂ ratios.

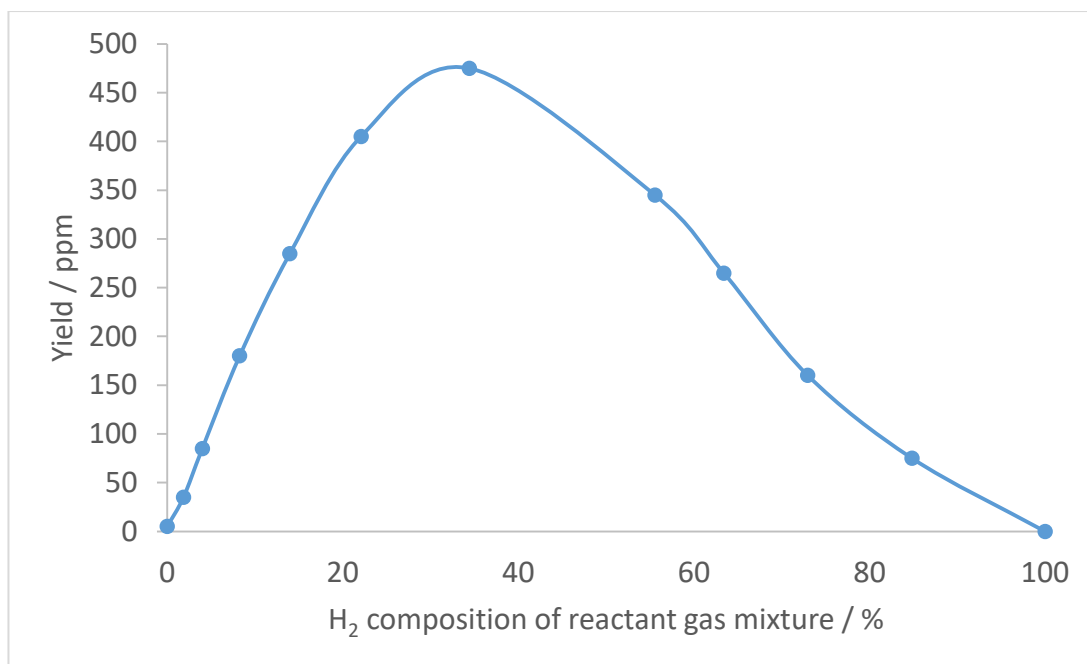


Figure 3.7 - The effect of H₂ partial pressure as a percentage of total reactant gas pressure on hydrogen peroxide synthesis yield.

Conditions: 30 min reaction time, 8.5 g H₂O solvent, 50 mL autoclave, 20°C, 1200 rpm, 10 mg 2.5 wt. % Au - 2.5 wt. % Pd/TiO₂ catalyst, 580 psi total pressure of H₂/CO₂ + O₂/CO₂, H₂ percentage of total (H₂ + O₂) pressure as indicated.

Figure 3.7 indicates that a peak yield of H₂O₂ is achieved at a gas composition of 34% H₂ 66% O₂ as partial pressures of total reactant gas pressure (*i.e.* ignoring diluent CO₂). At compositions consisting of less than 22% H₂, yield appears to increase close to linearly with increasing H₂ composition of the reactant gas mixture. The rate of H₂O₂ synthesis has previously been shown by Lunsford and co-workers⁹ to be first order with respect to H₂ concentration, therefore this suggests that system is operating under a kinetic regime and the rate of H₂O₂ synthesis is limited by the concentration of dissolved H₂ at these compositions. As there is very little deviation from linearity, this suggests that the subsequent degradation of H₂O₂ by hydrogenation is not highly active at these compositions.

Despite observing maximum yield at 34% H₂, we see a clear deviation from a linear increase in yield in response to an increase H₂ fraction in the reactant gas mixture. This suggests that either degradation via a hydrogenation pathway is more active at this composition or that the system is now operating in a mass transport limited

regime with respect to dissolved H_2 availability for H_2O_2 synthesis, or a combination of both of these factors.

At compositions above 34% H_2 , yield begins to decrease. Lunsford and co-workers⁹ also showed that the rate of H_2O_2 synthesis is zeroth order with respect to oxygen concentration, therefore a lower concentration of dissolved oxygen in solution should not limit the rate of synthesis if the system is in a kinetic regime; however the total availability of oxygen can limit the extent of H_2O_2 synthesis possible and therefore yield. A second factor contributing to lower H_2O_2 yields at high H_2 fractions is an increased rate of H_2O_2 degradation through hydrogenation. Previous studies within the Hutchings group have shown the hydrogenation reaction to be first order with respect to H_2 concentration and first order with respect H_2O_2 concentration.⁴⁵ Therefore at these majority H_2 gas compositions, the rate of hydrogenation will be increased and thus a greater proportion of synthesised H_2O_2 will be degraded *via* hydrogenation, leading to decreased yields.

H_2O_2 synthesis yield was also determined for 30 minute reactions at 20°C over a range of total pressures, using a constant reactant gas ratio of 34% H_2 / 66% O_2 , identical to that of 'standard conditions' defined in Chapter 2. These data are shown in Figure 3.8.

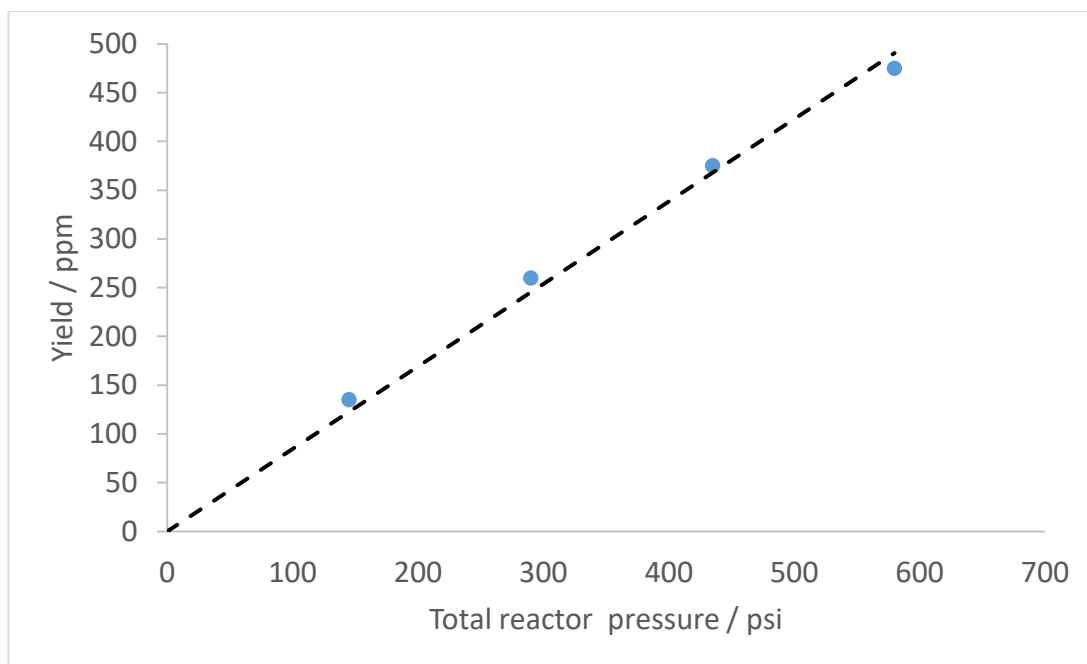


Figure 3.8 - The effect of total reactor pressure at a constant gas composition on hydrogen peroxide synthesis yield.

Conditions: 30 min reaction time, 8.5 g H₂O solvent, 50 mL autoclave, 20°C, 1200 rpm, 10 mg 2.5 wt. % Au - 2.5 wt. % Pd/TiO₂ catalyst, gas composition approximately 3.6% H₂, 6.9% O₂, balance CO₂, total pressure as indicated

Figure 3.8 shows that H₂O₂ yield is very close to directly proportional to total pressure at a given gas composition. This is to be expected if H₂O₂ synthesis is first order with respect to H₂ concentration and zeroth order with respect to O₂ as stated in the previously mentioned study by Hutchings and co-workers⁴⁵ for reactions performed in a 66% MeOH 34% H₂O medium. These data suggest that this rate equation also holds true for reactions in a pure H₂O solvent. It can therefore be assumed that in any commercial application of catalytic direct synthesis of H₂O₂ in H₂O, yield will increase close to linearly with dissolved hydrogen concentration (provided there is sufficient dissolved oxygen in solution), therefore at conditions of low dissolved hydrogen concentration (e.g. low hydrogen partial pressure), yields are very likely to be low.

3.2.5. The effect of catalyst mass on hydrogen peroxide synthesis and degradation using 2.5 wt. % Au - 2.5 wt. % Pd/TiO₂ at 20°C

H₂O₂ synthesis productivity and yield were determined for 30 minute reactions at 20°C over a range of catalyst masses. These data are shown in Figure 3.9 and Figure 3.10, respectively.

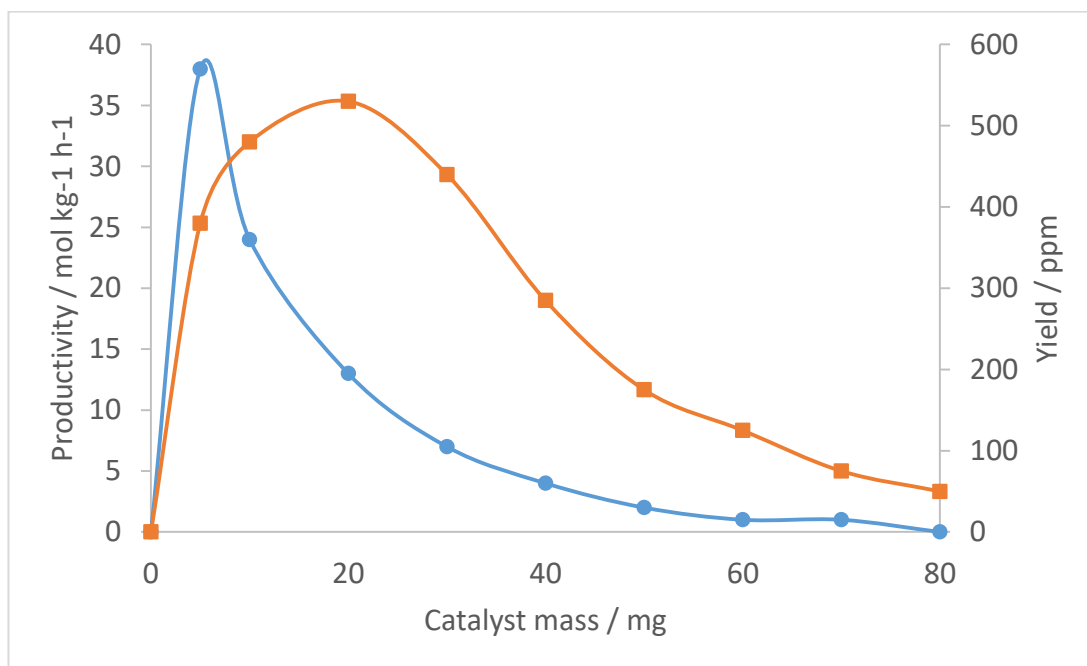


Figure 3.9 - The effect of catalyst mass on H₂O₂ synthesis productivity and yield.

● – Productivity, ■ – Yield

Conditions: 30 min reaction time, 8.5 g H₂O solvent, 50 mL autoclave, 20°C, 1200 rpm, 2.5 wt. % Au - 2.5 wt. % Pd/TiO₂ catalyst, mass as indicated, 420 psi H₂/CO₂ + 160 psi O₂/CO₂

Figure 3.9 shows that synthesis productivity peaks at a catalyst mass of 5 mg. Productivity is a measure of yield per unit mass per unit time, therefore a peak productivity is achieved at a low mass, as low mass of catalyst in the system can achieve a very high turnover rate as it is not limited by reactant availability or mass transfer limits, therefore is operating in a kinetic regime. The 2.5 wt. % Au - 2.5 wt. % Pd/TiO₂ catalyst is also active for the decomposition and hydrogenation of H₂O₂⁴⁴ therefore at low catalyst masses the extent of these degradation processes is decreased, and as such yields are less negatively impacted by subsequent degradation of produced hydrogen peroxide, leading to greater productivity.

In Figure 3.9 the results are also analysed in terms of absolute yield of H_2O_2 , this shows a peak yield at a catalyst loading of 20 mg. There is not a linear increase in yield when catalyst mass is increased up to 20 mg, this shows that the system is either limited by mass transport/availability of hydrogen or that the activity of degradation pathways increases to a greater extent with increasing catalyst mass than the activity of the synthesis reaction.

Figure 3.9 shows a marked decrease in productivity/yield at catalyst masses greater than 30 mg. As absolute yield is lower at catalyst masses ≥ 30 mg than those ≤ 20 mg, it must be assumed that degradation pathways are significantly more active at larger catalyst masses than at lower masses, however the synthesis reaction does not increase in activity to the same extent.

To fully examine the change in activity of the reaction pathways with catalyst mass, H_2O_2 degradation via hydrogenation and decomposition were also determined for 30 minute reactions at 20°C over a range of catalyst masses. These data are shown in Figure 3.10.

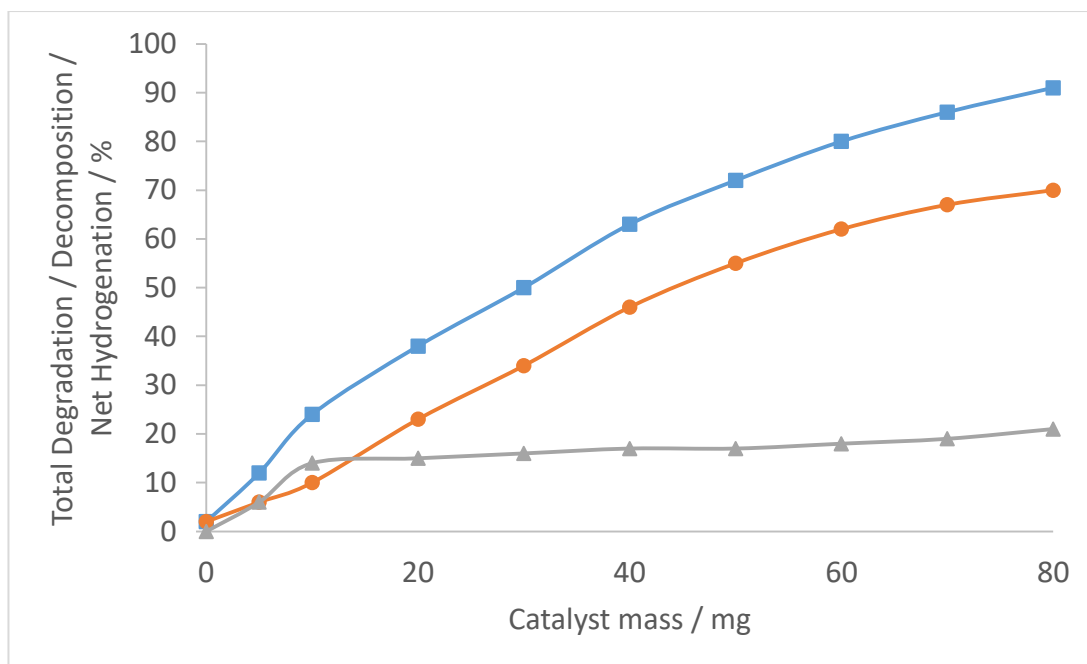


Figure 3.10 - The effect of catalyst mass on H₂O₂ decomposition, net hydrogenation and total degradation.

■ – Total Degradation^[a], ● – Decomposition^[b], ▲ - Net Hydrogenation^[a].

Conditions: 30 min reaction time, 7.82 g H₂O solvent + 0.68 g 50 wt.% H₂O₂ solution, 50 mL autoclave, 20°C, 1200 rpm, 2.5 wt. % Au - 2.5 wt. % Pd/TiO₂ catalyst, mass as indicated.

[a]: 420 psi H₂/CO₂

[b]: 420 psi O₂/CO₂

Figure 3.10 shows that the extent of degradation increases markedly with catalyst mass, reaching 91% degradation at a catalyst loading of 80 mg. This confirms that the decreased yields at high catalyst masses observed in Figure 3.9 are indeed due to a very high activity of the degradation pathways destroying a large fraction of the synthesised H₂O₂.

At catalyst masses ≤20 mg, the extent of hydrogenation and decomposition of H₂O₂ are comparable, however above these masses the extent of hydrogenation significantly plateaus, while the extent of degradation increases close to linearly with catalyst mass. Hydrogenation requires both H₂O₂ and dissolved H₂, therefore the rate of hydrogenation is likely to be limited due to the availability of hydrogen, and therefore an increase in active sites provided by increase in catalyst mass does little to increase the extent of hydrogenation. Conversely, decomposition requires solely

H₂O₂, therefore at a given concentration of H₂O₂ an increase in active sites provided by increase in catalyst mass leads to an increase in the rate of decomposition.

These findings highlight a need to design a catalyst which minimises the decomposition pathway, as this has been shown to be the dominant pathway by which H₂O₂ catalytically degrades in a water solvent at 20°C when a sufficient mass of catalyst is present. If a catalyst is designed with a significantly decreased decomposition activity, there is potential to produce high concentrations of H₂O₂ by performing reactions utilising an increased mass of catalyst.

3.2.6. Henry's constants for the solubility of H₂ and O₂ in H₂O and MeOH

Temperature dependant Henry's gas solubility constants for H₂O, MeOH and a 34% H₂O/66% MeOH mixture were generated from calculations based on Henry's law. For both H₂ and O₂ in H₂O, values for Henry's coefficients and temperature constants were obtained from the work of Sander.⁴⁶ For hydrogen in MeOH, temperature corrected Henry's coefficients were obtained from the empirical correlation put forward by Descamps *et al.*⁴⁷ For oxygen in MeOH, Henry's coefficients and temperature constants were calculated from experimental data presented by Fischer and Wilkin.⁴⁸ At a constant partial pressure of gas, gas solubility will be directly proportional to Henry's constants. There is potential for the total amount of dissolved gas in solution at a given time in a H₂O₂ direct synthesis reaction to be affected by other factors such as the nature of the diluent gas, the headspace of the reactor and reactor stirring dynamics.^{49, 50} In the previously presented datasets, these additional factors are constant, therefore while the exact Figures are estimations based on available data, the trends in Henry's constants displayed for H₂ (Figure 3.11) and O₂ (Figure 3.12) offer a useful lens through which to analyse the previous data sets.

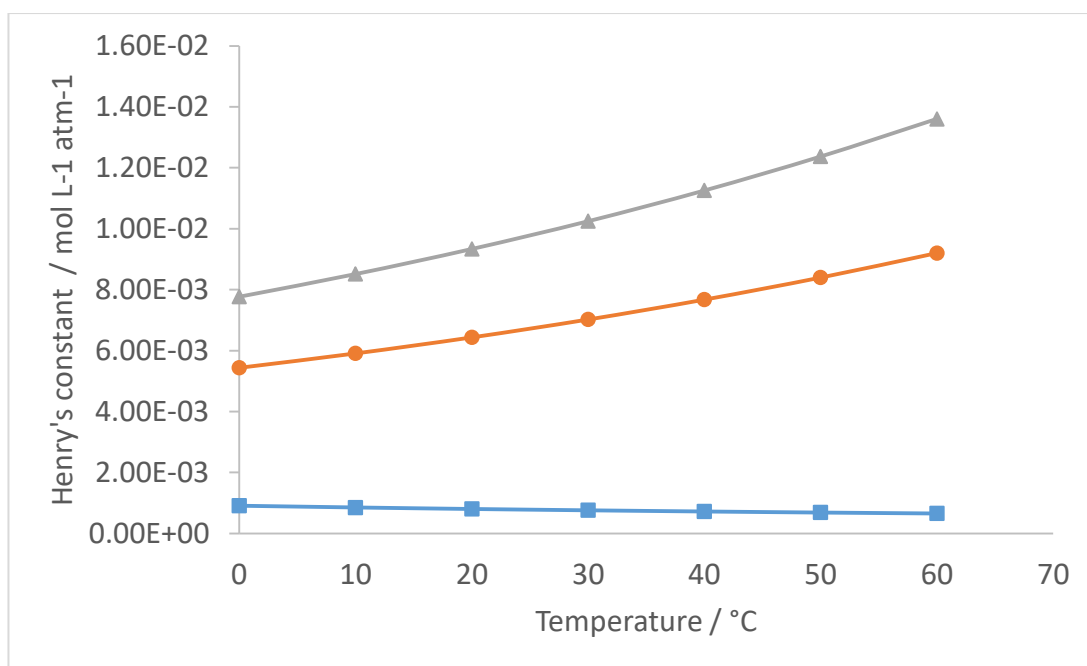


Figure 3.11 - Variation of Henry's constants (H_{CP}) with temperature for Hydrogen solubility in H_2O , 34% H_2O / 66% MeOH and MeOH solvent systems.

■ – H_2O , ● – 34% H_2O / 66% MeOH, ▲ - MeOH.

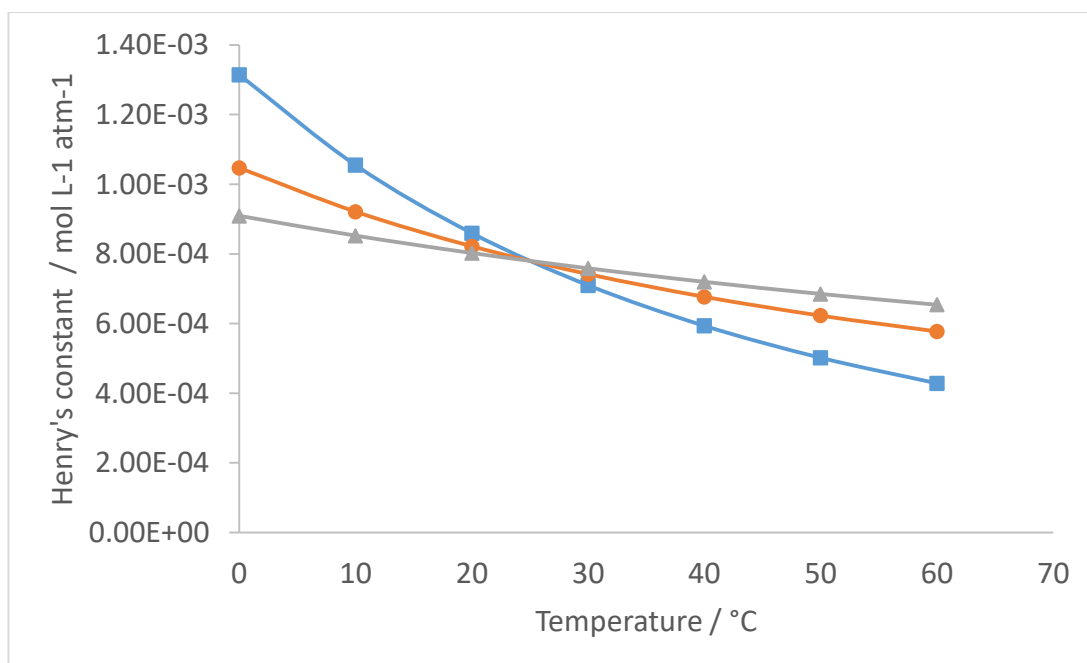


Figure 3.12 - Variation of Henry's constants (H_{CP}) with temperature for Oxygen solubility in H_2O , 34% H_2O / 66% MeOH and MeOH solvent systems.

■ – H_2O , ● – 34% H_2O / 66% MeOH, ▲ - MeOH.

Figure 3.11 compares the solubility of H₂ in the three solvent compositions and shows that H₂ solubility is around an order of magnitude higher in MeOH compared to H₂O, with Henry's constant (H_{CP}) values at 20°C of $9.34 \times 10^{-3} \text{ mol atm}^{-1} \text{ L}^{-1}$ and $8.04 \times 10^{-4} \text{ mol atm}^{-1} \text{ L}^{-1}$ respectively. This explains the significantly greater rates of H₂O₂ synthesis and hydrogenation – both processes in which the rate depends on the concentration of dissolved H₂ – in MeOH containing solvent compositions relative to H₂O. The solubility of H₂ in H₂O was found to decrease with increasing temperatures, explaining one factor in the observed decrease in yield of H₂O₂ with increasing temperature and the reason for the 'plateauing' of hydrogenation at higher temperatures, as shown in Section 3.2.2.

Figure 3.12 shows that O₂ solubility shows far less variance between H₂O and MeOH when compared to H₂ and in fact at *c.a.* 25°C the O₂ solubilities are identical for the different solvents. Therefore any differences in behaviour between experiments performed in H₂O and MeOH are likely to be solely due to differences in H₂ concentration.

3.2.7. The effect of solution pH on hydrogen peroxide synthesis and degradation using 2.5 wt. % Au - 2.5 wt. % Pd/TiO₂ at 20°C

The effect of acid addition has previously been studied in a 66% MeOH 34% H₂O solvent composition at 2°C by Hutchings and co-workers,⁴² however no studies have been performed in a purely aqueous reaction media or at ambient temperature. Using AuPd/TiO₂, synthesis, decomposition and hydrogenation reactions were studied at a range of solution pHs in H₂O at 20°C; these data are shown in Figure 3.13. The pH of the reaction solution was tuned by the addition of an appropriate amount of concentrated HNO₃ or NaOH solution to achieve pH levels less than or greater than 7, respectively. The addition of halides was deliberately avoided as these species are known to alter the performance of the catalyst.^{15, 17, 18, 42}

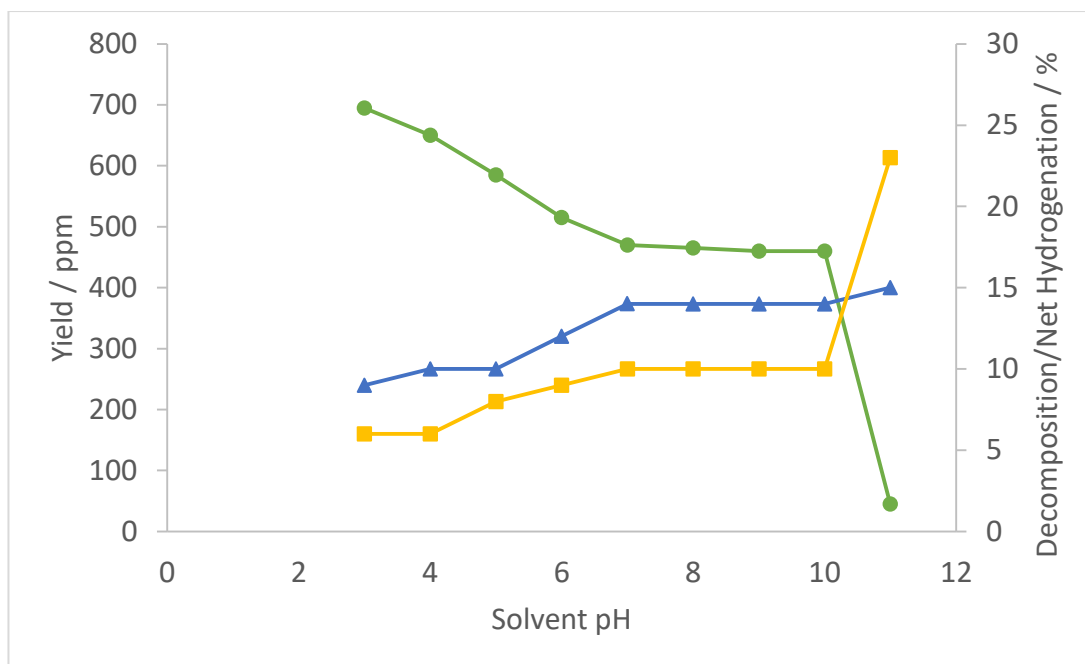


Figure 3.13 – The effect of pre-reaction solvent pH on H₂O₂ synthesis yield, decomposition and net hydrogenation

● – Yield^[a], ■ – Decomposition^[b], ▲ - Net Hydrogenation^[c].

Conditions: 30 min reaction time, 50 mL autoclave, 20°C, 1200 rpm, 10 mg 2.5 wt. % Au - 2.5 wt. % Pd/TiO₂ catalyst, pH adjusted as indicated

[a]: 8.5 g H₂O solvent, 420 psi H₂/CO₂ + 160 psi O₂/CO₂

[b]: 7.82 g H₂O solvent + 0.68 g 50 wt. % H₂O₂, 420 psi O₂/CO₂

[c]: 7.82 g H₂O solvent + 0.68 g 50 wt. % H₂O₂, 420 psi H₂/CO₂

Decreasing solvent pH through the addition of acid increases H₂O₂ and decreases degradation via both decomposition and hydrogenation. Similar trends have been shown in previous literature for an Au-Pd/MgO catalyst in a H₂O / MeOH solvent composition⁴² and for a Pd/SiO₂ catalyst in ethanol.⁹ The 2.5 wt. % Au - 2.5 wt. % Pd/TiO₂ catalyst was found to be stable to reactions performed in a solvent of pH 3 (0.001M HNO₃). This was confirmed by consistent catalyst activity upon recovery and re-use of the catalyst and MP-AES analysis of the reaction solution showing an absence of dissolved Au or Pd.

Increasing solvent pH has little effect on yield or either degradation process until a pH of 10 is exceeded, at which condition a significantly decreased yield and increased decomposition of hydrogen peroxide is observed.

The mechanism(s) through which acid addition decreases degradation and increases yield are not agreed upon. Early studies by Pospelova and co-workers^{51, 52} showed that acid promoters were necessary to achieve high yields with supported Pd catalysts, with the rationale that the decomposition pathway is base-catalysed, thus acid addition mitigates degradation via decomposition. Choudhary and co-workers¹² further showed that non-halide acids give a moderate decrease in the activity degradation pathways in reactions using a Pd/C catalyst and thus an increase in yield, however leaching of Pd was observed at concentrations above 0.05 M H₂SO₄ or 0.3M H₃PO₄.

Lunsford and co-workers⁹ showed that in an ethanol solvent, no H₂O₂ is produced with use of a Pd/SiO₂ catalyst in the absence of acid promoters, but significant yields are produced above 1M H₂SO₄. It is argued that base catalysed degradation and the abatement of such is only a minor factor in the promotion effect seen from acid addition. Lunsford states that in the aforementioned reaction in the absence of acidic promoters, H₂ is consumed through combustion, but no H₂O₂ is produced; acid addition vastly reduces the extent of combustion and allows for the synthesis of H₂O₂. Lunsford states that the exact role of protons is unclear, but that they play “a very positive but largely indirect role” in the direct synthesis reaction, possibly due to influencing the electronic state of surface palladium atoms on the catalyst.

Strukul and co-workers⁵³ have put forward a mechanism in which protons are directly involved in the direct synthesis of hydrogen peroxide on Pd surfaces. They propose that O₂ first non-dissociatively chemisorbs on the surface, followed by reaction with a proton to form an OOH⁺ surface intermediate, which then reacts with H₂ in solution to form H₂O₂ and regenerate a proton.

More recently Flaherty and co-workers⁵⁴ have proposed a reaction mechanism for the direct synthesis of hydrogen peroxide over Pd clusters which proceeds via heterolytic reaction pathways involving successive proton then electron transfer, first to surface bound O₂ to form OOH intermediates, then again to these intermediates to form H₂O₂.

Therefore both Strukul and Flaherty reject the previously accepted Langmuir-Hinshelwood style mechanism outlined by Hutchings and co-workers⁴⁰ in which H₂ adsorbs and dissociates on the surface where it reacts with adsorbed O₂ to first form an OOH intermediate, then to form H₂O₂. As protons are directly involved in the synthesis of H₂O₂ in Strukul and Flaherty’s proposed mechanisms, it follows that a decrease in pH, *i.e.* an increase in the concentration of protons in solution, will increase the rate of synthesis and thus achieve a greater yield of H₂O₂ and vice versa.

3.2.8. The effect of dissolved ions on hydrogen peroxide synthesis using 2.5 wt. % Au - 2.5 wt. % Pd/TiO₂ at 20°C

For potential commercial implementations of the direct synthesis of H₂O₂ in H₂O, it may be beneficial to produce H₂O₂ directly in tap water, rather than have a necessary distillation/de-ionisation of water step. Therefore the effects of common ions found in tap water on the direct synthesis of H₂O₂ was investigated. Table 3.1 shows the average and upper acceptable limit concentrations of some common tap water ions, which were used to guide the ranges of ion concentrations investigated.

Table 3.1 – Average and acceptable limit concentrations of common dissolved ions in drinking water, as defined by Welsh Water.⁵⁵

Ion	Average concentration / mg L⁻¹	Limit concentration / mg L⁻¹
Sodium	18	200
Chloride	21	250
Sulfate	34	250
Nitrate	8	50
Iron	0.014	0.2
Phosphorus	0.65	2.2

The effect of the ions quantified in Table 3.1 and other ions commonly found in tap water on the hydrogen peroxide synthesis and total degradation reactions were studied, as shown in Figures 3.14 - 3.24.

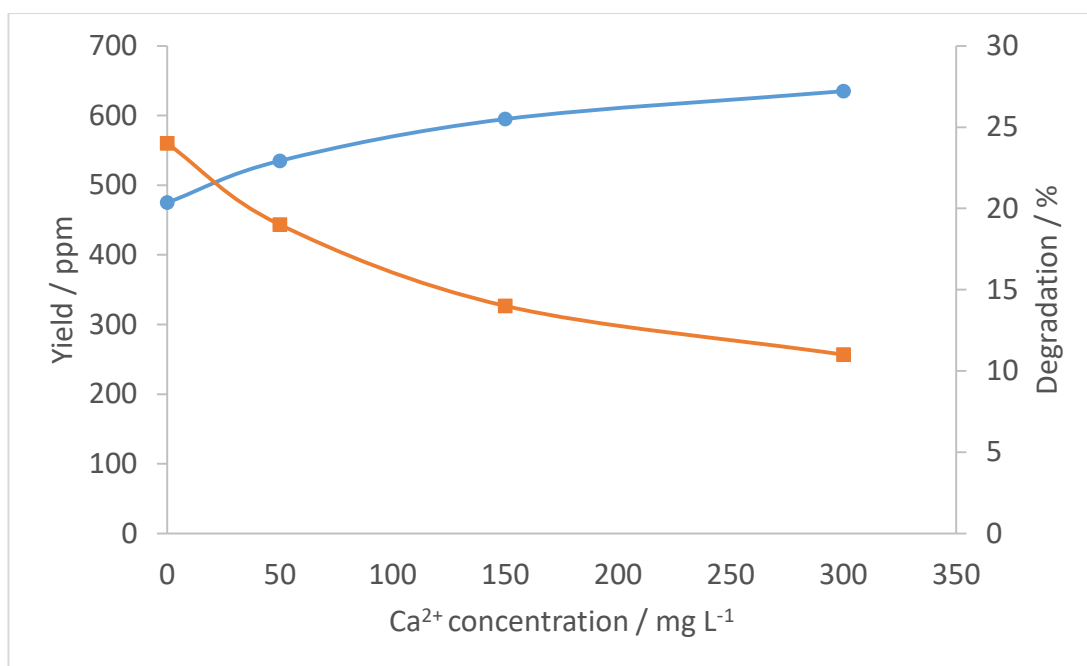


Figure 3.14 – The effect of Ca²⁺ (as CaCl₂) concentration on H₂O₂ synthesis yield and total degradation.

● – Yield^[a], ■ – Degradation^[b]

Conditions: 30 min reaction time, 50 mL autoclave, 20°C, 1200 rpm, 10 mg 2.5 wt. % Au - 2.5 wt. % Pd/TiO₂ catalyst

[a]: 8.5 g H₂O solvent, 420 psi H₂/CO₂ + 160 psi O₂/CO₂

[b]: 7.82 g H₂O solvent + 0.68 g 50 wt. % H₂O₂, 420 psi H₂/CO₂

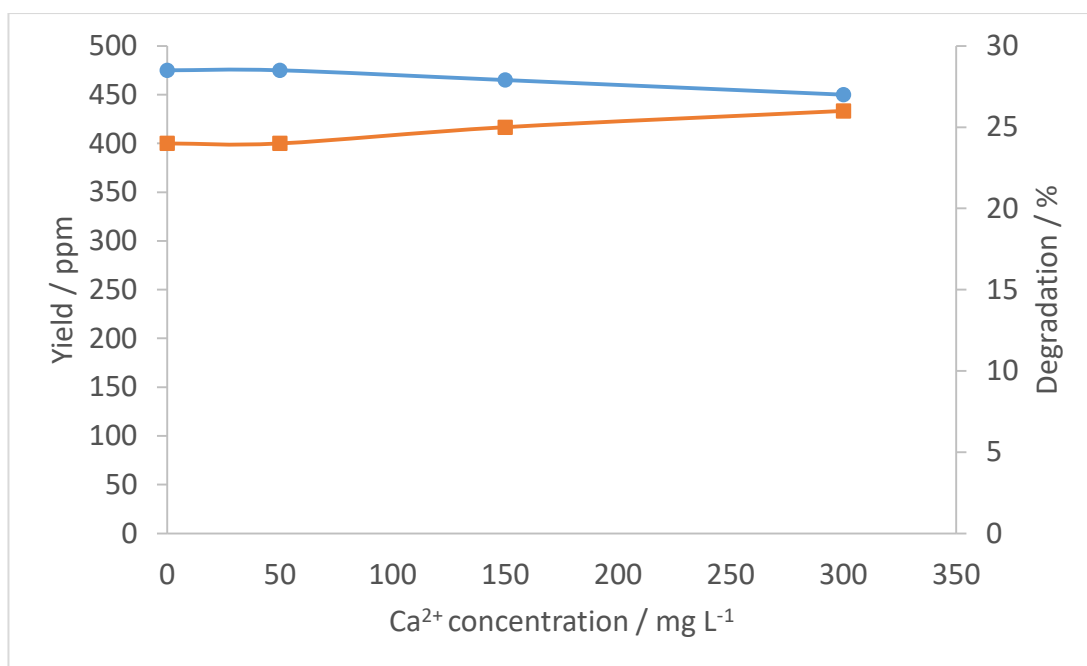


Figure 3.15 – The effect of Ca²⁺ (as Ca(NO₃)₂) concentration on H₂O₂ synthesis yield and total degradation.

● – Yield^[a], ■ – Degradation^[b]

Conditions: 30 min reaction time, 50 mL autoclave, 20°C, 1200 rpm, 10 mg 2.5 wt. % Au - 2.5 wt. % Pd/TiO₂ catalyst

[a]: 8.5 g H₂O solvent, 420 psi H₂/CO₂ + 160 psi O₂/CO₂

[b]: 7.82 g H₂O solvent + 0.68 g 50 wt. % H₂O₂, 420 psi H₂/CO₂

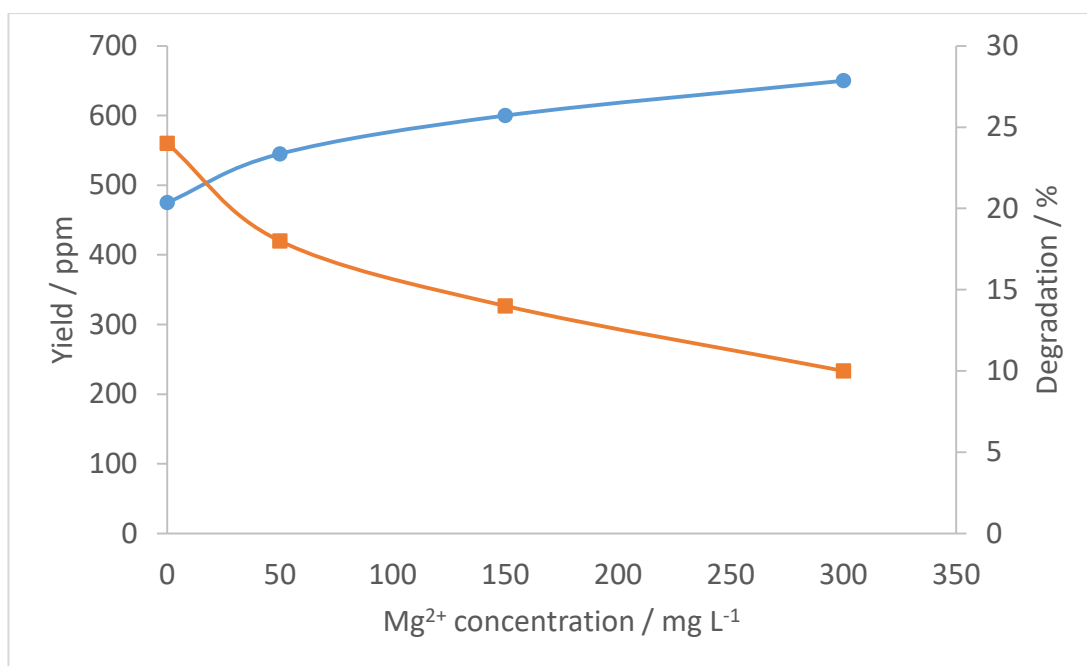


Figure 3.16 – The effect of Mg²⁺ (as MgCl₂) concentration on H₂O₂ synthesis yield and total degradation.

● – Yield^[a], ■ – Degradation^[b]

Conditions: 30 min reaction time, 50 mL autoclave, 20°C, 1200 rpm, 10 mg 2.5 wt. % Au - 2.5 wt. % Pd/TiO₂ catalyst

[a]: 8.5 g H₂O solvent, 420 psi H₂/CO₂ + 160 psi O₂/CO₂

[b]: 7.82 g H₂O solvent + 0.68 g 50 wt. % H₂O₂, 420 psi H₂/CO₂

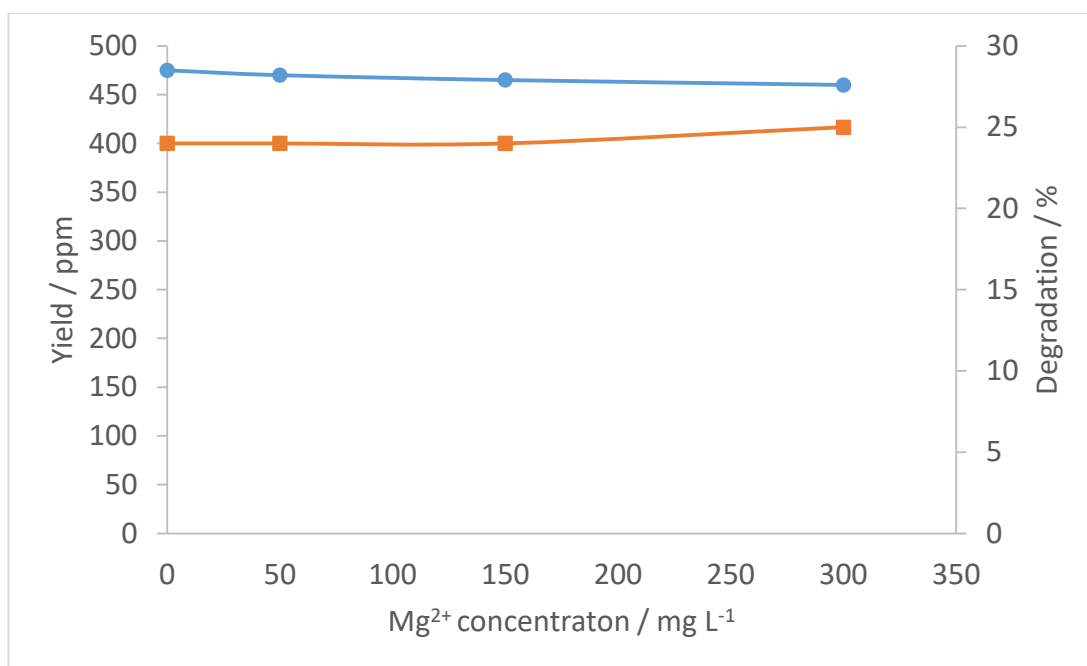


Figure 3.17 – The effect of Mg²⁺ (as Mg(NO₃)₂) concentration on H₂O₂ synthesis yield and total degradation.

● – Yield^[a], ■ – Degradation^[b]

Conditions: 30 min reaction time, 50 mL autoclave, 20°C, 1200 rpm, 10 mg 2.5 wt. % Au - 2.5 wt. % Pd/TiO₂ catalyst

[a]: 8.5 g H₂O solvent, 420 psi H₂/CO₂ + 160 psi O₂/CO₂

[b]: 7.82 g H₂O solvent + 0.68 g 50 wt. % H₂O₂, 420 psi H₂/CO₂

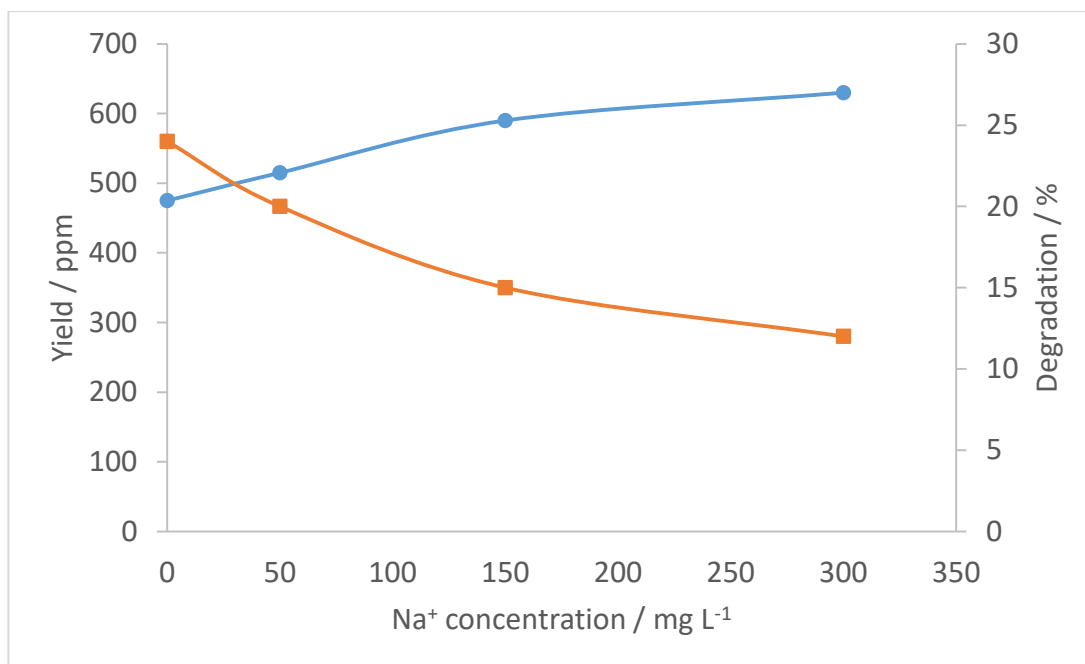


Figure 3.18 – The effect of Na⁺ (as NaCl) concentration on H₂O₂ synthesis yield and total degradation.

● – Yield^[a], ■ – Degradation^[b]

Conditions: 30 min reaction time, 50 mL autoclave, 20°C, 1200 rpm, 10 mg 2.5 wt. % Au - 2.5 wt. % Pd/TiO₂ catalyst

[a]: 8.5 g H₂O solvent, 420 psi H₂/CO₂ + 160 psi O₂/CO₂

[b]: 7.82 g H₂O solvent + 0.68 g 50 wt. % H₂O₂, 420 psi H₂/CO₂

The data displayed in Figures 3.14 through 3.18 indicate that an increase in the concentration of dissolved alkali metal chlorides has the effect of significantly increasing H₂O₂ yield and decreasing extent of degradation. Conversely an increased concentration of dissolved alkali metal nitrates has the effect of modestly decreasing H₂O₂ yield and decreasing extent of degradation. The effect on the direct synthesis observed by the addition of CaCl₂, MgCl₂ and NaCl is almost identical suggesting that the metal ions either have no effect on the reaction or affect the reaction in an analogous manner to each other.

The use of chloride (and other halides) as a promoter for the synthesis of hydrogen peroxide is widely reported and utilised by many groups. Halides act to stabilise the O-O bond, both in the surface OOH species, which serves to increase the rate of synthesis and in produced H₂O₂, which reduces the rate of degradation. The combined effect of these processes is an increase in H₂O₂ yield.^{9, 17, 18, 20, 42}

The effect of nitrate on the direct synthesis of hydrogen peroxide has not previously been investigated. From the above data it cannot be conclusively determined whether the modest decrease in yield and increase in degradation seen when alkali metal nitrate salts are added to the reaction is due to effects rising from the alkali metal ions, nitrate ions or both.

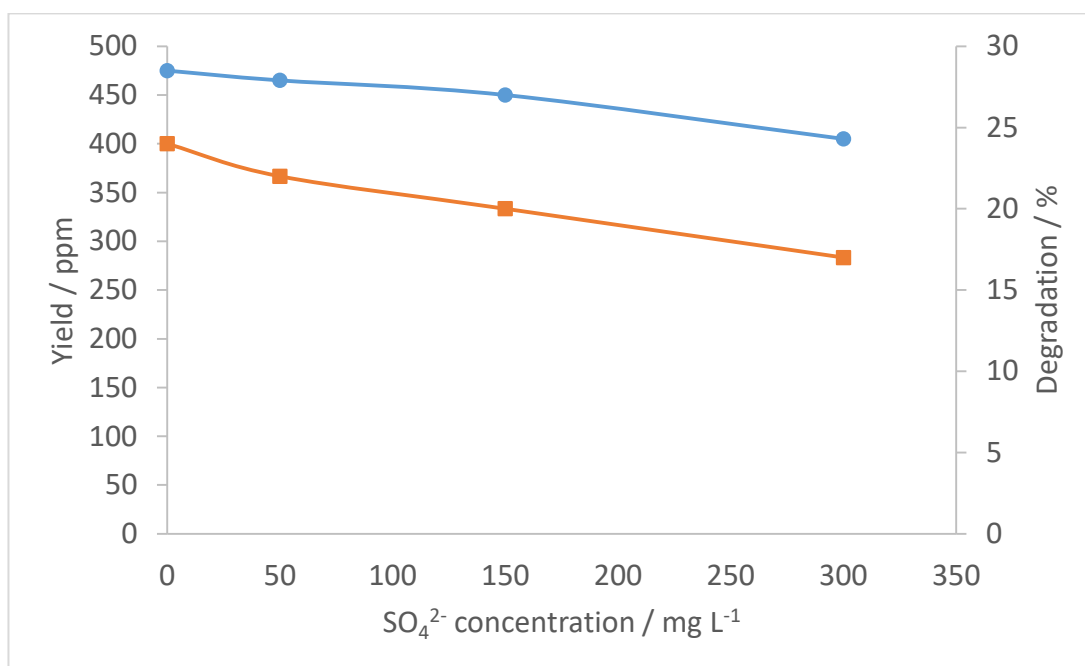


Figure 3.19 – The effect of SO₄²⁻ (as CaSO₄) concentration on H₂O₂ synthesis yield and total degradation.

● – Yield^[a], ■ – Degradation^[b]

Conditions: 30 min reaction time, 50 mL autoclave, 20°C, 1200 rpm, 10 mg 2.5 wt. % Au - 2.5 wt. % Pd/TiO₂ catalyst

[a]: 8.5 g H₂O solvent, 420 psi H₂/CO₂ + 160 psi O₂/CO₂

[b]: 7.82 g H₂O solvent + 0.68 g 50 wt. % H₂O₂, 420 psi H₂/CO₂

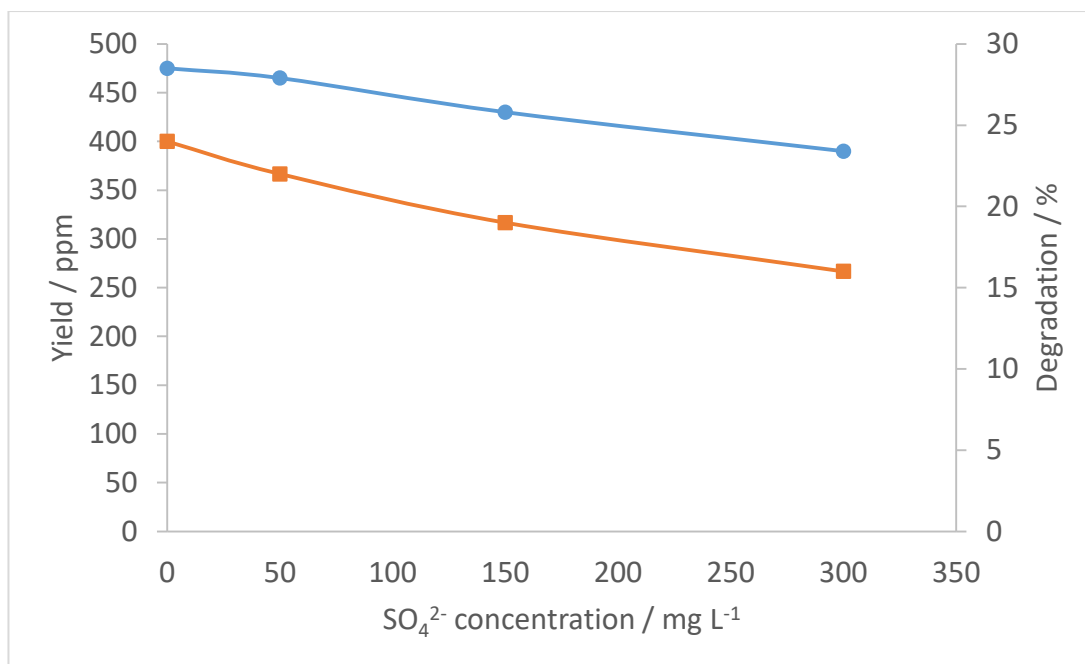


Figure 3.20 – The effect of SO₄²⁻ (as MgSO₄) concentration on H₂O₂ synthesis yield and total degradation.

● – Yield^[a], ■ – Degradation^[b]

Conditions: 30 min reaction time, 50 mL autoclave, 20°C, 1200 rpm, 10 mg 2.5 wt. % Au - 2.5 wt. % Pd/TiO₂ catalyst

[a]: 8.5 g H₂O solvent, 420 psi H₂/CO₂ + 160 psi O₂/CO₂

[b]: 7.82 g H₂O solvent + 0.68 g 50 wt. % H₂O₂, 420 psi H₂/CO₂

The data displayed in Figures 3.19 and 3.20 shows a concomitant decrease in yield and degradation activity with the addition of alkali metal sulfate salts. Again we see no significant difference in the behaviour of Ca²⁺ and Mg²⁺ salts, suggesting that any effect of these ions on the direct synthesis reactions is analogous. The effects of sulfate salts strongly suggests poisoning of the catalyst; platinum group metal poisoning by sulphur is a well-documented effect⁵⁶ and it is known that Pd is vital for the activity of hydrogen peroxide production catalysts.^{2, 57, 58} These data suggest that use of Pd-based catalysts for the direct synthesis of H₂O₂ in a water stream containing high concentrations of sulphurous compounds may not be feasible and that catalysts would require regular regeneration to remove sulfur (for example by heating under H₂) if used in such an environment.⁵⁹

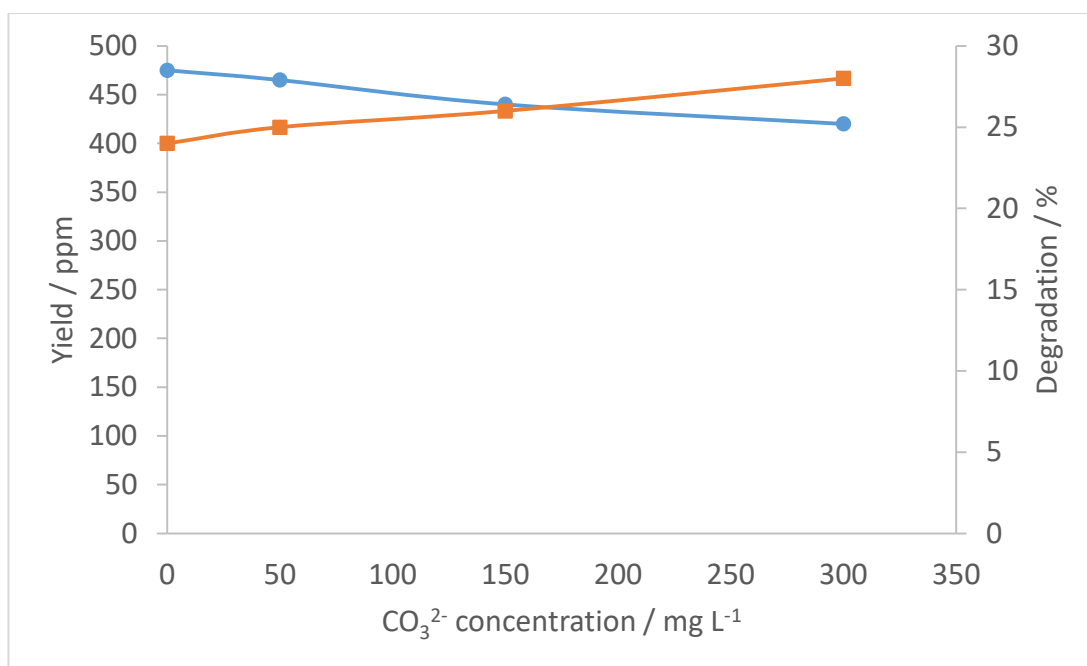


Figure 3.21 – The effect of CO₃²⁻ (as K₂CO₃) concentration on H₂O₂ synthesis yield and total degradation.

● – Yield^[a], ■ – Degradation^[b]

Conditions: 30 min reaction time, 50 mL autoclave, 20°C, 1200 rpm, 10 mg 2.5 wt. % Au - 2.5 wt. % Pd/TiO₂ catalyst

[a]: 8.5 g H₂O solvent, 420 psi H₂/CO₂ + 160 psi O₂/CO₂

[b]: 7.82 g H₂O solvent + 0.68 g 50 wt. % H₂O₂, 420 psi H₂/CO₂

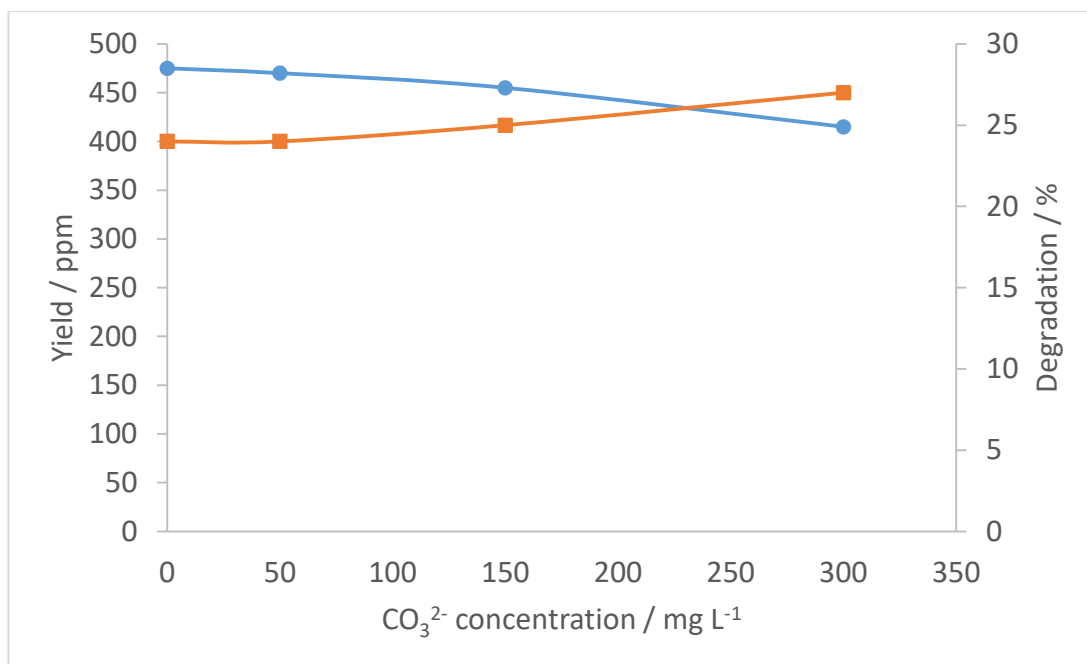


Figure 3.22 – The effect of CO₃²⁻ (as CaCO₃) concentration on H₂O₂ synthesis yield and total degradation.

● – Yield^[a], ■ – Degradation^[b]

Conditions: 30 min reaction time, 50 mL autoclave, 20°C, 1200 rpm, 10 mg 2.5 wt. % Au - 2.5 wt. % Pd/TiO₂ catalyst

[a]: 8.5 g H₂O solvent, 420 psi H₂/CO₂ + 160 psi O₂/CO₂

[b]: 7.82 g H₂O solvent + 0.68 g 50 wt. % H₂O₂, 420 psi H₂/CO₂

The data displayed in Figures 3.21 and 3.22 indicate that the addition of carbonate salts have the effect of decreasing hydrogen peroxide production and increasing degradation activity. This is probably due to the basic nature of carbonate increasing the pH of the reaction media. The deleterious effects of an increase in pH on the direct synthesis reaction has previously been discussed in Section 3.2.7.

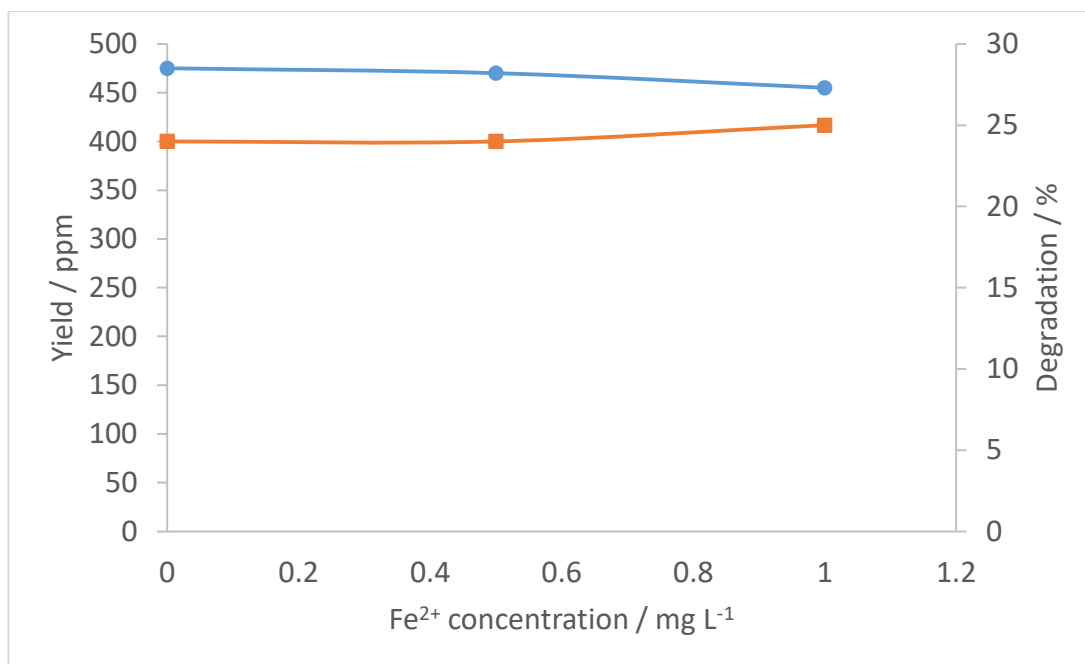


Figure 3.23 – The effect of Fe²⁺ (as FeCl₂) concentration on H₂O₂ synthesis yield and total degradation.

● – Yield^[a], ■ – Degradation^[b]

Conditions: 30 min reaction time, 50 mL autoclave, 20°C, 1200 rpm, 10 mg 2.5 wt. % Au - 2.5 wt. % Pd/TiO₂ catalyst

[a]: 8.5 g H₂O solvent, 420 psi H₂/CO₂ + 160 psi O₂/CO₂

[b]: 7.82 g H₂O solvent + 0.68 g 50 wt. % H₂O₂, 420 psi H₂/CO₂

Figure 3.23 shows that concentrations of 1 mg L⁻¹ or below of iron (greater than the concentration that is acceptable in tap water) has only a minor effect on the direct synthesis reaction, slightly increasing degradation and thus decreasing yield. As previously discussed, chloride ions serve to decrease degradation of H₂O₂ and increase yield, however as shown in Figures 3.14 and 3.15, at the concentrations <2 mg L⁻¹ these effects would be very slight or negligible.

The use of homogeneous ferrous iron in conjunction with H₂O₂ as “Fenton’s chemistry”, an umbrella term that describes the reaction between H₂O₂ and Fe²⁺ to form OH[•] and OOH[•] radicals, which then can act as powerful oxidants.⁶⁰ It is possible that addition of Fe²⁺ to the reaction solution at greater concentrations would result in a greater increase in degradation and decrease in yield, however at concentrations of iron which are acceptable in tap water, the effect is very small.

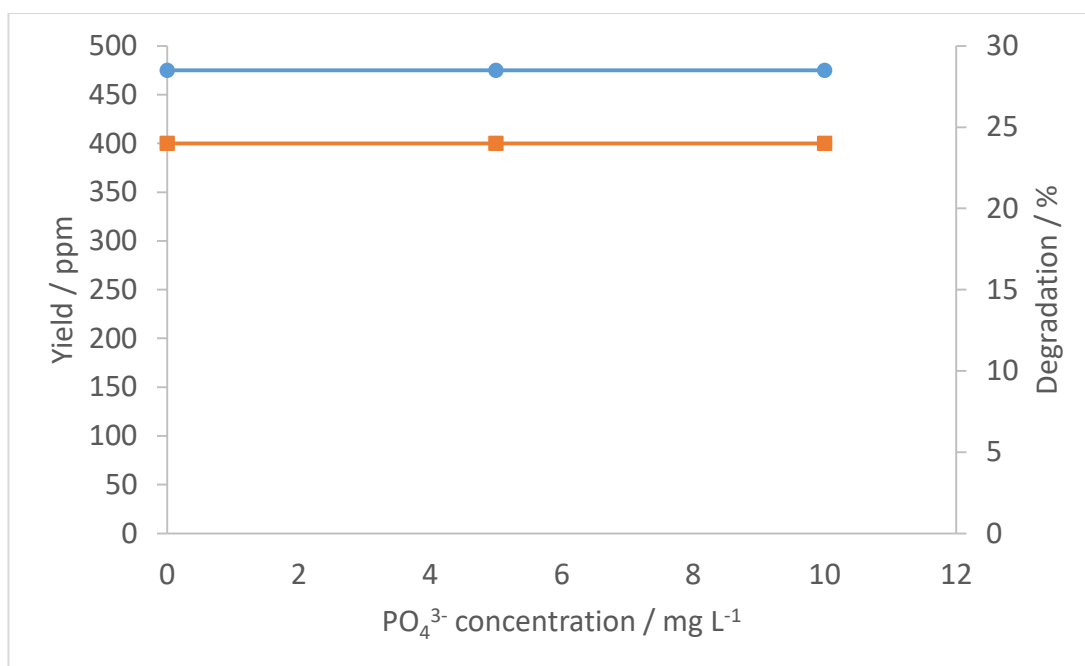


Figure 3.24 – The effect of PO₄³⁻ (as Na₃PO₄) concentration on H₂O₂ synthesis yield and total degradation.

● – Yield^[a], ■ – Degradation^[b]

Conditions: 30 min reaction time, 50 mL autoclave, 20°C, 1200 rpm, 10 mg 2.5 wt. % Au - 2.5 wt. % Pd/TiO₂ catalyst

[a]: 8.5 g H₂O solvent, 420 psi H₂/CO₂ + 160 psi O₂/CO₂

[b]: 7.82 g H₂O solvent + 0.68 g 50 wt. % H₂O₂, 420 psi H₂/CO₂

Figure 3.24 shows that at concentration which are acceptable in tap water, phosphate has no effect on the direct synthesis of hydrogen peroxide reaction.

3.2.9. The effect of using N₂ diluent gas on hydrogen peroxide synthesis using 2.5 wt. % Au - 2.5 wt. % Pd/TiO₂ at 20°C

The use of a diluent gas in addition to H₂ and O₂ in the direct synthesis of H₂O₂ is a necessary safety step if explosive gas mixtures are to be avoided. Some early investigations have been performed in explosive regimes⁶¹, while others have used novel reactor designs such as membranes to keep the gasses separate,^{62, 63} however the majority of recent studies have incorporated the use of gas mixtures with a sufficient amount of diluent gas to remain outside the explosive regime.⁴ Furthermore, for commercial applications of the direct synthesis of H₂O₂, it is highly likely that for health and safety considerations a non-explosive gas mixture will be required.

The Hutchings group has extensively used CO₂ as a diluent, due to two beneficial properties. Firstly, the explosive regime of H₂ and O₂ is narrower in a CO₂ diluent, allowing greater concentrations of H₂ to be used, whilst maintaining a safe mixture. Secondly, if the reaction solvent contains H₂O some CO₂ dissolves into the solvent forming carbonic acid, which acts as an *in-situ* promotor, for reasons discussed in Section 3.2.7.

It has been previously reported that the use of an inert diluent such as N₂ results in significantly lower H₂O₂ yields compared to those obtained with a CO₂ diluent. However, use of an N₂ diluent gas is a step towards practical commercial implementation of a H₂O₂ direct synthesis process which does not use gas cylinders as a reagent source, rather H₂ from electrolytic water splitting combined with O₂ and N₂ from air.⁵⁷

In analogous experiments to those presented in Section 3.2.3. H₂O₂ synthesis yield and the extent of the two degradation processes, decomposition and hydrogenation, were determined for 30 minute reactions at 20°C over a range of H₂O and MeOH solvent compositions, however in these studies N₂ was used as a diluent gas. These data are shown in Figure 3.25.

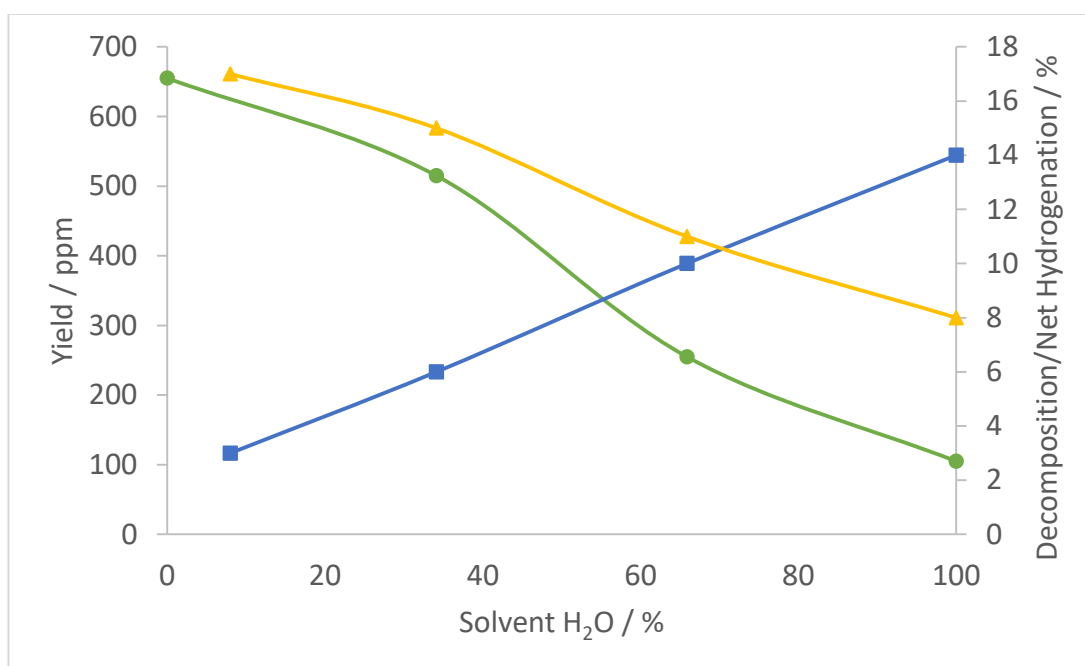


Figure 3.25 - The effect of solvent composition (H₂O / MeOH) on H₂O₂ synthesis yield, decomposition and net hydrogenation

● – Yield^[a], ■ – Decomposition^[b], ▲ - Net Hydrogenation^[c].

Conditions: 30 min reaction time, 50 mL autoclave, 20°C, 1200 rpm, solvent H₂O percentage as indicated (remainder MeOH), 10 mg 2.5 wt. % Au - 2.5 wt. % Pd/TiO₂ catalyst.

[a]: 8.5 g solvent, 420 psi H₂/N₂ + 160 psi O₂/N₂

[b]: 7.82 g solvent + 0.68 g 50 wt. % H₂O₂, 420 psi O₂/N₂

[c]: 7.82 g solvent + 0.68 g 50 wt. % H₂O₂, 420 psi H₂/N₂

Figure 3.25 shows that use of an N₂ diluent gas results in significantly different behaviour of the system comparative to use of a CO₂ diluent gas (Figure 3.6). The yield of H₂O₂ in H₂O is significantly decreased with use of an N₂ diluent gas, whereas the yield of H₂O₂ in MeOH is only slightly reduced. This shows the magnitude of the *in-situ* promotion effects of carbonic acid in H₂O are very significant. Carbonic acid is not produced in a methanol solvent, however a small decrease in yield and a more significant decrease in extent of hydrogenation are observed comparative to a system with a CO₂ diluent. The findings of Gemo *et al.* state that “H₂ solubility in methanol was confirmed to grow with the amount of CO₂,”⁴⁹ which explains the increase in both yield and hydrogenation observed in a MeOH solvent with a CO₂ diluent.

Decomposition follows a similar trend in CO₂ and N₂ diluted systems, with slightly more decomposition occurring in H₂O with a N₂ diluent relative to a CO₂ diluent, most likely due to the stabilising effect of lowered pH from carbonic acid formed by CO₂.

These findings show that for a potential application of the direct synthesis of H₂O₂ in water at 20°C with a N₂ diluted gas feed, low yields and high rates of H₂O₂ decomposition are serious challenges to overcome. If no promoters such as acid or halides are to be added to such a system, a catalyst which is highly active for the synthesis pathway, but very minimally or not active for the decomposition pathway would be required.

3.3. Conclusions

An efficient process of direct synthesis of H₂O₂ in water at ambient temperature represents highly economical and practical conditions for point-of-use generation of hydrogen peroxide and potential water-cleaning applications. However, as conditions are changed from those used previously in the Hutchings group (defined in Section 3.1) to conditions of a water solvent and ambient temperature, we see a marked decrease in H₂O₂ yield.

This decrease is due in part to the increased extent of H₂O₂ degradation that occurs with both an increase in temperature and an increased ratio of H₂O in the solvent. The decreased yield is also due to a reduced rate of H₂O₂ synthesis due to reduced H₂ solubility that again occurs with both an increase in temperature and an increased ratio of H₂O in the solvent. The concomitant positive effect of reduced H₂ solubility in water at ambient temperature is that the hydrogenation of H₂O₂ is relatively less of a concern than under previously studied conditions.

For the successful synthesis of H₂O₂ in water at ambient temperatures, a catalyst must be designed with limited or no activity for the decomposition of hydrogen peroxide, as we observe that at increasing catalyst masses, this degradation pathway dominates and can significantly limit yield. There is a possibility that catalysts that are highly active for both synthesis and hydrogenation under the previously used conditions may prove more effective in a water solvent at ambient temperature, as we observe that hydrogenation of H₂O₂ is relatively less of a concern in a water solvent relative to a methanol solvent, even when large masses of catalyst are used.

The pH and dissolved ions in water can affect the synthesis of H_2O_2 ; pH ranges less than 10 are probably not feasible for this reaction as we see very low yields and high rates of decomposition. Conversely, if a water source has acidic impurities, the data suggest this is actually beneficial to the direct synthesis reaction and will result in greater yields. Similarly if chlorides are present in the reaction media, the data suggest this will also increase yield. Carbonates have been shown to decrease yield, however in normal ranges for UK tap water this effect is fairly small. An element which could potentially cause issues if present in the reaction media is sulfur, as the data suggest that this poisons the catalyst, leading to lower activity and most likely eventually deactivation of the catalyst.

Based on the findings of the data contained herein, catalyst design should be primarily focussed on exhibiting activity for the direct synthesis of H_2O_2 while exhibiting low to no degradation activity. Furthermore, removal or decreased loading of precious metal would serve to reduce the cost of the catalyst and thereby potentially make implementation of the catalytic process more attractive. As a further benefit, there is a possibility that if catalytic activity for H_2O_2 synthesis is achieved with use of a metal other than Pd, the problem of poisoning by sulfur will be avoided.

3.4. References

1. G. Blanco-Brieva, M. C. Capel-Sanchez, M. P. de Frutos, A. Padilla-Polo, J. M. Campos-Martin and J. L. G. Fierro, *Industrial & Engineering Chemistry Research*, 2008, 47, 8011-8015.
2. C. Samanta, *Applied Catalysis A: General*, 2008, 350, 133-149.
3. J. K. Edwards, B. Solsona, E. N. N, A. F. Carley, A. A. Herzing, C. J. Kiely and G. J. Hutchings, *Science*, 2009, 323, 1037-1041.
4. J. K. Edwards, S. J. Freakley, R. J. Lewis, J. C. Pritchard and G. J. Hutchings, *Catalysis Today*, 2015, 248, 3-9.
5. J. Edwards, B. Solsona, P. Landon, A. Carley, A. Herzing, C. Kiely and G. Hutchings, *Journal of Catalysis*, 2005, 236, 69-79.
6. Y. Han and J. Lunsford, *Journal of Catalysis*, 2005, 230, 313-316.
7. Y. F. Han and J. H. Lunsford, *Catalysis Letters*, 2005, 99, 13-19.
8. Q. Liu and J. Lunsford, *Journal of Catalysis*, 2006, 239, 237-243.
9. Q. Liu and J. H. Lunsford, *Applied Catalysis A: General*, 2006, 314, 94-100.
10. V. R. Choudhary, A. G. Gaikwad and S. D. Sansare, *Catalysis Letters*, 2002, 83, 235-239.
11. V. R. Choudhary, C. Samanta and A. G. Gaikwad, *Chemical Communications*, 2004, 10, 2054-2055.
12. V. Choudhary and C. Samanta, *Journal of Catalysis*, 2006, 238, 28-38.
13. V. R. Choudhary, C. Samanta and T. V. Choudhary, *Journal of Molecular Catalysis A: Chemical*, 2006, 260, 115-120.
14. V. Choudhary and P. Jana, *Journal of Catalysis*, 2007, 246, 434-439.
15. V. R. Choudhary, C. Samanta and P. Jana, *Applied Catalysis A: General*, 2007, 317, 234-243.
16. V. R. Choudhary, C. Samanta and P. Jana, *Industrial and Engineering Chemistry Research*, 2007, 46, 3237-3242.
17. C. Samanta and V. R. Choudhary, *Catalysis Communications*, 2007, 8, 2222-2228.
18. C. Samanta and V. R. Choudhary, *Chemical Engineering Journal*, 2008, 136, 126-132.
19. V. R. Choudhary and P. Jana, *Applied Catalysis A: General*, 2009, 352, 35-42.
20. S. Park, J. C. Jung, J. G. Seo, T. J. Kim, Y.-M. Chung, S.-H. Oh and I. K. Song, *Catalysis Letters*, 2009, 130, 604-607.
21. S. Park, T. J. Kim, Y.-M. Chung, S.-H. Oh and I. K. Song, *Catalysis Letters*, 2009, 130, 296-300.
22. S. Park, S. Lee, S. Song, D. Park, S. Baeck, T. Kim, Y. Chung, S. Oh and I. Song, *Catalysis Communications*, 2009, 10, 391-394.
23. S. Park, J. G. Seo, J. C. Jung, S.-H. Baeck, T. J. Kim, Y.-M. Chung, S.-H. Oh and I. K. Song, *Catalysis Communications*, 2009, 10, 1762-1765.
24. S. Park, S.-H. Baeck, T. J. Kim, Y.-M. Chung, S.-H. Oh and I. K. Song, *Journal of Molecular Catalysis A: Chemical*, 2010, 319, 98-107.
25. S. Park, T. J. Kim, Y.-M. Chung, S.-H. Oh and I. K. Song, *Research on Chemical Intermediates*, 2010, 36, 639-646.
26. S. Park, D. R. Park, J. H. Choi, T. J. Kim, Y.-M. Chung, S.-H. Oh and I. K. Song, *Journal of Molecular Catalysis A: Chemical*, 2010, 332, 76-83.
27. S. Park, D. R. Park, J. H. Choi, T. J. Kim, Y.-M. Chung, S.-H. Oh and I. K. Song, *Journal of Molecular Catalysis A: Chemical*, 2011, 336, 78-86.
28. S. Park, J. H. Choi, T. J. Kim, Y.-M. Chung, S.-H. Oh and I. K. Song, *Catalysis Today*, 2012, 185, 162-167.

29. S. Park, J. H. Choi, T. J. Kim, Y.-M. Chung, S.-H. Oh and I. K. Song, *Journal of Molecular Catalysis A: Chemical*, 2012, 353-354, 37-43.
30. S. Park, J. Lee, J. H. Song, T. J. Kim, Y.-M. Chung, S.-H. Oh and I. K. Song, *Journal of Molecular Catalysis A: Chemical*, 2012, 363-364, 230-236.
31. P. Biasi, F. Menegazzo, F. Pinna, K. Eränen, P. Canu and T. O. Salmi, *Industrial and Engineering Chemistry Research*, 2010, 49, 10627-10632.
32. D. Gudarzi, O. A. Simakova, J. R. Hernández Carucci, P. D. Biasi, K. Eränen, E. Kolehmainen, I. Turunen, D. Y. Murzin and T. Salmi, *Chemical Engineering Transactions*, 2010, 21, 925-930.
33. P. Biasi, S. Zancanella, F. Pinna, P. Canu and T. O. Salmi, *Chemical Engineering Transactions*, 2011, 24, 49-54.
34. P. Biasi, P. Canu, F. Menegazzo, F. Pinna and T. O. Salmi, *Industrial & Engineering Chemistry Research*, 2012, 51, 8883-8890.
35. N. Gemo, P. Biasi, P. Canu and T. O. Salmi, *Chemical Engineering Journal*, 2012, 207-208, 539-551.
36. P. Biasi, F. Menegazzo, P. Canu, F. Pinna and T. O. Salmi, *Industrial & Engineering Chemistry Research*, 2013, DOI: 10.1021/ie4011782, 130916123939006.
37. S. Sterchele, P. Biasi, P. Centomo, P. Canton, S. Campestrini, T. Salmi and M. Zecca, *Applied Catalysis A: General*, 2013, 468, 160-174.
38. P. Biasi, J. García-Serna, A. Bittante and T. Salmi, *Green Chemistry*, 2013, 15, 2502.
39. M. G. Walter, E. L. Warren, J. R. McKone, S. W. Boettcher, Q. Mi, E. A. Santori and N. S. Lewis, *Chemical Reviews*, 2010, 110, 6446-6473.
40. E. Ntainjua N, J. K. Edwards, A. F. Carley, J. A. Lopez-Sanchez, J. A. Moulijn, A. A. Herzing, C. J. Kiely and G. J. Hutchings, *Green Chemistry*, 2008, 10, 1162.
41. J. K. Edwards, E. Ntainjua, A. F. Carley, A. A. Herzing, C. J. Kiely and G. J. Hutchings, *Angewandte Chemie*, 2009, 48, 8512-8515.
42. N. E. Ntainjua, M. Piccinini, J. C. Pritchard, J. K. Edwards, A. F. Carley, J. A. Moulijn and G. J. Hutchings, *ChemSusChem*, 2009, 2, 575-580.
43. J. K. Edwards, A. F. Carley, A. A. Herzing, C. J. Kiely and G. J. Hutchings, *Faraday Discussions*, 2008, 138, 225.
44. J. K. Edwards, A. Thomas, A. F. Carley, A. A. Herzing, C. J. Kiely and G. J. Hutchings, *Green Chemistry*, 2008, 10, 388.
45. S. J. Freakley, M. Piccinini, J. K. Edwards, E. N. Ntainjua, J. A. Moulijn and G. J. Hutchings, *ACS Catalysis*, 2013, 3, 487-501.
46. R. Sander, *Atmos. Chem. Phys.*, 2015, 15, 4399-4981.
47. C. Descamps, C. Coquelet, C. Bouallou and D. Richon, *Thermochimica Acta*, 2005, 430, 1-7.
48. K. Fischer and M. Wilken, *The Journal of Chemical Thermodynamics*, 2001, 33, 1285-1308.
49. N. Gemo, P. Biasi, T. O. Salmi and P. Canu, *The Journal of Chemical Thermodynamics*, 2012, 54, 1-9.
50. A. Lekhal, R. V. Chaudhari, A. M. Wilhelm and H. Delmas, *Chemical Engineering Science*, 1997, 52, 4069-4077.
51. T. A. Pospelova and N. I. Kobozev, *Zhurnal Fiz. Khimii*, 1961, 35, 535-542.
52. T. A. Pospelova, N. I. Kobozev and E. N. Eremin, *Zhurnal Fiz. Khimii*, 1961, 35, 298-305.
53. S. Abate, G. Centi, S. Melada, S. Perathoner, F. Pinna and G. Strukul, *Catalysis Today*, 2005, 104, 323-328.
54. N. M. Wilson and D. W. Flaherty, *Journal of the American Chemical Society*, 2016, 138, 574-586.
55. *Drinking Water Compliance Summary - Cardiff East*, Welsh Water, 2013.

56. P. Albers, J. Pietsch and S. F. Parker, *Journal of Molecular Catalysis A: Chemical*, 2001, 173, 275-286.
57. J. K. Edwards and G. J. Hutchings, *Angewandte Chemie*, 2008, 47, 9192-9198.
58. S. Chinta and J. H. Lunsford, *Journal of Catalysis*, 2004, 225, 249-255.
59. L. J. Hoyos, M. Primet and H. Praliaud, *Journal of the Chemical Society, Faraday Transactions*, 1992, 88, 113-119.
60. E. Neyens and J. Baeyens, *Journal of hazardous materials*, 2003, 98, 33-50.
61. B. Zhou and L. K. Lee, Hydrocarbon Technologies, Inc., 2001.
62. V. R. Choudhary, A. G. Gaikwad and S. D. Sansare, *Angewandte Chemie - International Edition*, 2001, 40, 1776-1779.
63. S. Melada, F. Pinna, G. Strukul, S. Perathoner and G. Centi, *Journal of Catalysis*, 2005, 235, 241-248.

4. THE DESIGN OF STABLE AND SELECTIVE CATALYSTS FOR THE DIRECT SYNTHESIS OF HYDROGEN PEROXIDE

4.1. Introduction

As noted in Chapter 1, when the catalytic direct synthesis of hydrogen peroxide (H_2O_2) was first patented in 1914 by Henkel and Weber¹, a Pd catalyst was used and since many studies have focussed on Pd catalysts. The most common form of these Pd catalysts is supported metal nano-particle catalysts such as those studied extensively by Choudhary and co-workers, Lunsford and co-workers, Salmi and co-workers, Song and co-workers and Hutchings and co-workers. Other forms of Pd catalysts such as bulk metal surfaces, colloidal Pd and modified membranes have also been studied.²⁻⁶

In all forms, Pd catalysts are active for the direct synthesis of H_2O_2 , however selectivity towards H_2O_2 is generally lower than would be desirable for practical implementation. It has been reported by many groups that Pd surfaces present as Pd^{II} are more selective than surfaces present as Pd^0 , as such treatments such as heating under an oxygen containing atmosphere and treatment with oxidising agents such as perchloric acid and halogen salts have been utilised to enhance selectivity.⁷⁻

11

Also noted by multiple groups is the effect of the catalyst support on selectivity, with a selectivity increase brought about by the use of highly acidic supports such as HNO_3 -washed SiO_2 or sulphonated ZrO_2 . The promotion effect of acidic supports has been attributed to the reduction of the base catalysed H_2O_2 degradation pathways.¹²⁻¹⁷

An increasing Pd particle size is generally reported to correlate positively with selectivity, with Strukul commenting that a “smooth metal particle surface” which is free of defects and with limited high energy edge sites is optimal for H_2O_2 synthesis.¹⁸ Kim and co-workers noted that for their Pd core-porous SiO_2 shell catalyst, those synthesised with the largest mean Pd particle diameter (4.2 nm) displayed greater productivity and selectivity than those with the smallest mean particle diameter (3.2 nm). This is attributed to the greater proportion of high energy edge and corner sites

on smaller Pd particles which dissociate O-O bonds, leading to the formation of water via combustion and the degradation pathways.¹⁹ This effect was showed through theoretical studies by Flaherty and co-workers who calculated that as a Pd cluster decreases in diameter from 7 nm to 0.7 nm, ΔH^\ddagger for H₂O formation decreases by 14 kJ mol⁻¹.²⁰ Similarly, Iwamoto and co-workers used DFT calculations to show that on a (111) surface of Pd, H₂O₂ would be produced with little to no degradation or combustion, whereas at edge sites, these undesired H₂O forming reactions would be significantly more favourable.²¹

Similar trends of increased selectivity with increased Pd particle size were found by Salmi and co-workers²² and Abate *et al.*²³ however in the latter study, it was found that catalysts with smaller particles were similarly or more productive than those with larger particles, despite being less selective. A study by Lee and co-workers²⁴ came to a similar conclusion, with Pd nano-octahedrons showing decreasing selectivity with size in the range of 7.5-18 nm diameter due to an increase in the proportion of edge and corner sites causing an increase in degradation. However, once high energy sites were blocked by doping with Br⁻, the catalysts with smaller particle sizes were more productive than those with larger particles. This suggests that if the unfavourable combustion and degradation reactions which occur preferentially on edge and defect sites can be controlled, smaller Pd particles are preferable due to their potential for greater H₂O₂ productivity.

A further way to enhance the selectivity of supported Pd catalysts for the direct synthesis of H₂O₂ is the alloying of Pd with Au, first reported by Hutchings and co-workers.²⁵ Supported Au-Pd catalysts have since gained much attention for improving upon Pd catalysts significantly in terms of selectivity and also in activity under most conditions. Further work from Hutchings and co-workers showed that Au-Pd catalysts consisting of randomly alloyed structures and large (>25 nm) nanoparticles are the most selective.²⁶⁻²⁸

The selectivity enhancement observed in the use of Au-Pd catalysts was attributed primarily to a geometric effect by Han and co-workers who found that a Pd atom surrounded by Au atoms is the optimal site for H₂O₂ synthesis, whereas continuous arrays of Pd atoms are active for the hydrogenation reaction.²⁹ A second effect is electronic, where a charge transfer from Au to Pd causes a decrease in the extent of O-O cleavage, increasing selectivity.³⁰

As both Pd and Au are significantly costly metals and may face supply issues and fluctuations in price, there is an interest in developing catalysts using more abundant

and economically attractive metals if the direct synthesis of H_2O_2 is to become industrially viable. Hutchings and co-workers have reported studies of supported Sn-Pd nanoparticle catalysts which displayed good activity as well as high stability and near total selectivity for the direct synthesis of H_2O_2 . Also reported in this study were various other supported metal nanoparticle catalysts of the type Pd-M (M= Ni, Ga, Co, In and Zn) which also display near total selectivity for the direct synthesis of H_2O_2 , in addition to high stability.³¹ This chapter will detail the design, testing, optimisation and characterisation of these catalysts.

4.2. Results and discussion

4.2.1. Metal Screening

With the eventual aim of designing an economically attractive H_2O_2 synthesis catalyst that utilises a low proportion or no noble metals, a range of mono-metallic catalysts were prepared and tested. This allowed for screening for potentially active metals and establishing of baseline activities of known active metals under the given conditions. The catalysts prepared included metals that have been studied in previous literature for H_2O_2 production (Pd, Au, Pt, Ru, Rh)^{10, 32-36} or metals which have literature precedent for utilisation in catalysts for other selective hydrogenation processes (Ni, Co, Ga, Fe, Zn, Cu, Ag)³⁷⁻⁴⁹. Catalysts that had undergone both oxidative and reductive heat treatments were tested. Catalysts containing only Au or Pd were heat treated at 400°C for 3 h as per literature precedents,²⁷ all other catalysts were heat treated at 500°C for 3 h which was sufficient to decompose all precursors as per literature values.⁵⁰ The testing data for this series of catalysts is displayed in Table 4.1.

Table 4.1 - Productivity and degradation testing data for various mono-metallic catalysts as indicated. All catalysts were prepared by standard impregnation. Chloride salt metal precursors were used for Au, Ni and Ga catalysts; nitrate salt metal precursors were used for all other catalysts.

Conditions: 50 ml Parr autoclave, 30 min, 20°C, 1200 rpm, 10 mg catalyst;

[a] 420 psi H₂/CO₂ +160 psi O₂/CO₂, 8.5g water;

[b] 420 psi H₂/CO₂, 7.82 g water + 0.68 g H₂O₂

Catalyst	Productivity / mol kg⁻¹ h⁻¹[a]	Degradation / %^[b]
5 wt. % Pd/TiO₂ reduced	20	38
5 wt. % Pd/TiO₂ oxidised	29	27
5 wt. % Au/TiO₂ reduced	0	2
5 wt. % Au/TiO₂ oxidised	0	2
5 wt. % Ni/TiO₂ reduced	0	2
5 wt. % Ni/TiO₂ oxidised	0	2
5 wt. % Ga/TiO₂ reduced	0	2
5 wt. % Ga/TiO₂ oxidised	0	2
5 wt. % Co/TiO₂ reduced	0	2
5 wt. % Co/TiO₂ oxidised	0	2
5 wt. % Cu/TiO₂ reduced	0	4
5 wt. % Cu/TiO₂ oxidised	0	2
5 wt. % Zn/TiO₂ reduced	0	2
5 wt. % Zn/TiO₂ oxidised	0	2
5 wt. % Ag/TiO₂ reduced	0	10
5 wt. % Ag/TiO₂ oxidised	0	10
5 wt. % Fe/TiO₂ reduced	0	6
5 wt. % Fe/TiO₂ oxidised	0	4
5 wt. % Ru/TiO₂ reduced	0	2

5 wt. % Ru/TiO₂ oxidised	0	2
5 wt. % Pt/TiO₂ reduced	3	72
5 wt. % Pt/TiO₂ oxidised	2	65
5 wt. % Rh/TiO₂ reduced	1	96
5 wt. % Rh/TiO₂ oxidised	2	28

The data displayed in Table 4.1 shows that under the given conditions, only Pd, Pt and Rh display any activity for H₂O₂ synthesis; none of the base metal catalysts tested produced measureable concentrations of H₂O₂. Pd catalysts are clearly the most suited to H₂O₂ synthesis, giving high productivity and moderate degradation activity. Pt catalysts display some activity for H₂O₂ synthesis in both oxidised and reduced states, however also display high degradation activity in both states. Rh catalysts in both oxidised and reduced states are capable of synthesising low concentrations of hydrogen peroxide, however notable is the extremely high degradation activity of the reduced Rh catalyst, with 96% of a 4% H₂O₂ solution undergoing hydrogenation or decomposition in 30 minutes. Ag, Fe and reduced Cu all show some degradation activity but no synthesis activity. Further testing showed that all degradation activity from these catalysts is from the decomposition pathway, which suggests that the active sites on these metals are capable of O-O bond scission, leading to H₂O₂ decomposition, but not the dissociation of hydrogen necessary for synthesis or hydrogenation of H₂O₂.

4.2.2. Pd-Pt Catalysts

Multiple studies have explored the addition of Pt to Pd supported metal catalysts to enhance activity for the direct synthesis of H₂O₂. A study by Lunsford and co-workers found that the addition of 5 atom% Pt to a 0.5 wt. % Pd/SiO₂ catalyst increased the activity of the catalyst 2.5 fold.³³ Strukul and co-workers found that Pd-Pt coatings on membrane type catalyst gave greater productivity compared to those with only Pd coatings.⁵¹ Another study from Strukul and co-workers found addition of Pt to a supported Pd catalyst resulted in increased selectivity and activity, with an optimum Pd/Pt ratio of 18.³² Biasi *et al.* found a significant increase in selectivity but a small decrease in productivity from the addition of a 0.1 wt. % Pt to a 1 wt. % Pd catalyst.

Greater Pt loading further decreased activity, hypothesised to be due to the poisoning of Pt sites by strong chemisorption of the synthesised H₂O₂.³⁵

None of the previous studies have explored the use of Pd-Pt catalysts in a water solvent at ambient temperature, therefore a range of Pd-Pt/TiO₂ catalysts were prepared by standard impregnation and tested for H₂O₂ synthesis, hydrogenation and decomposition activity. This data is shown in Table 4.2.

Table 4.2 – Productivity, net hydrogenation and degradation testing data for various Pd-Pt/TiO₂ catalysts as indicated. All catalysts were prepared by standard impregnation and heat treated in an air atmosphere at 500°C for 3h

Conditions: 50 ml Parr autoclave, 30 min, 20°C, 1200 rpm, 10 mg catalyst;

[a] 420 psi H₂/CO₂ +160 psi O₂/CO₂, 8.5g H₂O;

[b] 420 psi H₂/CO₂, 7.82 g H₂O + 0.68 g H₂O₂

[c] 420 psi O₂/CO₂, 7.82 g H₂O + 0.68 g H₂O₂

Catalyst	H ₂ O ₂ yield / ppm ^[a]	Productivity / mol kg ⁻¹ h ⁻¹ ^[a]	Net Hydrogenation / % ^[b]	H ₂ O ₂ Decomposition / % ^[c]
0.5 wt. % Pt - 4.5 wt. % Pd/TiO ₂	435	22	30	20
0.25 wt. % Pt - 4.75 wt. % Pd/TiO ₂	560	28	14	21
0.1% wt. Pt - 4.9 wt. % Pd/TiO ₂	595	30	13	18

The data displayed in Table 4.2 shows that a 0.1 wt. % Pt - 4.9 wt. % Pd/TiO₂ catalyst produces more H₂O₂ than 5 wt. % Pd/TiO₂ (30 vs 29 mol kg⁻¹ h⁻¹), but 0.25 wt. % Pt - 4.75 wt. % Pd/TiO₂ and 0.5 wt. % Pt - 4.5 wt. % Pd/TiO₂ both produce less H₂O₂ than 5 wt. % Pd/TiO₂. This data is in agreement with the previously cited studies which found an increase in H₂O₂ yield upon addition of small amounts of Pt to a Pd catalyst, but a decrease in yield with an increasing Pt content. These data differ to the previously cited papers by Strukul and co-workers³² and Biasi *et al*³⁵ in the effect of

additional Pt on catalyst selectivity. All Pt-Pd catalysts tested in this study had a decreased selectivity (as determined by a greater total degradation activity), relative to a 5 wt. % Pd/TiO₂ catalyst.

A 0.1 wt. % Pt - 4.9 wt. % Pd/TiO₂ catalyst is the most productive catalyst tested under the given conditions, however it is also less selective than 5 wt. % Pd/TiO₂ and 2.5 wt. % Au – 2.5 wt. % Pd/TiO₂. A high selectivity catalyst is desirable for the direct synthesis of H₂O₂, although there is scope for engineering solutions such as low contact time flow systems to be implemented successfully with high activity, low selectivity catalysts.⁵² However, in all cases it is critical that a catalyst is stable to metal loss and does not decrease in productivity with use. The previously tested series of Pt-Pd catalysts were tested for stability and re-usability; these data are displayed in Table 4.3.

Table 4.3 – Productivity re-use testing data for various Pd-Pt/TiO₂ catalysts as indicated. Catalyst preparation as in Table 4.2. Metal loss is determined by MP-AES analysis and comparison of un-used and post-reaction catalyst samples.

Conditions: 50 ml Parr autoclave, 30 min, 20°C, 1200 rpm, 10 mg catalyst, 420 psi H₂/CO₂ +160 psi O₂/CO₂, 8.5g H₂O.

Catalyst	1st use productivity / mol kg⁻¹ h⁻¹	2nd use productivity / mol kg⁻¹ h⁻¹	Metal loss?
0.1 wt. % Pt - 4.9 wt. % Pd/TiO₂	30	25	Yes
0.25% wt. Pt - 4.75% wt. Pd/TiO₂	28	24	Yes
0.5 wt. % Pt - 4.5 wt. % Pd/TiO₂	22	17	Yes

The data in Table 4.3 show that Pt-Pt catalysts heat treated in static air at 500°C are not stable to metal loss and as such do not give consistent productivity in successive H₂O₂ synthesis testing. A range of 0.1 wt. % Pt - 4.9 wt. % Pd/TiO₂ catalysts were further prepared and heat treated in static air at temperatures up to 700°C, however

none of these catalysts were found to be stable to metal loss and consistent in successive testing.

4.2.3. Pd-M bi-metallic screening

Studies by Hutchings and co-workers found that bi-metallic Au-Pd catalysts were significantly more selective than equally loaded mono-metallic Pd catalysts and do not suffer from loss of active metal in the course of a H₂O₂ synthesis reaction.²⁵ The increase in selectivity was mainly attributed to a geometric effect by Han and co-workers who found Au atoms disrupt continuous arrays of Pd atoms, which are active for the hydrogenation of H₂O₂.²⁹ There has not been significant research on the potential combinations of Pd with secondary metals to find further metal combinations which display increased selectivity over mono-metallic Pd catalysts. Furthermore, this has never been done under the 'water solvent, ambient temperature' conditions used in this work. Thus, several bi-metallic catalysts consisting of Pd and a second metal were prepared and tested for H₂O₂ synthesis and degradation activity; these data are displayed in Table 4.4.

Table 4.4 - Productivity and degradation testing data for various bi-metallic 2.5 wt. % Pd- 2.5 wt. % 'M'/TiO₂ catalysts as indicated and 2.5 wt. % Pd/TiO₂ for reference. All catalysts were prepared by standard impregnation and heat treated at 500°C in static air.

Conditions: 50 ml Parr autoclave, 30 min, 20°C, 1200 rpm, 10 mg catalyst;

[a] 420 psi H₂/CO₂ +160 psi O₂/CO₂, 8.5g H₂O;

[b] 420 psi H₂/CO₂, 7.82 g H₂O + 0.68 g H₂O₂

Catalyst	Productivity / mol kg ⁻¹ h ⁻¹ [a]	Degradation / % ^[b]
2.5 wt. % Pd/TiO₂	22	33
2.5 wt. % Pd 2.5 wt. % Au/TiO₂	24	24
2.5 wt. % Pd 2.5 wt. % Ru/TiO₂	9	28
2.5 wt. % Pd 2.5 wt. % Co/TiO₂	13	12
2.5 wt. % Pd 2.5 wt. % Ni/TiO₂	23	12
2.5 wt. % Pd 2.5 wt. % Zn/TiO₂	12	11
2.5 wt. % Pd 2.5 wt. % Ga/TiO₂	17	16

The data presented in Table 4.4 indicates that Pd-Au outperforms mono-metallic Pd and all other metal combinations which were tested in terms of productivity and shows enhanced selectivity relative to monometallic Pd. When a bi-metallic catalyst consists of Pd with Ru, Co, Zn or Ga, both productivity and degradation activity are decreased with respect to mono-metallic Pd. These decreases in activity are most likely due to a combination of alloying breaking up continuous Pd arrays, the coverage of high energy edge sites and coverage of active sites by the secondary metal. Pd-Ni displays a productivity similar to that of mono-metallic Pd but a significant decrease in degradation activity. Furthermore, Ni is an economically attractive and abundant co-metal, thus additional investigation into Pd-Ni bi-metallic catalysts was performed.

4.2.4. Pd-Ni catalysts

A series of Pd-Ni/TiO₂ catalysts with varied Pd and Ni loading and a total metal loading of 5 wt. % were prepared and tested for H₂O₂ synthesis and degradation activity; these data are displayed in Figure 4.1.

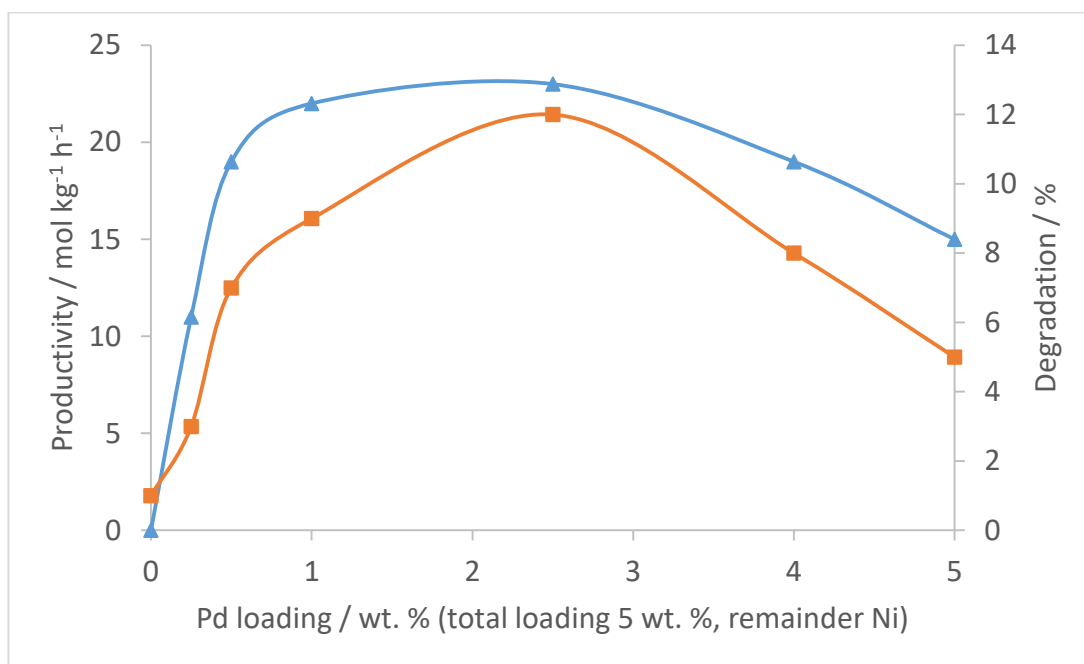


Figure 4.1 – Productivity and total degradation activity for Pd-Ni/TiO₂ catalysts with varied Pd and Ni loadings totalling 5 wt. %. All catalysts prepared by standard impregnation and heat treated in static air at 500°C for 3 h.

▲ - Productivity ^[a], ■ – Degradation ^[b]

Conditions: 50 ml Parr autoclave, 30 min, 20°C, 1200 rpm, 10 mg catalyst;

[a] 420 psi H₂/CO₂ +160 psi O₂/CO₂, 8.5g H₂O;

[b] 420 psi H₂/CO₂, 7.82 g H₂O + 0.68 g H₂O₂

The data displayed in Figure 4.1 show that catalysts containing 0.5 to 1 wt. % Pd exhibit a productivity near to that of a 2.5 wt. % Pd - 2.5 wt. % Ni/TiO₂ catalyst, whilst also exhibiting a lesser degree of degradation. These Pd-Ni catalysts with 0.5 to 1 wt. % Pd may represent high performing catalysts for the direct synthesis of hydrogen peroxide which use a significantly lower proportion of noble metals than successful catalysts in previous literature, such as 2.5 wt. % Au - 2.5wt. % Pd/TiO₂.

The stability of Pd-Ni catalysts to metal loss or deactivation was unknown, therefore a portion of the previously tested series of Pd-Ni catalysts were tested for stability and re-usability; these data are displayed in Table 4.5.

Table 4.5 – Productivity re-use testing data for Pd-Ni/TiO₂ catalysts, as indicated. All catalysts prepared by impregnation and heat treated at 500°C in static air for 3 hr. Metal loss determined by MP-AES analysis.

Conditions: 50 ml Parr autoclave, 30 min, 20°C, 1200 rpm, 10 mg catalyst, 420 psi H₂/CO₂ +160 psi O₂/CO₂, 8.5g H₂O.

Catalyst	1st test productivity / mol kg_{cat}⁻¹ hr⁻¹	2nd test productivity / mol kg_{cat}⁻¹ hr⁻¹	Metal loss?
0.25 wt. % Pd – 4.75 wt. % Ni/TiO₂	11	7	Yes
0.5 wt. % Pd – 4.5 wt. % Ni/TiO₂	19	11	Yes
1 wt. % Pd – 4 wt. % Ni/TiO₂	22	15	Yes
2.5 wt. % Pd – 2.5 wt. % Ni/TiO₂	23	15	Yes

The data in Table 4.6 shows that there is a significant decrease in productivity upon re-use of Pd-Ni catalysts which have been heat treated in static air at 500°C. MP-AES analysis of the reaction solutions confirms that the catalysts suffer from loss of both Pd and Ni.

To investigate whether these catalysts could be treated in a manner that produced stability upon re-use, many 0.5 wt.% Pd - 4.5 wt. % Ni/TiO₂ catalysts were prepared by impregnation and heat treated in an oxidative (air) or reductive (5% H₂/Ar) environment at various temperatures. The data obtained from testing these catalysts for re-use productivity is displayed in Table 4.6.

Table 4.6 – Productivity re-use testing data for 0.5 wt. % Pd – 4.5 wt. % Ni/TiO₂ catalysts that have undergone a range of heat treatments, as indicated. All catalysts prepared by impregnation and heat treated for 3 hr. Metal loss determined by MP-AES analysis.

Conditions: 50 ml Parr autoclave, 30 min, 20°C, 1200 rpm, 10 mg catalyst, 420 psi H₂/CO₂ +160 psi O₂/CO₂, 8.5g H₂O.

Treatment of 0.5 wt. % Pd - 4.5 wt. % Ni/TiO ₂	1st test productivity / mol kg _{cat} ⁻¹ hr ⁻¹	2nd test productivity / mol kg _{cat} ⁻¹ hr ⁻¹	Metal loss?
500°C oxidation	19	11	Yes
600°C oxidation	8	5	Yes
700°C oxidation	5	5	No
800°C oxidation	5	5	No
500°C reduction	16	10	Yes
600°C reduction	13	6	Yes
700°C reduction	12	5	Yes

The data in Table 4.6 show that high temperature ($\geq 700^\circ\text{C}$) oxidative heat treatment produces catalysts which give stable productivities and do not show signs of metal loss when the reaction solution is analysed by MP-AES, however these catalysts have relatively low productivity. No reductively treated catalysts appear to be stable.

4.2.5. Oxidation-Reduction-Oxidation treatment of Pd-Ni catalysts

A successive oxidation-reduction-oxidation (ORO) heat treatment technique, which has been shown in a previous study by Freakley *et al.*³¹ to achieve stability and increase selectivity for Pd-Sn/SiO₂ and Pd-Sn/TiO₂ catalysts was also investigated. A series of 0.5 wt. % Pd - 4.5 wt. % Ni/TiO₂ catalysts were heat treated in varied combinations of successive oxidation by heating treatment in static air at 500°C for 3 hr (O) and reduction by heat treatment in H₂/Ar at 200°C for 2 hr (R), as used previously for Pd-Sn catalysts. The data obtained from testing these catalysts is displayed in Table 4.7.

Table 4.7 – Re-use productivity and degradation testing data for 0.5 wt. % Pd - 4.5 wt. % Ni/TiO₂ catalysts, heat treated as indicated – O: static air, 500°C, 3 hr; 'R': H₂/Ar, 200°C, 2 hr. All catalysts were prepared by standard impregnation.

Conditions: 50 ml Parr autoclave, 30 min, 20°C, 1200 rpm, 10 mg catalyst;

[a] 420 psi H₂/CO₂ +160 psi O₂/CO₂, 8.5g H₂O;

[b] 420 psi H₂/CO₂, 7.82 g H₂O + 0.68 g H₂O₂

Catalyst	1st test productivity / mol kg_{cat}⁻¹ hr⁻¹ [a]	2nd test productivity / mol kg_{cat}⁻¹ hr⁻¹ [a]	Degradation / %^[b]
0.5 wt. % Pd - 4.5 wt. % Ni/TiO₂ O	19	11	7
0.5 wt. % Pd - 4.5 wt. % Ni/TiO₂ OR	22	12	13
0.5 wt. % Pd - 4.5 wt. % Ni/TiO₂ RO	16	12	6
0.5 wt. % Pd - 4.5 wt. % Ni/TiO₂ ORO	8	10	2
0.5 wt. % Pd - 4.5 wt. % Ni/TiO₂ OROR	12	12	5

The data displayed in Table 4.7 show that the only catalysts which do not decrease in productivity on re-use are the catalysts which have undergone an ORO or OROR treatment. For both of these catalysts, MP-AES analysis indicates that there is no Ni or Pd present in the post-reaction solution and digestion of used catalysts confirmed there was no metal loss relative to un-used catalysts. Thus it can be concluded that 0.5 wt. % - Pd 4.5 wt. % Ni/TiO₂ ORO and OROR catalysts are stable for H₂O₂ synthesis under the given conditions. No other combination of heat treatments produced a stable catalyst.

0.5 wt. % - Pd 4.5 wt. % Ni/TiO₂ ORO is stable and moderately productive with only 0.5% Pd, but importantly the data indicate that it has no activity for the degradation of hydrogen peroxide above that which is observed in a blank reaction (*i.e.* 2%). This lack of degradation activity has only previously been observed for an acid-washed

Au-Pd/TiO₂ catalyst by Edwards *et al.*⁵³ and for Pd-Sn/SiO₂ and Pd-Sn/TiO₂ ORO catalysts by Freakley *et al.*³¹

The testing data for 0.5 wt. % - Pd 4.5 wt. % Ni/TiO₂ ORO indicate that there is a slight increase in productivity on re-use. The testing data for 0.5 wt. % - Pd 4.5 wt. % Ni/TiO₂ OROR indicates that the productivity of this catalyst is slightly greater than that of the ORO catalyst, both on the first and subsequent use of the ORO catalyst. A probable explanation to the increase in productivity upon re-use of the ORO catalyst is the partial reduction of surface Pd by H₂ in the reaction mixture, moving the ORO catalyst behaviour towards that of the OROR catalyst. 0.5 wt. % - Pd 4.5 wt. % Ni/TiO₂ OROR does exhibit a small degree of degradation activity, therefore it is probable that a slight increase in degradation activity as a 0.5 wt. % - Pd 4.5 wt. % Ni/TiO₂ ORO catalyst is re-used will occur.

As treating 0.5 wt. % - Pd 4.5 wt. % Ni/TiO₂ with an oxidation-reduction-oxidation heat treatment cycle achieved a stable and selective catalyst, Pd-Ni/TiO₂ catalysts of different metal ratios were prepared, heat treated in an identical manner and tested. This data is displayed in Figure 4.2.

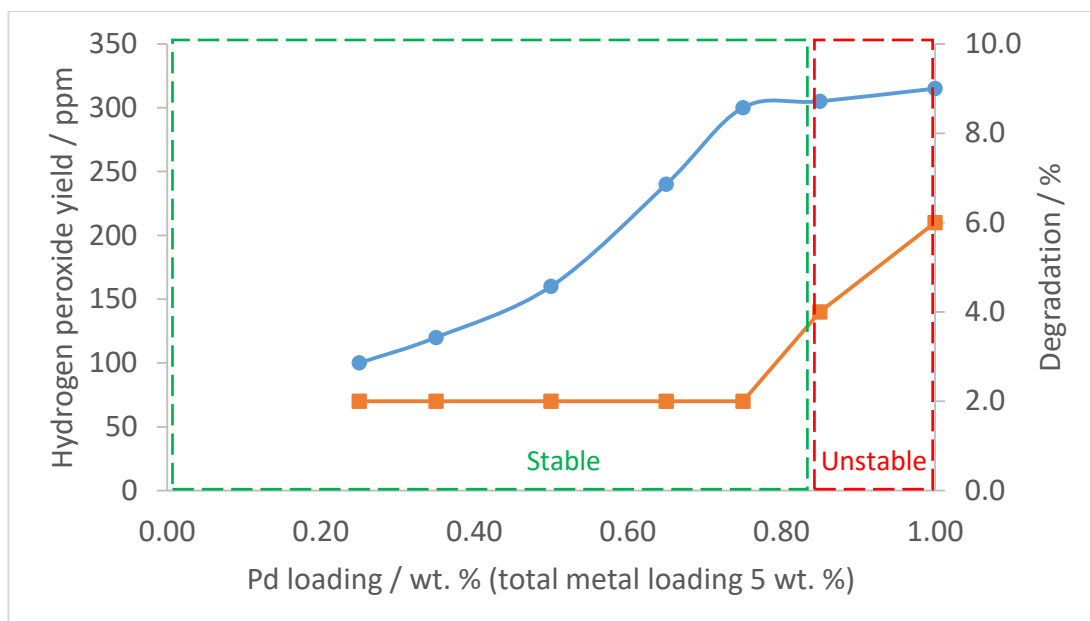


Figure 4.2 – Yield and total degradation activity for Pd-Ni/TiO₂ ORO catalysts with varied Pd and Ni loadings totalling 5 wt. %. All catalysts prepared by standard impregnation and heat treated successively in static air at 500°C for 3 h, 5% H₂/Ar at 200°C for 2 h and again in static air at 500°C for 3 h. Metal loss determined by MP-AES analysis.

● – Yield ^[a], ■ – Degradation ^[b]

Conditions: 50 ml Parr autoclave, 30 min, 20°C, 1200 rpm, 10 mg catalyst;

[a] 420 psi H₂/CO₂ +160 psi O₂/CO₂, 8.5g H₂O;

[b] 420 psi H₂/CO₂, 7.82 g H₂O + 0.68 g H₂O₂

The data in Figure 4.2 shows that all ORO treated catalysts in the range between 0.25 wt. % - Pd 4.75 wt. % Ni/TiO₂ and 0.75 wt. % - Pd 4.25 wt. % Ni/TiO₂ are stable, giving consistent productivity on re-use and showing no sign of metal loss by MP-AES analysis. These catalysts also display no degradation activity above that which is recorded for a blank reaction (2 %). However it was observed that catalysts with a relatively greater proportion of Pd are not stable, exhibiting both decreasing productivity on re-use and loss of Pd from the catalyst. These unstable catalysts also display some activity for degradation.

To study the effect of met ratio in Pd-Ni/TiO₂ catalysts with varied total metal loading, catalysts with a constant Pd loading of 0.5 wt. %, but a varied loading of Ni were prepared. The data obtained from testing these catalysts is displayed in Table 4.8.

Table 4.8 – Productivity, degradation and stability (no metal loss and consistent re-use testing) testing data for 0.5 wt. % Pd – x wt. % Ni/TiO₂ ORO catalysts. All catalysts were prepared by standard impregnation.

Conditions: 50 ml Parr autoclave, 30 min, 20°C, 1200 rpm, 10 mg catalyst;

[a] 420 psi H₂/CO₂ +160 psi O₂/CO₂, 8.5g H₂O;

[b] 420 psi H₂/CO₂, 7.82 g H₂O + 0.68 g H₂O₂

Catalyst	Productivity / mol kg _{cat} ⁻¹ hr ⁻¹ [a]	Degradation % ^[b]	Stable?
0.5 wt. % Pd - 4.5 wt. % Ni/TiO ₂ ORO	8	2	Yes
0.5 wt. % Pd - 9.5 wt. % Ni/TiO ₂ ORO	3	2	Yes
0.5 wt. % Pd - 2.5 wt. % Ni/TiO ₂ ORO	9	4	No

The data in Table 4.8 shows that increasing Ni loading at a consistent Pd loading leads to a decrease in productivity, but the resulting catalyst is still both stable and highly selective. Decreasing Ni loading at a consistent Pd loading leads to an unstable catalyst which also displays some activity for H₂O₂ degradation. These data suggest that it is not the absolute loading of Pd which determines whether a Pd-Ni/TiO₂ ORO will be stable, but rather the relative loadings of Pd and Ni. Figure 4.2 shows that for loading Pd-Ni catalysts with a total metal loading of 5 wt. %, catalysts with a greater proportion of Pd than 0.75 wt. % - Pd 4.25 wt. % Ni/TiO₂ (1:10.2 Pd:Ni atomic ratio) are unstable. In combination with the finding that 0.5 wt. % - Pd 2.5 wt. % Ni/TiO₂ ORO (1:9.06 Pd:Ni atomic ratio) is an unstable catalyst, these data suggest that there may be a minimum ratio of c.a. 1:10 Pd:Ni necessary to produce stable and selective structures on these catalysts.

A 0.5 wt. % Pd – 4.5 wt. % Ni/TiO₂ 'OOO' catalyst was prepared, for which the temperature and duration of heat treatment was identical to the ORO catalyst, however all treatment was performed in an oxidative (air) atmosphere. This catalyst was prepared to investigate whether the cycling of oxidation and reduction is necessary to create a stable and selective catalyst, or if similar results can be achieved with solely extended oxidative heat treatment. The results of testing this catalyst are displayed in Table 4.9.

Table 4.9 – Productivity and degradation testing data for a 0.5 wt. % Pd - 4.5 wt. % Ni/TiO₂ catalyst prepared by standard impregnation and heat treated in static air successively at 500°C for 3 h, 200°C for 2 h and again at 500°C for 3 h

Conditions: 50 ml Parr autoclave, 30 min, 20°C, 1200 rpm, 10 mg catalyst;

[a] 420 psi H₂/CO₂ +160 psi O₂/CO₂, 8.5g H₂O;

[b] 420 psi H₂/CO₂, 7.82 g H₂O + 0.68 g H₂O₂

Catalyst	Productivity / mol kg _{cat} ⁻¹ hr ⁻¹ [a]	Degradation / % [b]
0.5 wt. % Pd – 4.5% wt. Ni/TiO₂ ‘OOO’	1	2

The data in Table 4.9 shows that ‘OOO’ treatment almost entirely deactivates the catalyst. This shows that the activity, stability and selectivity of 0.5 wt. % Pd - 4.5 wt. % Ni/TiO₂ ORO is not simply a function of extended heat treatment and that an oxidation-reduction-oxidation cycle forms active and stable surface metal structures which cannot be formed by oxidative treatment alone.

The H₂O₂ degradation activity of a catalyst is a useful proxy measurement for determining a H₂O₂ synthesis catalyst’s selectivity, as degradation accounts for the 2 major un-selective pathways, hydrogenation and degradation. Direct combustion of H₂ is generally a lesser concern in liquid phase H₂O₂ synthesis and also tends to occur concomitantly with degradation activity,^{4,6} thus using degradation activity as an indicator for selectivity is generally valid. It is however still useful to directly measure H₂ selectivity towards H₂O₂ by gas analysis. Selectivity, productivity and degradation data for the widely used 2.5 wt. % Au - 2.5 wt. % Pd/TiO₂ catalyst, the newly formulated 0.5 wt. % Pd – 4.5% wt. Ni/TiO₂ ORO catalyst and a 0.5 wt. % Pd/TiO₂ ORO catalyst are displayed in Table 4.10.

Table 4.10 – Productivity, degradation and H₂ selectivity testing data for a range of catalysts prepared by standard impregnation. H₂ selectivity determined by GC analysis.

Conditions: 50 ml Parr autoclave, 30 min, 20°C, 1200 rpm, 10 mg catalyst;

[a] 420 psi H₂/CO₂ +160 psi O₂/CO₂, 8.5g H₂O;

[b] 420 psi H₂/CO₂, 7.82 g H₂O + 0.68 g H₂O₂

Catalyst	Productivity / mol kg _{cat} ⁻¹ hr ⁻¹ [a]	Degradation / % [b]	H ₂ Selectivity / %
2.5 wt. % Au - 2.5 wt. % Pd/TiO ₂ (400°C, 3 h oxidation)	24	24	64
0.5 wt. % Pd – 4.5% wt. Ni/TiO ₂ ORO	8	2	>97
0.5 wt. % Pd/TiO ₂ ORO	6	12	75

The data in Table 4.10 show that 0.5 wt. % Pd – 4.5% wt. Ni/TiO₂ ORO is a highly selective catalyst, displaying very little to no combustion activity in addition to degradation activity. Under the given conditions, 0.5 wt. % Pd – 4.5% wt. Ni/TiO₂ ORO is significantly more selective than 2.5 wt. % Au - 2.5 wt. % Pd/TiO₂, a catalyst which previously significantly improved upon the selectivity of early Pd catalysts.⁵⁴ These data also show that a mono metallic 0.5 wt. % Pd/TiO₂ catalyst which has undergone ORO heat treatment is slightly more active than 0.5 wt. % Pd – 4.5% wt. Ni/TiO₂ ORO, however does not exhibit the same degree of near total selectivity.

4.2.6. The use of varied supports for Pd-Ni catalysts

Thus far the catalysts prepared and tested in these studies have entirely made use of TiO₂ supports. To determine whether the structures which lead to stable and selective catalysts can solely be formed on TiO₂ or can be formed on different supports, analogous 0.5 wt. % Pd - 4.5 wt. % Ni ORO catalysts were prepared on other commonly used oxide supports and tested. The results of this testing are displayed in Table 4.11.

Table 4.11 – Productivity, degradation and stability testing data for a 0.5 wt. % Pd - 4.5 wt. % Ni ORO catalysts prepared on oxide supports.

Conditions: 50 ml Parr autoclave, 30 min, 20°C, 1200 rpm, 10 mg catalyst;

[a] 420 psi H₂/CO₂ +160 psi O₂/CO₂, 8.5g H₂O;

[b] 420 psi H₂/CO₂, 7.82 g H₂O + 0.68 g H₂O₂

Catalyst	Productivity / mol kg _{cat} ⁻¹ hr ⁻¹ [a]	Degradation / % [b]	Stable?
0.5 wt. % Pd - 4.5 wt. % Ni/TiO ₂ ORO	8	2	Yes
0.5 wt. % Pd - 4.5 wt. % Ni/SiO ₂ ORO	6	2	Yes
0.5 wt. % Pd - 4.5 wt. % Ni/ZrO ₂ ORO	5	2	Yes
0.5 wt. % Pd - 4.5 wt. % Ni/CeO ₂ ORO	5	2	Yes

The data in Table 4.11 show that TiO₂ is the support from which the most productive catalyst is prepared. Importantly, these data show that the method of producing active, stable and minimally hydrogenating catalysts is not exclusive to TiO₂ and is possible using other oxide supports.

Catalysts consisting of 0.5 wt. % Pd - 4.5 wt. % Ni supported onto materials other than metal oxides were also prepared in the now established ORO manner to further investigate the prerequisites for producing stable, selective. The results of testing these catalysts are displayed in Table 4.12.

Table 4.12 – Productivity, degradation and stability testing data for a 0.5 wt. % Pd - 4.5 wt. % Ni ORO catalysts prepared on non-oxide supports.

Conditions: 50 ml Parr autoclave, 30 min, 20°C, 1200 rpm, 10 mg catalyst;

[a] 420 psi H₂/CO₂ +160 psi O₂/CO₂, 8.5g H₂O;

[b] 420 psi H₂/CO₂, 7.82 g H₂O + 0.68 g H₂O₂

Catalyst	Productivity / mol kg _{cat} ⁻¹ hr ⁻¹ [a]	Degradation / % ^[b]	Stable?
0.5 wt. % Pd - 4.5 wt. % Ni/BN ORO	9	5	No
0.5 wt. % Pd - 4.5 wt. % Ni/SiC ORO	11	6	No

The data in Table 4.12 show that catalysts which are not prepared using an oxide support are not stable, exhibiting decreased productivity on re-use and loss of both Ni and Pd, as confirmed by MP-AES analysis. This suggests that an oxide support may be necessary to create Pd-Ni ORO catalysts which are active, stable and selective.

Catalysts consisting of Pd directly supported onto a nickel oxide support were prepared to investigate whether similar stable and selective catalysts can be formed as when a Pd and Ni are co-impregnated on to an oxide support such as TiO₂ or SiO₂. The results of testing these catalysts is shown in Table 4.13.

Table 4.13 – Productivity, degradation and stability testing data for a 0.5 wt. % Pd/NiO catalysts.

Conditions: 50 ml Parr autoclave, 30 min, 20°C, 1200 rpm, 10 mg catalyst;

[a] 420 psi H₂/CO₂ +160 psi O₂/CO₂, 8.5g H₂O;

[b] 420 psi H₂/CO₂, 7.82 g H₂O + 0.68 g H₂O₂

Catalyst	Productivity / mol kg _{cat} ⁻¹ hr ⁻¹ [a]	Degradation / % [b]	Stable?
0.5 wt. % Pd/NiO (500°C, 3hr, oxidation)	5	41	No
0.5 wt. % Pd/NiO ORO	3	33	Yes

The data in Table 4.13 show that catalysts prepared by directly supporting Pd onto NiO (both oxidised and ORO) are significantly less productive and selective than supported Pd-Ni ORO catalysts with an identical Pd loading. This suggests that simultaneous impregnation of Pd and Ni on to an oxide support is necessary to form the active, selective catalyst structures.

4.2.7. The effect of precursor salt and preparation pH for Pd-Ni catalysts

To this point all Pd-Ni catalysts have been prepared using NiCl₂ as an Ni precursor salt and a Pd(NO₃)₂ as a Pd precursor salt. These salts were used as they are analogous to the precursor salts used in the preparation of Pd-Sn ORO catalysts in the work by Freakley *et al.*³¹ from which this work follows. Chloride salts have been used successfully for producing H₂O₂ synthesis catalysts, with prior literature illustrating that chloride ions have positive effects on selectivity both when introduced into the reaction mixture and when incorporated into catalyst formulation.^{55, 56} It is also known that the choice of pre-cursor salt can have an effect on the morphology of surface metal structures, due to factors such as differences in the interactions between the precursor and the support, decomposition temperature of precursors and interactions between precursors, if multiple are utilised.^{22, 57} 0.5 wt. % Pd - 4.5 wt. % Ni/TiO₂ ORO catalysts were prepared using entirely nitrate or chloride precursors; the results of testing these catalysts is displayed in Table 4.14.

Table 4.14 – Productivity, degradation and stability testing data for a 0.5 wt. % Pd/NiO catalysts.

Conditions: 50 ml Parr autoclave, 30 min, 20°C, 1200 rpm, 10 mg catalyst;

[a] 420 psi H₂/CO₂ +160 psi O₂/CO₂, 8.5g H₂O;

[b] 420 psi H₂/CO₂, 7.82 g H₂O + 0.68 g H₂O₂

Catalyst	Metal Precursors	Productivity / mol kg _{cat} ⁻¹ hr ⁻¹ [a]	Degradation / % [b]	Stable?
0.5 wt. % Pd - 4.5 wt. % Ni/TiO ₂ ORO	Pd(NO ₃) ₂ , NiCl ₂	8	2	Yes
0.5 wt. % Pd - 4.5 wt. % Ni/TiO ₂ ORO	PdCl ₂ , NiCl ₂	8	2	Yes
0.5 wt. % Pd - 4.5 wt. % Ni/TiO ₂ ORO	Pd(NO ₃) ₂ , Ni(NO ₃) ₂	5	2	Yes

The data in Table 4.14 indicate that while a nitrate precursor preparation still produces a stable, selective hydrogen peroxide synthesis catalyst, the use of chloride precursors enhances activity. Chloride addition is generally considered to increase catalyst selectivity by reducing O-O bond cleavage, whether through ensemble effects or “long range electronic effects”,⁵⁶ therefore decreasing both combustion and hydrogenation activity. However, as shown previously, these catalysts show little to no activity for these unselective pathways, therefore the use of chloride precursors must increase productivity by a different mechanism.

The effect of the additional chloride and of tuning the pH of the impregnation solution used during catalyst preparation was investigated. In the absence of additional acid or base, an aqueous impregnation solution of chloride salts that is used to make 0.5 wt. % Pd - 4.5 wt. % Ni/TiO₂ ORO catalysts has a pH of 3. Various 0.5 wt. % Pd - 4.5 wt. % Ni/TiO₂ ORO catalysts were prepared using impregnation solutions of varied pH. These solutions were either acidified with HNO₃ (to reduce the pH but not add chloride) or HCl (to reduce the pH and add chloride) or alkalisied with NaOH (to increase the pH and avoid any effects of halides). The results of testing these catalysts are displayed in Figure 4.3.

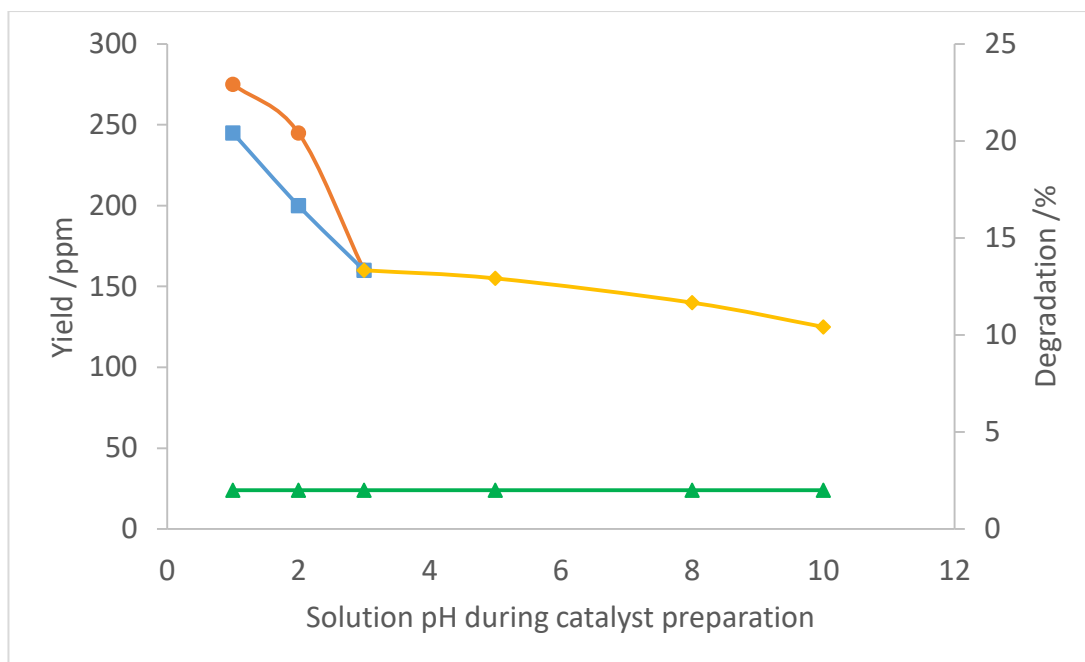


Figure 4.3 – Yield and total degradation activity for 0.5 wt. % Pd - 4.5 wt. % Ni/TiO₂ ORO catalysts prepared with impregnation solutions of varied pH.

● – Yield, HCl addition ^[a], ■ – Yield, HNO₃ addition ^[a], ◆ – Yield, NaOH addition ^[a], ▲ – Degradation ^[b]

Conditions: 50 ml Parr autoclave, 30 min, 20°C, 1200 rpm, 10 mg catalyst;

[a] 420 psi H₂/CO₂ +160 psi O₂/CO₂, 8.5g H₂O;

[b] 420 psi H₂/CO₂, 7.82 g H₂O + 0.68 g H₂O₂

The data displayed in Figure 4.3 indicates that acidifying the impregnation solution produces a more productive catalyst, with the addition of chlorine as HCl further increasing productivity to a maximum of 14 mol kg_{cat}⁻¹ hr⁻¹ (275 ppm yield from a 30 minute reaction). The pH of the preparation did not affect either the degradation activity, with all catalysts displaying no degradation activity above that observed in a blank reaction. All catalysts also maintained consistent productivity upon re-use and stability, showing no signs of metal loss by MP-AES analysis.

Both the addition of chloride and acid to the impregnation solution increase catalysts productivity/H₂O₂ yield, however as there is no net degradation activity for any of the catalysts tested, this increase in productivity cannot be due to increased selectivity. Therefore it is reasonable to conclude that both acid and chloride addition create more active metal structures on the catalyst surface. The addition of chloride has previously been noted by Sankar *et al.*⁵⁸ to facilitate the formation of [PdCl₄]²⁻ species which in

the cited work can form a more homogenous mixture with $[\text{AuCl}_4]^-$ species and therefore lead to improved dispersion in Au-Pd catalysts. It is reasonable to suggest that a similar mechanism may be occurring in this study, with chloride addition facilitating the formation of $[\text{PdCl}_4]^{2-}$ and $[\text{NiCl}_4]^{2-}$ species, which form a homogenous mixture in the impregnation solution, leading to highly dispersed Pd on the catalyst surface.

In the case of acid addition, this may in part be due to increasing the solubility of the PdCl_2 precursor salt, and thereby improving Pd dispersion during the impregnation process. Furthermore, Edwards *et al.*^{53, 59}, proposed that acid pre-treatment of TiO_2 and SiO_2 leads to “enhanced hydroxyl functionality” on the surface of the support. When these supports are used to prepare Pd or Au-Pd catalysts, there is increased Pd dispersion relative to untreated supports, which leads to enhanced activity. When acid is added to the impregnation solution used in this study, there is likely to be an increase in hydroxyl groups as a result of acid-support interaction, leading to a similar increase in Pd dispersion. When the pH of the impregnation solution is below the isoelectric point of the p25 TiO_2 support ($\text{IEP} \approx 6$)⁶⁰, the surface of the support will carry a positive charge. In the case of HCl addition to the impregnation solution, it is probable that $[\text{PdCl}_4]^{2-}$ and $[\text{NiCl}_4]^{2-}$ species are the predominant species in the solution, therefore there may also be a synergic effect on metal dispersion as the anionic metal species are attracted to the positively charged support surface.

4.2.8. Pd-Ga catalysts

Second to Pd-Ni, Pd-Ga was the next most productive of the Pd-M bi-metallic catalysts which were screened in Section 4.2.3. To investigate whether the properties of Pd-Ni/ TiO_2 ORO catalysts are unique to that metal combination, a series of Pd-Ga catalysts analogous to some of those which have been tested in the previous Sections of this Chapter were prepared. The results of testing these various Pd-Ga catalysts are displayed in Table 4.15.

Table 4.15 – Productivity, degradation and stability testing data for various Pd-Ga catalysts, heat treated as indicated – O: static air, 500°C, 3 hr; 'R': H₂/Ar, 200°C, 2 hr. All catalysts were prepared by standard impregnation.

Conditions: 50 ml Parr autoclave, 30 min, 20°C, 1200 rpm, 10 mg catalyst;

[a] 420 psi H₂/CO₂ +160 psi O₂/CO₂, 8.5g H₂O;

[b] 420 psi H₂/CO₂, 7.82 g H₂O + 0.68 g H₂O₂

Catalyst	Productivity / mol kg _{cat} ⁻¹ hr ⁻¹ [a]	Degradation / % [b]	Stable?
0.5 wt. % Pd – 4.5 wt. % Ga/TiO ₂ O (Pd(NO ₃) ₂ , GaCl ₃ precursors)	15	12	No
0.5 wt. % Pd – 4.5 wt. % Ga/TiO ₂ ORO (Pd(NO ₃) ₂ , GaCl ₃ precursors)	12	2	Yes
0.5 wt. % Pd – 4.5 wt. % Ga/TiO ₂ ORO (PdCl ₂ , GaCl ₃ precursors + HCl)	14	2	Yes
0.5 wt. % Pd – 4.5 wt. % Ga/SiO ₂ ORO	9	2	Yes
0.5 wt. % Pd – 4.5 wt. % Ga/SiC ORO	9	8	No
0.5 wt. % Pd/Ga ₂ O ₃ ORO	3	24	-

The data displayed in Table 4.15 shows that the general trends observed for Pd-Ni catalysts are also observed for analogous Pd-Ga catalysts. We observe that oxidative heat treatment alone is insufficient to produce a stable catalyst, but an ORO heat treatment is again successful in producing a stable catalyst with zero net degradation activity. As for 0.5 wt. % Pd - 4.5 wt. % Ni/TiO₂ ORO, an increase in productivity is observed for 0.5 wt. % Pd - 4.5 wt. % Ga/TiO₂ ORO when additional acid and chloride are introduced into the catalyst preparation solution, highly likely due to the same mechanisms. Selectivity measurements based on gas analysis confirm that H₂ selectivity towards H₂O₂ is >97% for 0.5 wt. % Pd - 4.5 wt. % Ga/TiO₂ ORO. Therefore it can be concluded that as with 0.5 wt. % Pd - 4.5 wt. % Ni/TiO₂ ORO, combustion is

not an active pathway and the catalyst is highly selective for the direct synthesis of H_2O_2 .

The data suggest that Pd-Ga ORO catalysts are stable and selective when prepared on oxide supports such as TiO_2 and SiO_2 , but not when prepared on non-oxide supports such as SiC, again analogous to Pd-Ni ORO catalysts. Furthermore, 0.5 wt. % Pd/ Ga_2O_3 ORO displays low activity and selectivity, again illustrating the necessity of co-impregnation of the metals on to a support to produce an active and selective catalyst.

Studies in Section 4.2.5 which investigated the fine tuning of metal ratios in Pd-Ni/ TiO_2 ORO catalysts with a total metal loading of 5 wt. % found that 0.75 wt. % Pd - 4.25 wt. % Ni/ TiO_2 ORO is a stable selective catalyst, but formulations with a proportionally greater loading of Pd become unselective and unstable. In an analogous manner, a series of Pd-Ga/ TiO_2 ORO catalysts of varied Pd:Ga ratios were prepared and tested. The results of this testing are displayed in Figure 4.4.

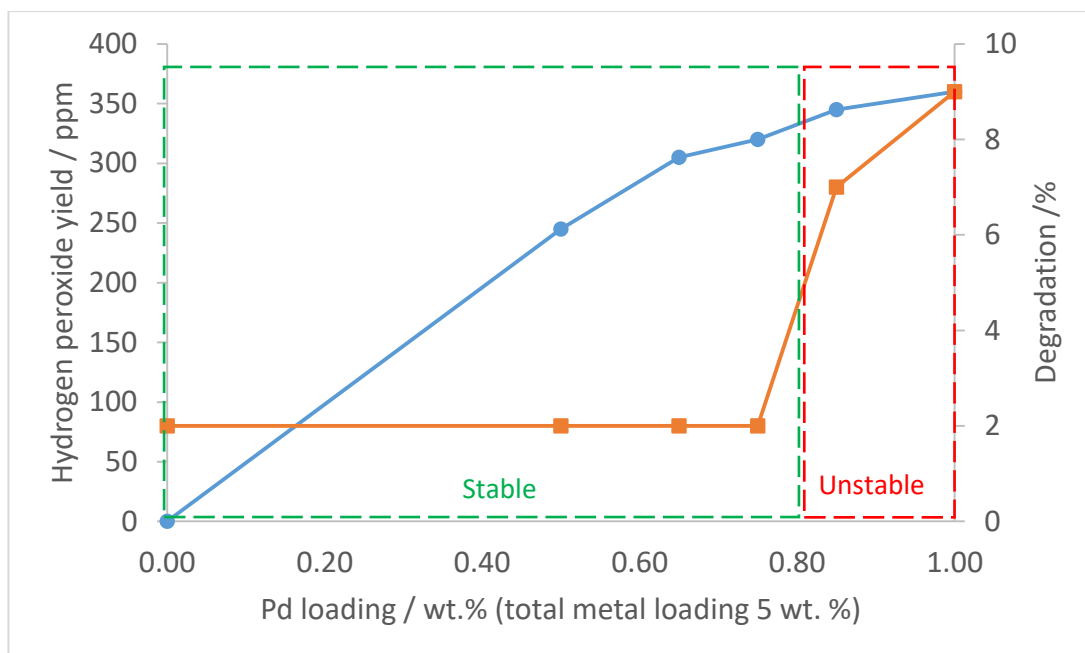


Figure 4.4 – Yield and total degradation activity for Pd-Ga/TiO₂ ORO catalysts with varied Pd and Ga loadings totalling 5 wt.%. All catalysts prepared by standard impregnation and heat treated successively in static air at 500°C for 3 h, 5% H₂/Ar at 200°C for 2 h and again in static air at 500°C for 3 h. Metal loss determined by MP-AES analysis.

● – Yield ^[a], ■ – Degradation ^[b]

Conditions: 50 ml Parr autoclave, 30 min, 20°C, 1200 rpm, 10 mg catalyst;

[a] 420 psi H₂/CO₂ +160 psi O₂/CO₂, 8.5g H₂O;

[b] 420 psi H₂/CO₂, 7.82 g H₂O + 0.68 g H₂O₂

The data in Figure 4.4 show a very similar trend to that seen in Figure 4.2 for Pd-Ni/TiO₂ ORO catalysts. For Pd-Ga/TiO₂ catalysts, it was found that 0.75 wt. % Pd - 4.25 wt. % Ni/TiO₂ ORO is a stable catalyst with no net degradation activity, however catalysts with a greater proportion of Pd than this were found to be unstable and show some degradation activity.

4.2.9. Further Pd-‘M’ ORO catalysts

Thus far in this work, it has been demonstrated that formulations of Pd-Ni and Pd-Ga in the correct ratios, supported on oxide materials (e.g. TiO₂) and heat treated in a cyclic oxidation-reduction-oxidation manner produce stable and highly selective H₂O₂ synthesis catalysts. In a previous study by Freakley *et al.*³¹ (to which portions of this work contributed) it was demonstrated that this is also the case for Pd-Sn ORO

catalysts. This work hypothesizes that the enhanced stability and selectivity of these catalysts is a function of a strong metal-support interaction (SMSI) between Pd and a thin, amorphous SnO_x layer on the catalyst surface which encapsulates small (<2 nm) Pd-rich particles while leaving larger (5-10 nm) Pd-Sn alloy particles exposed. These small Pd-rich nanoparticles are believed to be the primary active sites for the unselective hydrogenation and decomposition pathways, therefore once the small Pd-rich nanoparticles are 'covered' by a SnO_x layer, the unselective pathways are inhibited. The larger particles which remain exposed are composed of a Pd-Sn alloy, which is selective for the synthesis of H_2O_2 . TEM images suggested that the OR treatment is necessary to induce the SMSI effect which leads to 'coverage' of the small, unselective, Pd-rich nanoparticles. Pd^0 , even when incorporated into alloyed Pd-Sn structures, is active for the unselective hydrogenation and decomposition pathways. Therefore, a final oxidation step (*i.e.* a full ORO cycle) is necessary to generate Pd^{2+} as the predominant Pd state and therefore allow for a further increase in selectivity. A schematic of the proposed mechanism of surface structure development through the ORO cycle is illustrated in Figure 4.5.



Figure 4.5 – A schematic representation of the catalytic surface structures in a Pd-Sn/TiO₂ catalyst through an oxidation-reduction-oxidation heating cycle.³¹

It was further proposed in the study by Freakley *et al.*³¹ that there are three characteristics of the secondary metal which are necessary for producing a stable, selective Pd-'M' ORO catalyst. These characteristics are as follows: i) the secondary metal and its oxides should not decompose hydrogen peroxide. ii) the secondary metal should be able to form an alloy or mixed oxide phase with Pd. iii) the secondary metal can encapsulate small Pd-rich nanoparticles by strong metal-support interaction (SMSI). With three examples of catalysts with the general formulation of Pd-'M'/TiO₂ ORO proving to be stable and selective, many further transition metals

were tested as part of this formulation. A series of catalysts with the general nominal composition of 0.5 wt. % Pd - 4.5 wt. % 'M'/TiO₂ ORO were prepared and tested. The results of these tests are displayed in Table 4.16.

Table 4.16 – Productivity, degradation and stability testing data for various bi-metallic 0.5 wt. % Pd - 4.5 wt. % 'M'/TiO₂ ORO catalysts as indicated. All catalysts were prepared by standard impregnation.

Conditions: 50 ml Parr autoclave, 30 min, 20°C, 1200 rpm, 10 mg catalyst;

[a] 420 psi H₂/CO₂ +160 psi O₂/CO₂, 8.5g H₂O;

[b] 420 psi H₂/CO₂, 7.82 g H₂O + 0.68 g H₂O₂

Catalyst	Productivity mol kg⁻¹ h⁻¹ [a]	Degradation %^[b]	Stable?
0.5 wt. % Pd - 4.5 wt. % Ni/TiO₂ ORO	8	2	Yes
0.5 wt. % Pd - 4.5 wt. % Ga/TiO₂ ORO	12	2	Yes
0.5 wt. % Pd - 4.5 wt. % Zn/TiO₂ ORO	6	2	Yes
0.5 wt. % Pd - 4.5 wt. % Co/TiO₂ ORO	6	2	Yes
0.5 wt. % Pd - 4.5 wt. % In/TiO₂ ORO	7	2	Yes
0.5 wt. % Pd - 4.5 wt. % Cu/TiO₂ ORO	1	2	-
0.5 wt. % Pd - 4.5 wt. % Ru/TiO₂ ORO	8	20	No
0.5 wt. % Pd - 4.5 wt. % Ag/TiO₂ ORO	3	10	Yes
0.5 wt. % Pd - 4.5 wt. % Fe/TiO₂ ORO	2	5	-

The data displayed in Table 4.16 shows that Ni, Ga, Zn, In, or Co in the given combination with Pd, all produce active catalysts with minimal unselective degradation activity when treated with an ORO heating cycle. Furthermore, all of these selective 0.5 wt. % Pd - 4.5 wt. % 'M'/TiO₂ ORO catalysts display consistent productivity on re-use and do not suffer from metal loss as examined by MP-AES analysis. While some of these combinations of 0.5 wt. % Pd - 4.5 wt. % 'M'/TiO₂ ORO catalysts ('M' = Zn, Co, In) display little to no productivity increase over 0.5 wt. % Pd/TiO₂ ORO (Table 4.10), they are superior catalysts due to the significantly improved selectivity. It is believed that these stable, selective catalysts share a broadly similar surface metal structure to that observed for Pd-Sn/TiO₂ ORO.

However, when Pd is in combination with Cu or Fe, the catalysts exhibit negligible synthesis activity and when Pd is in combination with Ru, Ag or Fe, an extent of H₂O₂ degradation activity is recorded. Ag and Fe both display some degradation activity when tested as monometallic catalysts (Table 4.1), thus the failure of these metals to form selective catalysts is predicted by the three 'rules' set out previously. The alloying of Ru and Pd is documented to be a challenging process requiring sophisticated fabrication methods, with bulk alloying impossible and wet impregnation techniques forming random mixtures of mono-metallic nanoparticles.⁶¹ It therefore follows that Ru does not conform to the second of the 'rules' which were previously proposed and thus a stable, selective catalyst was not predicted by the 'rules' in this case. 0.5 wt. % Pd - 4.5 wt. % Cu/TiO₂ ORO displays both negligible synthesis and degradation activity, suggesting that there are very few Pd active sites available on the catalyst. Cu does not appear to infringe any of the outlined 'rules' as CuO_x does not degrade H₂O₂, although metallic Cu shows very slight activity (Table 4.1), further there are many accounts of Pd-Cu alloy formation⁶² and SMSI in Pd-Cu catalysts.⁶³ ⁶⁴ However, it is noted that SMSI in Pd-Cu/Nb₂O₅ leads to "drastically reduced" hydrogen chemisorption and turnover frequency in the hydrogenation of butadiene.⁶⁴ Other studies have documented the tendency for Pd-Cu/TiO₂ catalysts to form Pd core – CuO shell structures⁶⁵, therefore it could also be possible that similar structures are forming in the case of 0.5 wt. % Pd - 4.5 wt. % Cu/TiO₂ ORO, effectively 'covering' all Pd sites with a CuO layer, leading to inactivity.

In the study by Freakley *et al.*³¹, TEM images show total coverage of small Pd-rich nanoparticles by an SnO_x layer, which gives rise to the high selectivity of these catalysts. As outlined in Section 4.1, many studies suggest that it is specifically high energy edge and corner sites of Pd nanoparticles which are active for O-O bond dissociation and as such all unselective pathways in the direct synthesis of H₂O₂.^{18, 19}

Small nanoparticles have a relatively greater proportion of high energy edge and corner sites, hence a trend of increased selectivity with increased particle size is noted in many studies.²⁰ However, DFT studies by Iwamoto and co-workers show that a (111) surface of Pd is active for H₂O₂ synthesis with little to no activity for unselective pathways.²¹ Therefore, in the case of the stable, selective 0.5 wt. % Pd - 4.5 wt. % 'M'/TiO₂ ORO catalysts it is also possible that there are also small Pd-rich nanoparticles which are only partially encapsulated by the secondary metal oxide. In cases where high energy edge and corner sites are covered, but lower energy surfaces which are capable of selective H₂O₂ synthesis remain exposed, the resulting catalyst will theoretically still display near total selectivity.

To further explore the theory of edge and corner Pd sites acting as the predominant contributors to degradation activity, Pd sols were investigated. A monometallic Pd sol was prepared as described in the seminal work by Lopez-Sanchez *et al.*⁶⁶, half of which was immobilised on a TiO₂ support. Due to inherent problems of metal deposition when using sols in a stainless steel autoclave, simple H₂O₂ decomposition reactions were performed in a glass reaction vessel. The results of this testing is displayed in Table 4.17.

Table 4.17 – Decomposition testing data for free and immobilised Pd sols (each 0.1 mg Pd). Sol prepared with PdCl₂, poly vinyl acetate (PVA/Pd = 0.65, mol/mol) and NaBH₄ (NaBH₄/Pd = 5, mol/mol).

Conditions: 50 ml glass reactor, 30 min, 20°C, 1200 rpm, 7.82 g H₂O + 0.68 g H₂O₂, catalyst as indicated

Catalyst	Decomposition /%
Pd sol (0.1 mg Pd)	6
1 wt. % Pd/TiO ₂ (10 mg)	34

The data in Table 4.17 show that for catalysts of equivalent Pd mass, an immobilised Pd sol catalyst displays greater than five times the activity for H₂O₂ decomposition than a free Pd sol. In a free sol, Pd particles will generally facet into configurations of lower energy ((111), (110) and (100)) planes,^{67, 68} whereas when immobilised, high energy sites form at the interface of the Pd particle and the support.⁶⁹ Thus it is reasonable to conclude that these high energy interfacial edge sites are responsible for the vast increase in degradation activity observed.

4.2.10. Pd-Ni ORO performance under varied reaction conditions

Due to the zero net degradation activity and stability of 0.5 wt. % Pd - 4.5 wt. % Ni/TiO₂ ORO, multiple reactions were performed in succession to investigate whether it was possible to produce higher concentrations of hydrogen peroxide. After completion of a 30 minute reaction the autoclave was vented and re-charged with gases while remaining sealed; the concentration of hydrogen peroxide was then tested after 3 and 5 subsequent reactions. The results of this testing are displayed in Figure 4.6.

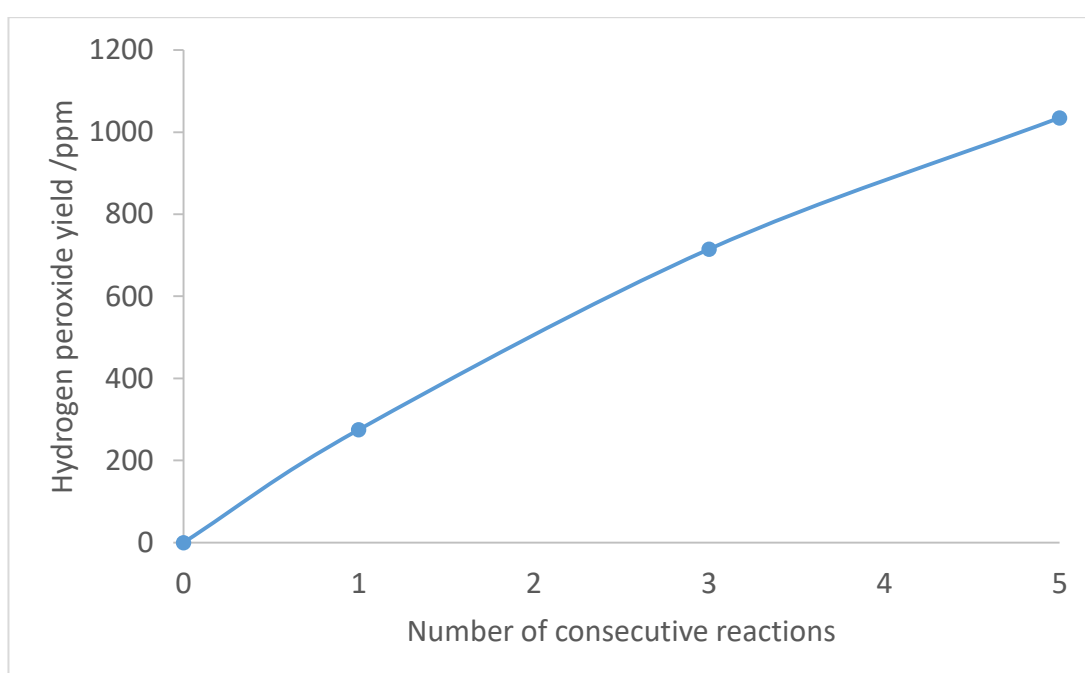


Figure 4.6 – Sequential synthesis reactions using a 0.5 wt. % Pd - 4.5 wt. % Ni/TiO₂ ORO (HCl, pH1) catalyst. The autoclave was fully vented and recharged with reactant gasses after each reaction, while the reaction solution and catalyst remained unchanged.

Conditions: 50 ml Parr autoclave, 30 min (per reaction), 20°C, 1200 rpm, 10 mg catalyst, 420 psi H₂/CO₂ +160 psi O₂/CO₂, 8.5g H₂O.

The results in Figure 4.6 show that 0.5 wt. % Pd - 4.5 wt. % Ni/TiO₂ ORO is active over multiple reaction cycles and is capable of sequentially producing significant yields of H₂O₂ when reactant gasses are replenished. The extent of H₂O₂ degradation appears to remain low, even at extended reaction time scales with relatively high concentrations of H₂O₂ present.

The effect of using an increased mass of 0.5 wt. % Pd - 4.5 wt. % Ni/TiO₂ ORO for both H₂O₂ synthesis and degradation reactions was also investigated. Similar tests were previously performed using a 2.5 wt. % Au - 2.5 wt. % Pd/TiO₂ catalyst, the results of which (displayed in Figure 3.10). The results of those tests showed that degradation activity increases significantly with catalyst mass, resulting in a degradation activity of 91% for a reaction utilising 80 mg catalyst. As degradation increases so markedly with catalyst mass, at masses greater than 20 mg, total yield begins to decrease as degradation processes dominate. It was hypothesised that due to the very low degradation activity of 0.5 wt. % Pd - 4.5 wt. % Ni/TiO₂ ORO, such a domination by degradation processes would not be observed, even at high masses. Therefore this would potentially allow for relatively high yields of H₂O₂ when increased masses of 0.5 wt. % Pd - 4.5 wt. % Ni/TiO₂ ORO were utilised. The results of testing varied masses of 0.5 wt. % Pd - 4.5 wt. % Ni/TiO₂ ORO for degradation activity and synthesis yield, along with previously presented analogous results for 2.5 wt. % Au - 2.5 wt. % Pd/TiO₂ are displayed in Figures 4.7 and 4.8, respectively.

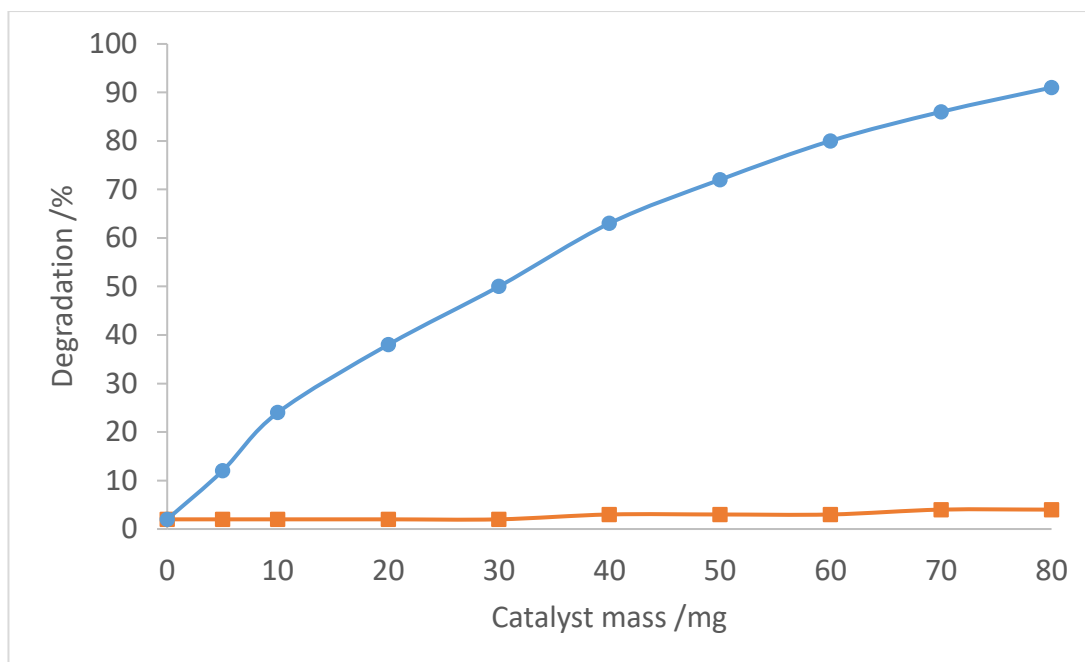


Figure 4.7 – H₂O₂ degradation activity for reactions using varied masses of 0.5 wt. % Pd - 4.5 wt. % Ni/TiO₂ ORO (HCl, pH1) and 2.5 wt. % Au - 2.5 wt. % Pd/TiO₂ catalysts.

● – 2.5 wt. % Au - 2.5 wt. % Pd/TiO₂, ■ – 0.5 wt. % Pd - 4.5 wt. % Ni/TiO₂ ORO (HCl, pH1)

Conditions: 50 ml Parr autoclave, 30 min, 20°C, 1200 rpm, mass of catalyst as indicated, 420 psi H₂/CO₂ +160 psi O₂/CO₂, 8.5g H₂O.

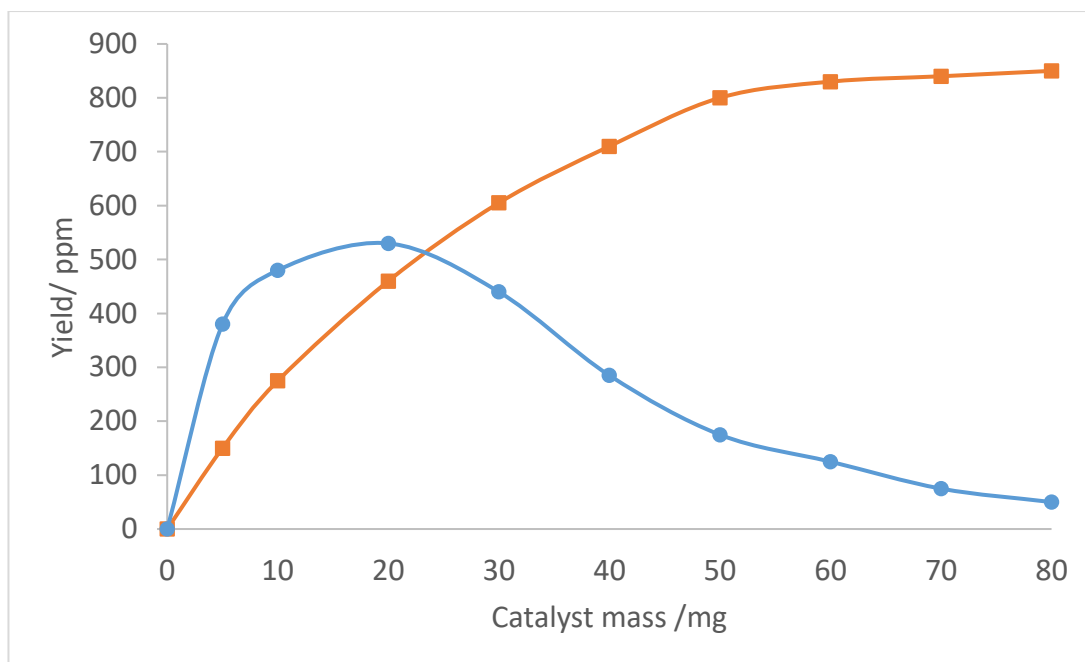


Figure 4.8 – Yield of H₂O₂ from synthesis reactions using varied masses of 0.5 wt. % Pd - 4.5 wt. % Ni/TiO₂ ORO (HCl, pH1) and 2.5 wt. % Au - 2.5 wt. % Pd/TiO₂ catalysts.

● – 2.5 wt. % Au - 2.5 wt. % Pd/TiO₂, ■ – 0.5 wt. % Pd - 4.5 wt. % Ni/TiO₂ ORO (HCl, pH1)

Conditions: 50 ml Parr autoclave, 30 min, 20°C, 1200 rpm, mass of catalyst as indicated, 420 psi H₂/CO₂ +160 psi O₂/CO₂, 8.5g H₂O.

The data displayed in Figures 4.7 and 4.8 show the advantage of using the highly selective 0.5 wt. % Pd - 4.5 wt. % Ni/TiO₂ ORO catalyst over the highly active 2.5 wt. % Au - 2.5 wt. % Pd/TiO₂ catalyst. Figure 4.7 shows that as catalyst mass is increased the degradation activity of 2.5 wt. % Au - 2.5 wt. % Pd/TiO₂ increases significantly, whereas 0.5 wt. % Pd - 4.5 wt. % Ni/TiO₂ ORO displays very little degradation activity, with only 4% degradation when using 80 mg catalyst. This result highlights the extremely low activity of 0.5 wt. % Pd - 4.5 wt. % Ni/TiO₂ ORO towards either decomposition or hydrogenation pathways, even with a high catalyst to substrate ratio.

Figure 4.8 shows that at catalyst masses of 20 mg and below, 0.5 wt. % Pd - 4.5 wt. % Ni/TiO₂ ORO is less productive 2.5 wt. % Au - 2.5 wt. % Pd/TiO₂. However, at masses above 20 mg the yield from 2.5 wt. % Au - 2.5 wt. % Pd/TiO₂ begins to decrease as explained previously, whereas due to the very low degradation activity of 0.5 wt. % Pd - 4.5 wt. % Ni/TiO₂ ORO, H₂O₂ yield continues to increase with increased catalyst mass up to 80 mg. This increase is not linear, with diminishing

returns in terms of yield per unit mass of catalyst, most likely resulting from mass transport effects and decreased availability of H₂. These results show that due to the extremely high selectivity of 0.5 wt. % Pd - 4.5 wt. % Ni/TiO₂ ORO, the ability to produce significant yields of H₂O₂ is possible when large catalyst masses are utilised.

It was previously shown in Section 3.2.9 that in a batch liquid/gas system using a 2.5 wt. % Au - 2.5 wt. % Pd/TiO₂ catalyst that use of an N₂ diluent leads to a significantly reduced yield relative to use of a CO₂ diluent. A standard synthesis reaction using a CO₂ diluent produces 470 ppm H₂O₂, whereas an analogous synthesis reaction using an N₂ diluent only produces 105 ppm H₂O₂. Decomposition activity was also increased when an N₂ diluent was used relative to a CO₂ diluent; believed to be due to a stabilising effect of carbonic acid formed *in-situ* when a CO₂ diluent is used. Similar tests were performed with 0.5 wt. % Pd - 4.5 wt. % Ni/TiO₂ ORO to assess the feasibility of using this catalyst with an N₂ diluted reactant stream, as would be the case for potential applications. The results of these tests are displayed in Table 4.18.

Table 4.18 – Productivity and degradation testing data for 0.5 wt. % Pd - 4.5 wt. % Ni/TiO₂ ORO (HCl, pH1) using both CO₂ and N₂ diluted gas streams.

Conditions: 50 ml Parr autoclave, 30 min, 20°C, 1200 rpm, 10 mg catalyst;

[a] 420 psi H₂/CO₂ +160 psi O₂/CO₂, 8.5g H₂O;

[b] 420 psi H₂/CO₂, 7.82 g H₂O + 0.68 g H₂O₂

Catalyst	Gas diluent	H ₂ O ₂ yield / ppm ^[a]	Degradation / % ^[b]
0.5 wt. % Pd - 4.5 wt. % Ni/TiO ₂ ORO (HCl, pH1)	CO ₂	275	2
0.5 wt. % Pd - 4.5 wt. % Ni/TiO ₂ ORO (HCl, pH1)	N ₂	145	2

The results in Table 4.18 show that 0.5 wt. % Pd - 4.5 wt. % Ni/TiO₂ ORO (HCl, pH1) maintains minimal degradation activity when an N₂ diluent is used, so an acidic medium, whether from acid additives or *in-situ* generated carbonic acid, is not necessary for the high selectivity of the catalyst. H₂O₂ yield for an N₂ diluent decreases significantly (*c.a.* 47%) relative to a CO₂ diluent, probably due to decreased H₂ solubility as outlined in Section 3.2.9. However, the relative decrease in yield upon

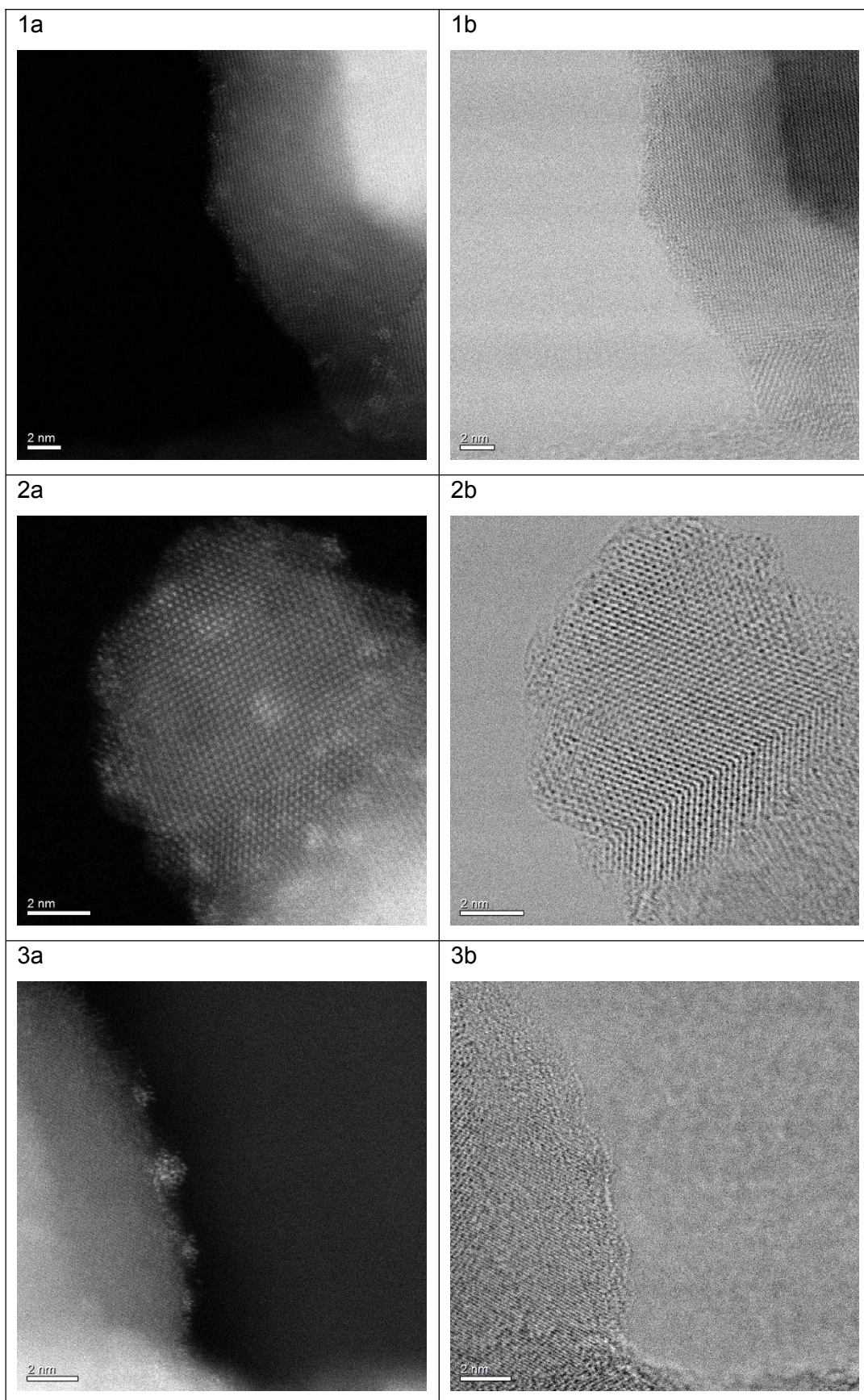
moving from a CO₂ to N₂ diluent is significantly less for 0.5 wt. % Pd - 4.5 wt. % Ni/TiO₂ ORO (HCl, pH1) compared to 2.5 wt. % Au - 2.5 wt. % Pd/TiO₂.

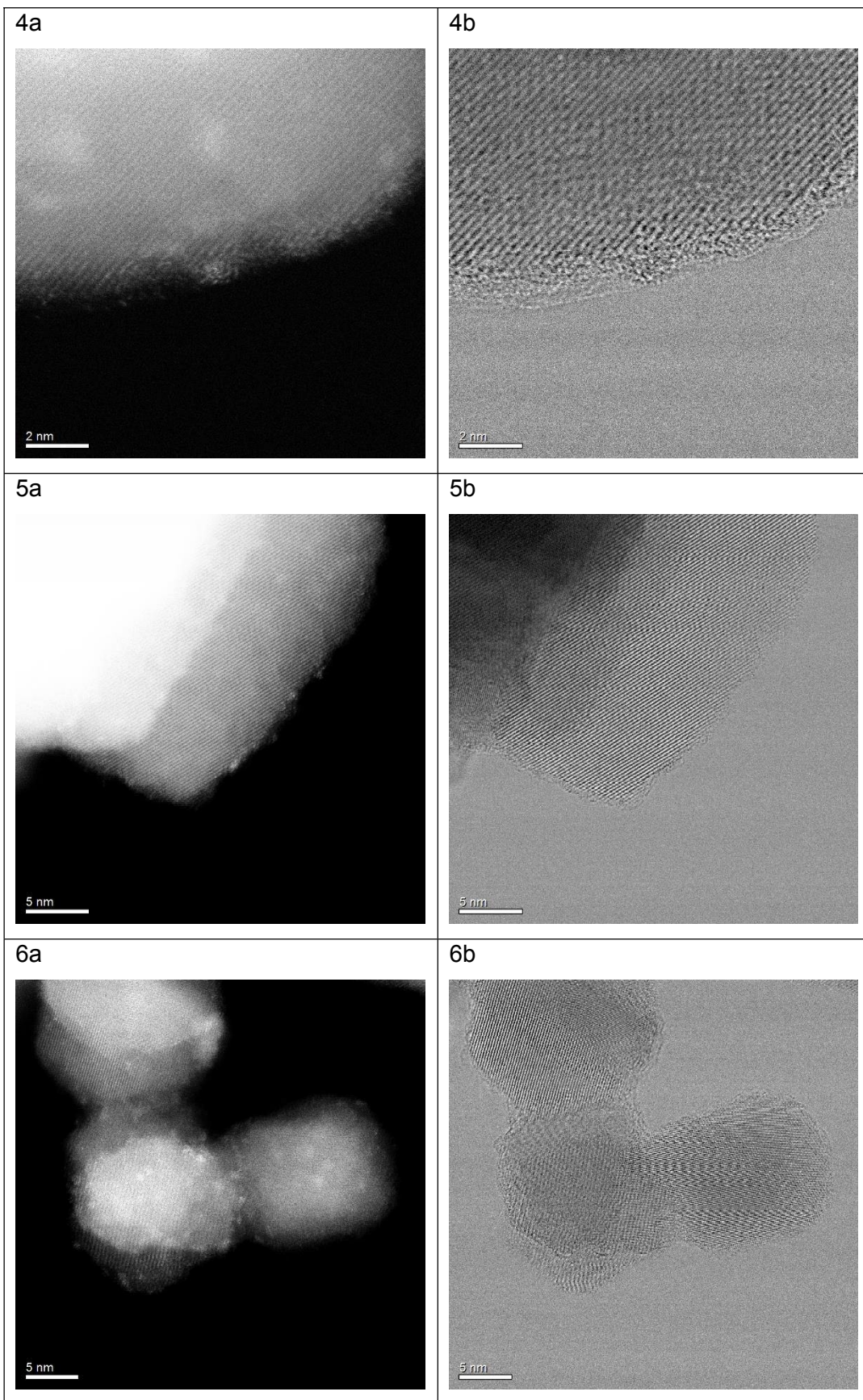
4.3. Characterisation

Characterisation efforts focussed on 0.5 wt. % Pd - 4.5 wt. % Ni/TiO₂ ORO catalysts as these were the most extensively tested throughout this work. Characterisation was performed with an aim towards identifying and understanding the stable surface metal structures responsible for the highly selective synthesis of H₂O₂ by these catalysts.

4.3.1. – STEM

STEM images were recorded to directly inspect a 0.5 wt. % Pd - 4.5 wt. % Ni/TiO₂ catalyst at all stages of the ORO cycle. An illustrative portion of these images are displayed in Figure 4.9.





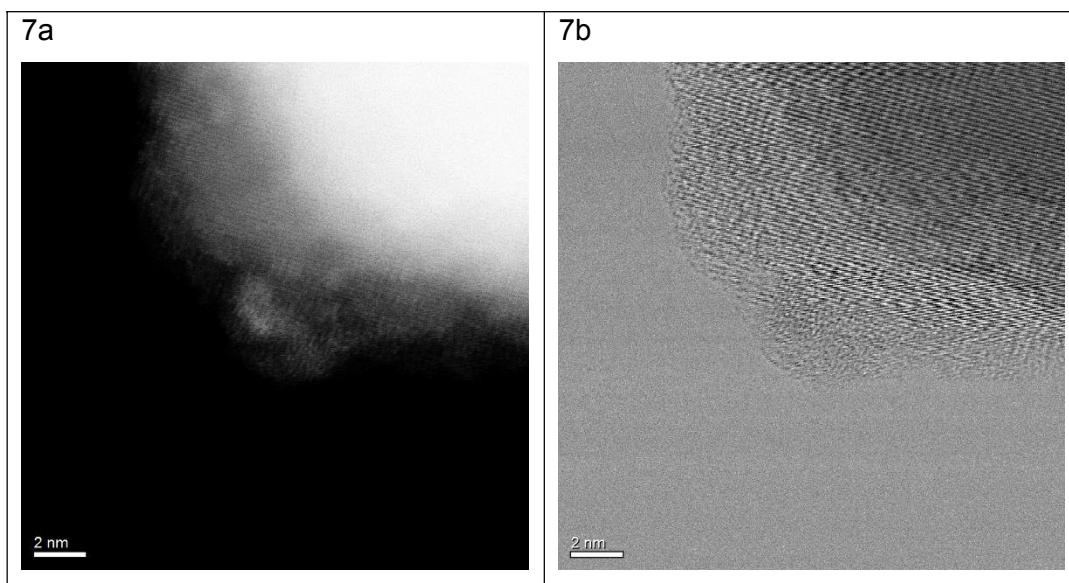


Figure 4.9 – STEM images of 0.5 wt. % Pd - 4.5 wt. % Ni/TiO₂ at each stage of an ORO heat treatment cycle. Images collected by Prof. Chris Kiely and co-workers at Lehigh Microscopy School.

Rows 1-2: O; Rows 3-4: OR; Rows 5-7: ORO

Column a: High-angle annular dark field/Z-contrast images, Column b: Bright field images

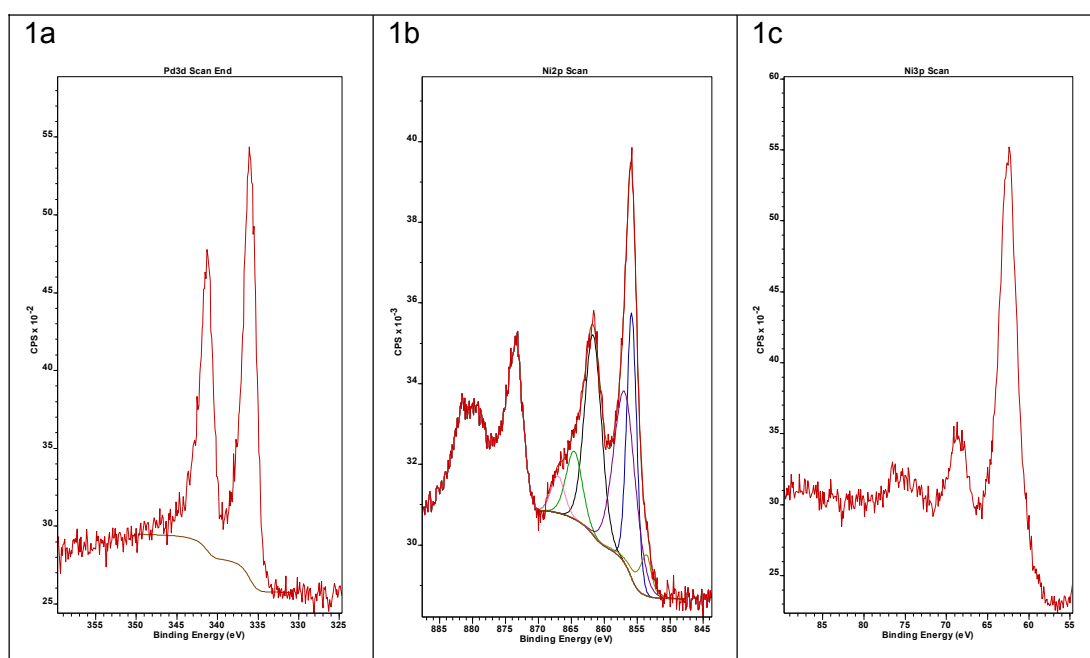
The images displayed in Figure 4.9 show that at all stages of heat treatment, the 0.5 wt. % Pd - 4.5 wt. % Ni/TiO₂ catalyst has very small Pd-rich particles, identifiable as bright spots in the 'Z-contrast' images (Column a) due to the relatively high atomic number of Pd. Almost all of these Pd-rich particles imaged having a diameter of less than 2 nm and the majority of particles having a diameter of 0.5 – 1 nm. Similar very small, Pd-rich particles were observed on Pd-Sn/TiO₂ catalysts in the prior study by Freakley *et al.*³¹, however imaging of Pd-Sn/TiO₂ catalysts also found many larger (5 -10 nm) Pd-Sn alloyed particles. Imaging of 0.5 wt. % Pd - 4.5 wt. % Ni/TiO₂ found no analogous larger Pd-Ni alloyed particles in images of the O or OR samples and only one such particle in the ORO sample (Image 7a/b, Pd-Ni composition confirmed by EDS). STEM imaging inherently focuses on a relatively small area of a catalyst, so is not always possible to extrapolate findings to broad statistical generalisations, however this finding suggests that these alloyed structures may be less common in 0.5 wt. % Pd - 4.5 wt. % Ni/TiO₂ ORO catalysts than Pd-Sn/TiO₂ catalysts.

Bright field images of 0.5 wt. % Pd - 4.5 wt. % Ni/TiO₂ ORO catalysts (Images 5b, 6b and 7b) show an amorphous layer covering the catalyst surface which is clearly visible at support edges. EDS analysis confirms this layer to be predominately NiO_x

with some TiO_x . This amorphous layer primarily consisting of the secondary supported metal is analogous to the structures previously observed in Pd-Sn/ TiO_2 ORO catalysts. In the images of 0.5 wt. % Pd - 4.5 wt. % Ni/ TiO_2 ORO, this amorphous $\text{NiO}_x/\text{TiO}_2$ layer does not appear to fully encapsulate the many small Pd-rich nanoparticles. It is therefore likely that the active selective structures in 0.5 wt. % Pd - 4.5 wt. % Ni/ TiO_2 ORO are primarily partially encapsulated small Pd-rich nanoparticles, in which high energy interfacial sites which are responsible for unselective reaction pathways are covered by an amorphous $\text{NiO}_x/\text{TiO}_x$ layer.

4.3.2. – XPS

XPS analysis was performed on 0.5 wt. % Pd - 4.5 wt. % Ni/ TiO_2 catalysts at each stage of the ORO treatment to probe the oxidation state of all surface species present on the catalysts. Relevant energy ranges from recorded XPS spectra are displayed in Figure 4.10.



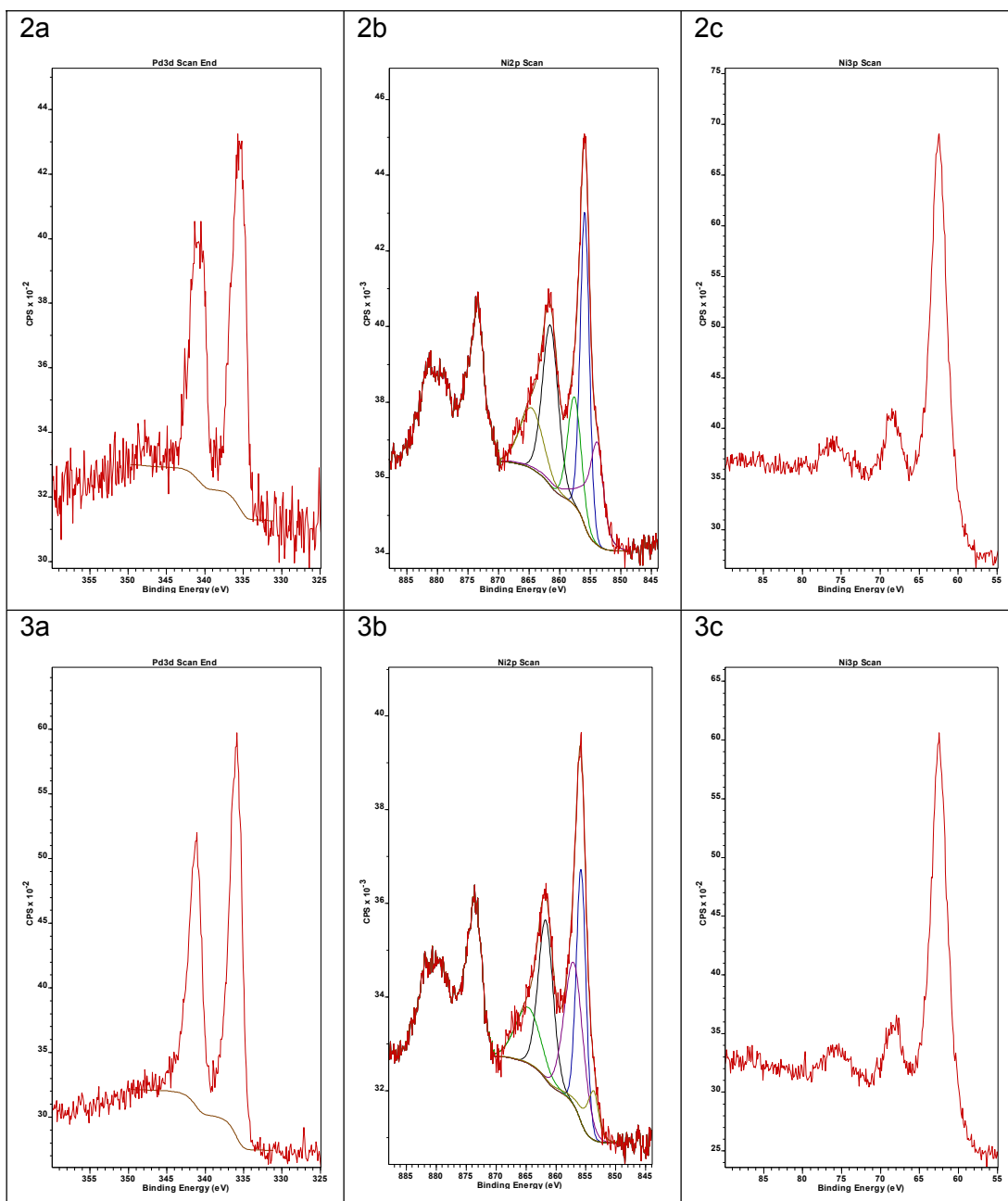


Figure 4.10 – XPS spectra images of 0.5 wt. % Pd - 4.5 wt. % Ni/TiO₂ at each stage of ORO treatment.

Row 1: O; Row 2: OR; Row 3: ORO

Column a: Pd 3d, Column b: Ni 2p, Column c: Ni 3p

From the XPS data presented in Figure 4.10, we observe that Pd is present as Pd²⁺ in O and ORO catalysts (336.1 eV) and present as Pd⁰ in the OR sample (335.4 eV).⁷⁰ This proves that Pd is in fact reduced during the ‘R’ heat treatment process. Pd behaves analogously throughout the heat treatment cycle in terms of oxidation state in these 0.5 wt. % Pd - 4.5 wt. % Ni/TiO₂ catalysts as was previously observed

in Pd-Sn/TiO₂ ORO catalysts.³¹ This also fits with testing data for the catalysts, as OR samples displayed high H₂O₂ synthesis activity, yet also high degradation activity, a noted feature of Pd⁰ catalysts.⁶

Ni is present in both metallic (Ni⁰) and oxidic (Ni²⁺) states in all samples. The O and ORO samples contain a large majority of Ni²⁺ while the OR sample shows a higher Ni⁰ content, but significant Ni²⁺ remains.⁷¹ It is possible that there is some rapid re-oxidation on Ni⁰ upon exposure to air after reductive heat treatment, potential future *in-situ* XPS studies could tell us whether there is full reduction of surface Ni during the reductive heat treatment step.

4.3.3. – CO DRIFTS

CO DRIFTS analysis was performed in absorption mode to probe the binding mode of CO on exposed Pd surfaces for 0.5 wt. % Pd - 4.5 wt. % Ni/TiO₂ through all stages of the ORO cycle. High energy Pd sites such as edges and defects would be expected to bind CO in a linear configuration, whereas lower energy planes would be expected to bind CO in bridged and three-fold conformations.^{72, 73} Therefore, our current working theory would predict a relative decrease in linear bound CO as a catalyst progresses through an ORO cycle and high energy Pd sites are covered by an amorphous NiO_x/TiO_x layer. The recorded spectra for 0.5 wt. % Pd - 4.5 wt. % Ni/TiO₂ are shown in Figure 4.11.

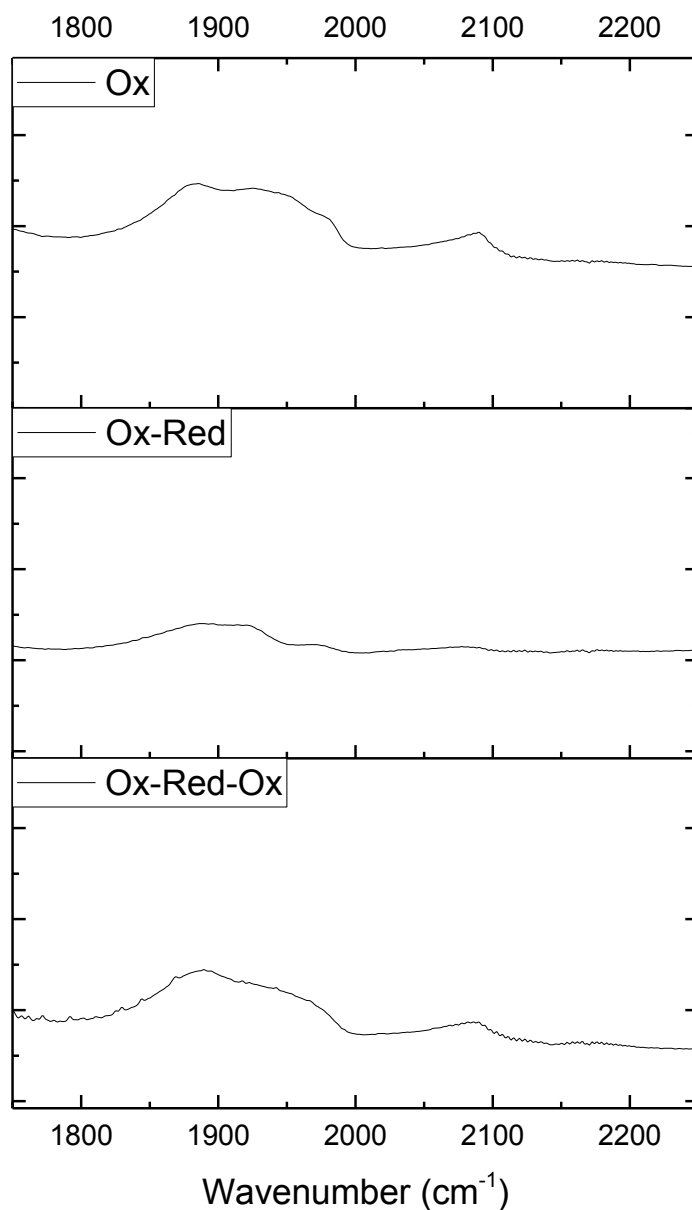


Figure 4.11 – Absorption mode DRIFTS spectra of CO on 0.5 wt. % Pd - 4.5 wt. % Ni/TiO₂ at each stage of ORO treatment.

Integration of the spectra displayed in Figure 4.11 shows the ratio of linear adsorbed CO (absorption peak 2000 - 2100 cm⁻¹) to bridged and three-fold adsorbed CO (absorption peak 1800 - 2000 cm⁻¹) is 1:7.00 for 0.5 wt. % Pd - 4.5 wt. % Ni/TiO₂ O and 1:9.7 for 0.5 wt. % Pd - 4.5 wt. % Ni/TiO₂ ORO. The differences in these spectra are relatively subtle, however these data suggest that there are relatively less high energy Pd sites on the ORO heat treated catalyst than the O treated catalyst, as predicted by the proposed model of the catalyst. The change in ratio of linear to bridged and threefold binding configurations between the O and ORO sample is not

large and there remains sites of sufficiently high energy to bind CO linearly on the ORO sample. The difference in H₂O₂ synthesis selectivity between O and ORO samples is marked, therefore it appears that sites which are of sufficiently high energy to bind CO linearly are not analogous to sites which are of sufficiently high energy to catalyse H₂O₂ degradation. However, this data represents some further evidence of the existence of relatively fewer high energy Pd sites in an ORO catalyst, relative to an O catalyst.

4.3.4. – CO Chemisorption

CO chemisorption was performed on a 0.5 wt. % Pd - 4.5 wt. % Ni/TiO₂ catalyst in both the O and ORO states. This was performed to probe volume of CO which adsorbs on to exposed Pd surfaces. In simple systems, a single type of CO binding mode can be assumed and the volume of adsorbed CO can be used to estimate active metal surface area and therefore metal dispersion. However, as outlined in Section 4.3.3, a 0.5 wt. % Pd - 4.5 wt. % Ni/TiO₂ catalyst binds CO in multiple configurations, the ratios of which change during an ORO heat cycle. However, if the working theory postulating an amorphous NiO_x/TiO_x layer ‘growing’ through the heat treatment cycles to partially cover Pd particles is correct, measured volume of CO adsorbed should decrease from an O to a ORO sample. The measured data from CO chemisorption is displayed in Table 4.19

Table 4.19 – CO chemisorption data for 0.5 wt. % Pd - 4.5 wt. % Ni/TiO₂ in O and ORO states.

Catalyst	Specific CO volume adsorbed / $\mu\text{L g}_{\text{cat}}^{-1}$
0.5 wt. % Pd - 4.5 wt. % Ni/TiO ₂ O	128.2
0.5 wt. % Pd - 4.5 wt. % Ni/TiO ₂ ORO	104.2

The data in Table 4.19 shows that there is a decrease in volume of CO adsorbed when an oxidised 0.5 wt. % Pd - 4.5 wt. % Ni/TiO₂ catalyst undergoes successive reduction and oxidation (ORO) treatment. These data are consistent with the current working theory of coverage of high energy Pd sites by an amorphous NiO_x/TiO_x layer increasing through ORO treatment.

4.3.5. – XRD

Powder XRD analysis was performed to analyse the crystal phases present in a range of the catalysts studied in this work. Collected X-ray diffraction patterns are displayed in Figures 4.12 – 4.14.

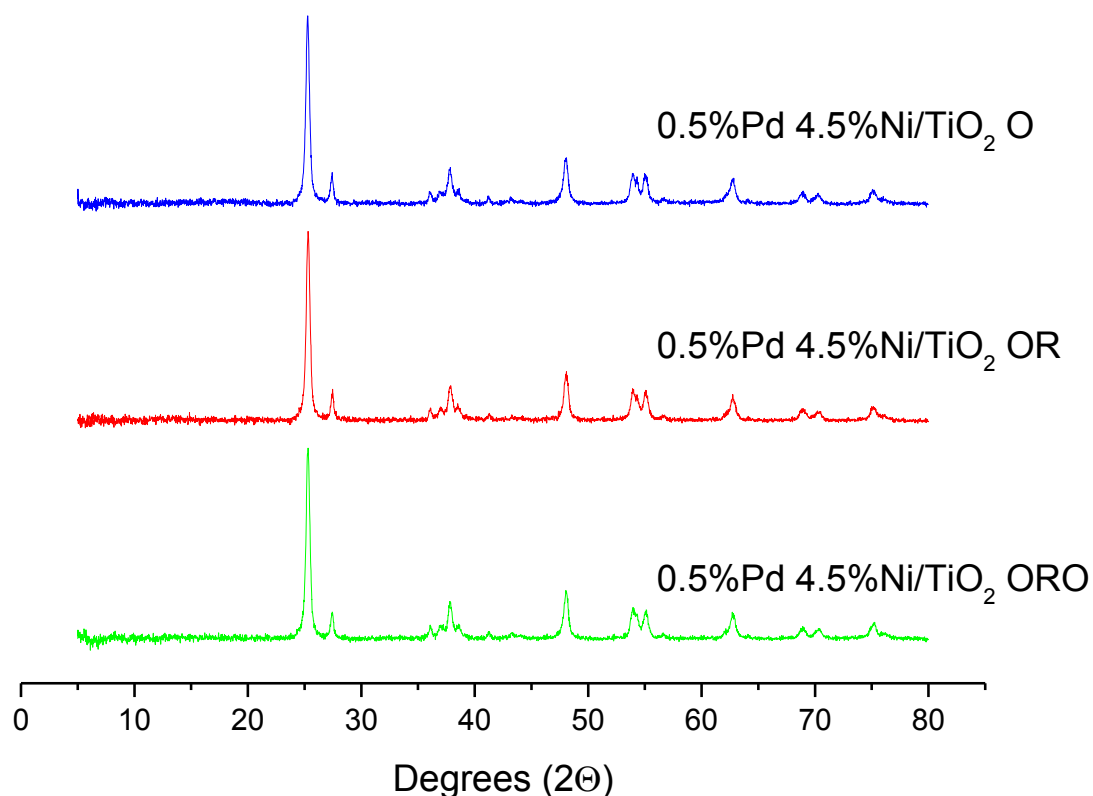


Figure 4.12 – XRD patterns of 0.5 wt. % Pd - 4.5 wt. % Ni/TiO₂ at each stage of ORO treatment

The patterns in Figure 4.12 show no significant changes between 0.5 wt. % Pd - 4.5 wt. % Ni/TiO₂ catalysts at each stage of the ORO treatment. Primary reflections corresponding to PdO ($2\theta = 34.352$)⁷⁴ or Pd ($2\theta = 40.366$)⁷⁵ are not visible not in any of the catalysts. This is consistent with the STEM imaging suggesting very small Pd nanoparticles as these produce weak reflections due containing very few crystal planes which can cause any reflection to be lost in background noise. The primary reflection corresponding to NiO ($2\theta = 43.30$)⁷⁶ is visible but very weak in both O and ORO samples. This suggests that there is some crystalline NiO present, but the NiO_x layer is largely amorphous.

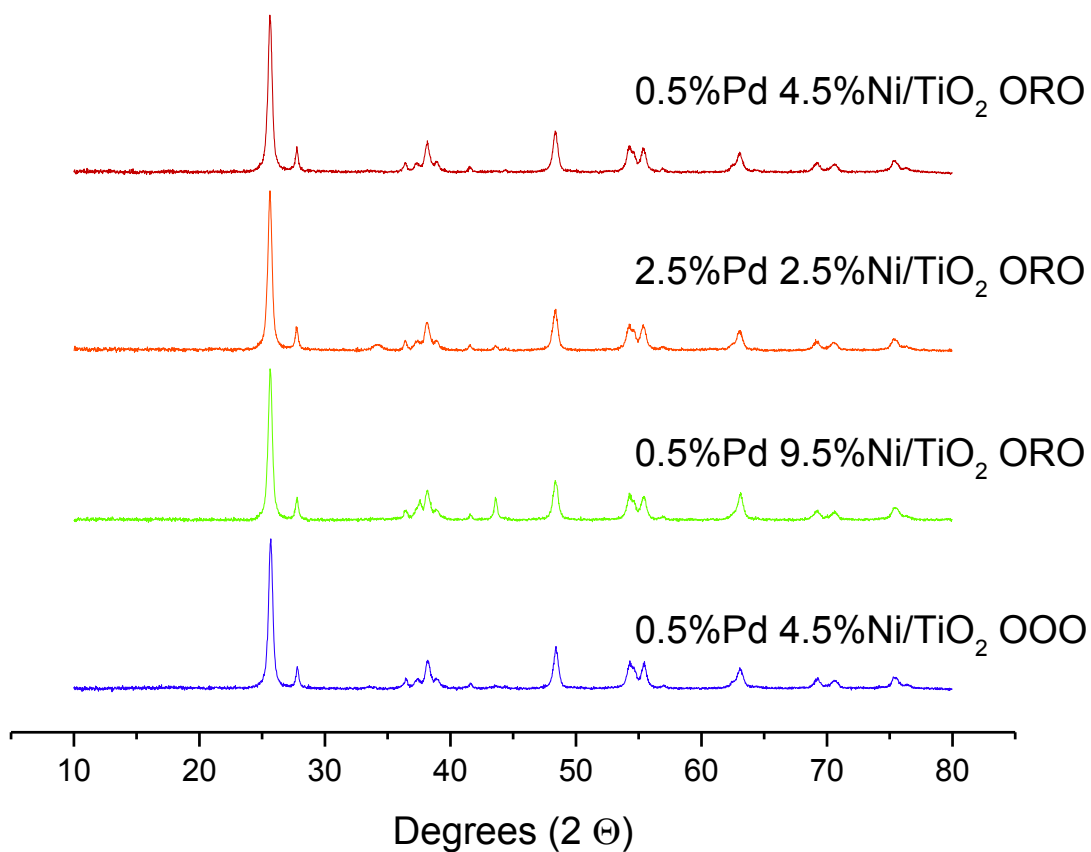


Figure 4.13 – XRD patterns of varied weight loadings and heat treatments of Pd - Ni/TiO₂.

The patterns in Figure 4.13 show a clear primary NiO reflection ($2\theta = 43.30$) in the 0.5 wt. % Pd - 9.5 wt. % Ni/TiO₂ ORO catalyst, indicating that when there is an increased loading of Ni there is a significant presence of crystalline NiO on the surface. A broad, fairly weak primary PdO reflection ($2\theta = 34.352$) is visible in the 2.5 wt. % Pd - 2.5 wt. % Ni/TiO₂ ORO catalyst, suggesting that increased Pd loading leads to the formation of larger Pd particles, causing a measureable reflection.

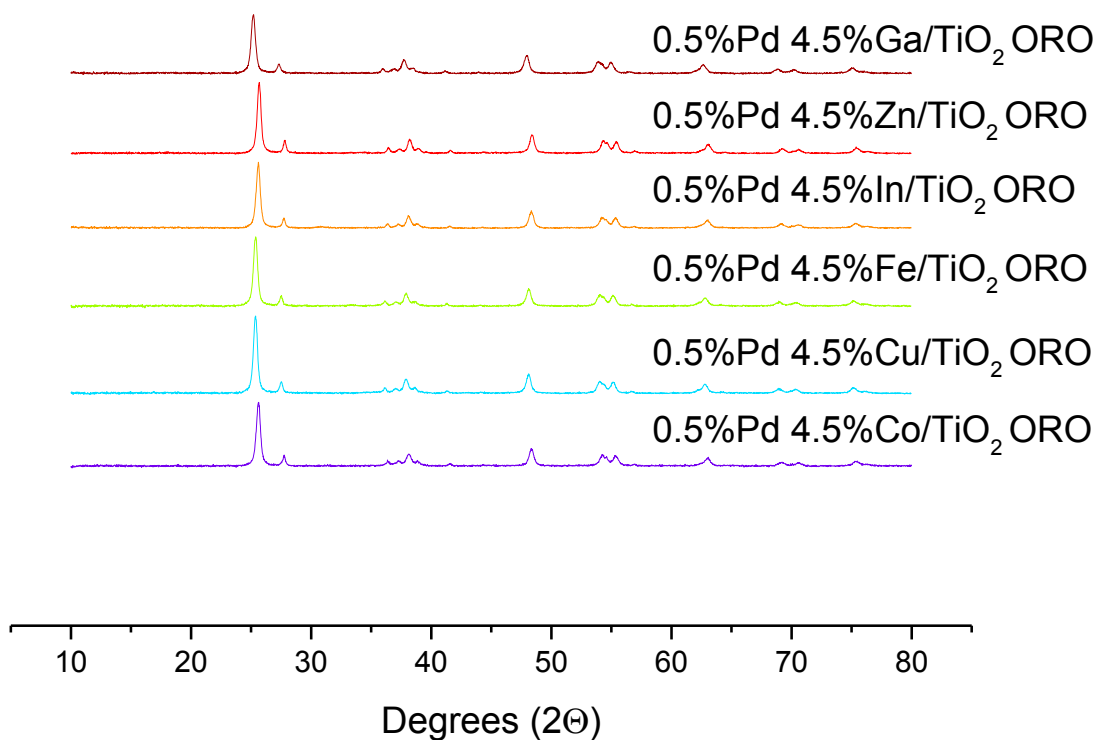


Figure 4.14 – XRD patterns of various compositions of 0.5 wt. % Pd - 4.5 wt. % 'M'/TiO₂ ORO.

The patterns in Figure 4.14 do not contain an observable Pd/PdO reflection for any of the catalysts, suggesting very small Pd rich nanoparticles for all variations of 0.5 wt. % Pd - 4.5 wt. % 'M'/TiO₂ ORO catalysts. No strong reflections corresponding to secondary metal oxides are observed, suggesting the presence of secondary metal oxides in an amorphous state.

4.3.6 – TPR

TPR analysis was performed to probe the reducibility of materials in 0.5 wt. % Pd/TiO₂ ORO, 2.5 wt. % Pd - 2.5 wt. % Ni/TiO₂ ORO and 0.5 wt. % Pd - 4.5 wt. % Ni/TiO₂ ORO catalysts. The TPR traces from analysis of these catalysts are displayed in Figures 4.15 - 4.17.

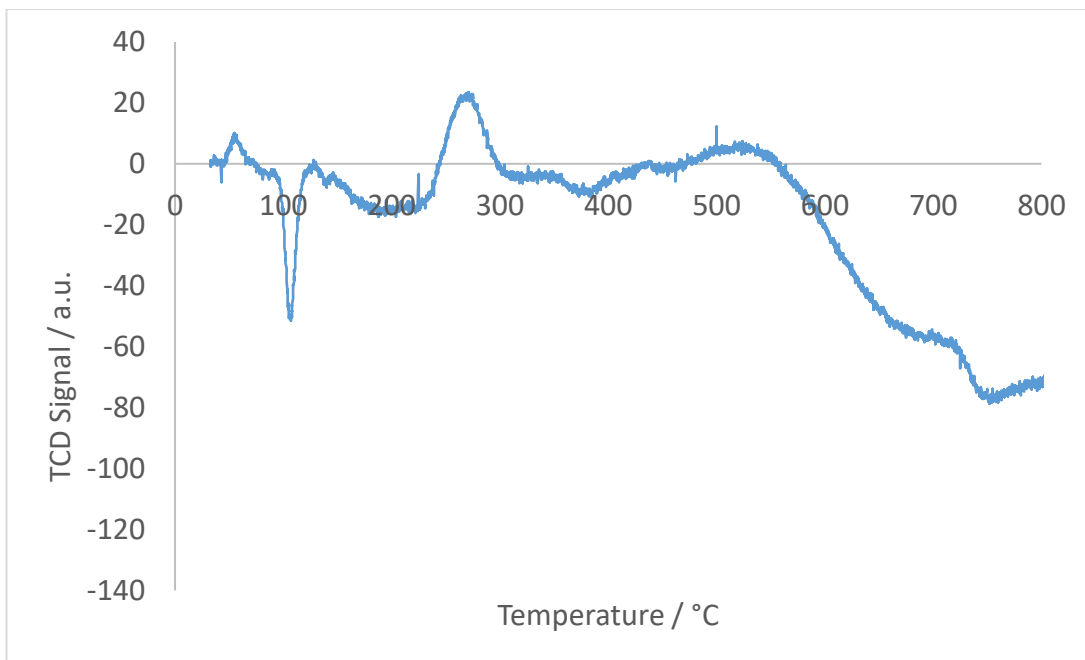


Figure 4.15 – TPR trace for of 0.5 wt. % Pd/TiO₂ ORO.

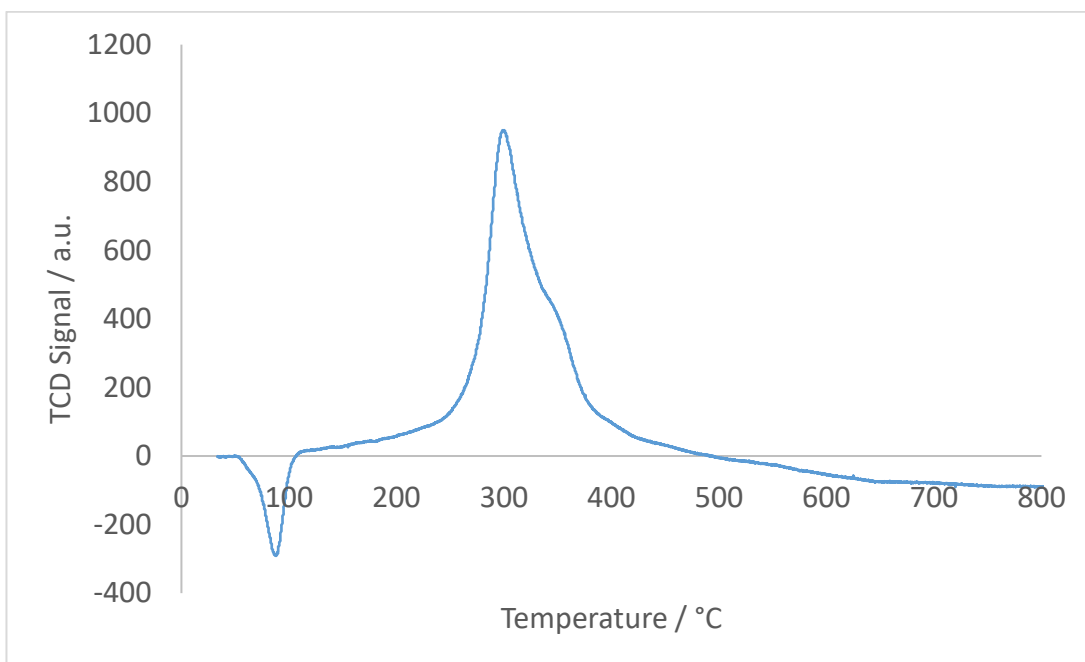


Figure 4.16 – TPR trace for of 2.5 wt. % Pd - 2.5 wt. % Ni/TiO₂ ORO.

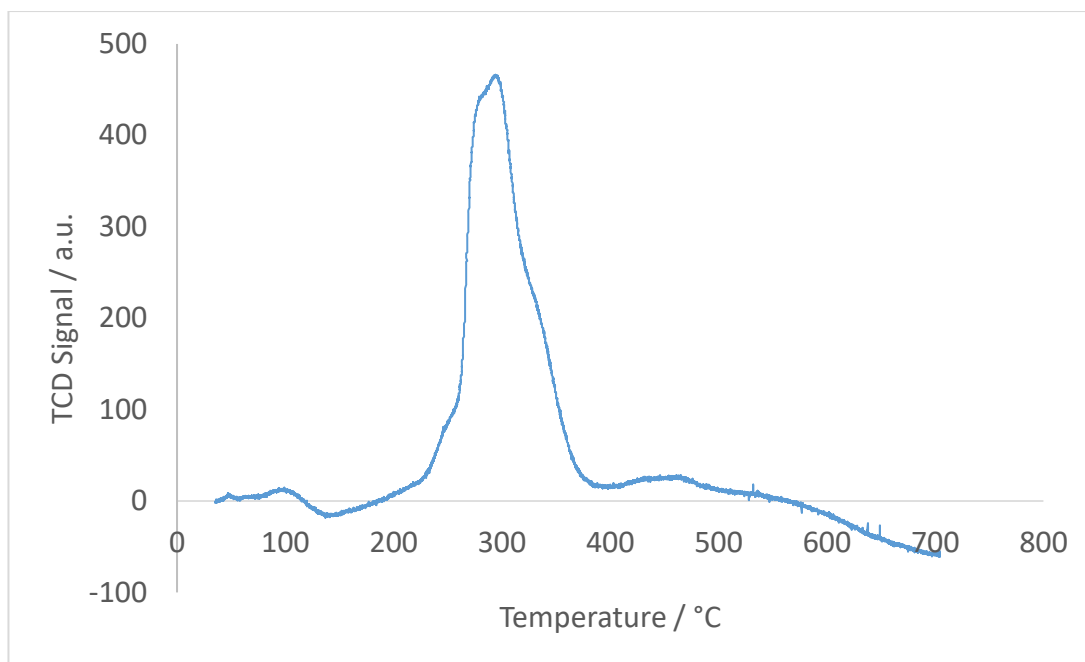


Figure 4.17 – TPR trace for of 0.5 wt. % Pd - 4.5 wt. % Ni/TiO₂ ORO.

Figure 4.15 and 4.16 (0.5 wt. % Pd ORO and 2.5 wt. % Pd - 2.5 wt. % Ni/TiO₂ ORO, respectively) both show a clear β -hydride decomposition peak around 100°C. No β -hydride decomposition peak is evident in Figure 4.17 for 0.5 wt. % Pd - 4.5 wt. % Ni/TiO₂ ORO. The formation of Pd hydride species is strongly dependant on Pd particle size, with hydride formation increasing with increasing particle size.⁷⁷ Prior studies have shown that Pd particles with a diameter smaller than 2.6 nm do not form Pd hydride phases.⁷⁸ This further confirms that very small (0.5 - 1 nm) median particle size in the 0.5 wt. % Pd - 4.5 wt. % Ni/TiO₂ ORO catalyst. The presence of β -hydride decomposition peaks in the traces for both 0.5 wt. % Pd ORO and 2.5 wt. % Pd - 2.5 wt. % Ni/TiO₂ ORO suggests that the average Pd particle size in these catalysts is significantly larger than that of 0.5 wt. % Pd - 4.5 wt. % Ni/TiO₂ ORO catalysts.

4.4. Conclusions

When first tested for H₂O₂ synthesis, the now extensively studied 2.5 wt. % Au – 2.5 wt. % Pd/TiO₂ catalyst represented a significant improvement in selectivity and activity over previous Pd based catalysts.²⁵ While these catalysts display fairly high

selectivity, they are still active for unselective reaction pathways, leading to inefficient use of reactant gasses and thus reduced economy in use. Furthermore, significant Au loading means catalyst production would rely on procurement of a metal which is relatively scarce, highly valued and extensively traded, therefore costly and prone to price fluctuation. Due to these characteristics, development of highly selective catalysts, preferably with minimal use of costly metals, is desirable.

Arguably the most significant development in catalyst design for H₂O₂ synthesis since the discovery of Au-Pd catalysts is the study by Freakley *et al.*³¹ reporting on supported Sn-Pd 'oxidised-reduced-oxidised' nanoparticle catalysts which display good activity, high stability and near total selectivity for H₂O₂. The work contained herein has demonstrated that various further supported metal nanoparticle catalysts of the type Pd-M (M= Ni, Ga, Co, In and Zn) ORO also display near total selectivity for the direct synthesis of H₂O₂, in addition to good activity and high stability.

Focussing on Pd-Ni catalysts, it was initially found that relatively high activity could be achieved with low (<1%) Pd loading in oxidised catalysts, however stable catalysts were only achieved after use of an ORO heat treatment. Even with use of an ORO heat treatment, Pd-Ni catalysts with relatively too little Ni still do not achieve stability or near total selectivity. TiO₂ was primarily used as a support material throughout this work, however it was shown that the stable and selective Pd-Ni ORO catalysts can be prepared on various other metal and semi-metal oxide supports. Attempts to directly support Pd onto a secondary metal oxide (eg. NiO) did not yield highly selective catalysts with any heat treatment, therefore it appears that the presence of Pd with a secondary metal supported onto a primary oxide support is necessary for the high selectivity exhibited by Pd-M ORO catalysts. Specifically for the preparation of a 0.5 wt. % Pd - 4.5 wt. % Ni/TiO₂ ORO catalyst, it was found that the use of chloride precursor salts and the addition of acid and chloride to the catalyst preparation lead to a more productive catalyst which remained almost totally selective.

The high selectivity of these Pd-M ORO catalysts allows for the use of high catalyst masses and extended reaction times to produce significant concentrations of H₂O₂, as demonstrated in Section 4.2.10 using an optimised 0.5 wt. % Pd - 4.5 wt. % Ni/TiO₂ ORO catalyst. The use of similar high catalyst masses and extended reaction times using a 2.5 wt. % Au - 2.5 wt. % Pd/TiO₂ does not allow for high yields of H₂O₂, instead producing low yields as degradation processes dominate. In addition, the significantly lower precious metal loading (and therefore decreased cost) of 0.5 wt. % Pd - 4.5 wt. % Ni/TiO₂ ORO comparative to 2.5 wt. % Au - 2.5 wt. % Pd/TiO₂ and the high stability

of 0.5 wt. % Pd - 4.5 wt. % Ni/TiO₂ ORO show the potential applicability of 0.5 wt. % Pd - 4.5 wt. % Ni/TiO₂ ORO to high catalyst mass, high throughput applications without concern of inefficient use of reactants from unselective reaction processes which will occur with less selective catalysts.

Using both catalyst testing and characterisation data, a model of the structures on 0.5 wt. % Pd - 4.5 wt. % Ni/TiO₂ ORO (and by extension, most likely the series of catalysts with similar behaviour) responsible for the selective synthesis of H₂O₂ can be proposed. STEM images show that the predominant Pd containing structures are 0.5 – 1 nm Pd-rich clusters (present as PdO in the ORO samples), with only very few larger (5 – 10 nm) alloyed Pd-Ni structures. There appears to be a near continuous layer of amorphous NiO or mixed NiO_x/TiO_x on the catalyst which partially covers the Pd-rich clusters as the catalyst is subjected to the ORO heat treatment. This partial coverage of the Pd-rich clusters appears to afford the selectivity to the catalyst, as the highest energy interfacial and corner Pd sites which are believed to be active for degradation pathways are blocked. Furthermore, the partial/ encapsulation of the Pd-rich clusters also may afford stability to the catalyst by preventing the loss of Pd from these particles or the removal of particles from the catalyst surface. Lower energy Pd planes are believed to remain exposed and act as active sites for the selective synthesis of H₂O₂. A revised schematic diagram of this proposed model is displayed in Figure 4.19.

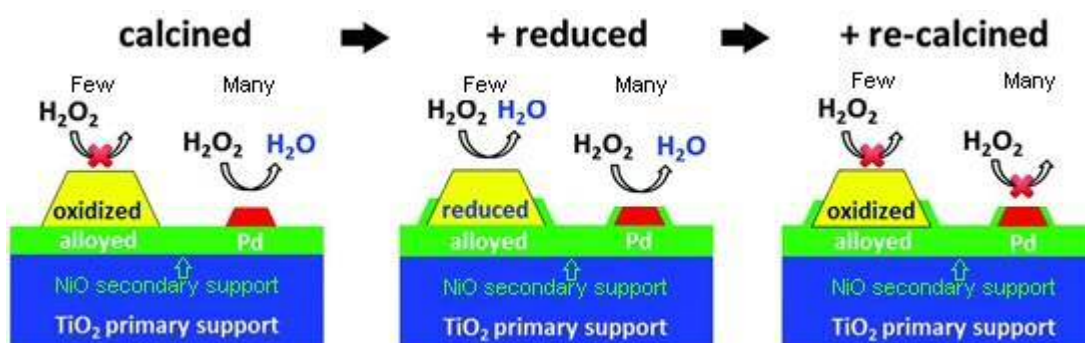


Figure 4.19 – A schematic diagram of the working model for the surface structures responsible for the highly selective synthesis of H₂O₂ by 0.5 wt. % Pd - 4.5 wt. % Ni/TiO₂ ORO and similar catalyst. Diagram adapted from Freakley *et al.*³¹

4.5. References

1. H. Henkel and W. Weber, *US Patent 1,108,752*, 1914.
2. R. Dittmeyer, J. D. Grunwaldt and A. Pashkova, *Catalysis Today*, 2015, 248, 149-159.
3. Y. H. Yi, L. Wang, G. Li and H. C. Guo, *Catalysis Science & Technology*, 2016, 6, 1593-1610.
4. J. K. Edwards, S. J. Freakley, R. J. Lewis, J. C. Pritchard and G. J. Hutchings, *Catalysis Today*, 2015, 248, 3-9.
5. J. K. Edwards and G. J. Hutchings, *Angewandte Chemie*, 2008, 47, 9192-9198.
6. C. Samanta, *Applied Catalysis A: General*, 2008, 350, 133-149.
7. V. R. Choudhary, A. G. Gaikwad and S. D. Sansare, *Catalysis Letters*, 2002, 83, 235-239.
8. V. R. Choudhary, C. Samanta and A. G. Gaikwad, *Chemical Communications*, 2004, 10, 2054-2055.
9. V. R. Choudhary and P. Jana, *Applied Catalysis A: General*, 2009, 352, 35-42.
10. V. R. Choudhary, C. Samanta and T. V. Choudhary, *Applied Catalysis A: General*, 2006, 308, 128-133.
11. N. Gemo, S. Sterchele, P. Biasi, P. Centomo, P. Canu, M. Zecca, A. Shchukarev, K. Kordas, T. O. Salmi and J.-P. Mikkola, *Catalysis Science & Technology*, 2015, 5, 3545-3555.
12. P. Biasi, P. Canu, F. Menegazzo, F. Pinna and T. O. Salmi, *Industrial & Engineering Chemistry Research*, 2012, 51, 8883-8890.
13. P. Biasi, F. Menegazzo, P. Canu, F. Pinna and T. O. Salmi, *Industrial & Engineering Chemistry Research*, 2013, DOI: 10.1021/ie4011782, 130916123939006.
14. S. Park, J. C. Jung, J. G. Seo, T. J. Kim, Y.-M. Chung, S.-H. Oh and I. K. Song, *Catalysis Letters*, 2009, 130, 604-607.
15. S. Park, T. J. Kim, Y.-M. Chung, S.-H. Oh and I. K. Song, *Catalysis Letters*, 2009, 130, 296-300.
16. S. Park, J. G. Seo, J. C. Jung, S.-H. Baeck, T. J. Kim, Y.-M. Chung, S.-H. Oh and I. K. Song, *Catalysis Communications*, 2009, 10, 1762-1765.
17. S. Park, S.-H. Baeck, T. J. Kim, Y.-M. Chung, S.-H. Oh and I. K. Song, *Journal of Molecular Catalysis A: Chemical*, 2010, 319, 98-107.
18. S. Melada, F. Pinna, G. Strukul, S. Perathoner and G. Centi, *Journal of Catalysis*, 2005, 235, 241-248.
19. S. Kim, D.-W. Lee, K.-Y. Lee and E. A. Cho, *Catalysis Letters*, 2014, 144, 905-911.
20. N. M. Wilson and D. W. Flaherty, *Journal of the American Chemical Society*, 2016, 138, 574-586.
21. T. Deguchi and M. Iwamoto, *The Journal of Physical Chemistry C*, 2013, DOI: 10.1021/jp4056297, 130828083551006.
22. S. Sterchele, P. Biasi, P. Centomo, A. Shchukarev, K. Kordas, A. R. Rautio, J. P. Mikkola, T. Salmi, P. Canton and M. Zecca, *Chemcatchem*, 2016, 8, 1564-1574.
23. S. Abate, K. Barbera, G. Centi, G. Giorgianni and S. Perathoner, *J. Energy Chem.*, 2016, 25, 297-305.
24. H. E. Jeong, S. Kim, M. G. Seo, D. W. Lee and K. Y. Lee, *J. Mol. Catal. A-Chem.*, 2016, 420, 88-95.
25. P. Landon, P. J. Collier, A. J. Papworth, C. J. Kiely and G. J. Hutchings, *Chemical Communications*, 2002, DOI: 10.1039/b205248m, 2058-2059.

26. J. K. Edwards, A. Thomas, B. E. Solsona, P. Landon, A. F. Carley and G. J. Hutchings, *Catalysis Today*, 2007, 122, 397-402.
27. J. Edwards, B. Solsona, P. Landon, A. Carley, A. Herzing, C. Kiely and G. Hutchings, *Journal of Catalysis*, 2005, 236, 69-79.
28. J. K. Edwards, A. F. Carley, A. A. Herzing, C. J. Kiely and G. J. Hutchings, *Faraday Discussions*, 2008, 138, 225.
29. L. Ouyang, G.-j. Da, P.-f. Tian, T.-y. Chen, G.-d. Liang, J. Xu and Y.-F. Han, *Journal of Catalysis*, 2014, 311, 129-136.
30. F. Gao and D. W. Goodman, *Chemical Society reviews*, 2012, 41, 8009-8020.
31. S. J. Freakley, Q. He, J. H. Harrhy, L. Lu, D. A. Crole, D. J. Morgan, E. N. Ntainjua, J. K. Edwards, A. F. Carley, A. Y. Borisevich, C. J. Kiely and G. J. Hutchings, *Science*, 2016, 351, 965-968.
32. S. Melada, F. Pinna, G. Strukul, S. Perathoner and G. Centi, *Journal of Catalysis*, 2006, 237, 213-219.
33. Q. Liu, J. C. Bauer, R. E. Schaak and J. H. Lunsford, *Applied Catalysis A: General*, 2008, 339, 130-136.
34. E. N. Ntainjua, S. J. Freakley and G. J. Hutchings, *Topics in Catalysis*, 2012, 55, 718-722.
35. S. Sterchele, P. Biasi, P. Centomo, P. Canton, S. Campestrini, T. Salmi and M. Zecca, *Applied Catalysis A: General*, 2013, 468, 160-174.
36. J. K. Edwards, J. Pritchard, L. Lu, M. Piccinini, G. Shaw, A. F. Carley, D. J. Morgan, C. J. Kiely and G. J. Hutchings, *Angewandte Chemie*, 2014, 53, 2381-2384.
37. R. C. Reuel and C. H. Bartholomew, *Journal of Catalysis*, 1984, 85, 78-88.
38. J. C. Rodriguez, A. J. Marchi, A. Borgna and A. Monzon, *Journal of Catalysis*, 1997, 171, 268-278.
39. T. Riedel, M. Claeys, H. Schulz, G. Schaub, S. S. Nam, K. W. Jun, M. J. Choi, G. Kishan and K. W. Lee, *Appl. Catal. A-Gen.*, 1999, 186, 201-213.
40. E. J. Shin and M. A. Keane, *Industrial & Engineering Chemistry Research*, 2000, 39, 883-892.
41. E. L. Rodrigues and J. M. C. Bueno, *Appl. Catal. A-Gen.*, 2004, 257, 201-211.
42. F. Studt, F. Abild-Pedersen, T. Bligaard, R. Z. Sørensen, C. H. Christensen and J. K. Nørskov, *Science*, 2008, 320, 1320-1322.
43. R. M. Bullock, *Catalysis without Precious Metals*, 2010.
44. P. Yuan, Z. Y. Liu, W. Q. Zhang, H. J. Sun and S. C. Liu, *Chinese Journal of Catalysis*, 2010, 31, 769-775.
45. A. G. Sergeev, J. D. Webb and J. F. Hartwig, *Journal of the American Chemical Society*, 2012, 134, 20226-20229.
46. Y. F. He, L. L. Liang, Y. N. Liu, J. T. Feng, C. Ma and D. Q. Li, *Journal of Catalysis*, 2014, 309, 166-173.
47. C. M. Li, Y. D. Chen, S. T. Zhang, J. Y. Zhou, F. Wang, S. He, M. Wei, D. G. Evans and X. Duan, *Chemcatchem*, 2014, 6, 824-831.
48. C. P. Jimenez-Gomez, J. A. Cecilia, D. Duran-Martin, R. Moreno-Tost, J. Santamaria-Gonzalez, J. Merida-Robles, R. Mariscal and P. Maireles-Torres, *Journal of Catalysis*, 2016, 336, 107-115.
49. Y. Y. Chen, C. A. Wang, H. Y. Liu, J. S. Qiu and X. H. Bao, *Chemical Communications*, 2005, DOI: 10.1039/b50909595f, 5298-5300.
50. C. Sigma-Aldrich, *Aldrich chemistry 2012-2014 : Handbook of Fine Chemicals*, 2011.
51. S. Abate, S. Melada, G. Centi, S. Perathoner, F. Pinna and G. Strukul, *Catalysis Today*, 2006, 117, 193-198.
52. J. García-Serna, T. Moreno, P. Biasi, M. J. Cocero, J.-P. Mikkola and T. O. Salmi, *Green Chemistry*, 2014, DOI: 10.1039/c3gc41600c.

53. J. K. Edwards, B. Solsona, E. N. N, A. F. Carley, A. A. Herzing, C. J. Kiely and G. J. Hutchings, *Science*, 2009, 323, 1037-1041.
54. P. Landon, P. J. Collier, A. F. Carley, D. Chadwick, A. J. Papworth, A. Burrows, C. J. Kiely and G. J. Hutchings, *Physical Chemistry Chemical Physics*, 2003, 5, 1917-1923.
55. V. R. Choudhary, C. Samanta and T. V. Choudhary, *Journal of Molecular Catalysis A: Chemical*, 2006, 260, 115-120.
56. Q. Liu and J. Lunsford, *Journal of Catalysis*, 2006, 239, 237-243.
57. M. L. Toebes, J. A. van Dillen and K. P. de Jong, *Journal of Molecular Catalysis A: Chemical*, 2001, 173, 75-98.
58. M. Sankar, Q. He, M. Morad, J. Pritchard, S. J. Freakley, J. K. Edwards, S. H. Taylor, D. J. Morgan, A. F. Carley, D. W. Knight, C. J. Kiely and G. J. Hutchings, *ACS Nano*, 2012, 6, 6600-6613.
59. J. K. Edwards, S. F. Parker, J. Pritchard, M. Piccinini, S. J. Freakley, Q. He, A. F. Carley, C. J. Kiely and G. J. Hutchings, *Catalysis Science & Technology*, 2013, 3, 812.
60. K. Suttiponparnit, J. Jiang, M. Sahu, S. Suvachittanont, T. Charinpanitkul and P. Biswas, *Nanoscale Res Lett*, 2010, 6, 27.
61. D. Wu, K. Kusada and H. Kitagawa, *Science and Technology of Advanced Materials*, 2016, 17, 583-596.
62. M. Fernández-García, J. A. Anderson and G. L. Haller, *The Journal of Physical Chemistry*, 1996, 100, 16247-16254.
63. M.-S. Kim, S.-H. Chung, C.-J. Yoo, M. S. Lee, I.-H. Cho, D.-W. Lee and K.-Y. Lee, *Applied Catalysis B: Environmental*, 2013, 142-143, 354-361.
64. M. M. Pereira, F. B. Noronha and M. Schmal, *Catalysis Today*, 1993, 16, 407-415.
65. J. Radnik, M. M. Pohl, V. N. Kalevaru and A. Martin, *The Journal of Physical Chemistry C*, 2007, 111, 10166-10169.
66. J. A. Lopez-Sanchez, N. Dimitratos, P. Miedziak, E. Ntainjua, J. K. Edwards, D. Morgan, A. F. Carley, R. Tiruvalam, C. J. Kiely and G. J. Hutchings, *Physical chemistry chemical physics : PCCP*, 2008, 10, 1921-1930.
67. J. S. Bradley, in *Clusters and Colloids*, Wiley-VCH Verlag GmbH, 2007, DOI: 10.1002/9783527616077.ch6, pp. 459-544.
68. A. R. Tao, S. Habas and P. Yang, *Small*, 2008, 4, 310-325.
69. M. Cargnello, V. V. T. Doan-Nguyen, T. R. Gordon, R. E. Diaz, E. A. Stach, R. J. Gorte, P. Fornasiero and C. B. Murray, *Science*, 2013, 341, 771-773.
70. M. Brun, A. Berthet and J. C. Bertolini, *Journal of Electron Spectroscopy and Related Phenomena*, 1999, 104, 55-60.
71. M. C. Biesinger, B. P. Payne, A. P. Grosvenor, L. W. M. Lau, A. R. Gerson and R. S. C. Smart, *Applied Surface Science*, 2011, 257, 2717-2730.
72. J. W. Niemantsverdriet, in *Spectroscopy in Catalysis*, Wiley-VCH Verlag GmbH & Co. KGaA, 2007, DOI: 10.1002/9783527611348.ch8, pp. 217-249.
73. A. Goursot, I. Papai and D. R. Salahub, *Journal of the American Chemical Society*, 1992, 114, 7452-7458.
74. A. G. Christy and S. M. Clark, *Physical Review B*, 1995, 52, 9259-9265.
75. W. P. Davey, *Physical Review*, 1925, 25, 753-761.
76. N. Dharmaraj, P. Prabu, S. Nagarajan, C. H. Kim, J. H. Park and H. Y. Kim, *Materials Science and Engineering: B*, 2006, 128, 111-114.
77. M. Bonarowska, J. Pielaszek, W. Juszcyk and Z. Karpiński, *Journal of Catalysis*, 2000, 195, 304-315.
78. M. W. Tew, J. T. Miller and J. A. van Bokhoven, *The Journal of Physical Chemistry C*, 2009, 113, 15140-15147.

5. THE IMPLEMENTATION OF GAS AND LIQUID FLOW SYSTEMS FOR THE DIRECT SYNTHESIS OF HYDROGEN PEROXIDE

5.1. Introduction

Flow reactors allow for varied rates of solvent and/or reactant gas flow through a catalyst bed and as such, allow for control of contact time between reactants and the catalyst. In the direct synthesis of H₂O₂, increased contact time theoretically leads to an increased extent H₂O₂ synthesis, but also an increased extent of the undesired decomposition and hydrogenation reactions. Therefore a contact time at which yield is optimised via a maximising synthesis rate and minimising degradation rate can theoretically be found.

Investigations have shown that high productivities can be achieved with the use of micro-reactors which have tightly packed, <1 mm diameter channels. This stops bulk mixing of hydrogen and oxygen, allowing for high concentration reactant gasses to be used with a vastly decreased risk of explosion. However, as these reactors are very small they have low throughputs and are both expensive and difficult to construct.¹⁻³

Operating outside the explosive regime of reactant gas mixtures, larger fixed bed reactors in which flows of gas and liquid are passed through a secured mass of powdered or pelletized catalyst can also be operated continuously. These reactors allow tailoring of reaction conditions such as reactant gas and solvent flow rates, gas composition and pressure, which can be used to optimise activity and selectivity. It was shown by Biasi *et al.* that these conditions are not necessarily the same for all catalysts when employed in an identical reactor.⁴ Table 5.1 displays the conditions and productivities obtained in various reactor systems as reported in literature, however direct comparison of such results is problematic as studies tend to differ on multiple reaction metrics such as reactor type, catalyst formulation, solvent and additives, all of which greatly affect results.

Table 5.1 – A comparison of literature reported reactor systems and productivities, adapted from Freakley *et al.*⁵

Study author	Reactor system	Catalyst	Temp / K
Paskova ⁶	Semi-batch	5% Pd/Al ₂ O ₃	293
Inoue ⁷	Microreactor; particle size ~50 μm	5% Pd/Al ₂ O ₃	293
Inoue ⁸	Microreactor	5% Pd/various	293
Kim ⁹	Up-flow fixed bed	0.24% Pd/resin	295
Biasi ⁴	Trickle bed reactor; particle size 0.5 - 1 mm	2.5% Pd/CeO ₂ , ZrO ₂	263
Biasi ¹⁰	Trickle bed reactor	2.5% Au-Pd/CeO ₂ , ZrO ₂	263
Freakley ⁵	Fixed bed; particle size 200 - 500 μm	1% Au-Pd/TiO ₂	275

Study author	Pressure / bar	Solvent	Productivity / mol kg _(Pd) ⁻¹ h ⁻¹
Paskova ⁶	70	MeOH	6500
Inoue ⁷	9.5	H ₂ O + Acid + NaBr	Up to 3000
Inoue ⁸	10	H ₂ O + Acid + NaBr	900
Kim ⁹	50	MeOH + HBr	5290
Biasi ⁴	10	MeOH	40 - 50
Biasi ¹⁰	10	MeOH	Up to 180
Freakley ⁵	10	66% MeOH + 34% H ₂ O	400

A fixed bed flow system probably represents the most practical solution for small scale, on-site implementation of the direct synthesis of H₂O₂, allowing for continuous operation, recycling of unreacted gasses to increase conversion and the potential for high throughputs.^{5, 11, 12} The efficient direct synthesis of H₂O₂ in water in a flow system would also be a very attractive process for potential water cleaning technologies.

The direct synthesis of H₂O₂ has also been demonstrated in absence of solvent with an example in patent literature illustrating direct combination of hydrogen and oxygen in gaseous phase at elevated temperatures and pressures.¹³ The system reported in this patent necessitates the use of acid and halides to act as stabilisers. However, in a recent study by Akram *et al.* Au-Pd/TiO₂ catalysts were employed to form H₂O₂ in a

gas phase flow system at atmospheric pressure, without the use of acid or halide stabilisers.¹⁴ Whilst there have been few studies into the synthesis of H₂O₂ in the gas phase, this reaction offers the potential advantages of a simpler process design over a liquid/gas flow system and the removal of any issues with gas solubility into a solvent limiting potential yield.

In this work, the direct synthesis of H₂O₂ in both gas and gas/liquid flow systems will be investigated, using both well studied 2.5 wt. % Au - 2.5 wt. % Pd/TiO₂ catalysts and the highly selective 0.5 wt. % Pd - 4.5 wt. % Ni/TiO₂ and 0.5 wt. % Pd - 4.5 wt. % Ga/TiO₂ catalysts which were reported in Chapter 4.

5.2. Results

5.2.1. Gas phase flow reactions using Au-Pd/TiO₂ catalysts

A gas phase H₂O₂ synthesis reactor was constructed as outlined in Chapter 2.3.5. The results of testing the blank reactor for synthesis and degradation activity are shown in Table 5.2. As a single cylinder of 2% H₂/air was used for these reactions, it is not possible to decouple the decomposition and hydrogenation reactions, therefore the total degradation is reported.

Table 5.2 – H₂O₂ production and degradation activity for the blank gas phase reactor. Conditions: 16hr reaction time, ≈25°C, H₂/air, 50 ml min⁻¹, 20 bar, 4% H₂O₂ solution used for degradation tests

Catalyst	H ₂ O ₂ produced /moles	Degradation /%
None	0	52% (vs pre-reaction) 47% (vs 16hr control)

From these blank reactor tests it can be concluded that the reactor itself plays no part in any H₂O₂ synthesis, however it does contribute to the degradation of hydrogen peroxide, most likely due to catalysis of both the decomposition and hydrogenation pathways of H₂O₂ by the stainless steel walls of the reactor at elevated pressures in the presence of H₂ gas.

Previous studies of gas phase H_2O_2 synthesis by Hutchings and co-workers¹⁴ used a 16 hour reaction duration. Shorter reaction durations were not studied in this previous investigation, therefore a test was performed to compare yield from a 16 hour reaction and a 4 hour reaction. These data are displayed in Figure 5.1.

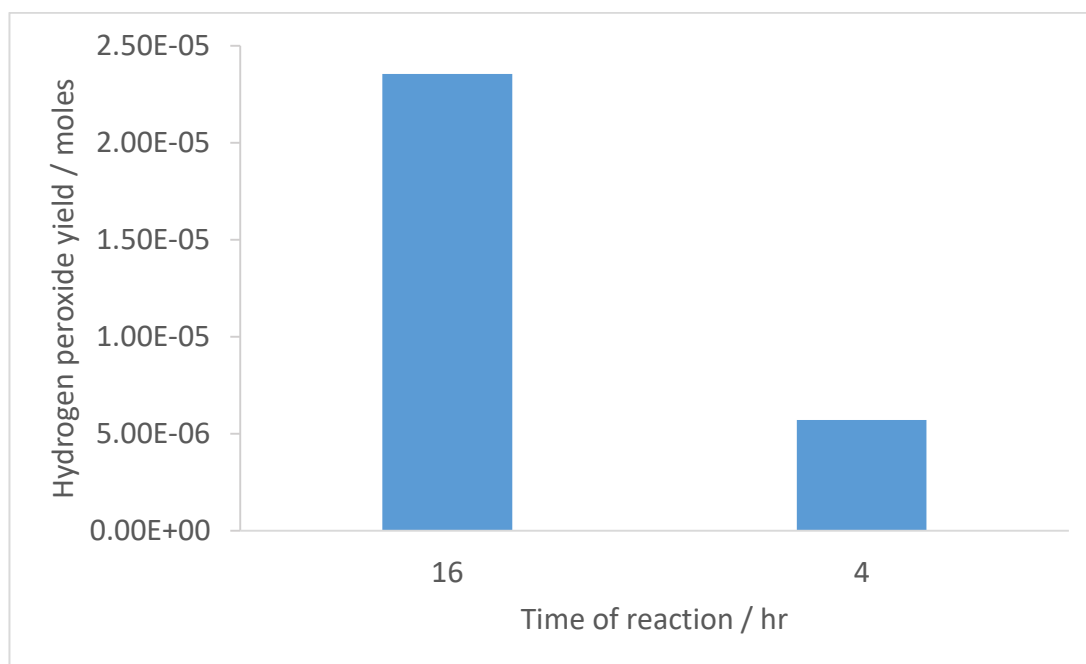


Figure 5.1 – Hydrogen peroxide yield for reactions performed for 4 and 16 hour durations. Conditions: Reaction time as indicated, $\approx 25^\circ\text{C}$, 2% H_2 /air, 50 ml min^{-1} , 20 bar, 50 mg 2.5 wt. % Au – 2.5 wt. % Pd/TiO₂ catalyst.

The data in Figure 5.1 show that for a gas phase reaction using an Au-Pd/TiO₂ catalyst the moles of H_2O_2 produced from a 16 hr reaction is approximately a factor of 4 greater than that produced from a 4 hr reaction. This suggests the rate of H_2O_2 production is constant over a 16 hr reaction.

It has been previously shown in Figure 3.8 that in a batch liquid/gas system, H_2O_2 yield is directly proportional to the pressure of reactant gasses, at a constant ratio. Tests were performed to measure H_2O_2 yield from reactions at varied pressures in a gas phase flow system, these data are displayed in Figure 5.2.

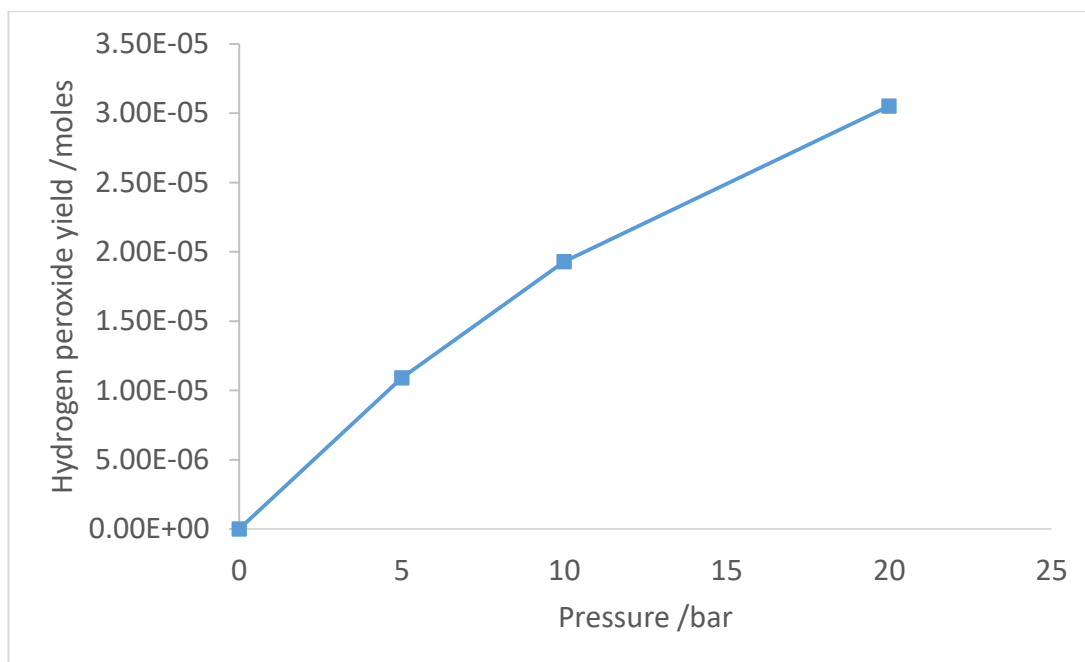


Figure 5.2 – Hydrogen peroxide yield for reactions performed using varied reactor pressures. Conditions: 16 hr reaction time, $\approx 25^{\circ}\text{C}$, 2% H_2/air , 50 ml min^{-1} , pressure as indicated, 50 mg 2.5 wt. % Au – 2.5 wt. % Pd/ TiO_2 catalyst.

The data displayed in Figure 5.2 show that H_2O_2 yield increases with pressure, as expected. This relationship appears to be almost directly proportional for pressures up to 10 bar, however the curve appears to deviate from direct proportionality for the data point at 20 bar. Activity of H_2O_2 synthesis, H_2O_2 hydrogenation and combustion all increase with increasing pressure; the decrease in H_2O_2 yield at 20 bar may be due to the heat generated in the catalyst bed from exothermic combustion and hydrogenation processes leading to an increased extent of H_2O_2 decomposition. As the reactor used could only be safely pressurised to 20 bar, greater pressures were not able to be tested.

The effect of the catalyst mass used in a reaction was also previously explored in a batch liquid/gas system (Figures 3.9 and 3.10). It was found that when an Au-Pd/ TiO_2 catalyst is employed, yield of H_2O_2 initially increases with an increased catalyst mass, but then decreases at high mass loadings as the degradation processes, primarily decomposition, become dominant reaction processes. The effect of catalyst mass used in a reaction was similarly investigated in a gas flow system. These data are displayed in Figure 5.3.

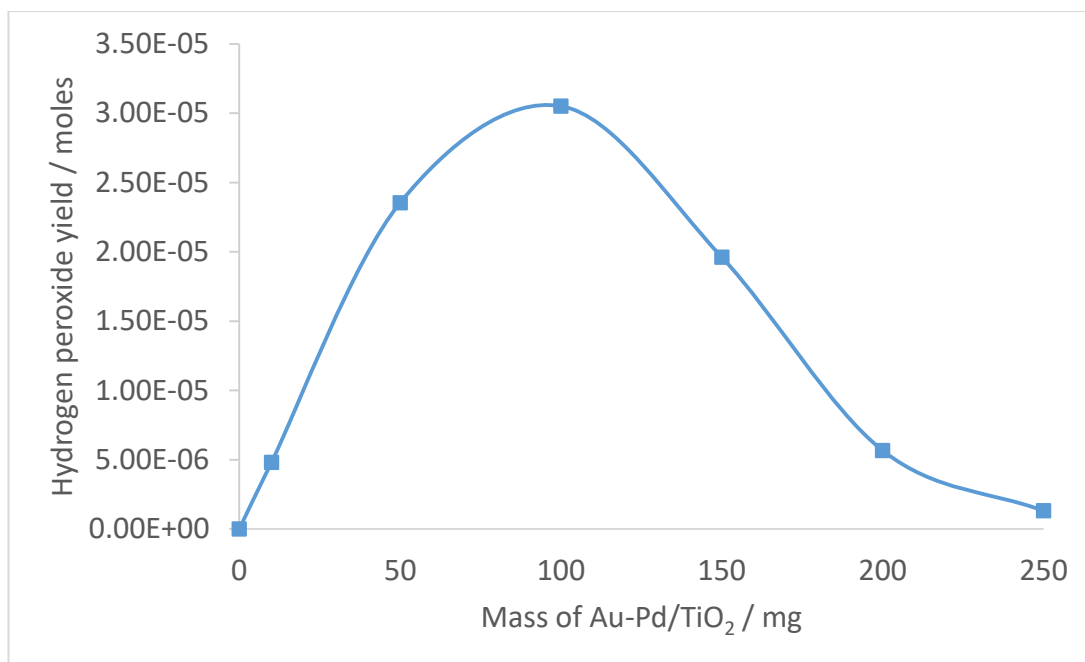


Figure 5.3 – Hydrogen peroxide yield for reactions performed using varied masses of Au-Pd/TiO₂ catalyst.

Conditions: 16 hr reaction time, ≈25°C, 2% H₂/air, 50 ml min⁻¹, 20 bar, catalyst mass as indicated, 2.5 wt.% Au – 2.5 wt.% Pd/TiO₂ catalyst.

The data displayed in Figure 5.3 show that there is an increase in yield up to a maximum of 30.5 μmol when catalyst mass is increased to 100 mg, with a close to directly proportional relationship between yield and mass of catalyst up to 50 mg. However, there is a decrease in yield with an increase in catalyst from 100 to 250 mg. This suggests an increase in the extent of the combustion of H₂ and/or the degradation of peroxide when a greater mass of Au-Pd catalyst is used. As the mass of catalyst used increases, the catalyst bed length increases, therefore the residence time of any synthesised H₂O₂ will also increase, which could result in a significant increase in the rate of H₂O₂ degradation and therefore a decrease in yield. A second possible cause could be increased temperature as the mass of catalyst/size of catalyst bed increases leading to a large increase in the rate of H₂ combustion and therefore a decrease in yield. Unfortunately, in the simple reactor configuration employed for this study, an intra-bed thermocouple could not be fit, therefore all hypothesis relating to catalyst bed temperature could only be formed from indirect measurements.

It was hypothesised that the addition of a non-reactive solid diluent to the active catalyst would limit temperature increase of the catalyst bed and potentially decrease

contact time between synthesised peroxide and the catalyst surface. These effects should theoretically decrease the extent of both combustion and degradation reactions, leading to an increased yield. Identical samples of Au-Pd/TiO₂ catalyst were tested alone as a finely ground powder and when mixed in 1:1 and 1:5 weight ratios with SiC, which acts as a non-reactive solid diluent in the catalyst bed. The data from these tests are displayed in Figure 5.4.

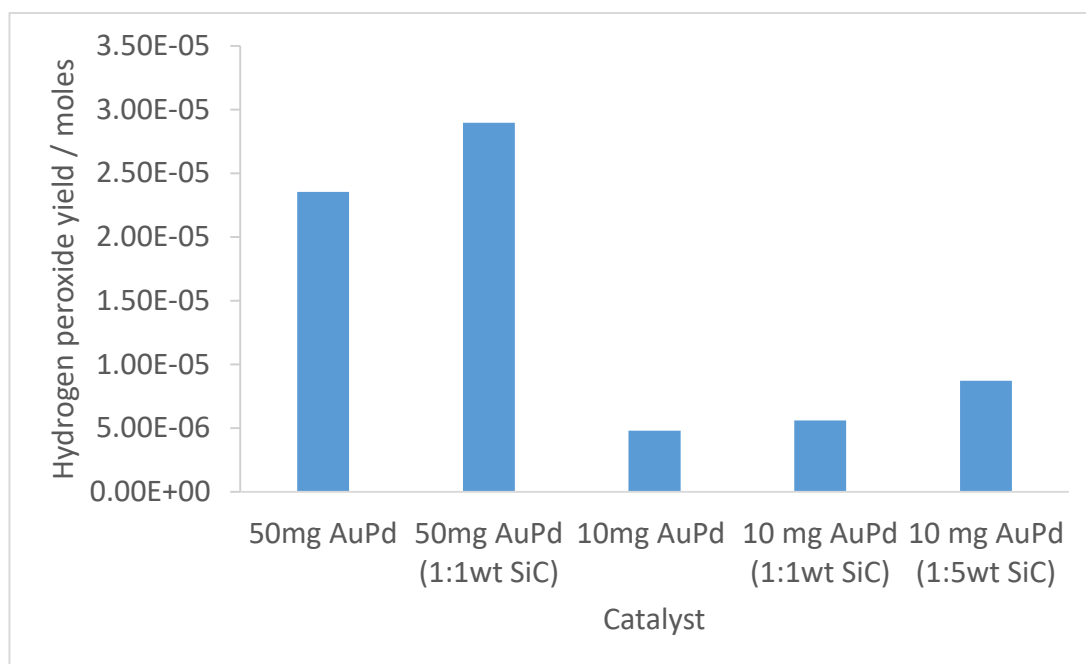


Figure 5.4 – Hydrogen peroxide yield for reactions performed using varied masses of Au-Pd/TiO₂ with and without SiC solid diluent.

Conditions: 16 hr reaction time, ≈25°C, 2% H₂/air, 50 ml min⁻¹, 20 bar, 10/50 mg 2.5 wt. % Au – 2.5 wt. % Pd/TiO₂ catalyst mixed with SiC in the mass ratios indicated.

The data in Figure 5.4 show that the addition of a solid SiC diluent has a positive effect on H₂O₂ yield and is therefore probably acting to limit the extent of degradation and/or combustion via the actions outlined previously.

Pressing the catalyst into pellets is another commonly used method to improve flow dynamics through a catalyst bed.¹⁵ Therefore, it was hypothesised that use of a pelletized catalyst would also increase yield via similar actions to those observed with the addition of SiC, namely improved thermal control and decreased residence time of the synthesised H₂O₂. Pelletized and powdered catalysts were first tested in a

batch reactor liquid/gas system and compared to assess any differences in catalyst performance upon pelletizing. This data is displayed in Table 5.3.

Table 5.3 – Batch reactor testing data for powdered and pelletized Au-Pd/TiO₂ catalyst

Conditions: 50 ml Parr autoclave, 30 min, 20°C, 1200 rpm, 10 mg catalyst;

[a] 420 psi H₂/CO₂ +160 psi O₂/CO₂, 8.5g H₂O;

[b] 420 psi H₂/CO₂, 7.82 g H₂O + 0.68 g H₂O₂

Catalyst	Productivity / mol kg_{cat}⁻¹ hr⁻¹[a]	H₂O₂ yield / ppm^[a]	H₂O₂ Degradation /%^[b]
2.5 wt.% Au - 2.5 wt.% Pd/TiO₂ powder	24	475	24
2.5 wt.% Au - 2.5 wt.% Pd/TiO₂ pellet	24	465	24

The data displayed in Table 5.3 shows that the Au-Pd/TiO₂ catalyst used for this investigation performs almost identically as both a powder and pellet for batch synthesis and degradation reactions.

The pelletized catalyst was then tested in the gas phase flow system and compared to previously obtained data for an analogous mass of powdered catalyst. These data are displayed in Figure 5.5.

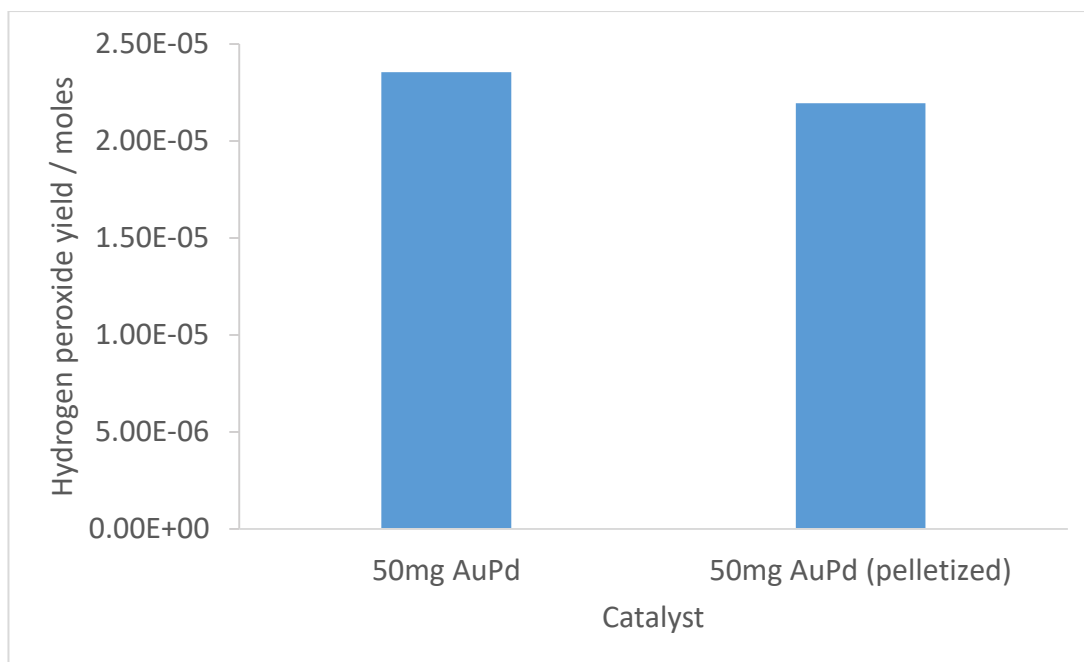


Figure 5.5 – Hydrogen peroxide yield for reactions performed with powdered and 600-425 micron pelletized Au-Pd/TiO₂ catalysts.

Conditions: 16 hr reaction time, ≈25°C, 2% H₂/air, 50 ml min⁻¹, 20 bar, 50 mg 2.5 wt. % Au – 2.5 wt. % Pd/TiO₂ as finely ground powder or 600-425 micron pellets.

The data displayed in Figure 5.5 suggest that pelletizing the Au-Pd catalyst has very little effect on the reaction, unlike the increases in yield observed with the addition of a SiC diluent. The batch testing data displayed in Table 5.3 suggests that a pelletized catalyst is just as productive as a powdered sample and it is reasonable to assume that this finding would hold constant in a gas phase flow system. Therefore it can be concluded that there is no decrease in combustion or degradation when a pelletized catalyst is used, relative to a powdered catalyst. This suggests that for this gas phase flow system, 600-425 micron catalyst pellets do not allow for any improvement in the thermal control of the catalyst bed or a decrease in contact time between synthesised H₂O₂ and the catalyst surface.

5.2.2. Gas phase flow reactions using Pd-Ni/TiO₂ and Pd-Ga/TiO₂ catalysts

In Chapter 4 the design of highly selective Pd-Ni catalysts for the synthesis of H₂O₂ was described. In a batch reactor liquid/gas system these catalysts display extremely low activity for H₂ combustion and H₂O₂ degradation, therefore H₂O₂ can be produced

with near total selectivity. Under the conditions employed repeatedly in the studies contained in Chapter 4, an optimised preparation of a 0.5 wt. % Pd - 4.5 wt. % Ni/TiO₂ catalyst is half as productive as 2.5 wt. % Au - 2.5 wt. % Pd/TiO₂ (12 mol kg_{cat}⁻¹ h⁻¹ vs 24 mol kg_{cat}⁻¹ h⁻¹), however the Pd-Ni/TiO₂ catalyst displays significantly improved H₂ selectivity (>95% vs 60%). Thus, an optimised preparation of a 0.5 wt. % Pd - 4.5 wt. % Ni/TiO₂ catalyst was employed in the gas phase flow system to study the effect of using a catalyst which is less active but more selective when compared to Au-Pd/TiO₂ in a batch liquid/gas system. The results of these tests are displayed in Figure 5.6.

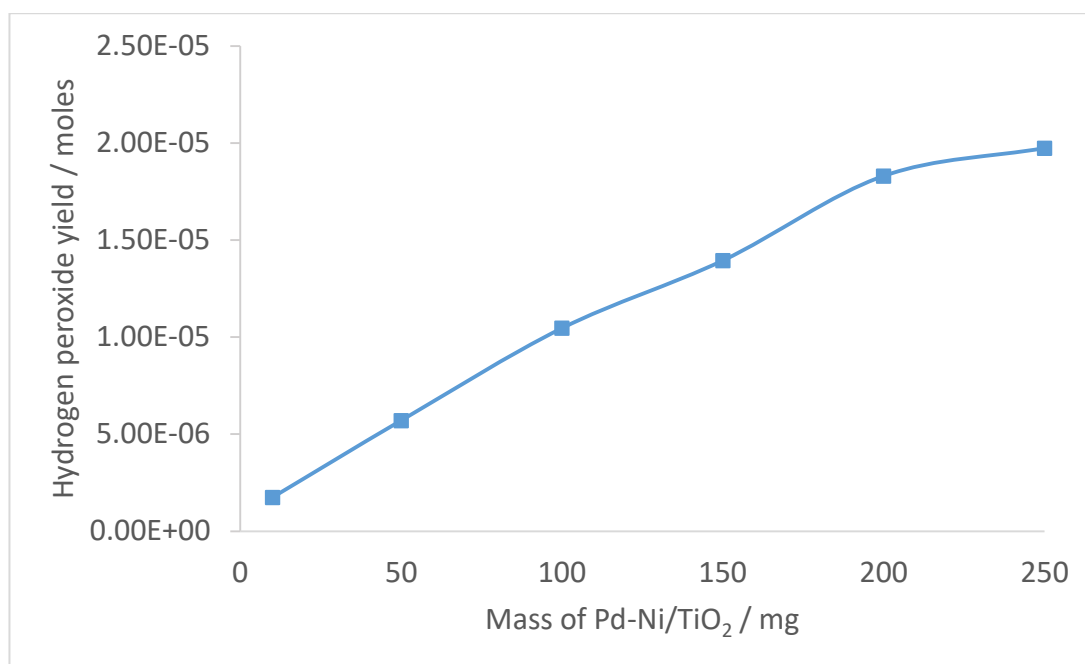


Figure 5.6 – Hydrogen peroxide yield for reactions performed with varied masses of powdered Pd-Ni/TiO₂ ORO catalysts.

Conditions: 16 hr reaction time, ≈25°C, 2% H₂/air, 50 ml min⁻¹, 20 bar, catalyst mass as indicated, 0.5 wt. % Pd – 4.5 wt. % Ni/TiO₂ ORO.

The data displayed in Figure 5.6 show that contrary to what is observed when an Au-Pd/TiO₂ catalyst is used; when a Pd-Ni/TiO₂ ORO catalyst is used the yield of hydrogen peroxide continues to increase with catalyst mass up to 250 mg. Below 200 mg, increases in yield are close to directly proportional to the increases in catalyst mass, however yield of H₂O₂ appears to begin to plateau at greater masses.

Pd-Ni/TiO₂ appears to be less active for the synthesis of H₂O₂ than Au-Pd/TiO₂; for example the yield of H₂O₂ obtained when using 50 mg Au-Pd/TiO₂ (23.5 μmol) is

approximately a factor of 4 greater than that obtained when using 50 mg Pd-Ni/TiO₂ (5.7 μmol). However, there was no decrease in yield at greater catalyst masses observed with Pd-Ni/TiO₂ (as was observed with Au-Pd/TiO₂), therefore the data suggest that Pd-Ni/TiO₂ has relatively lower degradation and combustion activities than Au-Pd/TiO₂ and as such is a more selective catalyst. These relative differences in the performance of the catalyst closely mirror what is observed in a batch liquid/gas system.

Pd-Ni/TiO₂ was tested both in pelletized form and diluted using SiC, in the same way as Au-Pd/TiO₂ previously. These two measures were hypothesised to improve the gas dynamics in the catalyst bed and decrease overheating, therefore potentially increasing selectivity and yield. The results of these tests are displayed in Figure 5.7.

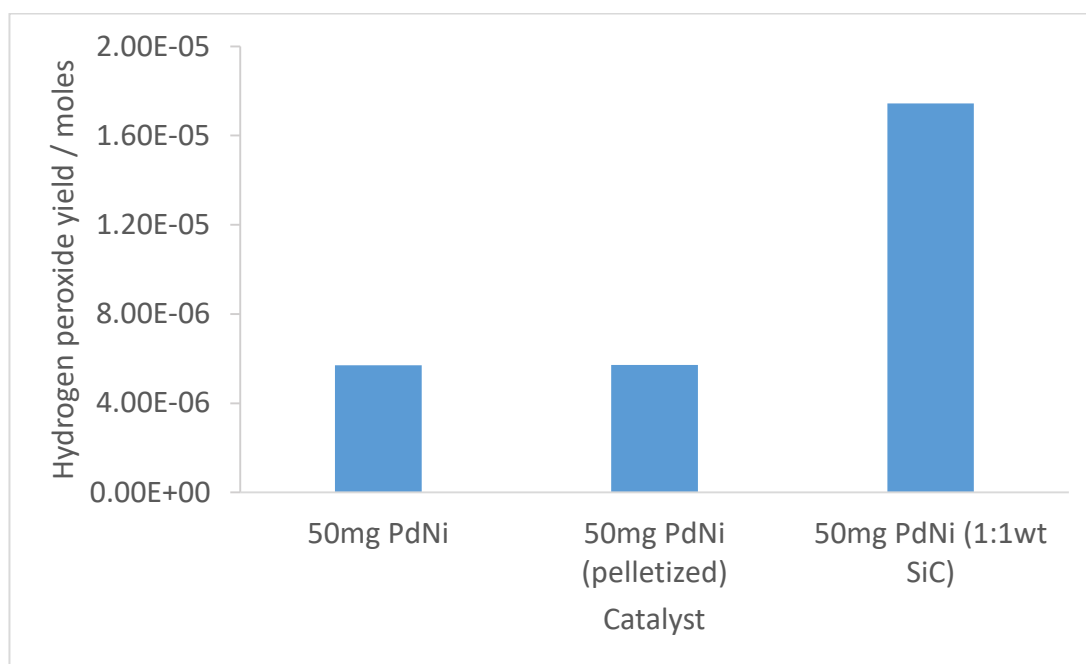


Figure 5.7 – Hydrogen peroxide yield for reactions performed with Pd-Ni/TiO₂ ORO catalysts as powder, pellet and powder mixed with a SiC solid diluent. Conditions: 16 hr reaction time, ≈25°C, H₂/air, 50 ml min⁻¹, 20 bar, 50 mg catalyst, 0.5 wt. % Pd – 4.5 wt. % Ni/TiO₂ ORO as finely ground powder, 600-425 micron pellets or finely ground powder mixed with SiC.

The data displayed in Figure 5.7 show that as was also observed with Au-Pd/TiO₂, pelletizing Pd-Ni/TiO₂ has a negligible effect on the performance of the catalyst. Similarly, mixing Pd-Ni/TiO₂ with a solid SiC diluent increases yield, as was also

observed with Au-Pd. This increase in yield (from 5.7 to 17.4 μmol) suggests that combustion of H_2 and degradation of synthesised H_2O_2 are reduced when a Pd-Ni/ TiO_2 catalyst is mixed with a solid diluent, but therefore are still significant factors in the reaction when a Pd-Ni/ TiO_2 catalyst is used alone.

In Section 4.2.8, it was also shown that Pd-Ga/ TiO_2 catalysts behave very similarly to Pd-Ni/ TiO_2 catalysts, with a similar near total selectivity and productivity that is approximately half that observed for Au-Pd/ TiO_2 . Therefore a 0.5 wt. % Pd - 4.5 wt. % Ga/ TiO_2 catalyst was tested in the gas phase flow system when mixed with a SiC diluent, as this reaction configuration had proved successful with Au-Pd and Pd-Ni/ TiO_2 previously. Figure 5.8 shows a comparison of the H_2O_2 yield obtained and Table 5.4 shows a comparison of H_2 consumption and selectivity towards H_2O_2 for these 3 catalysts.

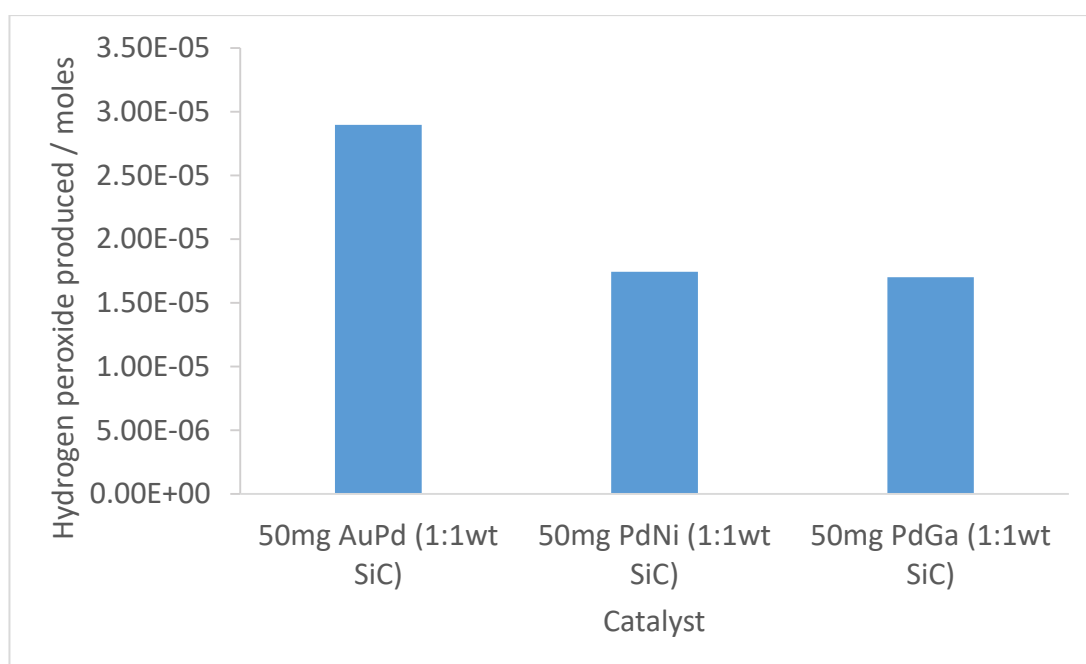


Figure 5.8 – Hydrogen peroxide yield for reactions performed with Au-Pd/ TiO_2 , Pd-Ni/ TiO_2 ORO and Pd-Ga/ TiO_2 ORO catalysts mixed with a SiC solid diluent. Conditions: 16 hr reaction time, $\approx 25^\circ\text{C}$, H_2/air , 50 ml min^{-1} , 20 bar, 50 mg catalyst, 2.5 wt. % Au – 2.5 wt. % Pd/ TiO_2 , 0.5 wt. % Pd – 4.5 wt. % Ni/ TiO_2 ORO or 0.5 wt. % Pd – 4.5 wt. % Ga/ TiO_2 ORO mixed with SiC in a 1:1 weight ratio.

Table 5.4 – Selectivity data from GC analysis of gas collected after the catalyst bed. Conditions as in Figure 5.8.

Catalyst	H ₂ consumed / %	Selectivity to H ₂ O ₂ / %
50mg 2.5 wt.% Au - 2.5 wt.% Pd /TiO ₂	100	0.06
50mg 2.5 wt.% Au - 2.5 wt.% Pd /TiO ₂ + 50mg SiC	100	0.07
50mg 0.5 wt. %Pd - 4.5 wt. %Ni / TiO ₂ + 50mg SiC	4.3	0.94
50mg 0.5 wt. % Pd - 4.5 wt. % Ga / TiO ₂ + 50mg SiC	5.0	0.80

The data in Figure 5.8 suggest that 0.5 wt. % Pd - 4.5 wt. % Ga/TiO₂ behaves very similarly to 0.5 wt. % Pd - 4.5 wt. % Ni/TiO₂ in a gas phase flow system, as is also observed in a liquid/gas phase batch system (Section 4.2.8). The selectivity data in Table 5.4 suggest that Pd-Ga/TiO₂ is slightly less selective towards the production of H₂O₂, a trait which is also seen in liquid/gas phase batch system when catalyst masses greater than 10 mg are used.

The data in Table 5.4 show that Au-Pd/TiO₂ consumes all of the H₂ that is fed to the reactor bed, resulting in a selectivity of less than 0.1%. The majority of this H₂ usage appears to be *via* combustion as it was noted that the reactor bed greatly increases in temperature in the course of the reaction, although accurate quantification of this effect was not possible due to the reasons outlined previously. Pd-Ni/TiO₂ and Pd-Ga/TiO₂, by comparison, consume 5% or less of the hydrogen in the gas feed, resulting in selectivities approaching 1%. The selectivity for gas phase flow synthesis with all catalysts tested is very low. However, use of Pd-Ni and Pd-Ga/TiO₂ catalysts result in significantly more selective processes than use of an Au-Pd/TiO₂ catalyst.

5.2.3. Liquid/gas phase flow reactions using 0.5 wt. % Pd – 4.5 wt. % Ni/TiO₂ ORO

A liquid/gas phase H₂O₂ synthesis reactor was constructed as outlined in Chapter 2 Section 2.3.5. The results of testing the blank reactor for synthesis and degradation activity are shown in Table 5.5.

Table 5.5 – H₂O₂ production and degradation activity for the blank liquid/gas phase flow reactor.

Conditions: 25°C, 175 ml/min 5% H₂/CO₂ + 35 ml/min 25% O₂/CO₂, 1 ml/min H₂O, 30 bar, 4% H₂O₂ solution used for degradation tests

Catalyst	H ₂ O ₂ produced / moles	Degradation / %
None	0	0

The data in Table 5.5 show that the reactor does not degrade peroxide at a pressure of 30 bar. Conditions for initial tests were based on the conditions used by Freakley *et al.*⁵; in the referenced study, conditions of 35 ml/min 5% H₂/CO₂ with 7 ml/min 25% O₂/CO₂ and 0.2 ml/min H₂O were used. This study was intended to investigate the synthesis of H₂O₂ in a greater throughput flow system, therefore the previous reaction parameters were increased by a factor of 5 to give the initial reaction conditions used in this study (175 ml/min 5% H₂/CO₂ with 35 ml/min 25% O₂/CO₂ and 1 ml/min H₂O).

Pelletized catalyst was used for all tests performed in the liquid / gas flow system as use of a powdered catalyst would not allow for efficient fluid dynamics through the catalyst bed and thus cause safety and performance issues from pressure build-ups. Tests were predominately performed with an optimised 0.5 wt. % Pd – 4.5 wt. % Ni / TiO₂ catalyst, which had undergone the ORO heat treatment. Comparative batch testing of powdered and pelletized samples of this catalyst were performed. This data is displayed in Table 5.6.

Table 5.6 – Batch reactor testing data for powdered and pelletized (425-600 μm) 0.5 wt. % Pd – 4.5 wt. % Ni/TiO₂ ORO catalyst.

Conditions: 50 ml Parr autoclave, 30 min, 20°C, 1200 rpm, 10 mg catalyst;

[a] 420 psi H₂/CO₂ +160 psi O₂/CO₂, 8.5g H₂O;

[b] 420 psi H₂/CO₂, 7.82 g H₂O + 0.68 g H₂O₂

Catalyst	Productivity / mol kg_{cat}⁻¹ hr⁻¹[a]	H₂O₂ yield / ppm^[a]	H₂O₂ Degradation / %^[b]
0.5 wt. % Pd – 4.5 wt. % Ni/TiO₂ ORO powder	14	275	2
0.5 wt. % Pd – 4.5 wt. % Ni/TiO₂ ORO pellet (425-600 μm)	12	240	2

The data in Table 5.6 show that the process of pelletizing the 0.5 wt. % Pd – 4.5 wt. % Ni/TiO₂ ORO catalyst slightly decreases the activity of the catalyst towards H₂O₂ synthesis. However, a degradation activity of 2% for the reaction, which is the same as is obtained in a blank reactor (Figure 3.10), is maintained for the pelleted catalyst.

A 10 hour H₂O₂ synthesis reaction was performed using pelleted 0.5 wt. % Pd – 4.5 wt. % Ni/TiO₂ ORO catalyst with the synthesised H₂O₂ sampled throughout the experiment. This allowed for assessment of the ability of the catalyst to produce a consistent concentration of H₂O₂ and evaluation of the stability of the catalyst in a flow system. The results of this test are displayed in Figure 5.9.

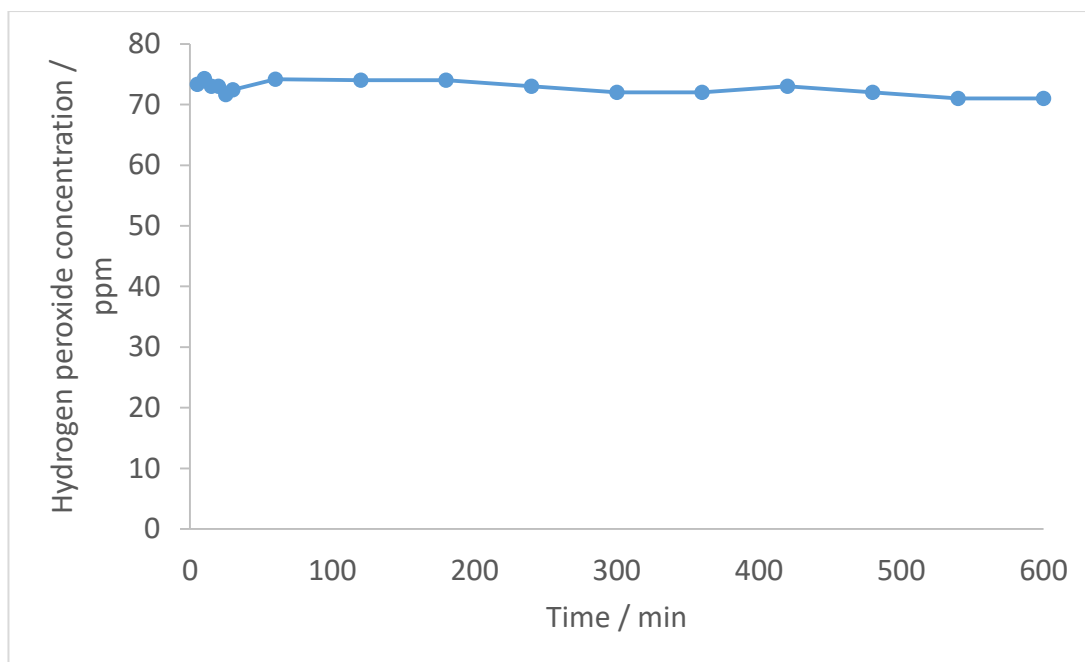


Figure 5.9 – Hydrogen peroxide concentration for a 10 h liquid gas/flow reactor reaction sampled in a time-on-line manner.

Conditions: $\approx 25^{\circ}\text{C}$, 250 mg 0.5 wt. % Pd – 4.5 wt. % Ni/TiO₂ ORO catalyst, 175 ml/min 5% H₂/CO₂ + 35 ml/min 25% O₂/CO₂, 1 ml/min H₂O, 30 bar

The data displayed in Figure 5.9 show that at the given conditions, 1 ml/min hydrogen peroxide at ca. 75 ppm can be produced consistently for 10 hours. The studies reported in Section 4.2.7 show 0.5 wt. % Pd – 4.5 wt. % Ni / TiO₂ ORO catalysts to be highly stable in liquid/gas phase batch reactions in water, with a productivity of 14 mol kg_{cat}⁻¹ hr⁻¹ maintained over at least two uses of the catalyst. The data displayed in Figure 5.9 suggest that Pd-Ni / TiO₂ ORO catalyst is stable over a 10 hour period in a gas/liquid flow system, as a consistent catalyst productivity was measured throughout the test. Post reaction catalyst digestion and MP-AES analysis showed no loss of metal when compared to an unused sample.

5.2.4. The effect of pressure on liquid/gas phase flow reactions using 0.5 wt. % Pd – 4.5 wt. % Ni/TiO₂ ORO

The effect of pressure in the gas/liquid flow system was studied by performing H₂O₂ syntheses at varied pressures. For a practical implementation of the direct synthesis of H₂O₂, use of a low operating pressure is desirable to maximise energy efficiency and safety of the process. These results of these tests are displayed in Figure 5.10.

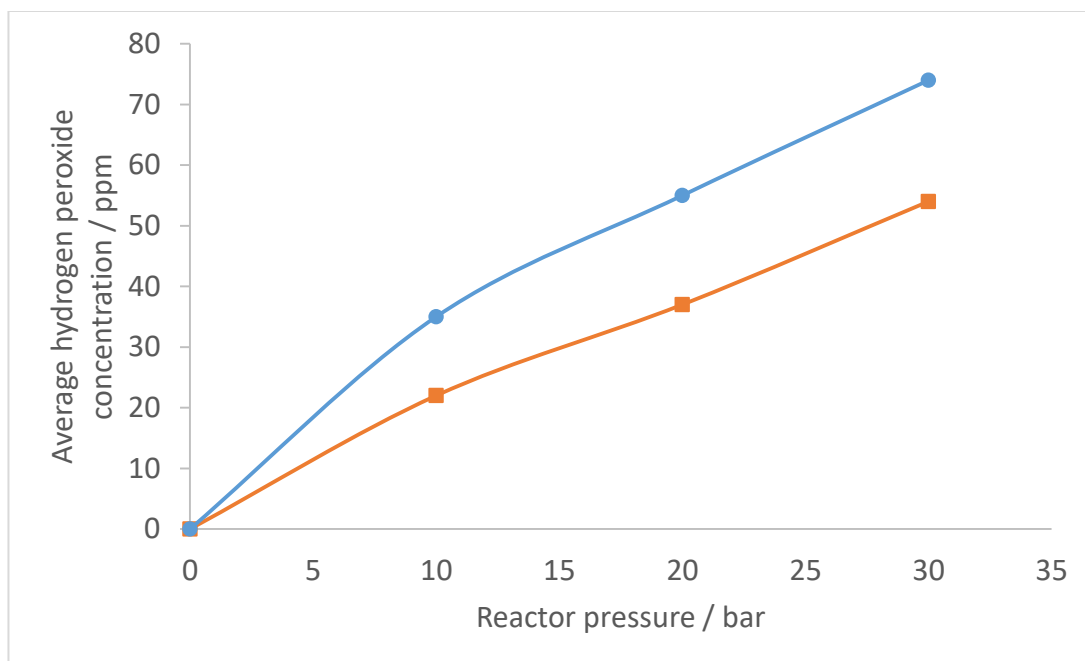


Figure 5.10 – Average hydrogen peroxide concentration produced using a 0.5 wt. % Pd – 4.5 wt. % Ni/TiO₂ catalyst, at varied pressures in a liquid/gas flow reactor.

● – 250 mg catalyst, ■ – 100 mg catalyst

Conditions: ≈25°C, 0.5 wt. % Pd – 4.5 wt. % Ni/TiO₂ ORO catalyst mass as indicated, 175 ml/min 5% H₂/CO₂ + 35 ml/min 25% O₂/CO₂, 1 ml/min H₂O, pressure as indicated.

The data displayed in Figure 5.10 show that the relationship between the reactant gas pressure and the concentration of H₂O₂ produced is close to proportional for 100 mg of 0.5 wt. % Pd – 4.5 wt. % Ni/TiO₂ catalyst. When 250 mg of the catalyst is used, there is a greater deviation from a linear relationship between pressure and yield; this is potentially due to a decrease in the selectivity of the process when a greater mass of catalyst is used or inefficient reactor dynamics with a larger catalyst bed. It was previously shown in Figure 3.8 that for batch liquid/gas system reactions with 10 mg of 2.5 wt. % Au - 2.5 wt. % Pd/TiO₂ catalyst, the concentration of H₂O₂ produced is directly proportional to pressure up to 580 psi (40 bar). These data support the mechanism proposed by Hutchings and co-workers⁵ stating H₂O₂ synthesis is first order with respect to H₂ concentration and zeroth order with respect to O₂.

5.2.5. The effect of catalyst mass on liquid/gas phase flow reactions using 0.5 wt. % Pd – 4.5 wt. % Ni/TiO₂ ORO

The effect of catalyst mass on both the concentration of H₂O₂ produced and the H₂ selectivity towards H₂O₂ was investigated. The data from these tests is displayed in Figure 5.11.

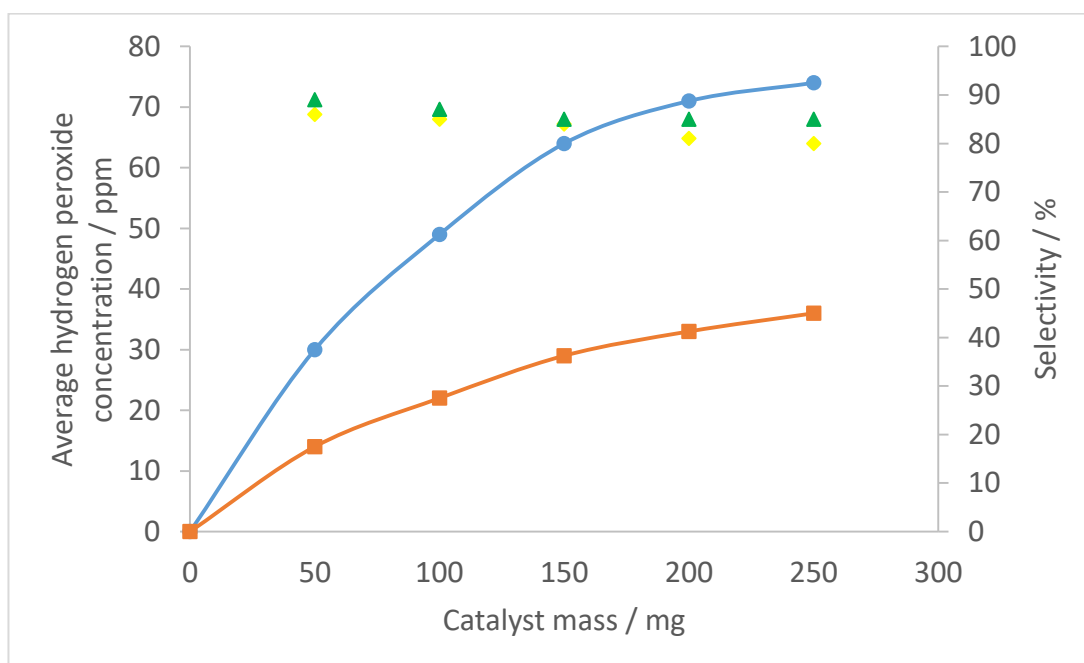


Figure 5.11 – Average hydrogen peroxide concentration and selectivity at varied catalyst masses in a liquid gas/flow reactor at 30 and 10 bar pressure.

● – 30 bar H₂O₂ production (left axis), ■ – 10 bar H₂O₂ production (left axis), ◆ – 30 bar H₂O₂ selectivity (right axis), ▲ – 10 bar H₂O₂ selectivity (right axis)

Conditions: ≈25°C, 0.5 wt. % Pd – 4.5 wt. % Ni/TiO₂ ORO catalyst mass as indicated, 175 ml/min H₂/CO₂ + 35 ml/min O₂/CO₂, 1 ml/min H₂O, pressure as indicated

The data in Figure 5.11 show that at both 30 and 10 bar, increasing catalyst mass increases the concentration of H₂O₂ produced, however the relationship is not directly proportional, with a decrease in incremental gains in H₂O₂ concentration at greater catalyst masses. Selectivity falls slightly as catalyst mass increases but, remains in the range of 80 - 90% for all catalyst masses and pressures studied. Whilst high, this selectivity is lower than that recorded for the same catalyst in a batch liquid/gas system (Table 4.10). The decreasing proportional yields as catalyst mass is increased is partially explained by the small decrease in selectivity as catalyst mass is increased.

This fall could also be due to limited availability of dissolved hydrogen in the reactant stream.

The selectivity, which is lower than that measured in batch tests, and the decrease in selectivity with increasing catalyst mass could be due to the nature of the reactor dynamics. In gas/liquid flow reactors of small diameters, a flow dynamic named the Taylor flow is commonly observed.⁵ Taylor flow is characterized by alternate gas bubbles and liquid slugs, where the gas bubbles are greater in length than the diameter of the reactor. Whilst confirmation of the flow regime was not possible in the reactor configuration used, a similar flow regime that contains large gas bubbles is almost certain, given the relatively greater gas flow comparative to liquid flow.¹¹ Thus there are periods in which only gas (H_2 , O_2 and a CO_2 or air diluent) flows over the catalyst and a small amount of direct gas phase reactant to catalyst surface interaction may occur. As seen in Table 5.4, the interaction of gas phase reactants with a Pd-Ni/ TiO_2 catalyst represents a very unselective H_2O_2 synthesis process, with significant amounts of H_2 combustion. Thus, it is possible that there is a degree of gas phase reactant interaction with the catalyst in a gas/liquid flow system, leading to H_2 combustion and therefore lower selectivities than those recorded in batch liquid/gas testing.

5.2.6. The effect of solvent flow rate on liquid/gas phase flow reactions using 0.5 wt. % Pd – 4.5 wt. % Ni/ TiO_2 ORO

Tests were performed to investigate the effect of H_2O flow rate on H_2O_2 production in the liquid/gas flow system. These data are displayed both in terms of the concentration of H_2O_2 produced and the total moles of H_2O_2 produced per minute in Figures 5.12 and 5.13, respectively.

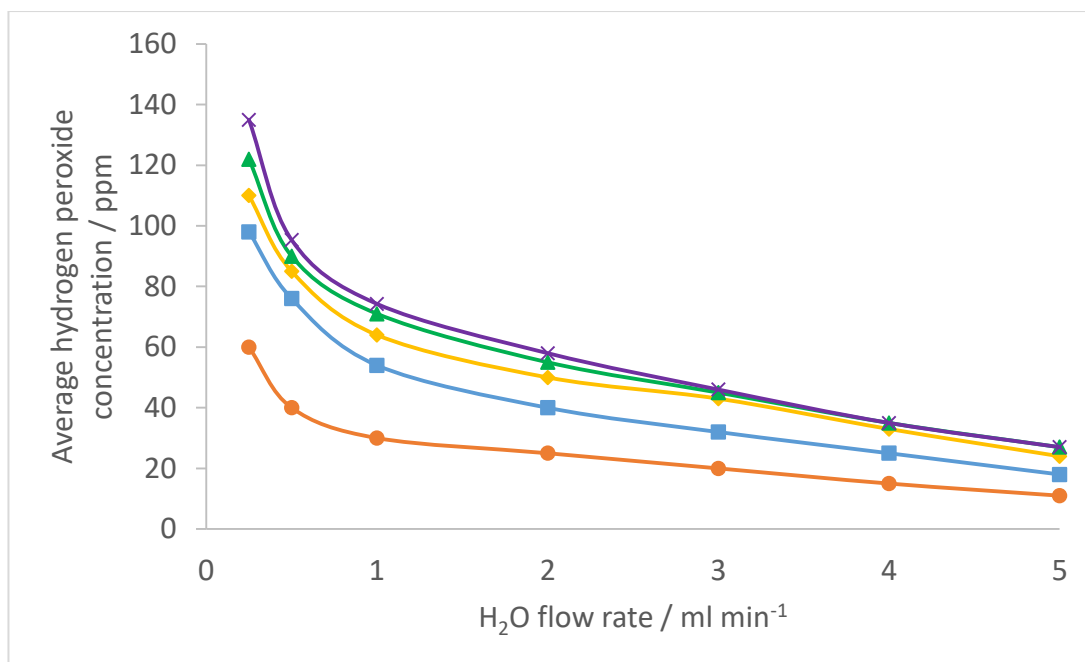


Figure 5.12 – Average hydrogen peroxide yield at varied H₂O flow rates for various catalyst masses.

● – 50 mg, ■ – 100 mg, ◆ – 150 mg, ▲ – 200 mg, ✕ – 250 mg

Conditions: ≈25°C, 0.5 wt. % Pd – 4.5 wt. % Ni/TiO₂ ORO catalyst mass as indicated, 175 ml/min H₂/CO₂ + 35 ml/min O₂/CO₂, H₂O solvent flow rate as indicated, 30 bar.

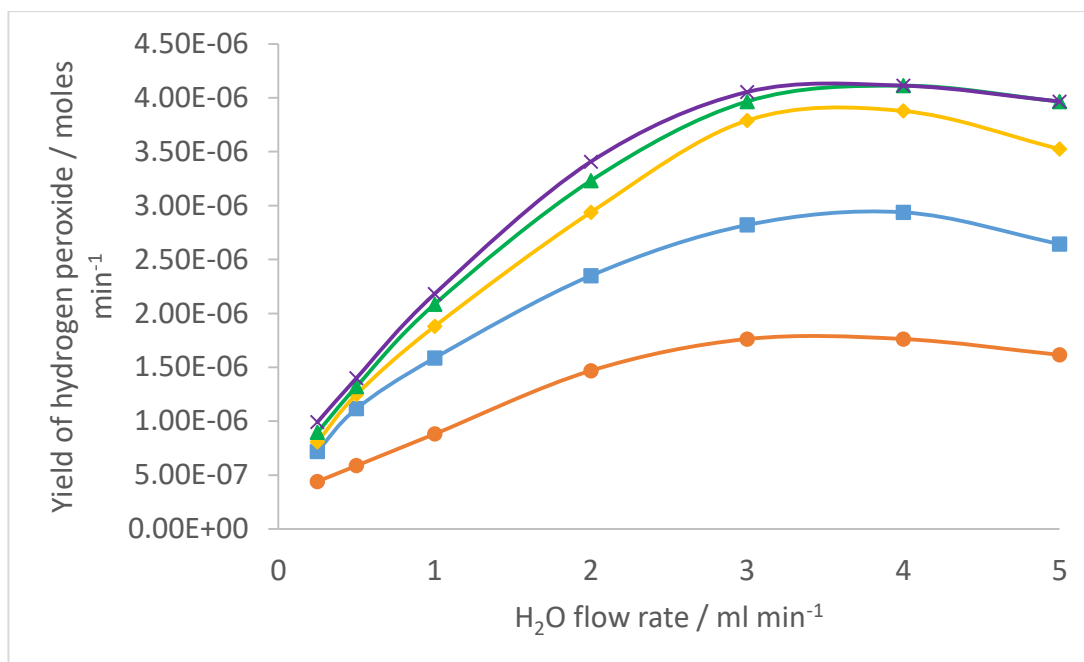


Figure 5.13 – Average hydrogen peroxide yield per minute at varied H₂O flow rates for various catalyst masses

● – 50 mg, ■ – 100 mg, ◆ – 150 mg, ▲ – 200 mg, × – 250 mg

Conditions: ≈25°C, 0.5 wt. % Pd – 4.5 wt. % Ni/TiO₂ ORO catalyst mass as indicated, 175 ml/min H₂/CO₂ + 35 ml/min O₂/CO₂, H₂O solvent flow rate as indicated, 30 bar

The data in Figure 5.12 show that a greater rate of H₂O flow leads to a decreased concentration of produced H₂O₂. This decrease in concentration with increasing flow rate is probably primarily due to the dilution effect when greater masses of solvent are utilised. However, as shown in Figure 5.13, the greatest yield in terms of total moles does not occur at the greatest H₂O flow rates, therefore there must be other contributing factors beyond dilution. One factor which may contribute to a decreased yield of H₂O₂ at flow rates greater than 4 ml/min is a potentially decreased concentration of dissolved reactant gasses in the solvent at greater flow rates as there is a greater mass of solvent present with a constant amount of reactant gasses. A second factor which may contribute to a decreased yield is the decreased residence time of the dissolved reactant gasses in the catalyst bed at greater liquid flow rates, thus limiting turnover and therefore yield.

The data in Figure 5.13 shows that the most efficient production of H₂O₂ in terms of total moles produced occurs at 3 to 4 ml/min for all catalyst masses. For the test performed using 50 mg catalyst and a H₂O flow rate of 3 ml/min, the catalyst productivity per kg of active metal (as used in Table 5.1) is 423 mol_{H₂O₂} kg_(Pd)⁻¹ h⁻¹.

This compares favourably to the results obtained under flow conditions in the absence of promoters by Freakley⁵ and Biasi^{4, 10}. There are notable differences between the conditions used in this test and those in the referenced studies; this test uses a greater reactor pressure than the references studies (30 bar vs 10 bar), but this study also uses significantly greater throughputs and a H₂O solvent as opposed to MeOH or a H₂O/MeOH used in the referenced studies.

At high flow rates, the system is most likely limited by a combination of the reasons discussed in the previous paragraph. At low flow rates, there is a lesser mass of solvent present, therefore the moles of reactant gasses which can dissolve into the solvent are limited, thus limiting the availability of reactants and the possible yield of H₂O₂. Thus we observe decreased yields at both low and high flow rates. At flow rates greater than 3 ml/min we also see very little or no difference in concentration/total yield in the range of 150 to 250mg of catalyst. This suggests that the system not limited by a the number of catalyst active sites available, instead it is probably due to a limited concentration of dissolved reactant gasses present at the given gas flow rates and pressure.

5.2.7. The effect of gas flow rate on liquid/gas phase flow reactions using 0.5 wt. % Pd – 4.5 wt. % Ni/TiO₂ ORO

The effect of varying gas flow rate, while maintaining all other reaction conditions, was also investigated. The total rate of gas flow was varied, but not the gas ratio, which was kept constant at 1:1 H₂:O₂, the optimal ratio for the direct synthesis of H₂O₂ (Freakley *et al.*)⁵ The results of these tests are shown in Figure 5.14.

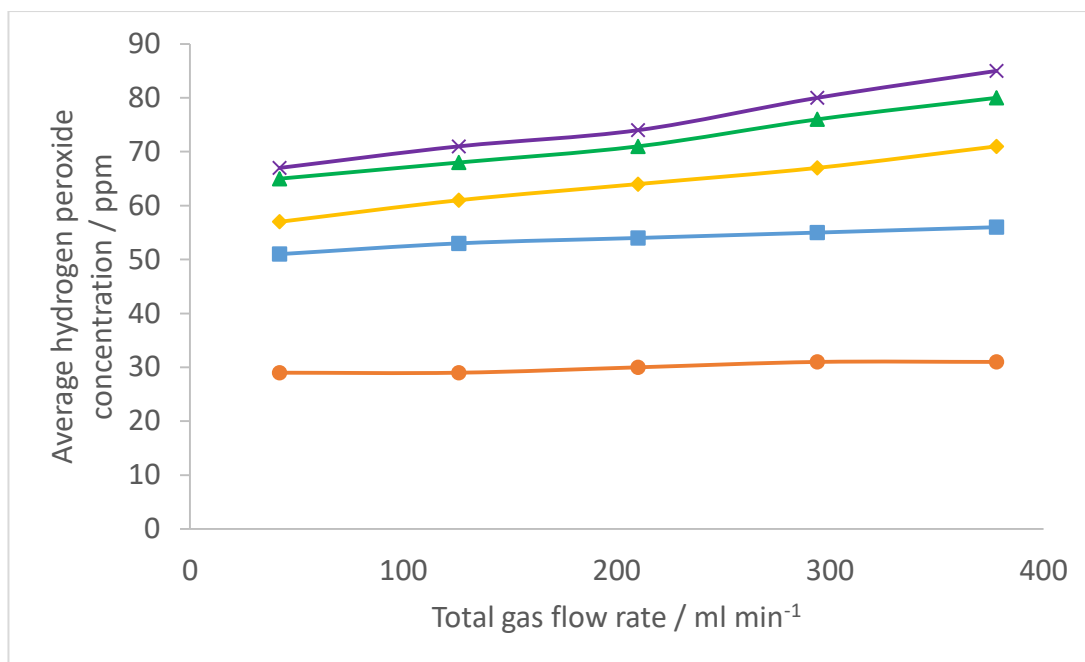


Figure 5.14 – Average hydrogen peroxide concentration at varied reactant gas flow rates at a constant ratio for various catalyst masses

● – 50 mg, ■ – 100 mg, ◆ – 150 mg, ▲ – 200 mg, X – 250 mg

Conditions: $\approx 25^{\circ}\text{C}$, 0.5 wt. % Pd – 4.5 wt. % Ni/TiO₂ ORO catalyst mass as indicated, 1:1 H₂:O₂ (7.5 % each) with CO₂ diluent (85 %) total gas flow as indicated, 1 ml/min H₂O, 30 bar.

Similar to the findings in the study by Freakley *et al.*,⁵ the data displayed in Figure 5.14 show that there is a minor increase in produced H₂O₂ concentration with total gas flow. Freakley hypothesised that this increase was due to greater mass transfer between gas and liquid and the reduction of stagnant regions which occurs at higher flow rates. The extent to which produced H₂O₂ concentration observed in this case is lesser than that seen in the previous reported study. This could be due to the larger throughputs used in this study, which may already have efficient hydrodynamics even at the lowest flow rates, which correspond to some of the highest flow rates used in the previous study.

5.2.8. Liquid/gas phase flow reactions using 0.5 wt. % Pd – 4.5 wt. % Ga/TiO₂ ORO

In Section 4.2.8 and Figure 5.8, it was also shown that Pd-Ga catalysts behave very similarly to Pd-Ni catalysts in both batch liquid/gas and gas phase flow systems, respectively. Therefore a 425 - 600 μm pelleted 0.5 wt. % Pd - 4.5 wt. % Ga/TiO₂

catalyst was tested in the gas/liquid phase flow system under analogous conditions to those which Pd-Ni had been tested under. Figure 5.15 shows a comparison of the concentration of H₂O₂ produced obtained and H₂ selectivity towards H₂O₂ for Pd-Ga and Pd-Ni.

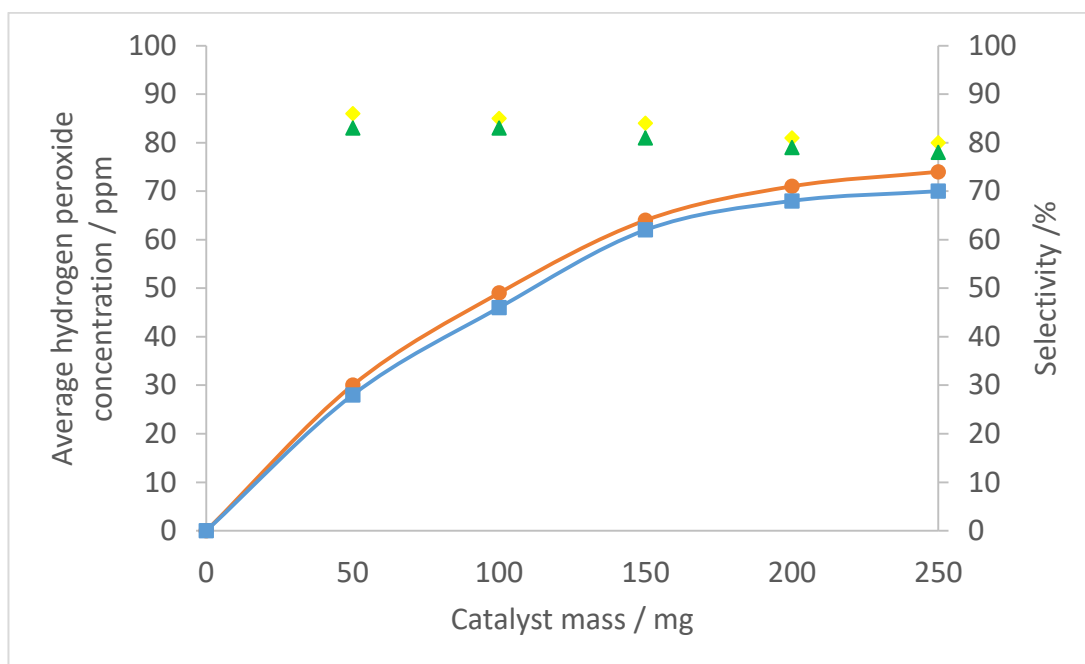


Figure 5.15 – Average hydrogen peroxide concentration and selectivity at varied catalyst masses for 0.5 wt. % Pd – 4.5 wt. % Ni/TiO₂ ORO and 0.5 wt. % Pd – 4.5 wt. % Ga/TiO₂ ORO catalysts

● – Pd-Ni H₂O₂ production (left axis), ■ – Pd-Ga H₂O₂ production (left axis), ◆ – Pd-Ni H₂O₂ selectivity (right axis), ▲ – Pd-Ga H₂O₂ selectivity (right axis)

Conditions: ≈25°C, 0.5 wt. % Pd – 4.5 wt. % Ni/TiO₂ ORO or 0.5 wt. % Pd – 4.5 wt. % Ga/TiO₂ ORO catalyst mass as indicated, 175 ml/min H₂/CO₂ + 35 ml/min O₂/CO₂, 1 ml/min H₂O, 30 bar.

The data in Figure 5.15 echo previous findings in Section 4.2.8 and Figure 5.8 with Pd-Ga/TiO₂ behaving very similarly to Pd-Ni/TiO₂. We observe a marginally decreased concentration of H₂O₂ produced and H₂ selectivity when a Pd-Ga catalyst is used relative to a Pd-Ni catalyst in a gas/liquid flow system, but these catalysts have broadly the same activity in all systems under which they have been tested.

5.2.9. The effect of using an N₂ diluent on liquid/gas phase flow reactions using 0.5 wt. % Pd – 4.5 wt. % Ni/TiO₂ ORO

For implementation of the direct synthesis of H₂O₂, use of a dilute H₂ in O₂/N₂ reactant stream, such as those which can be produced through electrolysis of water and recombination with air, is desirable from an economic and practical consideration. The effect of using a low concentration (2%) H₂ in air (20±1% O₂) reactant gas mixture was studied under varied conditions in a flow liquid/gas system. These tests are matched for total (H₂, O₂ and diluent) gas flow, which therefore means they are inherently not matched for H₂ content of gas flow. However, Figure 5.14 has shown that concentration of H₂O₂ produced does not change greatly over the range of H₂ content of gas flows at the pressure and liquid flow which are tested herein, therefore it is assumed that H₂ concentration in the solvent is close to equilibrium for the conditions and reactor dynamics are efficient. The results of these tests are displayed in Figures 5.16 and 5.17.

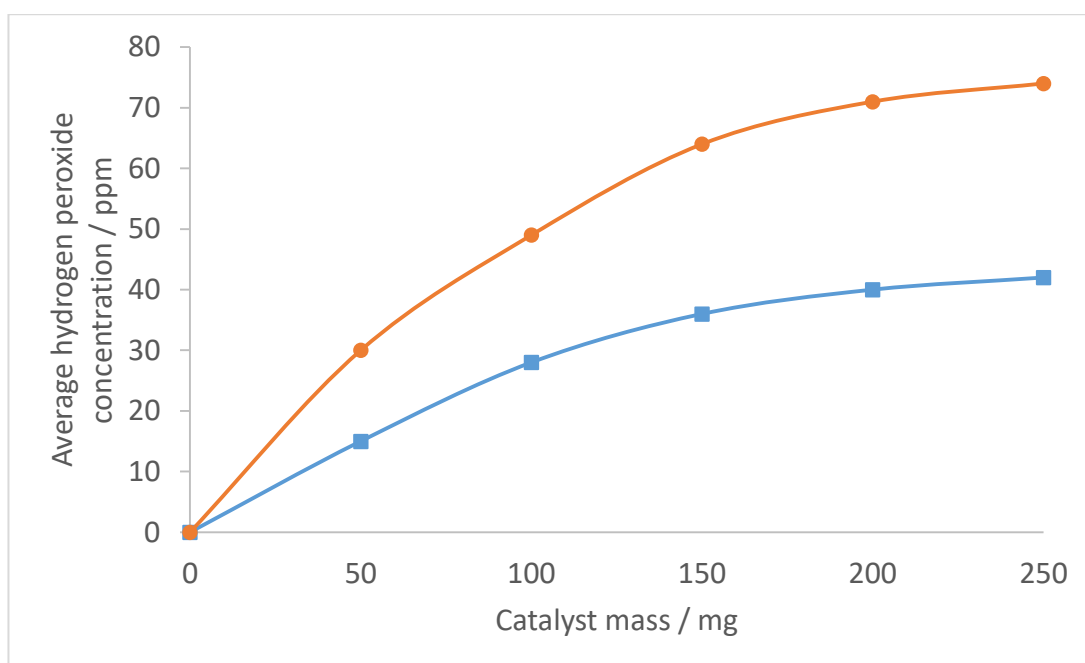


Figure 5.16 – Average hydrogen peroxide concentration at varied catalyst masses rates for CO₂ and air gas diluents

- – 1:1 H₂:O₂ (7.5 % each) with CO₂ diluent (85 %), ■ – 2% H₂ with air diluent

Conditions: ≈25°C, 0.5 wt. % Pd – 4.5 wt. % Ni/TiO₂ ORO catalyst mass as indicated, 210 ml/min total gas flow compositions as indicated, 1 ml/min H₂O, 30 bar.

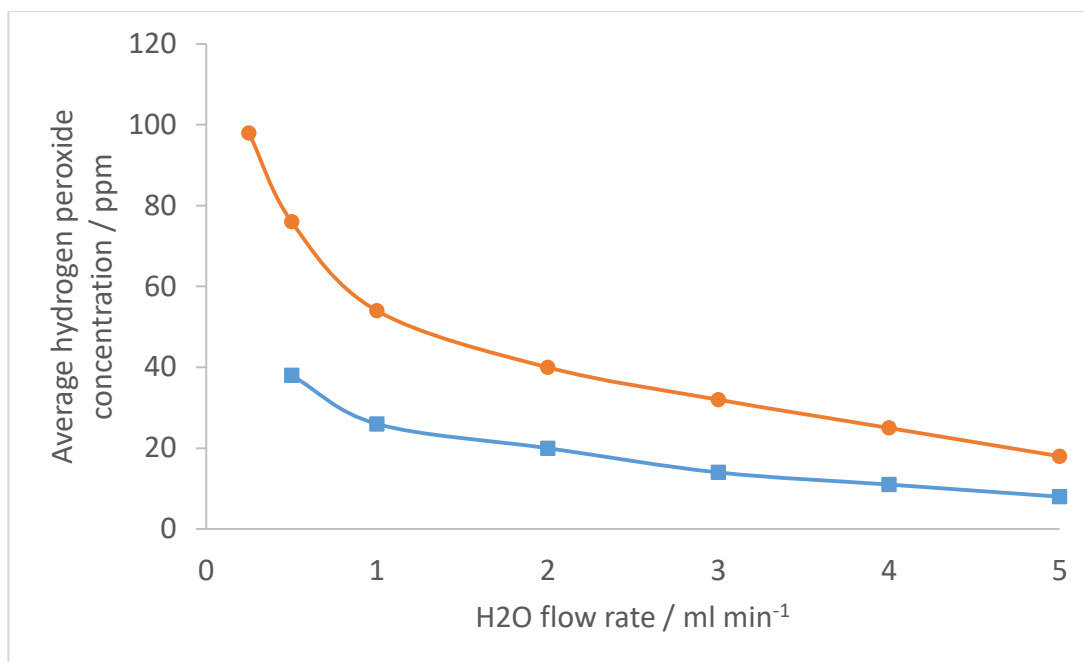


Figure 5.17 – Average hydrogen peroxide concentration at varied H₂O flow rates for CO₂ and air gas diluents

- – 1:1 H₂:O₂ (7.5 % each) with CO₂ diluent (85 %), ■ – 2% H₂ with air diluent

Conditions: ≈25°C, 100mg 0.5 wt. % Pd – 4.5 wt. % Ni/TiO₂ ORO, 210 ml/min total gas flow compositions as indicated, H₂O solvent flow rate as indicated, 30 bar.

The data displayed in Figures 5.16 and 5.17 shows that the concentration of H₂O₂ produced is approximately 40 - 50% reduced when an air diluent is used, relative to a CO₂ diluent. This decrease is fairly consistent across all reaction conditions which were tested. It was previously shown in Table 4.18 that in a batch liquid/gas system use of an N₂ diluent leads to a similar reduction in yield relative to use of a CO₂ diluent than is observed in Figures 5.16 and 5.17. A selectivity measurement of 82% was recorded for the air diluent condition at 1 ml/min H₂O and 150 mg catalyst; the selectivity value measured under analogous conditions with a CO₂ diluent is 84%. Therefore we observe that selectivity is very slightly decreased, but remains high when an air diluent is used.

The predominant reason for the difference in yield and selectivity in these tests is again probably due to the significant *in-situ* promotional effect of carbonic acid which occurs with the use of a CO₂ diluent.¹² A second, lesser effect causing a reduced H₂O₂ yield in the air diluent conditions, especially at greater catalyst masses (Figure 5.16) and greater liquid flow rates (Figure 5.17) could be H₂ availability. As previously stated, the tests were matched for total gas flow, therefore the air diluent condition

necessarily had a decreased H₂ flow by nature of the gas mixes used. While the data in Figure 5.14 suggest the reactant gasses are in excess and changes in gas flows do not cause large changes in yield, there is a small effect, therefore it is reasonable to conclude that the relatively decreased H₂ in the air diluent conditions also contributes to a decreased yield.

5.2.10. The effect of using a 'hard water' solvent on liquid/gas phase flow reactions using 0.5 wt. % Pd – 4.5 wt. % Ni/TiO₂ ORO

Another consideration for the practical implementation of the direct synthesis of H₂O₂ is the possible use of water which contains a range of dissolved ions. The ability to produce H₂O₂ in a stream which contains dissolved ions is vital for potential water cleaning applications of this technology. Furthermore, for applications which require aqueous H₂O₂, such as bleaching, if H₂O₂ can be produced at a useful concentration in a real world water stream which contains dissolved ions, it would remove the need for a preliminary distillation or deionisation step, which would reduce energetic and economic demands.

Section 3.2.8 details the effects of varied concentrations of individual ions on the H₂O₂ yield and degradation in a batch liquid/gas system using a 2.5 wt. % Au – 2.5 wt. % Pd/TiO₂ catalyst. It was shown that the ions which cause the greatest deleterious effect to the direct synthesis of H₂O₂ process are sulfate, carbonate and iron. A model 'hard water' solution was prepared by dissolution of the relevant salts in HPLC grade water to achieve dissolved ions levels which are at or near the legislated UK limits for tap water as reported by Welsh Water.¹⁶ The composition of this model 'hard water' is shown in Table 5.7. The results of tests performed using this 'hard water' as a reaction solvent are shown in Figure 5.18 for CO₂ and air diluents in addition to previous results obtained using HPLC grade for comparison.

Table 5.7 – Concentrations of dissolved ions present in the prepared ‘hard water’ sample.

Ion identity	Concentration / mg/L
K^+	155
Na^+	190
Mg^{2+}	60
Ca^{2+}	150
SO_4^{2-}	250
CO_3^{2-}	250
NO_3^-	30
Cl^-	100
Fe^{3+}	0.2

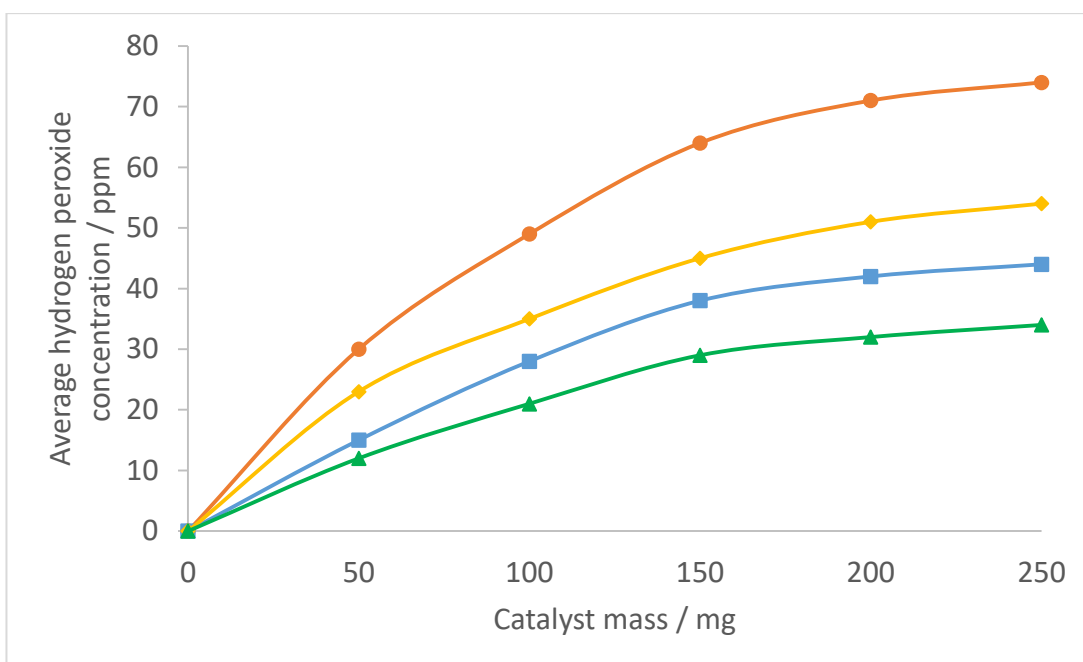


Figure 5.18 – Average hydrogen peroxide concentration at varied catalyst masses rates for CO₂ and air gas diluents in HPLC grade and ‘hard’ water

● – 1:1 H₂:O₂ (7.5 % each) with CO₂ diluent (85 %) in HPLC grade water, ■ – 2% H₂ with air diluent in HPLC grade water, ◆ – 1:1 H₂:O₂ (7.5 % each) with CO₂ diluent (85 %) in ‘Hard water’, ▲ – 2% H₂ with air diluent in ‘Hard water’

Conditions: ≈25°C, 0.5 wt. % Pd – 4.5 wt. % Ni/TiO₂ O.R. mass as indicated, 210 ml/min total gas flow compositions as indicated, 1ml/min H₂O solvent flow rate, 30 bar.

The data in Figure 5.18 shows an approximately 20-25% decreased yield in 'hard water' compared to HPLC grade water, both with use of a CO₂ and air diluent. This is consistent with the magnitude of decreased yields found from sulfate, carbonate and iron in Section 2.3.8. The mechanism of the productivity decreasing effect of these individual ions is fully explained in Section 2.3.8 and it is believed that the same mechanisms are active in this scenario. Selectivity measurements of 80% and 79% were recorded for 150 mg catalyst in 'hard water' solvent with CO₂ and air diluents respectively. The slight decrease in selectivity in the 'hard water' solvent relative to HPLC grade water solvent is probably due to increased degradation as a result of increased pH from the addition of carbonate ions, a phenomena previous shown in Figure 3.21 and 3.22.

5.3. Conclusions

The studies presented herein reporting the direct synthesis of H₂O₂ in the gas phase represent preliminary and proof of concept work in an area that has extremely little literature precedent. It is proposed in multiple studies pertaining to the epoxidation of propene using Au catalysts, wherein H₂ is added to O₂ reactant streams as a sacrificial reductant, that H₂O₂ is formed in the gas phase on the Au particle surface before participating in the selective oxidation reaction.¹⁷⁻²⁰ However, H₂O₂ is not directly observed in any of these studies. A 2001 patent¹³ reports this reaction, however in addition to elevated pressures (as used in this study), the process requires an elevated temperature and the presence of acid and halides in the gas phase as stabilisers to produce H₂O₂.

A more recent study by Akram *et al.*¹⁴ utilised conditions more comparable to those in this study. In the aforementioned study, the process was performed using Au-Pd/TiO₂ catalysts in a gas phase flow system, without the use of acid or halide stabilisers, although tests were performed at atmospheric pressure and 40-80°C. A reactor capable of containing high pressure gas flows was constructed for this study, therefore contrary to the study by Akram, the results herein are obtained at elevated pressures (5 - 20 bar) and ambient temperature (25±1°C). As there is significant overlap in conditions used, data can be compared between this work and that of Akram. At conditions of 50 ml/min 2% H₂/air flow, 50 mg 2.5 wt. % Au – 2.5 wt. % Pd/TiO₂ catalyst and 16 hr reaction time, Akram produced 1.001 x 10⁻⁶ moles of H₂O₂

at ambient pressure and 60°C, whereas in this work 2.350×10^{-5} moles of H_2O_2 were produced at 20 bar and ambient temperature, with greater yields achievable at greater catalyst masses.

Therefore, whilst these are preliminary studies, this work highlights that there is scope for greatly increasing yields in this process with engineering modifications. Conversion data is not provided in the study by Akram, therefore relative differences in selectivity cannot be commented on; however within this study it was shown that adding a solid diluent in the form of SiC increases yield and selectivity.

Furthermore, the use of newly designed Pd-Ni and Pd-Ga ORO catalysts provides a significant increase in selectivity over the use of Au-Pd. This again highlights potential scope for future work to refine the gas phase direct synthesis process and achieve greater H_2O_2 yields, possibly by exploring the use of greater masses of selective Pd-Ni or Pd-Ga catalysts or implementing a recycle loop to re-circulate unreacted H_2 and O_2 through the catalyst bed. The use of varied temperatures in addition to elevated pressures could also be explored.

Gas/liquid phase flow reactor tests show that the optimised Pd-Ni catalyst presented in Chapter 4 is able to give a constant H_2O_2 synthesis activity and resist loss of active metal over a 10 hour test period. This finding highlights the high stability of the catalyst, which is a necessity for practical implementation of a direct synthesis of H_2O_2 system. For the test performed using 50 mg catalyst and a H_2O flow rate of 3 ml/min at 30 bar (Figure 5.13), the catalyst productivity per kg of active metal (as used in Table 5.1) is $423 \text{ mol}_{\text{H}_2\text{O}_2} \text{ kg}_{(\text{Pd})}^{-1} \text{ h}^{-1}$. This is the greatest productivity recorded in this system. For the test performed using 100 mg catalyst and a H_2O flow rate of 1 ml/min at 10 bar, the catalyst productivity per kg of active metal is $78 \text{ mol}_{\text{H}_2\text{O}_2} \text{ kg}_{\text{Pd}}^{-1} \text{ h}^{-1}$. These results are comparable to the results obtained under flow conditions using MeOH/ H_2O solvent mixes in the absence of promoters by Freakley *et al.*⁵ and Biasi *et al.*^{4, 10}, as presented in Table 5.1. However, the selectivities of up to 89% recorded in this study are greater than those recorded in any of the referenced studies.

Previous work by Biasi *et al.*⁴ showed that for supported Pd catalysts (2.5 wt. % Pd; SiO_2 , ZrO_2 , sulfated ZrO_2 and sulfated CeO_2 supports) an increase in selectivity and productivity was observed when the catalysts were tested in a trickle bed reactor, relative to a semi-batch reactor. For the catalysts featuring sulfonated supports, selectivities of 70% were achieved in the trickle bed reactor, where a maximum selectivity of only 30% had been achieved in a semi-batch reactor. The authors emphasise that optimising reactor design and operating conditions to find an optimum

contact time between the catalyst and the reactant gasses/solvent is key for high productivity and selectivity. However, the data presented in Figure 5.11 suggests that these enhancements in selectivity and productivity are not always observed when moving from a semi-batch or batch system to a flow system.

The Pd-Ni catalyst, used extensively in the studies herein, is a highly selective catalyst in a batch system, where there is the possibility for extended contact time between produced H_2O_2 and the catalyst surface. Therefore, when contact time is greatly decreased in a flow system, we do not observe a rise in selectivity, as would be expected via a reduction in the extent of degradation, were a less selective catalyst used. In contrast, we observe a slight decrease in selectivity upon moving to a flow system, potentially from a degree of concurrent gas phase combustion, as previously outlined. When using a highly selective catalyst such as Pd-Ni/ TiO_2 , the best results may be obtained from a semi-batch reactor, which would allow for sufficient reactants to be delivered to the catalyst active sites and an extended contact time which would allow for a greater extent of synthesis and due to the nature of the catalyst would not lead to decreased yield via degradation.

In the flow system tested herein, as in a batch system tested in Chapters 3 and 4, H_2O_2 yield shows a close to proportional relationship to H_2 partial pressure when a selective catalyst such as Pd-Ni is used. This is because H_2 solubility increases with pressure and the synthesis reaction is believed to be first order with respect to available hydrogen concentration.^{21, 22} For this reason, it is unlikely that low pressure direct synthesis of H_2O_2 is feasible in either of these systems at low operating pressures. Alternate engineering solutions could be explored to attempt to increase the dissolution of H_2 into the solvent at lower pressures to allow for increased yields at low pressures.

A potentially useful method of generating the necessary H_2 reactant gas for the direct synthesis of H_2O_2 is the electrolysis of water as this would not require the purchase and storage of supplementary gas cylinders. This method of generating H_2 without relying on external gas cylinders would necessitate the use of air as a diluent gas (to keep the gas stream outside of the explosive H_2 in O_2 regime), which precludes the use of CO_2 as a diluent. The beneficial effects of a CO_2 diluent have been discussed in Chapter 3 of this work as well as multiple previous studies.^{12, 23} In this study we observe a decrease in yield of approximately 40 - 50% upon using an air diluent, relative to tests performed with a CO_2 diluent under otherwise identical conditions. However, selectivity only displays a very small decrease, suggesting that the use of

air as a diluent is feasible as high yields can still be obtained if engineering measures to improve conversion, such as recycling of unreacted gasses, are implemented.

Performing tests with model 'hard water' we observe a decrease in yield of approximately 20 - 25%, relative to using HPLC grade water. However, again we only observe a small decrease in selectivity, suggesting that high yields could be obtainable with improved reactor engineering. A group of species that may present problems in an implementation of the direct synthesis of H_2O_2 where impure water streams are used are sulfur containing molecules. Due to the well documented effect of sulfur containing molecules poisoning Pd sites, a water stream which contains high levels of these species would incrementally decrease catalyst activity and necessitate catalyst regeneration. Therefore the direct synthesis of H_2O_2 may not be feasible in water streams which contain sulfur compounds.

5.4. References

1. T. Inoue, J. Adachi, K. Ohtaki, M. Lu, S. Murakami, X. Sun and D. F. Wang, *Chemical Engineering Journal*, 2015, 278, 517-526.
2. Y. Voloshin, R. Halder and A. Lawal, *Catalysis Today*, 2007, 125, 40-47.
3. P. Biasi, S. Zancanella, F. Pinna, P. Canu and T. O. Salmi, *Chemical Engineering Transactions*, 2011, 24, 49-54.
4. P. Biasi, P. Canu, F. Menegazzo, F. Pinna and T. O. Salmi, *Industrial & Engineering Chemistry Research*, 2012, 51, 8883-8890.
5. S. J. Freakley, M. Piccinini, J. K. Edwards, E. N. Ntainjua, J. A. Moulijn and G. J. Hutchings, *ACS Catalysis*, 2013, 3, 487-501.
6. A. Pashkova, K. Svajda and R. Dittmeyer, *Chemical Engineering Journal*, 2008, 139, 165-171.
7. T. Inoue, K. Ohtaki, S. Murakami and S. Matsumoto, *Fuel Processing Technology*, 2013, 108, 8-11.
8. T. Inoue, M. A. Schmidt and K. F. Jensen, *Industrial & Engineering Chemistry Research*, 2007, 46, 1153-1160.
9. J. Kim, Y.-M. Chung, S.-M. Kang, C.-H. Choi, B.-Y. Kim, Y.-T. Kwon, T. J. Kim, S.-H. Oh and C.-S. Lee, *ACS Catalysis*, 2012, 2, 1042-1048.
10. P. Biasi, F. Menegazzo, F. Pinna, K. Eranen, T. O. Salmi and P. Canu, *Chemical Engineering Journal*, 2011, 176, 172-177.
11. J. García-Serna, T. Moreno, P. Biasi, M. J. Cocero, J.-P. Mikkola and T. O. Salmi, *Green Chemistry*, 2014, DOI: 10.1039/c3gc41600c.
12. J. K. Edwards, S. J. Freakley, R. J. Lewis, J. C. Pritchard and G. J. Hutchings, *Catalysis Today*, 2015, 248, 3-9.
13. M. Nyström, J. Wangård and W. Herrmann, *US Patent 6299852 B1*, 2001.
14. A. Akram, S. J. Freakley, C. Reece, M. Piccinini, G. Shaw, J. K. Edwards, F. Desmedt, P. Miquel, E. Seuna, D. J. Willock, J. A. Moulijn and G. J. Hutchings, *Chemical Science*, 2016, 7, 5833-5837.
15. P. W. N. M. v. L. R.A. van Santen, J.A. Moulijn and B.A. Averill, in *Studies in Surface Science and Catalysis*, Elsevier, 2nd edn., 1999, DOI: [https://doi.org/10.1016/S0167-2991\(99\)80011-1](https://doi.org/10.1016/S0167-2991(99)80011-1), pp. 375-431.
16. *Drinking Water Compliance Summary - Cardiff East*, Welsh Water, 2013.
17. T. Hayashi, K. Tanaka and M. Haruta, *Journal of Catalysis*, 1998, 178, 566-575.
18. U. B. S., T. Susumu, H. Toshio and H. Masatake, *Chemistry Letters*, 1998, 27, 1277-1278.
19. T. A. Nijhuis, B. J. Huizinga, M. Makkee and J. A. Moulijn, *Industrial & Engineering Chemistry Research*, 1999, 38, 884-891.
20. T. A. Nijhuis, T. Visser and B. M. Weckhuysen, *Angewandte Chemie*, 2005, 44, 1115-1118.
21. Q. Liu and J. H. Lunsford, *Applied Catalysis A: General*, 2006, 314, 94-100.
22. R. Sander, *Atmos. Chem. Phys.*, 2015, 15, 4399-4981.
23. J. K. Edwards and G. J. Hutchings, *Angewandte Chemie*, 2008, 47, 9192-9198.

6. FUTURE WORK AND CONCLUSIONS

6.1. Conclusions

As detailed in Chapter 1 of this work, H_2O_2 is currently industrially produced via the anthraquinone process. This process is capable of achieving high H_2 selectivities at fairly mild conditions (*c.a.* 50°C, 4 bar). However, the process suffers from some drawbacks such as proving economically viable only on a very large scale, which requires potentially costly storage and transport of produced H_2O_2 and the addition of stabilisers to prevent decomposition of H_2O_2 . Furthermore, the process requires regular replenishment of anthraquinone which is lost to degradation, increasing both the costs and environmental impact associated with the process.¹⁻³

The disadvantages of the anthraquinone process and a continuing and growing demand for H_2O_2 have spurred studies into the catalysed direct synthesis of H_2O_2 from molecular H_2 and O_2 . This process could hypothetically allow for small scale, on-site production of H_2O_2 which is free from stabilisers and additives. The main challenge of this process is that of selectivity, as the majority of catalysts which are active for H_2O_2 synthesis are also active for subsequent degradation pathways.^{2, 4, 5}

Chapter 3 of this work explored the effect of reaction conditions on the direct synthesis of H_2O_2 using a 2.5 wt. % Au – 2.5 wt. % Pd/TiO₂ catalyst. The use of a 100% H_2O solvent and ambient temperature represents the most economic and ‘green’ conditions for this process and could potentially allow for significant uses in water purification. However, H_2 solubility is relatively low in H_2O compared to short-chain alcohols, which are commonly used as solvents for the direct synthesis of H_2O_2 . Furthermore, many previous studies have made use of sub-ambient temperatures and additives such as halides and acids to suppress degradation pathways and increase H_2O_2 yield.^{2, 4} As such, when the direct synthesis of H_2O_2 is performed in 100% H_2O and at ambient temperature, there is moderately high degradation activity (especially at high catalyst mass usage) and limited H_2O_2 yields.

Investigations into the potential direct synthesis of H_2O_2 in tap water, including hard water, demonstrated some potential challenges. Carbonates were shown to increase the degradation of H_2O_2 , thus decreasing the yield. This is believed to be primarily

due to base-catalysed decomposition of H_2O_2 . Sulfur species in water also appear to cause catalyst poisoning, leading to decreased yields and most likely eventual deactivation of the catalyst.

Based on the results in Chapter 3, it was decided that catalyst design should focus primarily on minimising the degradation activity of a catalyst. Chapter 4 details the design of such catalysts. A series of supported metal nanoparticle catalysts of a generalised formula 0.5 wt. % Pd – 4.5 wt. % M (M= Ni, Ga, Co, In and Zn) were prepared and treated with successive oxidative, reductive and oxidative (ORO) heat treatments. For catalysts of this type, ORO heat treatment was found to confer high stability and near-total selectivity towards H_2O_2 with moderate activity. The high selectivity of these catalysts was found to allow for the use of high catalyst masses to produce significant yields of H_2O_2 whilst maintaining very low degradation activity.

Catalyst optimisation and characterisation focussed primarily on Pd-Ni/ TiO_2 ORO catalysts. It was found that the presence of both Pd and Ni (or other suitable metal) on a secondary metal oxide support is necessary for stable and selective catalysts. Furthermore, a loading consisting of too much Pd or too little Ni also results in catalysts which are not highly selective or stable. Improvement of catalyst productivity could be achieved by the inclusion of acid and halides into the catalyst preparation while maintaining both high selectivity and stability.

A model of 0.5 wt. % Pd - 4.5 wt. % Ni/ TiO_2 ORO was proposed by consideration of catalyst testing and characterisation data. Z-contrast images obtained by STEM in combination with EDS analysis show that the predominant Pd-containing structures are 0.5 – 1 nm Pd-rich clusters with only few larger (5 – 10 nm) alloyed Pd-Ni structures. EDS analysis suggests there is a near-continuous layer of NiO or mixed $\text{NiO}_x/\text{TiO}_x$ on the catalyst, with the lack of defined NiO reflections in XRD analysis suggesting this layer to be amorphous. Bright field images suggest that this layer grows and partially covers the Pd-rich clusters as the catalyst is treated with an ORO heating cycle. This partial coverage of the Pd-rich clusters appears to confer the high selectivity to the catalyst as the interfacial and corner Pd sites, which are of the highest energy and primarily responsible for catalysing degradation pathways,^{6,7} are covered. This leaves lower energy Pd planes exposed for the selective synthesis of H_2O_2 .^{8,9} This partial encapsulation/edge coverage of the small Pd-rich nanoparticles also may prevent the loss of Pd from these particles or the loss of full particles from the catalyst surface, therefore allowing for a highly stable catalyst. XPS analysis confirms Pd to be present primarily as PdO in the ORO catalyst samples, whereas

there is significant Pd⁰ present in solely oxidation-reduction (OR) treated samples. This explains the necessity of the final oxidation step as Pd⁰ is known to be active for the degradation of H₂O₂ and therefore catalysts with significant Pd⁰ content are unselective.¹⁰

Chapter 5 reports the gas phase direct synthesis of H₂O₂, studies which are primarily 'proof of concept' in an area with very little prior literature. This process has been proposed as a step in the epoxidation of propene using Au catalysts,¹¹⁻¹⁴ but H₂O₂ was not directly observed in any of these studies. However, a study by Akram *et al.*¹⁵ used 2.5 wt. % Au – 2.5 wt. % Pd/TiO₂ catalysts in a gas phase flow system at atmospheric pressure and 40-80°C, to produce H₂O₂ in the gas phase without the use of acid or halide stabilisers. The studies contained in this work were performed on a reactor capable of containing high pressure gas flows, therefore results herein were obtained at elevated pressures (5 - 20 bar) and ambient temperature (25±1°C). The production of H₂O₂ in the gas phase is possible under these conditions with use of a 2.5 wt. % Au – 2.5 wt. % Pd/TiO₂ catalyst, however selectivity is extremely low, remaining under 0.1%. At conditions of 50 ml/min 2% H₂/air flow, 50 mg catalyst and 16 hour reaction time, Akram produced 1.001x10⁻⁶ moles of H₂O₂ at ambient pressure and 60°C, whereas in this work 2.350x10⁻⁵ moles of H₂O₂ were produced at 20 bar and ambient temperature. Greater yields are possible by increasing catalyst mass to a point (100 mg 2.5 wt. % Au – 2.5 wt. % Pd/TiO₂, under the above conditions), however yield begins to decrease at greater catalyst masses as degradation processes dominate. Yields and selectivity can also be increased by the addition of SiC, which acts as a solid diluent and improves thermal management of the catalyst bed.

The implementation of 0.5 wt. % Pd – 4.5 wt. % Ni/TiO₂ and 0.5 wt. % Pd – 4.5 wt. % Ga/TiO₂ ORO catalysts, which were introduced in Chapter 4, allows for selectivities approaching 1%. While this is low in absolute terms, it represents a significant increase in selectivity over the use of a 2.5 wt. % Au – 2.5 wt. % Pd/TiO₂ catalyst. Again, greater yields are recorded at increased catalyst masses, however no decrease in yield is seen when using catalyst masses up to 250 mg at the conditions described above. This again highlights the significantly improved selectivity of the newly designed Pd-M ORO series of catalysts over the heavily studied 2.5 wt. % Au – 2.5 wt. % Pd/TiO₂ catalyst.

Chapter 5 also reports studies performed in a gas/liquid phase flow reactor. It was shown that a 0.5 wt. % Pd – 4.5 wt. % Ni/TiO₂ ORO catalyst gives a constant yield of

H₂O₂ and is stable to metal loss over a 10 hour reaction. Productivities of up to 423 mol_{H₂O₂} kg_{Pd}⁻¹ h⁻¹ were recorded for this catalyst in a H₂O solvent flow system, which is comparable to previous studies by Freakley *et al.*¹⁶ and Biasi *et al.*^{17, 18} which have investigated the production of H₂O₂ in a flow system without the use of promoters in more favourable MeOH or MeOH/H₂O solvent compositions. Furthermore, the selectivities of up to 89% recorded in this study are greater than those recorded in these previous studies.¹⁶⁻¹⁸

In this study, it was found that selectivity in a flow system was decreased compared to that of a batch system, a reverse of the trend seen in previous studies wherein less selective catalysts were utilised.¹⁷ 0.5 wt. % Pd – 4.5 wt. % Ni/TiO₂ ORO has proven to be a near totally selective catalyst in a batch system, where there is significant contact time between the catalyst and reactants/products. Therefore, beneficial effects on selectivity are not observed in a liquid/gas flow system where contact time is significantly decreased. The small decrease in selectivity which is actually observed is potentially due to a degree of combustion occurring over the catalyst in the gas phase as gas ‘bubbles’ pass over the catalyst, allowing direct contact between gaseous reactants and the catalyst.

Studies investigating practical, ‘real-world’ conditions for the direct synthesis of H₂O₂ in a flow regime showed the near-directly proportional relationship between H₂ partial pressure and H₂O₂ yield when using a 0.5 wt. % Pd – 4.5 wt. % Ni/TiO₂ ORO catalyst. Therefore, the direct synthesis of H₂O₂ at low pressures appears to only produce low concentrations of H₂O₂. The process remains highly selective, therefore recycling of unused reactants is a possible method to increase yield. A potential method for the practical implementation of the direct synthesis of H₂O₂ involves the generation of H₂ from water electrolysis and dilution of this H₂ with air for use as a reactant stream. The use of air as a diluent, as opposed to CO₂ which is used extensively in this and many previous studies,^{4, 5} results in a decrease in yield of approximately 40 - 50%, however selectivity remains high. Tests performed using UK legislated acceptable limits of dissolved ions in tap water showed that this condition causes a decrease in yield of approximately 20 - 25%, relative to using HPLC grade water. Under this condition it was again observed that selectivity remains high while yield is decreased, suggesting that improved yields could be obtained with recycling of unused reactants.

In conclusion, this work first thoroughly investigated the effects of reaction conditions on the direct synthesis of H₂O₂, identifying the challenges of operating under environmentally friendly and economic conditions of a water solvent and ambient

reaction temperature. Secondly, this work investigated the design of highly selective H₂O₂ synthesis catalysts. A series of catalysts was prepared with the general formula 0.5 wt. % Pd – 4.5 wt. % 'M'/TiO₂ and heat treated with a sequential 'oxidation-reduction-oxidation' process, producing highly stable, near-totally selective H₂O₂ synthesis catalysts. Finally, this work studied the implementation of these catalysts, showing them to be significantly more selective than previous state-of-the-art catalysts in gas and gas/liquid flow regimes. Tests also show that it is possible to selectively produce H₂O₂ in practical 'real world' conditions of high flow rates, a hard water solvent and a dilute H₂ in air reactant stream.

6.2. Future work

6.2.1. Further catalyst optimisation and design

The vast majority of catalysts studied and designed in this work were prepared using a standard wet-impregnation method, as outlined in Chapter 2. However, previous literature shows catalysts which are active for the direct synthesis of H₂O₂ have been successfully prepared by many techniques including modified impregnation¹⁹, sol-immobilisation²⁰ and physical grinding²¹. Investigations into using alternate techniques such as these to initially prepare catalysts before ORO treatment could potentially lead to the discovery of more productive catalysts.

Optimisation of metal loading was performed for Pd-Ni/TiO₂ and Pd-Ga/TiO₂ ORO catalysts, but not for further successful Pd-M ORO combinations (i.e. M = Co, In and Zn). Performing these optimisations could allow for the creation of a range of highly productive catalysts and also potentially allow for the identification of trends in the metal ratios of optimised catalysts. Further enhancements in productivity of these catalysts could also be investigated through the optimisation of catalyst support, precursor salt and preparation solution pH, as performed in this work for Pd-Ni ORO. A further optimisation which could be explored for all catalysts is the temperature and duration of heat treatments. All ORO heat treatments in this work used the conditions first outlined by Freakley *et al.*²² for Pd-Sn/TiO₂ ORO catalysts, which proved successful to create 5 further examples of stable, selective catalysts. However it is possible that these catalysts could maintain stability and selectivity but achieve improved productivity with optimised heat treatment cycles.

Section 4.2.2 of this work showed a significant enhancement in activity of a 5 wt. % Pd/TiO₂ catalyst with the substitution of 0.1 wt. % Pd with Pt, however there was a

failure to produce stable preparations of these catalysts. A study investigating the addition of Pt to Au-Pd/TiO₂ catalysts for H₂O₂ synthesis by Pritchard *et al.*²³ found that a 2.4 wt. % Au – 2.4 wt. % Pd – 0.2 wt. % Pt/TiO₂ catalyst was 250% as productive as 2.5 wt. % Au – 2.5 wt. % Pd/TiO₂ with no increase in degradation activity. The addition of Pt to stable Pd-M ORO catalysts could be investigated to determine whether this can produce a similar enhancement in catalyst activity whilst maintaining stability.

It was hypothesised in Chapter 4 that the active structures for selective synthesis of H₂O₂ by Pd-M ORO catalysts is primarily small Pd-rich clusters which have their support interface and corner sites blocked, leaving lower energy planes exposed. Alternative routes to synthesising such structures could be explored. For example, the use of polymers such as PVA or PVP²⁴ in the synthesis of Pd catalysts could be investigated to see if this brings about a similar selectivity and stability to that seen in Pd-M ORO catalysts. Alternatively, stabilised colloidal catalysts could be further investigated, as results in Section 4.2.9 suggest that colloidal Pd does not have high activity for H₂O₂ decomposition, unlike supported Pd catalysts. A further potential option is the synthesis of mixed metal oxides of the type Pd-M, for example by a sol-gel method, to potentially synthesise bulk materials which contain Pd single atoms or small clusters partially encapsulated by secondary metal oxides.^{25, 26}

6.2.2. Use of Pd-M ORO catalysts in further reactions

Many catalysts have been tested for the direct synthesis of H₂O₂, however the vast majority of active catalysts display significantly lower selectivity than the Pd-M ORO series of catalysts presented in this work. These catalyst may also exhibit similar very high selectivity for other selective hydrogenation reactions which have literature precedent for employing Pd catalysts. Processes such as the selective hydrogenation of highly unsaturated aliphatic hydrocarbons or the chemo-selective hydrogenation of carbonyl compounds may benefit from the use of this newly developed series of selective Pd based hydrogenation catalysts.²⁷⁻²⁹

The work contained in this thesis focussed on the direct synthesis of H₂O₂ under conditions which are economic and environmentally friendly, however are not conducive to producing high yields of H₂O₂. The series of selective Pd-M ORO catalysts could also be fully tested under conditions which are more favourable for producing high yield of H₂O₂ to investigate how their performance compares to the current state-of-the-art. As detailed in Section 1.4.2, the addition of acids and/or

halides to the reaction solution is a commonly used method to increase the yield of H_2O_2 synthesis reactions. H_2O_2 synthesis using Pd-M ORO catalysts in conjunction with such additives could be tested to observe the maximum yields which are possible under these more favourable conditions.³⁰⁻³⁴ A sub-ambient temperature is commonly used in the direct synthesis of H_2O_2 to reduce the rates of H_2O_2 degradation and therefore improve selectivity. However, this work has shown that using Pd-M ORO catalysts, near-total selectivity is achieved at ambient temperatures. Therefore, tests at elevated temperatures could be performed to investigate the temperature at which selectivity begins to decrease. As the activity of the synthesis pathway also increases with temperature, greater yields may be obtainable at elevated temperatures, as long as selectivity is maintained.^{7, 35}

A MeOH solvent is very commonly used in the direct synthesis of H_2O_2 due to increased H_2 solubility comparative to H_2O ;^{36, 37} this generally leads to greater possible yields but also greater rates of H_2O_2 hydrogenation, as shown in Section 3.2.1. Therefore, H_2O_2 synthesis reactions using highly selective Pd-M ORO catalysts could be performed in a MeOH solvent in addition to longer chain alcohols to investigate whether high selectivities can be obtained. H_2 solubility in n-alcohols generally increases with chain length,³⁸ therefore the synthesis of H_2O_2 in long chain alcohol solvents (e.g. decan-1-ol) could be explored, either as a sole solvent with subsequent extraction of produced H_2O_2 or as a bi-phasic solvent system with H_2O . Super-critical CO_2 has previously been investigated as a solvent for the direct synthesis of H_2O_2 , primarily chosen due to very high H_2 solubility; however this process has generally been shown to be highly unselective.^{1, 39-41} Again, tests using the newly developed, highly selective Pd-M ORO catalysts in this system could be performed to investigate whether selectivities reported in previous literature can be improved upon.

The direct synthesis of H_2O_2 in water presents possibilities for use in water cleaning technologies. As outlined in Section 1.2.1, H_2O_2 is a powerful oxidant and is used to destroy many contaminants in water, regularly together with Fe^{2+} species as Fenton's reagent or in conjunction with UV treatment.^{3, 42-44} An exciting path for future work is the investigation of *in-situ* generation of H_2O_2 and the subsequent use of Fenton's chemistry or H_2O_2 /UV treatment to destroy contaminants in waste water streams. This could potentially lead to the development of water treatment processes which use H_2 generated by electrolysis of H_2O together with air to provide a gaseous reagent stream for the direct synthesis of H_2O_2 , and then use this generated H_2O_2 to oxidise pollutants *in-situ*.

6.2.3. Further flow system testing

For direct synthesis of H_2O_2 in a gas flow system, selectivity was found to be less than 1% for all catalysts tested, however measuring the extent of each unselective pathway (combustion, hydrogenation and decomposition) was not feasible in the reactor system utilised. Further tests to investigate which of these unselective pathways dominate the reaction process would allow for future improvements that specifically address these issues. For example, if combustion is found to dominate, performing reactions at a decreased temperature may help reduce the activity of this pathway and therefore increase H_2 selectivity. If hydrogenation or decomposition are found to be the dominant unselective processes, steps to reduce the contact time of produced H_2O_2 with the catalyst bed could be introduced, such as the implementation of multiple small catalyst beds with collection of produced H_2O_2 after each. For gas phase flow synthesis of H_2O_2 using Pd-Ni or Pd-Ga ORO catalysts, a H_2 consumption of 5% was recorded (Section 5.2.2). Therefore the implementation of a recycle loop to pass unreacted reagents back over the catalyst bed represents a relatively simple engineering modification that could allow for greatly improved H_2O_2 yield.

For direct synthesis of H_2O_2 in a liquid/gas flow system, again measuring the extent of each unselective pathway (combustion, hydrogenation and decomposition) would provide useful information. It is believed the small loss of selectivity arises from gas phase combustion, due to the negligible hydrogenation/decomposition active of Pd-Ni ORO catalysts in the liquid phase. If this is indeed the case, methods to reduce the extent of combustion could be investigated. These could include thermal management of the catalyst bed via dilution with an inert solid (e.g. SiC) or direct cooling of the catalyst bed. Methods of modifying the gas/liquid dynamics of the flow could also be investigated to attempt to produce a more thoroughly mixed reactant stream with smaller 'gas bubbles'. This could theoretically reduce the extent of gas phase interactions between the catalyst and the reactants. More intimate mixing of the gas and liquid stream components could also have the effect of improving the rate at which dissolved H_2 concentration reaches equilibrium due to a greater gas/liquid interfacial surface area.⁴⁵ This could potentially increase yield if under the conditions used within this work, H_2 dissolution equilibrium was not reached prior to the reactant stream reaching the catalyst bed.

In gas/liquid flow operation using selective Pd-M ORO catalysts, H₂ selectivity was high, but H₂ conversion was less than 1%. Therefore, implementation of a recycle loop used to re-circulate unreacted gasses over the catalyst bed would be a method to potentially greatly increase H₂O₂ yield. The use of alternative reactor types could also be investigated. Continuous or semi-continuous reactors with a longer contact time than that used in the liquid/gas flow studies in this work could be used to maximise the effectiveness of the highly selective Pd-M ORO catalysts. For example a semi-batch reactor would allow for sufficient reactants to be delivered to the catalyst active sites and an extended contact time which would allow for a greater extent of synthesis and due to the nature of the catalyst would not lead to decreased yield via degradation. The use of a slurry reactor could also be investigated, as this reactor type allows for control of contact time, through mixing of catalyst and reactants and good thermal control.⁴⁶

6.2.4. Characterisation

Characterisation presented in this work focussed on 0.5 wt. % Pd – 4.5 wt. % Ni/TiO₂ ORO and from this data a hypothesised model for the catalyst was proposed in Section 4.4. The identical preparation and analogous experimental performance of similar Pd-M ORO catalysts leads to the belief that they share largely similar features to those proposed for Pd-Ni ORO. However, characterisation of the types presented in Section 4.3 for other catalysts in the Pd-M ORO series would allow for the identification of similarities and any differences between the catalysts in the series.

STEM images in Section 4.3.1 suggest that the 0.5 wt. % Pd – 4.5 wt. % Ni/TiO₂ ORO catalyst has many partially encapsulated 0.5 – 1 nm Pd-rich nanoparticles and few larger alloyed Pd-Ni particles. A previous focussing on 3 wt. % Pd – 2 wt. % Sn/TiO₂ ORO and 1 wt. % Pd – 4 wt. % Sn/SiO₂ ORO catalysts by Freakley *et al.*²², found relatively more large (5-10 nm) Pd-Sn alloyed particles compared to small Pd-rich particles. Further investigations using STEM to compare catalysts could show the reasons for these differences. Preparing 0.5 wt. % Pd – 4.5 wt. % Sn/TiO₂ ORO and 3 wt. % Pd – 2 wt. % Ni/TiO₂ ORO catalysts and imaging these to study the presence of small Pd-rich and larger alloyed particles could tell us whether this apparent difference in relative abundance of each type of particle is a function of the ratio of metal loadings or due to the identity and characteristics of the secondary metal.

6.3. References

1. Y. H. Yi, L. Wang, G. Li and H. C. Guo, *Catalysis Science & Technology*, 2016, 6, 1593-1610.
2. C. Samanta, *Applied Catalysis A: General*, 2008, 350, 133-149.
3. J. M. Campos-Martin, G. Blanco-Brieva and J. L. Fierro, *Angewandte Chemie*, 2006, 45, 6962-6984.
4. J. K. Edwards, S. J. Freakley, R. J. Lewis, J. C. Pritchard and G. J. Hutchings, *Catalysis Today*, 2015, 248, 3-9.
5. J. K. Edwards and G. J. Hutchings, *Angewandte Chemie*, 2008, 47, 9192-9198.
6. S. Kim, D.-W. Lee, K.-Y. Lee and E. A. Cho, *Catalysis Letters*, 2014, 144, 905-911.
7. N. M. Wilson and D. W. Flaherty, *Journal of the American Chemical Society*, 2016, 138, 574-586.
8. S. Melada, F. Pinna, G. Strukul, S. Perathoner and G. Centi, *Journal of Catalysis*, 2005, 235, 241-248.
9. T. Deguchi and M. Iwamoto, *The Journal of Physical Chemistry C*, 2013, 117, 18540-18548.
10. V. R. Choudhary, A. G. Gaikwad and S. D. Sansare, *Catalysis Letters*, 2002, 83, 235-239.
11. T. Hayashi, K. Tanaka and M. Haruta, *Journal of Catalysis*, 1998, 178, 566-575.
12. U. B. S., T. Susumu, H. Toshio and H. Masatake, *Chemistry Letters*, 1998, 27, 1277-1278.
13. T. A. Nijhuis, B. J. Huizinga, M. Makkee and J. A. Moulijn, *Industrial & Engineering Chemistry Research*, 1999, 38, 884-891.
14. T. A. Nijhuis, T. Visser and B. M. Weckhuysen, *Angewandte Chemie*, 2005, 44, 1115-1118.
15. A. Akram, S. J. Freakley, C. Reece, M. Piccinini, G. Shaw, J. K. Edwards, F. Desmedt, P. Miquel, E. Seuna, D. J. Willock, J. A. Moulijn and G. J. Hutchings, *Chemical Science*, 2016, 7, 5833-5837.
16. S. J. Freakley, M. Piccinini, J. K. Edwards, E. N. Ntainjua, J. A. Moulijn and G. J. Hutchings, *ACS Catalysis*, 2013, 3, 487-501.
17. P. Biasi, P. Canu, F. Menegazzo, F. Pinna and T. O. Salmi, *Industrial & Engineering Chemistry Research*, 2012, 51, 8883-8890.
18. P. Biasi, F. Menegazzo, F. Pinna, K. Eranen, T. O. Salmi and P. Canu, *Chemical Engineering Journal*, 2011, 176, 172-177.
19. M. Sankar, Q. He, M. Morad, J. Pritchard, S. J. Freakley, J. K. Edwards, S. H. Taylor, D. J. Morgan, A. F. Carley, D. W. Knight, C. J. Kiely and G. J. Hutchings, *ACS Nano*, 2012, 6, 6600-6613.
20. J. A. Lopez-Sanchez, N. Dimitratos, P. Miedziak, E. Ntainjua, J. K. Edwards, D. Morgan, A. F. Carley, R. Tiruvalam, C. J. Kiely and G. J. Hutchings, *Physical Chemistry Chemical Physics*, 2008, 10, 1921-1930.
21. P. J. Miedziak, S. A. Kondrat, N. Sajjad, G. M. King, M. Douthwaite, G. Shaw, G. L. Brett, J. K. Edwards, D. J. Morgan, G. Hussain and G. J. Hutchings, *Catalysis Science & Technology*, 2013, 3, 2910-2917.
22. S. J. Freakley, Q. He, J. H. Harry, L. Lu, D. A. Crole, D. J. Morgan, E. N. Ntainjua, J. K. Edwards, A. F. Carley, A. Y. Borisevich, C. J. Kiely and G. J. Hutchings, *Science*, 2016, 351, 965-968.
23. J. K. Edwards, J. Pritchard, L. Lu, M. Piccinini, G. Shaw, A. F. Carley, D. J. Morgan, C. J. Kiely and G. J. Hutchings, *Angewandte Chemie*, 2014, 53, 2381-2384.

24. H. Erdogan, O. Metin and S. Ozkar, *Physical Chemistry Chemical Physics*, 2009, 11, 10519-10525.
25. N. N. M. Zorkipli, N. H. M. Kaus and A. A. Mohamad, *Procedia Chemistry*, 2016, 19, 626-631.
26. D. A. Ward and E. I. Ko, *Industrial & engineering chemistry research*, 1995, 34, 421-433.
27. A. Tungler, T. Tarnai, L. Hegedûs, K. Fodor and T. Máthé, *Platinum Metals Review*, 1998, 42, 108-115.
28. B. Coq and F. Figueras, *Journal of Molecular Catalysis A: Chemical*, 2001, 173, 117-134.
29. P. Mäki-Arvela, J. Hájek, T. Salmi and D. Y. Murzin, *Applied Catalysis A: General*, 2005, 292, 1-49.
30. N. E. Ntainjua, M. Piccinini, J. C. Pritchard, J. K. Edwards, A. F. Carley, J. A. Moulijn and G. J. Hutchings, *ChemSusChem*, 2009, 2, 575-580.
31. C. Samanta and V. R. Choudhary, *Chemical Engineering Journal*, 2008, 136, 126-132.
32. V. R. Choudhary, C. Samanta and P. Jana, *Industrial and Engineering Chemistry Research*, 2007, 46, 3237-3242.
33. C. Samanta and V. R. Choudhary, *Catalysis Communications*, 2007, 8, 2222-2228.
34. V. R. Choudhary, C. Samanta and P. Jana, *Applied Catalysis A: General*, 2007, 317, 234-243.
35. J. Li and K. Yoshizawa, *Catalysis Today*, 2015, 248, 142-148.
36. N. Gemo, P. Biasi, T. O. Salmi and P. Canu, *The Journal of Chemical Thermodynamics*, 2012, 54, 1-9.
37. C. Descamps, C. Coquelet, C. Bouallou and D. Richon, *Thermochimica Acta*, 2005, 430, 1-7.
38. J. V. H. d'Angelo and A. Z. Francesconi, *Journal of Chemical & Engineering Data*, 2001, 46, 671-674.
39. A. Pashkova, L. Greiner, U. Krtschil, C. Hofmann and R. Zapf, *Applied Catalysis A: General*, 2013, 464-465, 281-287.
40. R. Dittmeyer, J. D. Grunwaldt and A. Pashkova, *Catalysis Today*, 2015, 248, 149-159.
41. D. Hâncu, J. Green and E. J. Beckman, *Accounts of Chemical Research*, 2002, 35, 757-764.
42. W. Li, A. Bonakdarpour, E. Gyenge and D. P. Wilkinson, *ChemSusChem*, 2013, 6, 2137-2143.
43. K. V. Plakas, A. J. Karabelas, S. D. Sklari and V. T. Zaspalis, *Industrial & Engineering Chemistry Research*, 2013, 52, 13948-13956.
44. D. F. Bishop, G. Stern, M. Fleischman and L. S. Marshall, *Industrial & Engineering Chemistry Process Design and Development*, 1968, 7, 110-117.
45. R. Battino and H. L. Clever, *Chemical Reviews*, 1966, 66, 395-463.
46. C. G. Hill and T. W. Root, *Introduction to Chemical Engineering Kinetics and Reactor Design*, Wiley, 2014.